TRANSCRIPTIONAL REGULATION IN SKELETAL MUSCLE OF ZEBRAFISH IN RESPONSE TO NUTRITIONAL STATUS, PHOTOPERIOD AND EXPERIMENTAL SELECTION FOR BODY SIZE

Ian Porto Gurgel do Amaral

A Thesis Submitted for the Degree of PhD
at the
University of St Andrews

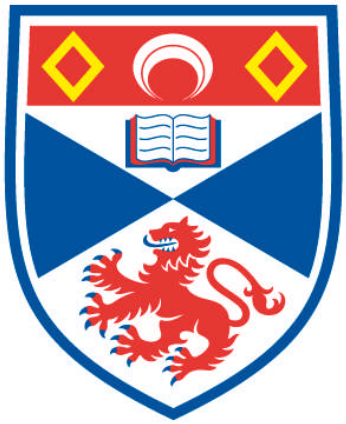

2012

Transcriptional regulation in skeletal muscle of zebrafish in response to nutritional status, photoperiod and experimental selection for body size

Ian Porto Gurgel do Amaral

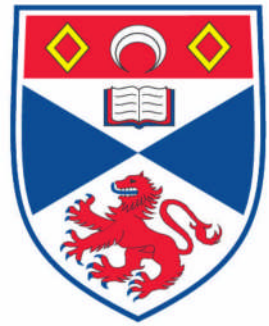

This thesis is submitted in partial fulfilment for the degree of PhD

at the

University of St Andrews

December of 2011

Transcriptional regulation in skeletal muscle of zebrafish in response to nutritional status, photoperiod and experimental selection for body size

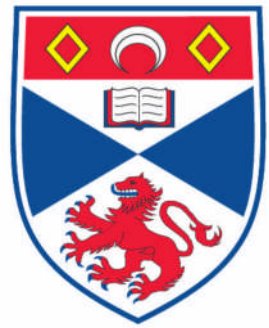

Ian Porto Gurgel do Amaral

This thesis is the result of four years of research under direct supervision of **Prof. Ian A. Johnston**, head of the Fish Muscle Research Group. The experiments of which were performed in the Scottish Oceans Institute of the University of St Andrews.

December of 2011

Declarations

1. Candidate's declarations:
I, Ian Porto Gurgel do Amaral, hereby certify that this thesis, which is approximately 38,000 words in length, has been written by me, that it is the record of work carried out by me and that it has not been submitted in any previous application for a higher degree.
I was admitted as a research student in October, 2007 and as a candidate for the degree of PhD in Biology in December, 2008; the higher study for which this is a record was carried out in the University of St Andrews between 2007 and 2011.

Date: 12 of December of 2011 Signature of candidate:

2. Supervisor's declaration:
I hereby certify that the candidate has fulfilled the conditions of the Resolution and Regulations appropriate for the degree of PhD in Biology in the University of St Andrews and that the candidate is qualified to submit this thesis in application for that degree.

Date: 12 of December of 2011 Signature of supervisor:

3. Permission for electronic publication:
In submitting this thesis to the University of St Andrews I understand that I am giving permission for it to be made available for use in accordance with the regulations of the University Library for the time being in force, subject to any copyright vested in the work not being affected thereby. I also understand that the title and the abstract will be published, and that a copy of the work may be made and supplied to any bona fide library or research worker, that my thesis will be electronically accessible for personal or research use unless exempt by award of an embargo as requested below, and that the library has the right to migrate my thesis into new electronic forms as required to ensure continued access to the thesis. I have obtained any third-party copyright permissions that may be required in order to allow such access and migration, or have requested the appropriate embargo below.

The following is an agreed request by candidate and supervisor regarding the electronic publication of this thesis:

Access to all of printed copy but embargo of chapters 3 and 4 of electronic publication of thesis for a period of 1 year on the following ground: publication would preclude future publication.

Date: 12 of December of 2011 Signature of candidate:

Date: 12 of December of 2011 Signature of supervisor:

To my family

Acknowledgements and Grants

I thank Prof. Ian A Johnston for giving me the opportunity of doing my PhD in his group, which was a great experience. Prof. Ian helped me in many circumstances before and during my PhD. Coming to St Andrews was only possible after Prof. Ian helped me in many ways to get the necessary funding to live here. During my PhD his great intellect and knowledge in the area of muscle physiology were fundamental for the progression of my work, but I also thank him for being a very understanding and patient person. I also thank Prof. Ian for his very kind words of support during the difficult times I encountered during my stay in St Andrews.

I thank Dr. Vera Vieira-Johnston, the first person I met when I arrived in St Andrews in 2007. Her help with fish husbandry was fundamental for this project. Maybe more importantly, she was a "foster mother" during my PhD, always helping me during the difficulties in adapting to living in Scotland. I also thank Vera for her very kind words of support during the difficult times I encountered during my stay in St Andrews, and for the Brazilian music. My stay in Scotland would have been much harder without her warm friendship.

I thank Prof. Luiz Bezerra de Carvalho Jr. and Ranilson de Souza Bezerra from the department of Biochemistry of Universidade Federal de Pernambuco. They were my supervisors during my undergraduate and master projects. Without their words of advice and good examples I wouldn't have pursued a PhD in St Andrews.

I thank present and past member of the Fish Muscle Research Group. Specially Dr. Neil Bower, Dr. Daniel MacQueen, Dr. Daniel Garcia and Dr. Hung-tai Lee for help and advice during my experiments. Olivia Mendivil, Clara Col, Tom Ashtom and Dr. Graham Scott are thanked for their great help in keeping the good mood and for being such great office mates and friends.
I thank my friends Jennifer Cadman, Aidan Marshal, Hannah Laws, Hailey Fowler, Giovanna Bacchidu, Ann Slimm, Sarah Ryan, Moises Lino e Silva, Renata França and Werlayne Mendes for being great friends, for the trips we took together, for cooking for me, and for sharing various moments of happiness during the four years I was in St Andrews.

During my PhD I received scholarships from Alban (E07D402823BR), Sir Harold Mitchel Fund, University of St Andrews and CAPES (BEX 0449-10-5). The experiments performed in this thesis were funded by LyfeCycle (FP7-222719).

I will always be grateful to you all

Publications

- Amaral, I. P. G. and Johnston, I. A. (2011). Insulin-like growth factor (IGF) signalling and genome-wide transcriptional regulation in fast muscle of zebrafish following a single-satiating meal. The Journal of Experimental Biology 214, 2125-2139.

  I performed all experiments, which were designed by me and Prof. Ian Johnston. I wrote the paper under supervision of Prof. Ian Johnston.

Conferences

- **Johnston, I.A., Amaral, I.P.G., Vieira-Johnston V.L.A.** *Annual main meeting of the Society of Experimental Biology (SEB)*, Marseille, France. Title: Intra-specific variation in muscle fibre phenotype. July, 2008. Oral presentation by Johnston, I.A.

- **Amaral, I.P.G. and Johnston, I.A.** *Post-graduate Conference*, University of St Andrews, Scotland. Title: Molecular control of muscle growth during growth and life-cycle transitions in aquaculture species. November, 2008. Poster presentation. This was part of the compulsory training during the PhD.

- **Amaral, I.P.G. and Johnston, I.A.** *Post-graduate Conference*, University of St Andrews, Scotland. Title: Molecular control of muscle growth during growth and life-cycle transitions in aquaculture species. November, 2009. Oral presentation. This was part of the compulsory training during the PhD.

- **Amaral, I.P.G. and Johnston, I.A.** *International Congress of Biology of Fish*, Barcelona, Spain. Title: Muscle gene expression analysis of insulin-like growth factor (IGF) signaling following a single-satiating meal in the zebrafish. July, 2010. Oral presentation.

- **Amaral, I.P.G. and Johnston, I.A.** *Annual main meeting of the Society of Experimental Biology (SEB)*, Glasgow, UK. Title: Effects of selection for body size on early-life traits and gene expression in the skeletal muscle of zebrafish (*Danio rerio*). July, 2011. Poster presentation.

- **Amaral, I.P.G. and Johnston, I.A.** *Sussex workshop.* Title: Circadian expression of clock and putative clock-controlled genes in skeletal muscle of the zebrafish (*Danio rerio*). July, 2011. Poster presentation by Johnston, I.A.

Index

Chapter 2

Chapter 3

Chapter 4

List of Figures

List of Tables

List of Abbreviations

akt	v-akt murine thymoma viral oncogene
bHLH	basic helix-loop-helix
BM	body mass
cAMP	cyclic adenosine monophosphate
CCGs	clock-controlled genes
cGMP	cyclic guanosine monophosphate
DAG	diacylglycerol
ECL	external cellular layer
FL	fork length
GH	growth hormone
GHr	growth hormone receptor
GO	gene ontology
Hh	hedgehog
IGF	insulin-like growth factor
IGFBP	insulin-like growth factor binding protein
MAPK	mitogen-activated protein kinase
MBT	mid-blastula transition
MPC	myogenic precursor cell
MRF	myogenic regulatory factor
MT	melatonin receptor
mTOR	mammalian target of rapamycin
pf	post-fertilization
PI3K	phosphatidylinositol 3-phosphate kinase
PKC	protein kinase C
PRL	Prolactin
qPCR	quantitative real-time polymerase chain reaction
ROR	retinoid orphan receptor
RZR	retinoid Z receptor
SL	standard length
STAT	signal transducers and activators of transcription
SUMO	small ubiquitin-like modifier
T3	triiodothyronine
T4	thyroxine
TGF-β	transforming growth factor – β
TL	total length
TSH	thyroid stimulating hormone
UPR	unfolded protein response
WGD	whole genome duplication
YSL	yolk syncytial layer

Abstract

In the present study, the ease of rearing, short generation time and molecular research tools available for the zebrafish model (*Danio rerio*, Hamilton) were exploited to investigate transcriptional regulation in relation to feeding, photoperiod and experimental selection.

Chapter 2 describes transcriptional regulation in fast skeletal muscle following fasting and a single satiating meal of bloodworms. Changes in transcript abundance were investigated in relation to the food content in the gut. Using qPCR, the transcription patterns of 16 genes comprising the insulin-like growth factor (IGF) system were characterized, and differential regulation between some of the paralogues was recorded. For example, feeding was associated with upregulation of *igf1a* and *igf2b* at 3 and 6h after the single-meal was offered, respectively, whereas *igf1b* was not detected in skeletal muscle. On the other hand, fasting triggered the upregulation of the *igf1* receptors and *igfbp1a/b*, the only binding proteins whose transcription was responsive to a single-satiating meal. In addition to the investigation of the IGF-axis, an agnostic approach was used to discover other genes involved in transcriptional response to nutritional status, by employing a whole-genome microarray containing 44K probes. This resulted in the discovery of 147 genes in skeletal muscle that were differentially expressed between fasting and satiation. Ubiquitin-ligases involved in proteasome-mediated protein degradation, and antiproliferative and pro-apoptotic genes were among the genes upregulated during fasting, whereas satiation resulted in an upregulation of genes involved in protein synthesis and folding, and a gene highly correlated with growth in mice and fish, the enzyme ornithine decarboxylase 1.

Zebrafish exhibit circadian rhythms of breeding, locomotor activity and feeding that are controlled by molecular clock mechanisms in central and peripheral organs. In chapter 3 the transcription of 17 known clock genes was investigated in skeletal muscle in relation to the photoperiod and food content in the gut. The hypothesis that myogenic regulatory factors and components of the IGF-pathway were clock-controlled was also tested. Positive (*clock1* and *bmal1* paralogues) and negative oscillators (*cry1a* and *per* genes*)* showed a strong circadian pattern in skeletal muscle in anti-phase with each other. MyoD was not clock-controlled in zebrafish in contrast to findings in mice,

whereas myf6 showed a circadian pattern of expression in phase with *clock* and *bmal*. Similarly, the expression of two IGF binding proteins (*igfbp3* and *5b*) was circadian and in phase with the positive oscillators *clock* and *bmal*. It was also found that some paralogues responded differently to photoperiod. For example, *clock1a* was 3-fold more responsive than *clock1b*. *Cry1b* did not show a circadian pattern of expression. These patterns of expression provide evidence that the molecular clock mechanisms in skeletal muscle are synchronized with the molecular clock in central pacemaker organs such as eyes and the pineal gland.

Using the short generation time of zebrafish the effects of selective breeding for body size at age were investigated and are described in chapter 4. Three rounds of artificial selection for small (S-lineage) and large body size (L-lineage) resulted in zebrafish populations whose average standard length were, respectively, 2% lower and 10% higher than an unselected control lineage (U-lineage). Fish from the L-lineage showed an increased egg production and bigger egg size with more yolk, possibly contributing to the larger body size observed in the early larval stage (6dpf) of fish from this lineage. Fish from S- and L-lineage exposed to fasting and refeeding showed very similar feed intake, providing evidence that experimental selection did not cause significant changes in appetite control. Investigation of the expression of the IGF-axis and nutritionally-response in skeletal muscle after fasting and refeeding revealed that the pattern of expression was not different between the selected lineages, but that a differential responsiveness was observed in a limited number of genes, providing evidence that experimental selection might have changed the way fish allocate the energy acquired through feeding. For example, a constitutive higher expression of *igf1a* was recorded in skeletal muscle of fish from the L-lineage whereas *igfbp1a*/b transcripts were higher in muscle of fish from the S-lineage. These findings demonstrate the rapid changes in growth and transcriptional response in skeletal muscle of zebrafish after only three rounds of selection. Furthermore, it provides evidences that differences in growth during embryonic and larval stages might be related to higher levels of energy deposited during oogenesis, whereas differences in adult fish were better explained by changes in energy allocation instead of energy acquisition.

In chapter 5 the main findings made during this study and their impact on the literature are discussed.

1. General Introduction

1.1. The zebrafish as a biological model system

Fish model species include the fugu (*Takifugu rubripes*) and the green spotted pufferfish (*Tetraodon nigroviridis*), the stickleback (*Gasterosteus aculeatus*) the medaka (*Oryzias latipes*) and the zebrafish (*Danio rerio*). In addition to having available information about their genes and genome organization, each of these fish display interesting characteristics as model species. For example, pufferfish are useful for studies of genome evolution due to their very compact genome, while stickleback is often used to model evolution of speciation in response to different environmental variables in separate populations. Medaka and zebrafish are used in many fields of biology as laboratory model species due to short generation time, genetic tractability, and ease of rearing and spawning in a controlled environment.

Among the fish model species zebrafish has attracted the most attention from the scientific community, resulting in the unravelling of its anatomy, behaviour and physiology. Although big progress has been made in understanding this model system much remains to be discovered as evidenced by the recent publication of an atlas of anatomy and histology of the whole body (Menke et al., 2011) and a 3D reconstruction of the zebrafish brain (Ullmann et al., 2010). There are many reasons for the great interest in the zebrafish, but what first made it so attractive to scientists interested in embryology and development was the transparency of the body during the early-life stages, which made the observation and characterization of the whole process of body and organ formation possible using light-microscopy. Apart from some important differences in physiology, the zebrafish is being more and more used for biomedical research with focus on human diseases, the reason being that most biological processes underlying pathogenesis are conserved even between invertebrates and higher vertebrates and are recapitulated in the fish model (Lieschke and Currie, 2007). Here again zebrafish excel in being an excellent model due to the low costs when compared to the mouse model (whose anatomy and physiology is more related to humans), to the genetic tractability and ease with which phenotypes can be followed visually, without the need for invasive, costly and time-demanding procedures. The body transparency

during embryonic and larval stages is important in a model in modern biomedical research allowing for direct observation of mutants and transgenesis, in the latter case with the use of fluorescent constructs. With effect, the zebrafish model has been successfully employed in a number of cases to model monogenic (e.g.: muscle dystrophy and iron-storage disorder) and polygenic human diseases (e.g.: oncogenesis and infection) making use of forward- and reverse-genetic experiments and transgenesis [reviewed in (Lieschke and Currie, 2007; Delvecchio et al., 2011)]. Forward-genetic experiments resulted in a number of mutants being generated that are publicly available from The Zebrafish Model Organism Database (www.zfin.org) and from the Zebrafish Mutant Project under development by the Sanger Institute (http://www.sanger.ac.uk/Projects/D_rerio/zmp/). While the ZFIN mutant fish lines relies on submission of information on and samples of mutants by the scientific community, the Sanger initiative set-out to mutate every single protein-coding gene, with 1,627 genes mutated so far, and make this information publicly available with the possibility to request mutate alleles from their website. The tractability of zebrafish has also proven useful in drug-discovery screening in which hundreds of embryos can be simultaneously exposed to candidate drugs [reviewed in (Lieschke and Currie, 2007)]. In fact, this model is in use by many pharmaceutical industries, including the giant Swiss-based pharmaceutical company Novartis (Delvecchio et al., 2011).

The zebrafish also has a great potential as a model for experiments in aquaculture. Advantages include previous studies of its bioenergetics (Chizinski et al., 2008), behaviour (Miller and Gerlai, 2007), growth (Siccardi et al., 2009) and swimming metabolism (Plaut and Gordon, 1994) that could be used in comparative studies with economically important fish for the aquaculture industry. Despite the acceptance and broad use of the zebrafish in biomedical sciences, the potential of this biological model is often overlooked in the aquaculture fields of nutrition, growth and disease.

1.1.1. The zebrafish genome, linkage map and whole genome duplication

Without question, the construction of linkage maps and the sequencing of the zebrafish genome were two important factors that helped the zebrafish model become so important for research. Linkage maps facilitated the investigation of mutant zebrafish lines through the use of synteny analysis and permitted a comparative analysis with

other vertebrate genomes (Woods et al., 2000). In addition, genetic maps are important for the analysis of quantitative trait loci (QTL), in which portions of the genome are analysed for their influence on a certain trait, and for the study of *cis*-regulation of expression among genes. In February 2001 the Sanger Institute started the Zebrafish genome sequencing project in collaboration with the zebrafish community. Ten years later, in May 2011 the ninth assembly version was released which shows that the zebrafish genome is composed of 25 autosomal chromosomes and 1 mitochondrial chromosome, in a total of 1.7 Giga base-pairs with around 18,000 known protein-coding genes (Table 1.1).

One known caveat of using zebrafish to model human diseases is that teleosts have undergone a whole genome duplication (WGD) after radiation of the tetrapods (Jaillon et al., 2004). WGD events are thought to be one of the possible mechanisms responsible for increasing the complexity of a genome. Following a WGD event two copies of every gene are found in the genome and are termed paralogues. Inter- and intrachromosomal rearrangements (e.g.: fusion and break) and a massive gene loss occurs in the unstable newly duplicated genome, resulting in the rediploidization of the genome (Jaillon et al., 2004; Volff, 2005). These genomic rearrangements allow for the paralogues to take different fates depending on their function and importance for the organism. While there is a possibility that the organism might benefit from the higher gene dose, it is believed that only 15% of paralogues are retained in extant species with most duplicated genes suffering loss of function due to detrimental mutations over evolutionary time and are lost from the genome (Jaillon et al., 2004). Additionally, in most cases retained paralogues show a divergence in their genomic sequence that affects the regulatory, intronic and coding sequences, usually resulting in differences in regulation of expression and biological activity. In rare events, the divergence in sequence leads to a beneficial completely new function for one of the paralogues, termed neofunctionalization (Force et al., 1999). Another possible fate is subfunctionalization, when two retained paralogues share different aspects of the same function (Force et al., 1999). It is thought that three main WGD events occurred in the vertebrates: the first before the lamprey (*Petromyzon marinus*, considered the least derived vertebrate), the second before the radiation of cartilaginous and bony fish, and the third before radiation of the teleosts. Other WGD duplications are thought to have occurred after radiation of the teleosts which affected several fish lineages, for example

a WGD duplication event is known to have occurred after the radiation of salmonids. A massive 50% loss of duplicated genes is thought to have occurred after WGD in salmonids (Allendorf, 1979). This means salmonids may have twice as many paralogues compared to other teleosts and four times as many as tetrapods. While it is considered a disadvantage in comparative studies of fish with tetrapods, the WGD events presents scientists with a unique opportunity to study genome evolution by comparing the different species that have undergone WGDs with their ancestral species and species that didn't experience a WGD. The importance of WGD in fish physiology becomes obvious when studying polygenic biological processes in which the retained paralogues may have evolved unique gene regulation and functions.

Table 1.1 – Comparison of the current state of some genome projects under investigation by the Sanger Institute*, with special attention to fish genomes.

Common name	Scientific name	Assembly version	Genome size (Mega base-pair)	Known protein-coding genes	Number of Genes (prediction)
C. elegans	***Caenorhabditis elegans***	WS220	103	20,389	N/A**
Fruitfly	***Drosophila melanogaster***	BDGP 5.25	168	13,781	19,437
Green spotted pufferfish	***Tetraodon nigroviridis***	TETRAODON 8.0	342	1,794	23,832
Fugu	***Takifugu rubripes***	FUGU 4.0	393	809	29,699
Stickleback	***Gasterosteus aculeatus***	BROAD S1	446	14	44,884
Medaka	***Oryzias latipes***	HdrR	700	1,631	123,380
Lamprey	***Petromyzon marinus***	PMAR3	831	N/A	161,311
Zebrafish	***Danio rerio***	Zv9	1,505	18,572	36,628
Human	***Homo sapiens***	GRCh37.p3	3,280	20,599	46,737
Mouse	***Mus musculus***	NCBIM37	3,420	21,873	46,375

* data retrieved from http://www.ensembl.org on September 2011.
** N/A – data not available

1.2. Fish Growth and Muscle development

1.2.1. Fish growth

The scope of growth of a fish is a function of the balance of acquisition and expenditure of energy. During embryonic and larval stages the energy supply comes from the yolk and is mostly used for development, whereas in juvenile and adult stages it comes from exogenous feeding and is mostly used for growth. For example, the zebrafish has a typical growth curve that fits a logistical equation in which an indeterminate growth pattern is observed [personal observations and (Eaton and Farley, 1974)] (Figure 1.1). In this type of curve, the growth rate (increment in size per day) increases steadily to reach a maximum (called point of inflection) at which point the growth rate starts to decrease. The growth rate and point of inflection are highly dependent on environmental factors and the genetic background of the fish.

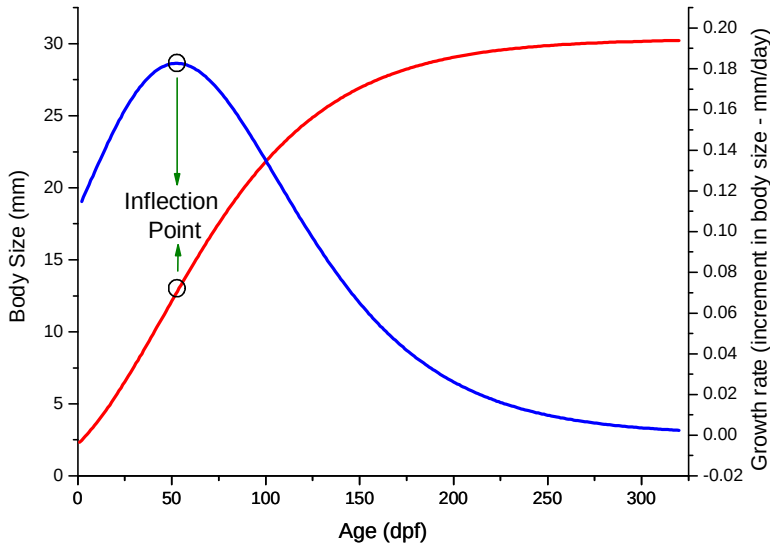

Figure 1.1 – Typical curves of growth (red) and growth rate (blue) of a zebrafish.

1.2.2. Structure and function of the adult teleost myotome

Depending on the degree of phylogenetic complexity and development of the organism, myotomes can be V or W-shaped segments of horizontally orientated muscle fibres surrounded by connective tissue (the myocommata, which is analogous to the epymisium in other vertebrates) (Van Leeuwen, 1999). The connective tissue is composed of cells (of which fibroblasts are the most abundant) and the extracellular matrix (composed of proteoglycans and proteins, of which collagen is the main component) (Velleman, 1999). In adult teleosts, the bulk of the myotome (~90%) is composed of fast-twitch fibres localized in the medial portion whereas the slow-twitch fibres are localized laterally and adjacent to the major horizontal septum and account for most of the remainder of the muscle fibres. In the developing and adult zebrafish myotomes, intermediate muscle fibres are found at the major horizontal septum between the regions of slow- and fast-twitch fibres (Johnston et al., 2009) (Figure 1.2). The organization of the different types of muscle fibres in discrete layers in the myotome is thought to reflect their distinct recruitment when different speeds are required (e.g., routine and burst swimming) (Johnston et al., 1977). Slow-twitch fibres are used for routine swimming, are rich in mitochondria, and have a constant supply of oxygen due to high vascularization, thus most energy comes from aerobic metabolism (Johnston et al., 1977; Johnston, 1982; Rome et al., 1984; Luther et al., 1995). On the other hand, fast-twitch fibres are used in fast-start swimming mostly during prey capture and evasion, have fewer mitochondria, and most energy comes from anaerobic metabolism due to the rapid use of energy allied with a low blood supply owing to the low vascularization of this tissue (Johnston, 1980, 1982; Luther et al., 1995). Intermediate muscle fibres share some properties from both slow- and fast-twitch muscle fibres. Thus the three discrete layers of muscle fibres are differentially recruited in the flowing order as the level of activity increases: slow-, intermediate-, and fast-twitch muscle fibres (Johnston et al., 1977).

Muscle fibres extend from the posterior to the anterior portion of the myotome and are inserted in the connective tissue through short tendons (Johnston, 1980; Yamaguchi et al., 1990). Bundles of muscle fibres are surrounded by the perymisium, while the endomysium encloses the individual muscle fibres. Individual muscle fibres contain myofibrils, which contain the basic contractile unit, the sarcomere (Figure 1.2).

When the sarcomere is observed by electron microscopy three vertical lines are observed: two Z-lines (or Z-discs) flanking each end of the sarcomere and one M-line in the middle of the sarcomere (Figure 1.2). The Z-line is composed mainly of α-actinin and provides support for the horizontal thin filaments which are perpendicularly oriented towards the M-line in both sides of the Z-line [reviewed in (Craig and Padrón, 2004)]. The M-line is composed of myomesin, M-protein and creatine kinase and provides support for the horizontal thick filaments which are perpendicularly oriented towards the Z-line in both sides of the M-line [reviewed in (Craig and Padrón, 2004)]. Titin is a giant elastic protein that spans from the Z-line to the M-line and closely associates with the thick filaments, playing a major role in the maintenance of the alignment and orientation of the thick filaments in the sarcomere (Figure 1.2) (John, 1992). The clear area observed between the Z- and M-lines is formed by the thin filaments and is called the I-zone whereas the dark area is formed by thick filaments and is called the A-zone (Figure 1.2) (Huxley and Hanson, 1954). Hundreds of actin molecules orientated in a helix form the backbone of the thin filament (the polymer is also called F-actin) with tropomyosin and troponin attached to the thin filament at regular intervals [reviewed by (Craig and Padrón, 2004)]. The two latter proteins regulate the contraction mechanism triggered by Ca^{2+}. The length of the thin filament is thought to be controlled by a giant protein, nebulin, although this function remains contentious (Figure 1.2) (John, 1992; McElhinny et al., 2003). The thick filament is mainly composed of myosin molecules comprising 6 polypeptides (2 heavy chains and 4 light chains), arranged in a α-helix at the C-terminal (also known as tail) and the globular heads on the N-terminal. The assembly of many molecules of myosin in a helical orientation result in the rod structure of the thick filament formed by the myosin tail on the axis and the head on the surface. The head region of the myosin molecule has actin-binding and ATPase properties. Shortening of the sarcomere and muscle contraction is based on the sliding of the thick and thin filaments which occurs through the interaction of the myosin head with the actin molecule, in a process that is dependent of Ca^{2+} and ATP (Huxley and Hanson, 1954).

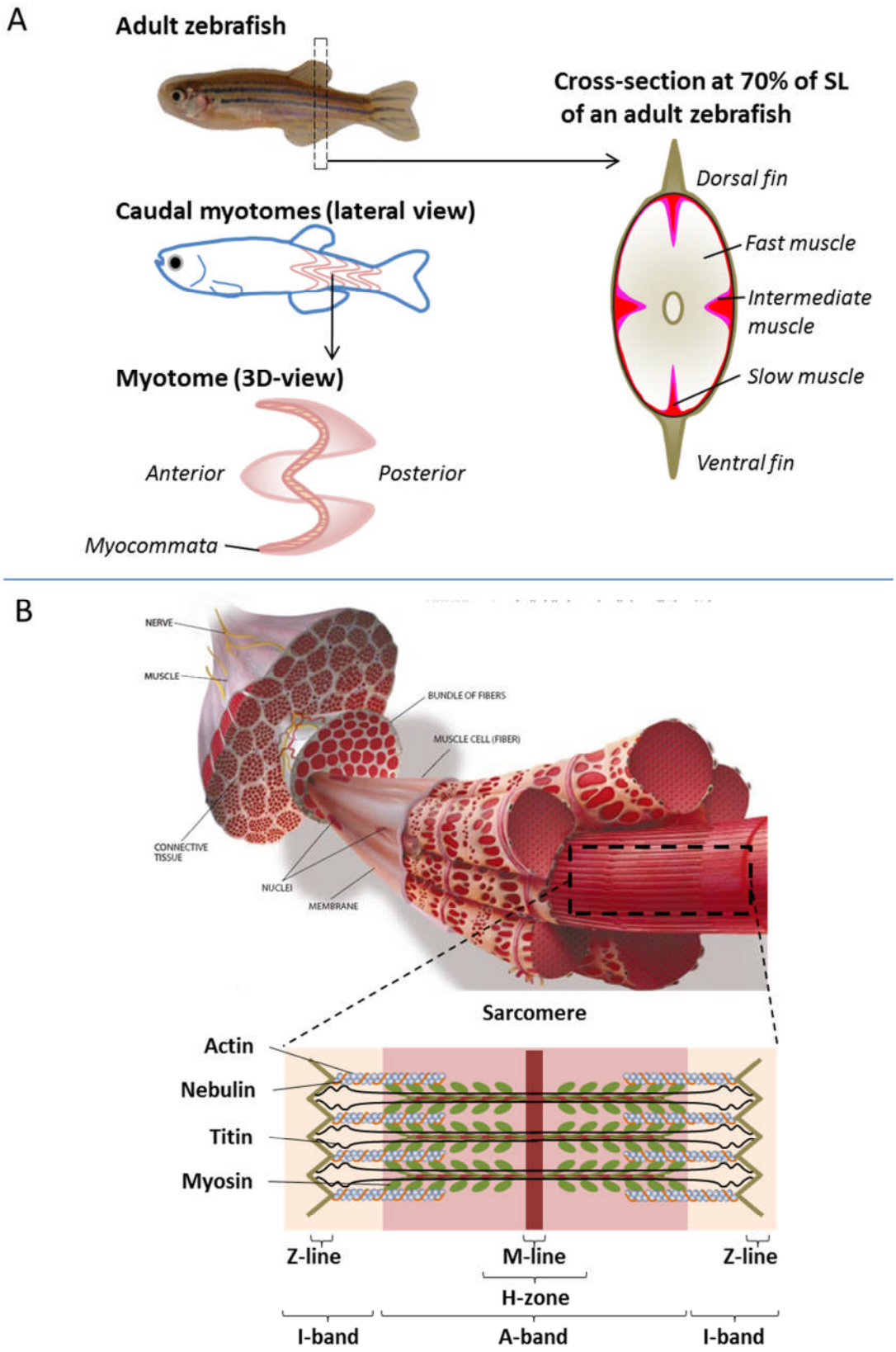

Figure 1.2 – (A) Muscle fibre types in a cross-section of adult zebrafish and myotome structure, and (B) a simplified drawing of the muscle and sarcomere structure, the contractile unit of skeletal muscle. Muscle structure was adapted from http://topvelocity.net/why-some-pitchers-throw-harder-than-others/

1.2.3. Zebrafish embryonic development, cell fate map and embryonic cell layers

The myotomes originate from the embryonic somites formed during development of the embryonic cell layer called mesoderm. In this section the morphogenetic movements that result in the formation of embryonic cell layers will be summarized using the staging system described by Kimmel et al. (1995).

After fertilization, the fish egg is composed of a single blastomere (the animal pole) on the top of the yolk (the vegetal pole) (Figure 1.3). The single blastomere undergoes a series of synchronous cell divisions, linearly increasing the number of blastomeres from 2 [around 45min post-fertilization (pf), beginning of the segmentation period] to 512 (around 2h45min pf, in the middle of the blastula period) (Figure 1.3). During the 512-cell stage a number of important changes occur in the cell cycle and zygotic activation: the blastomeres at the margin of the yolk release their cytoplasm and nucleus into the yolk cytoplasm, originating the yolk syncytial layer (YSL) which will lie between the yolk cell and the blastomeres; the cell cycle starts to lengthen and to become asynchronous; the lengthening of the interphase is concomitant with the increase of production of RNA (zygotic activation) and the motility of cells. These changes are collectively known as the mid-blastula transition (MBT). It is believed that maternally-deposited mRNAs control the basic cellular functions prior to MBT (Pelegri, 2003), but these transcripts are also believed to simply function as a nutritional reserve (Hunter et al., 2010). In chapter 4 the levels of maternal transcripts in selectively bred zebrafish are investigated. The progression of the asynchronous cell divisions after MBT results in the dome stage, when the YSL starts to dome towards the animal pole and, subsequently, tiers of blastomeres at the margin of the yolk cell (blastoderm) starts to move towards the vegetal pole (a process that is called epiboly) (Figure 1.3). When the blastoderm covers 50% of the yolk-cell (50% epiboly) the blastomeres in the front of migration to the vegetal pole start to involute towards the medial portion of the yolk-cell and marks the beginning of the gastrula period (~5.3hpf, Figure 1.3). Injection of blastomeres with tracer dye at this stage allowed for the construction of a cell fate map for the zebrafish, with the origin of many organs and structures in the embryo being traced back to specific regions in the blastoderm at the 50%-epiboly stage (Kimmel et al., 1990) (Figure 1.3). The continuation of epiboly results in the formation of a germ ring, a thick layer of blastomeres concentrated at the 50%-epiboly position. The blastoderm at the germ-ring consists of two layers of

blastomeres: the epiblast and the hypoblast, the two first embryonic cell layers. Movements of convergence start during the germ-ring stage and subsequently results in the formation of the shield (Figure 1.3). Movements of convergence entail the migration of blastomeres from all regions of the blastoderm to the future embryo axis. The region of the shield will originate the structures of the embryo head, allowing for the distinction of the future anterior-posterior axis. After the formation of the shield epiboly resumes and the blastoderm folds back upon itself, separating the epiblast and hypoblast by a fissure, the Brachet's cleft, at the 75%-epiboly stage (Figure 1.3). After the end of gastrulation, three embryonic layers are formed: the ectoderm is originated from the epiblast and will form the epidermis and central nervous system, while the mesoderm and endoderm originate from the hypoblast. Lineage tracer dye experiments reveal that cells from the endoderm will give rise to the intestine and pharynx whereas the mesoderm will give rise to blood cells, and somites among other structures and organs (Kimmel et al., 1990).

After completion of epiboly, around 10hpf, the segmentation of the paraxial mesoderm gives rise to the somites that at this stage have an epithelial aspect, with a layer of superficial cells surrounding a group of mesenchymal cells. Cell lineage dye tracing of the mesenchymal cells reveals that they will form the bulk of the myotome (Kimmel et al., 1995), whereas the cells on the superficial layer adjacent to the notochord (the medial somitic epithelium), called adaxial cells, are the slow muscle precursor cells (Thisse et al., 1993) (Figure 1.4). The ventromedial epithelium of the somites will give rise to sclerotome cells that will migrate between the adaxial cells and the notochord, and originate the vertebral cartilage and later the axial skeleton (Figure 1.4). A third derivative of the somite, the dermomyotome, is formed from the anterior-most layer of somitic cells and will form the external cell layer (ECL) (Figure 1.4). The morphogenetic movements involved in myogenesis and larval myotomal structure formation will be summarized in section 1.3.6.

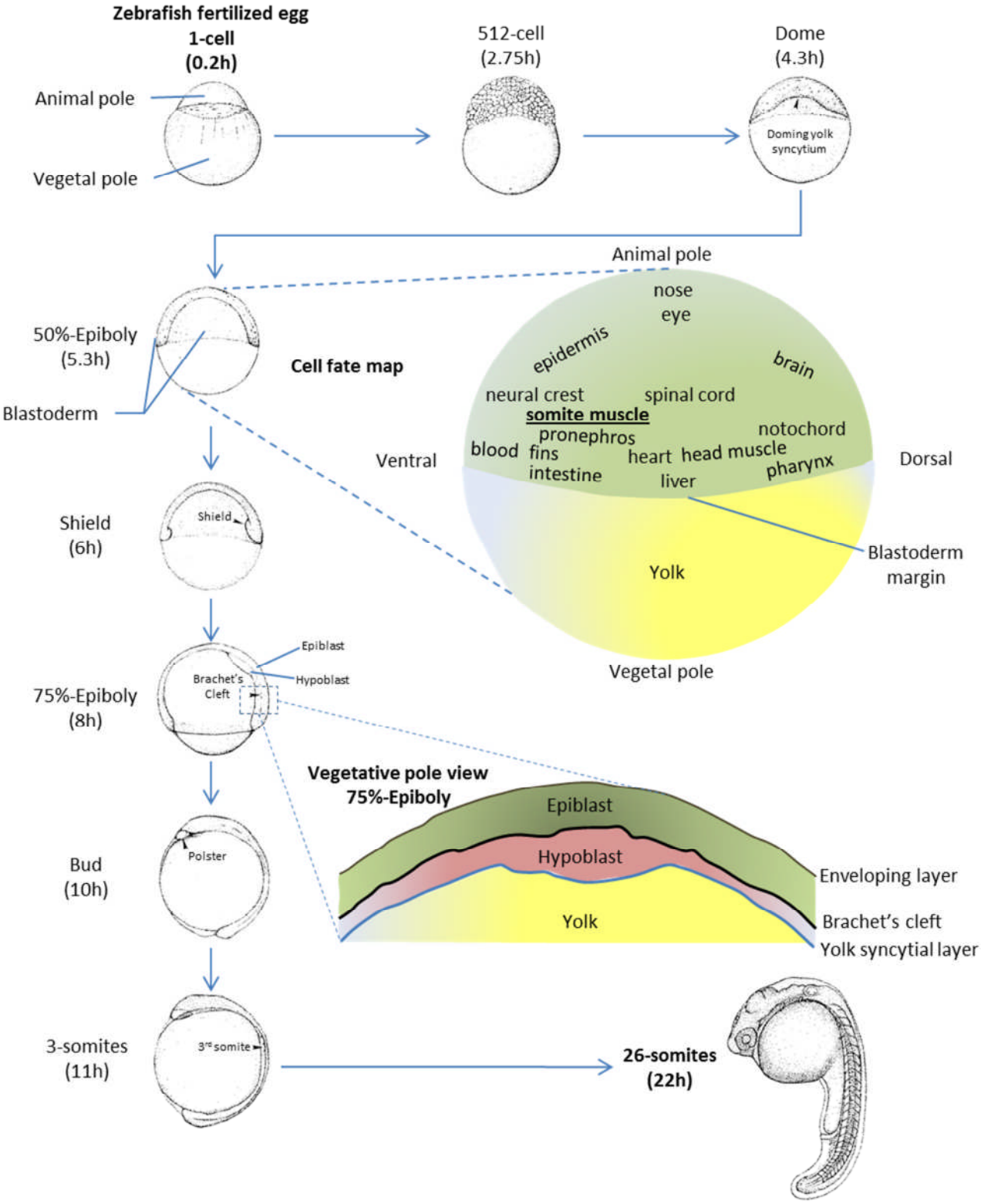

Figure 1.3 – Zebrafish development from 1-cell to 26-somite stage, with emphasis in the cell fate map during 50% epiboly and the two embryonic layers formed during gastrulation [adapted from (Kimmel et al., 1990; Kimmel et al., 1995)].

1.2.4. Transcription factors as master switches during myogenesis

During myogenesis muscle-specific transcription factors bind to the regulatory sequences of muscle genes to start specific transcriptional programs that will dictate the fate of the cells. Specific expression of the transcription factors serves as a molecular marker of cell lineage and metabolic status and has been fundamental for unravelling muscle development processes. Knockout and knockdown experiments in the mouse and zebrafish models, respectively, have been fundamental in the investigation of the function of the transcription factors in myogenesis by exploring the effects of loss-of-function of single genes or combination of genes of a pathway. In this section the fundamentals of knockout and knockdown experiments will be summarized together with the main evidences on the transcription factors that are important for myogenesis.

The mutation of embryonic stem cells with a vector containing the mutation of interest is the first step in the production knockout mice [reviewed in (Capecchi, 2005)]. Successful transformation of the target sequence is achieved by homologous recombination of the vector with the stem cell's DNA, which can be confirmed by chemical resistance screening. The mutated embryonic stem cell is then inserted into blastocysts and transferred to a pseudo-pregnant foster mother whose progeny will be heterozygous to the mutation and are called chimeras. Homozygous animals carrying the mutation can be produced by crossing two heterozygous chimeras. Using this technique the sequence of genes of interest can be specifically targeted and transformed into non-functional sequences or simply changed to a non-coding sequence (Capecchi, 2005). In morpholino-based knockdown experiments, a morpholino molecule containing a sequence complementary to the target mRNA blocks its splicing into mature mRNA and its translation into protein (Summerton and Weller, 1997; Nasevicius and Ekker, 2000). In contrast with the permanent effects of the knockout technique, knockdown by morpholino is transient and does not change the genome of the animal (Lawson and Wolfe, 2011). However, morpholino-based knockdown is still the technique of choice to investigate gene function in the zebrafish due to the lack of reverse-genetic techniques that targets specific sequences of DNA. New techniques that target and change specific genomic sequences in the zebrafish are currently under development [reviewed in (Lawson and Wolfe, 2011)].

MyoD, myf5, myf6 (also known as mrf4) and myog are members of the family of basic helix-loop-helix (bHLH) family of myogenic regulatory factors (MRFs) with

fundamental importance for myoblast specification (myoD, myf5 and myf6) and differentiation (myf6 and myog). Knockout and knockdown experiments show that the functions of some MRFs are redundant. For example, double knockout of myoD and myf5 produced mice without myoblasts and skeletal muscle (Rudnicki et al., 1993), whereas single knockout of either myoD or myf5 produced mice with a muscle phenotype similar to the wild-type (Braun et al., 1992; Rudnicki et al., 1992). This redundancy in function of myoD and myf5 was recapitulated in zebrafish embryos using the morpholino knockdown technology (Hammond et al., 2007; Hinits et al., 2009). In mice, myf6 functions in specification of myoblasts and their subsequent differentiation into muscle fibres. Evidence for myf6 role in specification and differentiation came from knockouts of myoD/myf5 and myog, respectively (Sumariwalla and Klein, 2001; Kassar-Duchossoy et al., 2004). Morpholino knockdown of myf6 in zebrafish embryos caused impaired myofibril alignment, causing a loss of fibre integrity and attachment (Wang et al., 2008). However, the function of myf6 in zebrafish muscle remains contentious since recent findings do not corroborate the function of myf6 in myofibril alignment (Hinits et al., 2009). Contrary to the situation in mouse, the zebrafish myf6 does not seem to be capable of specification of myoblasts as evidenced by lack of myf6 expression in double knockdown of myoD and myf5 (Hinits et al., 2007). Knockout of myog in mice is lethal and muscle fibres do not differentiate correctly (Hasty et al., 1993; Nabeshima et al., 1993). In the zebrafish, double ablation of myoD and myog results in loss of most fast muscle whereas single myog ablation had almost no effect on fast muscle phenotype, this led to the conclusion that myog is not essential to differentiation in zebrafish fast muscle (Hinits et al., 2009).

Other transcription factors play important roles in muscle development. For example, the myocyte enhancer factor 2 (mef2) is not synthesised until onset of MRF expression providing evidence that this transcription factor is not fundamental for muscle specification, but its expression greatly augments the differentiation of the developing muscle and it is involved in myofibrillar thick filament assembly (Hinits and Hughes, 2007). In addition, ablation of expression of *mef2* in zebrafish embryos led to impaired posterior somite formation, probably mediated by Hedgehog (*Hh*) signaling, defects in sarcomere assembly and impaired cardiac contractility (Wang et al., 2005; Wang et al., 2006).

Apart from the MRFs other proteins have important functions in muscle development and growth and have been the focus of attention due to the possibility of producing animals with increased muscle mass. For example, myostatin is a member of the transforming growth factor-β (TGF-β) superfamily with potent inhibitory functions of myogenesis which affects myoblast proliferation and differentiation (Lee, 2004). In knockdown experiments in zebrafish, suppression of myostatin expression caused an increase in myoD and myog expression together with an increase in the number of somites in early development (Amali et al., 2004) providing evidence of an augmented myogenesis. More recently, a double-muscle phenotype was observed in adult zebrafish when myostatin was suppressed using RNA interference technology, resulting in enhanced expression of myoD, myog, myf5 and myf6 (Lee et al., 2009). In addition, overexpression of follistatin, a negative regulator of proteins from the TGF-β superfamily, including myostatin, produced a significant increase in muscle mass in rainbow trout and zebrafish mediated by enhanced hyperplasia (Medeiros et al., 2009; Li et al., 2011).

1.2.5. Fish myogenesis

The organization of the adult myotome in discrete zones with different fibre types is determined during embryogenesis through complex morphogenetic processes. Most of what is known about fish myogenesis comes from the zebrafish model. The basic mechanisms of stem cell commitment to myogenic precursor cells (MPCs), subsequent differentiation into myoblast and migration and fusion into myotubes are shared among vertebrates [reviewed in (Johnston, 2006; Johnston et al., 2011)]. Important differences in myogenesis between fish and other vertebrates include the time of onset of the slow muscle precursors in fish, adaxial cells, which occurs before complete somite formation, and continued formation of fast muscle myotubes into adult stages (Rowlerson and Veggetti, 2001).

Myogenesis can be separated in three different phases: embryonic myogenesis, stratified hyperplasia and mosaic hyperplasia. Around 10 hours post-fertilization (hpf) the first somite is formed in the developing zebrafish embryo (Kimmel et al., 1995). The somites will differentiate into the ECL (also known as dermomyotome), the different skeletal muscle cells and the axial skeleton.

In zebrafish, myogenesis start in the early segmentation period of the embryonic development (~10hpf). MPCs flanking the notochord start to express the muscle-specific transcription factor myoD. Expression of myoD commits the MPCs to a slow muscle cell lineage fate and these are termed adaxial cells (Devoto et al., 1996). As somite formation progresses, three discrete cell populations are observed in the somite during the early segmentation period: the adaxial cells flanking the notochord (which express pax7 and myoD); the anterior somite localized to the rostral portion of the somite (which express pax3 and pax7); and the posterior somite localized to the caudal portion of the somite (expressing pax7, myoD and myog) (Figure 1.4) (Devoto et al., 1996; Stellabotte and Devoto, 2007). Time-elapsed analysis of single cell migration shows that during the mid-segmentation period the somite rotates 90º so the anterior and posterior regions of the early somite become laterally (the dermomyotome) and medially localized (fast-cell precursors) whereas the adaxial cells (slow-cell precursors) remain in their initial position (Figure 1.4) (Hollway et al., 2007). At this stage the notochord secretes glycoproteins from the *Hh* family, which signals for the adaxial cells to become slow-fibres. The nascent slow muscle fibres start to express myosin heavy chain, and change to a more elongated morphology. These are the first cells to show

contractile properties, and are termed pioneer muscle cells (Figure 1.4) (Devoto et al., 1996). The remainder of slow myoblasts migrate radially away from the medial region (Figure 1.4). At late-segmentation, the somite rotation and migration of slow myoblasts are complete, with the fast myoblasts in the most medial region of the somite and starting to differentiate into fast-twitch myotubes, and the slow myoblasts forming a layer of cells subcutaneously to the ECL (Hollway et al., 2007; Stellabotte and Devoto, 2007). The ECL will provide the skin and myotomes with MPCs (pax3 and pax7 positive), satellite cells (pax7 positive), and dermal cells (Hollway et al., 2007). The process of somite formation ends around 24hpf when ~30 somites can be observed in the zebrafish (Kimmel et al., 1995).

Stratified hyperplasia is observed when MPCs differentiate into myoblasts and start to form new slow-twitch myotubes mainly in the dorsal and ventral medial regions (termed germinal zones) whereas myoblasts originate fast-twitch myotubes at the periphery of the myotome (Figure 1.4) (Rowlerson and Veggetti, 2001). At this stage two processes are observed: myoblast to myoblast fusion, resulting in new myotubes; and myoblast to myotube fusion, resulting in myotube maturation. This phase of myogenesis is so called due to the discrete zones of myotube formation observed (Figure 1.5). In contrast with the differentiation of adaxial cells into slow myoblasts, the differentiation of MPCs in the germinal zones into new slow myoblasts is not entirely dependent on the *Hh* pathway (Barresi et al., 2001). However, ablation of this pathway led to formation of fewer slow myotubes when compared to wild-type zebrafish (Barresi et al., 2001). Stratified hyperplasia accounts for most slow-twitch muscle fibres produced during the larval stage in many fish, but slow-twitch myotubes continue to form from the germinal zones throughout the life-cycle of many fish [reviewed in (Johnston, 2006)].

In the last phase of myogenesis, mosaic hyperplasia, quiescent pax7-positive cells differentiate into myoblasts and fuse to existing fast-twitch myotubes throughout the myotome which results in a mosaic of muscle fibres with different diameters (Figure 1.5) (Stellabotte and Devoto, 2007) (Figure 1.5). Most fast muscle fibres that form in the late larval period and in adult stages are produced through mosaic hyperplasia (Johnston, 2006), which continues until ~50% of the maximum body length (Johnston et al., 2009).

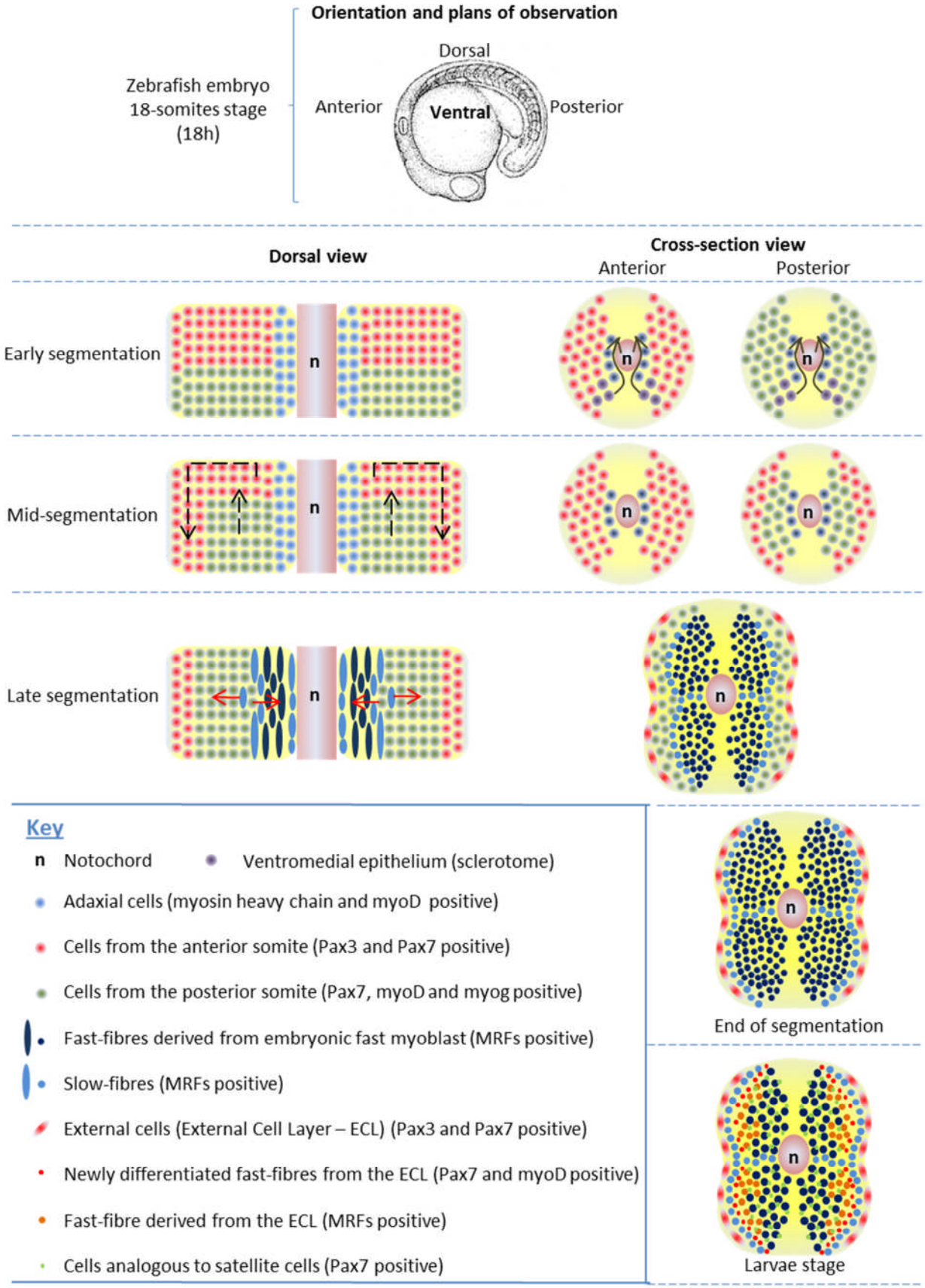

Figure 1.4 – Rotation of the somite during zebrafish embryonic myogenesis [adapted from (Kimmel et al., 1995; Devoto et al., 1996; Hollway et al., 2007; Stellabotte and Devoto, 2007)].

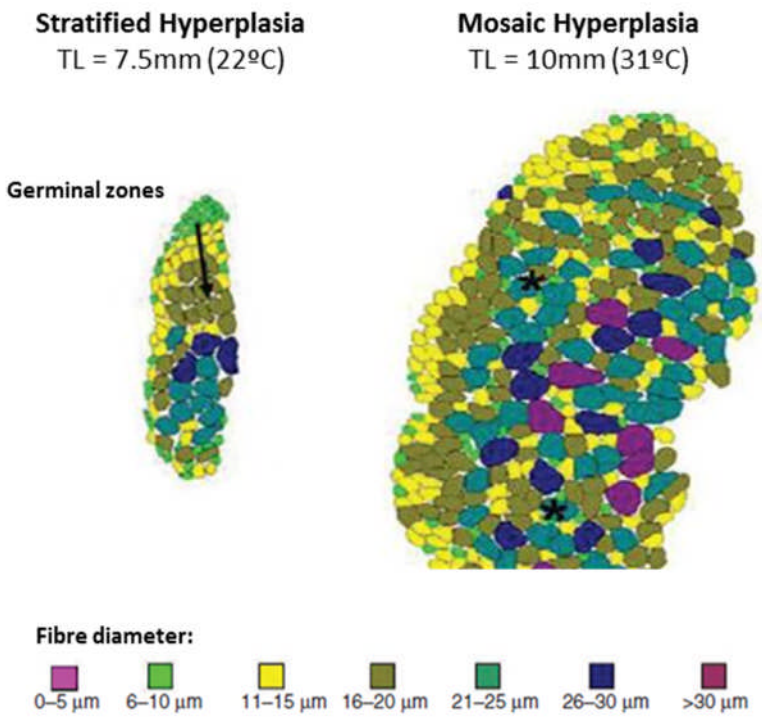

Figure 1.5 – Stratified and mosaic hyperplasia in zebrafish larvae [adapted from (Johnston et al., 2009)]. The arrow points to layers of increased fibre diameter and asterisks marks fibres surrounded by smaller fibres.

The maximum fibre number produced by stratified and mosaic hyperplasia is positively correlated with fish body size and is influenced by environmental temperature [reviewed in (Johnston, 2006; Johnston et al., 2011)]. Subsequent increase in muscle mass is achieved by hypertrophy whereby the muscle fibres expand in diameter and length by absorbing myoblasts [reviewed in (Johnston et al., 2011)]. This becomes evident when growth curves are compared to fibre recruitment curves, in which increments in body size are not followed by significant increments in fibre number when fish reach 50% of the maximum body size (Figure 1.6)

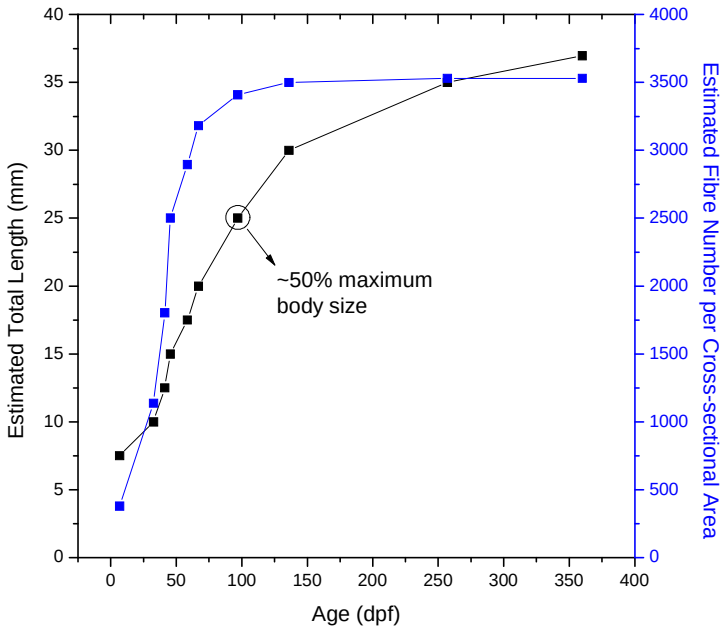

Figure 1.6 – Comparison between curves of body size and fibre number recruitment in the zebrafish. Data from growth were obtained from measurements of thousands of zebrafish kept at 27ºC from embryonic to adult stages (personal observations) and data for the fibre number curve are derived from (Johnston et al., 2009) (embryonic temperature of 26ºC, rearing at 26ºC).

1.3. Hormonal regulation of growth

Muscle fibres are metabolically active and receive molecular information from other tissues in the form of macromolecules and metabolites conveying information on environmental conditions (e.g. photoperiod length and periodicity), and are also capable of sensing their environment (e.g. nutrient levels and temperature). Mediated by hormonal signals, the transcriptional activity of muscle fibres is changed in response to the environment and molecular signals are produced, which will act in other tissues or locally. The molecular mechanisms triggering transcriptional change by some hormonal pathways are summarized in this section.

1.3.1. Growth Hormone (GH)

GH, produced in the pituitary gland, is a protein consisting of 191 amino acids with anabolic effects on metabolism, and its actions are realised by its binding to the ubiquitously expressed growth hormone receptor (GHr). Binding of GH to GHr on the plasma membrane triggers receptor dimerization and phosphorylation, with subsequent phosphorylation of the tyrosine kinases of the Janus Family (JAK). Phosphorylation of GH receptors and JAK activate several intracellular pathways including the mitogen-activated protein kinases (MAPK), phosphatidylinositol 3-phosphate kinase (PI3K), diacylglycerol (DAG), protein kinase C (PKC), intracellular calcium (Ca^{2+}) and the signal transducers and activators of transcription (STATs) that will affect the cellular metabolism at many levels [revisited by (CarterSu et al., 1996)]. For example, the uptake of glucose and control of cell survival are mediated by activation of the PI3K pathway. While many of these effects will be indirect and mediated by the different relevant pathways, phosphorylation of STATs (STAT1, STAT3, STAT5) will ultimately result in activation of GH-dependent gene expression and represent a direct effect of GH binding on cellular metabolism (Herrington et al., 2000). Some of the anabolic effects of GH are realised by the activation of the insulin-like growth factor (IGF) pathway (section 1.4.2). In fish, the level of circulating GH is modulated by many factors including temperature, salinity, photoperiod, nutrition and stress [reviewed in (Björnsson et al., 2002; Perez-Sanchez et al., 2002)]. Given its importance for the somatic growth axis, this hormone has been the focus of a few overexpression experiments, with the results varying from a 2.6- to a 10-fold increase in body size for the zebrafish and coho salmon (*Oncorhynchus kisutch*), respectively

(Devlin et al., 1995; Figueiredo et al., 2007). However, overexpression of GH in zebrafish can result in detrimental effects on the animal such as decreased transcription of the anti-oxidant defence system and the myogenic factors myoD and myog, and an accelerated senescence in adult fish (Rosa et al., 2010).

1.3.2. Insulin-like Growth Factors (IGF) pathway

The IGF pathway is composed of two ligands (igf1 and igf2), two receptors (igf1r and igf2r) and six binding proteins (igfbp1-6). IGFs' release in target tissue and their binding to their receptors is modulated by insulin-like growth factors binding proteins (IGFBPs) and proteases (Duan et al., 2010). Binding of the ligands to igf1r causes phosphorylation of a series of protein kinases that will ultimately lead to activation of the PI3K/AKT/mTor pathway, increasing protein synthesis (mediated by AKT and mTor) and decreasing protein degradation (mediated by AKT and FOXO transcription factor), thus promoting growth [reviewed in (Glass, 2003, 2005)]. On the other hand, binding to igf2r leads to lysosomal degradation of the ligand (Lau et al., 1994; Wang et al., 1994) and seems to be a mechanism of regulation of circulating IGF concentration. While IGF receptors are ubiquitously expressed, the liver is the main organ that produces circulating IGFs and IGFBPs. However, IGFs and IGFBPs are also produced by other peripheral tissues such as skeletal muscle in response to both GH and nutritional stimuli with possible paracrine and autocrine actions. Due to the whole genome duplication some teleosts have twice as many components in this pathway when compared to tetrapods. For example, the zebrafish has 16 known components, compared to 10 found in the mouse. The IGF system has been proven to be important not only for cellular growth, but also for normal development of the zebrafish as evidenced by *igf1ra/b* knockdown in which the IGF signaling was disrupted, with various detrimental effects on embryonic development including organ formation and muscle contractility (Schlueter et al., 2006; Schlueter et al., 2007). In addition, double-knockdown of *igf2a/b* caused malformation of the midline, and defects on kidney development (White et al., 2009). Changes in the level of IGFBP in fish have also been proven to be of importance for normal development and growth. For example, overexpression of *igfbp1* caused growth retardation and knockdown of this gene during hypoxia decreased the growth retardation (Kajimura et al., 2005). Knockdown of *igfbp2* and *igfbp3* caused

cardiovascular defects and retardation of development of pharynx and ear, respectively (Li et al., 2005; Wood et al., 2005b). However, knockout of single IGFBP genes in mice resulted in phenotypes not strikingly different from the wild-types [reviewed in (Duan et al., 2010)]. This suggests some caution is necessary when extrapolating results on the IGFBPs from the mice model to fish species.

The transcriptional regulation of the IGF pathway in response to nutritional levels in skeletal muscle and to the genetic background of the zebrafish is the focus of Chapters 2 and 3, respectively.

1.3.3. Cortisol

Cortisol is a glucocorticoid with anti-inflammatory and catabolic actions produced by the adrenal gland mainly in response to stressful conditions. Its molecular mechanism of action starts with the hormone binding to an inactive glucocorticoid receptor (GR) in the cytoplasm. Activated cortisol-GR complex is capable of causing its anti-inflammatory actions through a synergistic mechanism that includes (1) a transrepression cascade by inhibiting a series of kinases (p38, ERK1/2 and JNK) and NF-KappaB, and (2) directly inhibition of c-Jun- and c-Fos-dependent gene expression that would ultimately lead to expression of inflammatory cytokines (Barnes, 1998; Labeur and Holsboer, 2010). Cortisol-GR complexes also have direct activation and repression actions on gene expression which are realised by dimerization of activated cortisol-GR complexes. The dimers bind to responsive elements in the DNA and directly repress gene expression whereas interaction with other transcription factors (e.g., oct1, oct3, STAT5 and CREB) will activate gene expression (Schoneveld et al., 2004; Labeur and Holsboer, 2010). Most of what is known of cortisol mechanism of action comes from mammalian model species, with little information on the molecular pathways conserved in fish. However, in mammals and fish, cortisol seems to have similar functions during situations of stress to repress cellular growth, promote protein and glycogen breakdown and increase the circulating levels of glucose [reviewed in (Mommsen and Moon, 2001)]. For example, fish exposed to different stressors show increased circulating levels of cortisol (Bernier, 2006). Cortisol, in conjunction with prolactin and GH, is important for seawater and freshwater adaptation (McCormick, 2001; Sakamoto and McCormick, 2006). In a recent publication, cortisol was able to decrease the expression of interleukins 6 and 8, two

cytokines involved in inflammatory response, in a rainbow trout macrophage cell line (Castro et al., 2011) providing evidence of a conserved molecular action of this hormone in fish.

1.3.4. Thyroid hormones

In response to thyroid-stimulating hormone (TSH) produced by the pituitary gland, the thyroid produces thyroxine (T4) and triiodothyronine (T3), the thyroid hormones, which are considered anabolic since it causes a positive nitrogen balance (higher protein synthesis). They enter the cell cytoplasm through membrane transporters, where T4 is metabolised into the active T3 by iodothyronine deionidases (type I and II). In the cytoplasm, T3 can have a non-genomic molecular effect by activating the PI3K/AKT/mTor pathway (Yen, 2001; Moeller et al., 2006) that will ultimately lead to protein synthesis. In the nucleus, T3 activates the thyroid receptor/retinoid-x receptor complex (TR/RXR) which activates transcription of several genes involved in intermediary metabolism and cellular processes (e.g., carbohydrate and lipid metabolism, thermogenesis, muscle contraction, growth and cell cycle regulation) (Yen, 2001). Four transcripts for thyroid hormone receptors are found in fish and have probably arisen from a single gene (Power et al., 2001). Thyroid hormone actions are of great importance for the somatotropic axis as the thyroid receptors interact with the promoter of GH (Farchi-Pisanty et al., 1997) and integrates nutrition and other important physiological and developmental processes such as ossification (Saele et al., 2003), oocyte growth (Tyler and Sumpter, 1996) and muscle accretion and myofibre hypertrophy (Yang et al., 2007). Thyroid hormones are also known to play an important role in metamorphosis of fish and amphibians (Carr and Patino, 2011), and a recent report shows the importance of the pituitary-thyroid axis in adaptation of stickleback to freshwater environments (Kitano et al., 2010).

1.3.5. Melatonin and the molecular clock

Light perception is initiated by photoreceptor cells in the retina (common to mammals and fish) and pineal gland (fish only) mediated by the photopigment rhodopsin (Falcon, 1999; Falcon et al., 2007). The activation of this photopigment triggers a complex molecular cascade involving several enzymatic steps, of which arylalkylamine-N-

acetyltransferase (*aanat*) is considered the enzyme catalysing the limiting-rate step that produces the "time-keeping hormone" melatonin (Falcon et al., 2011). In the absence of light, *aanat* transcription is activated which is responsible for the peak levels melatonin during the night (Besseau et al., 2006; Falcon et al., 2011). In teleosts, two *aanat* genes (*aanat1* and *aanat2)* are found and they have probably resulted from gene duplication (Appelbaum et al., 2006). Melatonin receptors are found in the fish retina and brain, where it modulates the secretion of GH and prolactin (PRL) in the pituitary (Mazurais et al., 1999; Falcon et al., 2003). One low-affinity (*MT3*) and two high affinity (*MT1* and *MT2*) melatonin receptors have been described in fish (Barrett et al., 2003; Falcon et al., 2007). The former functions in detoxification processes and apparently does not have direct effects on somatic growth (Barrett et al., 2003) whereas the latter are seven-domain transmembrane receptors coupled to G-proteins (Falcon et al., 2007). Binding of melatonin to high-affinity receptors triggers the activation of several intracellular pathways including cyclic AMP (cAMP), phospholipase C (PLC) and cyclic GMP (cGMP), which are capable of depolarizing the cell membrane and causing changes in transcriptional activity (neuroendocrine actions of melatonin) (Falcon et al., 2007). Melatonin can also act directly on the nucleus mediated by the Retinoid Z Receptors (RZR) and Retinoid Orphan Receptors (ROR) (Hardeland, 2009). The rhythmic nocturnal production of melatonin coupled with its binding to nuclear receptors and subsequent transcriptional regulation make this hormone the central oscillator of circadian rhythms in vertebrates, conferring periodicity and rhythmicity to a molecular clock machinery that will, in turn, drive metabolic rhythmicity.

In addition to melatonin, light entrains an intrinsic and complex clock machinery that is based on transcriptional and post-translational regulation of protein synthesis. While melatonin is mainly produced by eyes and pineal tissues (considered the central pacemakers), the molecular clock components are found in the central pacemakers and in many other peripheral tissues, and integrates the photoperiod information perceived by the eye and pineal with metabolism and physiology in peripheral tissues. In mouse, the circadian system is highly hierarchical, with the central pacemakers entraining and controlling the rhythmicity and periodicity of peripheral circadian clocks (Ripperger et al., 2011). Research on the molecular mechanism in the zebrafish points to a more dispersed control of the circadian clocks as evidenced by a direct photoresponsiveness of internal organs to light (Whitmore et al., 1998; Weger et al., 2011). The exact mechanisms by which central pacemakers entrain

peripheral clocks remain to be established, but it is thought that a combination of neuronal and hormonal information (including melatonin and glucocorticoids) is relayed to peripheral tissues [reviewed in (Takahashi et al., 2008; Dibner et al., 2010)]. The core-clock molecular machinery is composed of a positive and negative arm that rhythmically control the transcription of the components of the clock, and an ancillary arm that fine-tunes the expression of the main oscillators of the main components of the clock machinery. The clock-drosophila homolog (*clock*) and the aryl hydrocarbon receptor nuclear translocator-like (*arntl*, but commonly known as *bmal*) are the components of the positive arm of the mechanism, they form heterodimers and activate the transcription of all core-clock components genes that are controlled by the clock-mechanism. Clock:bmal heterodimers also activate transcription of the negative oscillators period (per) and cryptochrome proteins (cry) which, after translation, form heterodimers in the cytoplasm, translocate to the nucleus and inhibit transcriptional activation by clock:bmal. The ancillary arm is composed of ROR and REV-erb, which are, respectively, positive and negative regulators of *clock* and *bmal* transcription. Due to the WGD that occurred at the base of teleost evolution, the zebrafish has as many as twice the number of copies of each gene in this pathway. In addition, unlike the mouse molecular clock, expression of two paralogues of negative oscillators namely *per2* and *cry1a* are directly responsive to light input (Tamai et al., 2007; Vatine et al., 2009), and a growing number of genes were recently reported as being light-responsive or clock-controlled in the zebrafish (Weger et al., 2011).

Thus, melatonin and the circadian clock machinery are responsible for the integration of physiology with the photoperiod, with direct influence on gene expression. The transcriptional regulation of the circadian machinery and some clock-controlled genes in skeletal muscle of the zebrafish is described in Chapter 3.

1.4. Biotic and abiotic factors affecting fish growth and myogenesis

Environmental factors are sensed by the organism and trigger an intricate physiological response leading to an output response mediated by neuroendocrine pathways (e.g., modulation of behaviour, respiration, metabolism, sexual maturity, and tissue differentiation). This change in physiological state in response to environmental variables is commonly known as phenotypical or developmental plasticity, is limited by the genetic variation of the population, and can have transient or persistent effects on the physiology and organism fitness. In this section some abiotic and biotic factors affecting fish growth and myogenesis will be summarized.

1.4.1. Temperature

Fish, as most biological systems, have an optimum temperature for growth and development. Exposure to temperatures slightly higher or lower than the optimum will lead to a decrease in growth due to the compensatory mechanisms elicited by the change in temperature. However, exposure to temperature much higher or lower than the optimum might result in malformation and lethality. In addition to the effects on adult individuals, embryonic temperature causes a persistent effect on final muscle fibre number in fish. For example, embryonic temperature affects the timing of development of fish larvae which includes the timing of myogenic progenitor cell recruitment and differentiation [reviewed in (Johnston, 2006)]. This was demonstrated in a number of studies in which fish were exposed to a range of temperatures during embryonic development and then transferred to a single rearing temperature for the remainder of development and growth (Vieira and Johnston, 1992; Johnston et al., 2001; Xie et al., 2001; Hall and Johnston, 2003; Fernandes et al., 2006; Macqueen et al., 2008). The conclusions point to the hypothesis that exposure to different temperatures during a critical stage of embryogenesis imprints the embryo to have a certain fate dependent on embryonic temperature, affecting the timing of MRF expression and cell recruitment (Vieira and Johnston, 1992; Johnston et al., 2001; Xie et al., 2001; Hall and Johnston, 2003; Fernandes et al., 2006; Macqueen et al., 2008).

The exact molecular basis of the changes in growth of adult fish induced by temperature remains to be established. The GH-IGF axis, an output of various systems involving acclimation and adaptation to different environmental conditions, is usually

studied to explain the effects of temperature on somatic growth. For example, sunshine bass, a hybrid fish produced for aquaculture purposes, acclimatized at 25 and 30ºC (optimum temperature for its growth) had higher levels of plasma igf1 when compared to fish acclimatized at lower temperatures (Davis and Peterson, 2006). This increase in igf1 levels were probably due to activation of transcription since the authors did not find a decreased plasma level of IGF binding proteins. Gabillard et al. (2003) have found that plasma level of GH was increased without an increased gene expression in the pituitary. In a recent review Gabillard et al. (2005) have discussed that the temperature-induced increase in growth affects both embryonic and post-embryonic phases of development and that this is mediated by the somatotropic axis. For example, higher expression of *igf2* was correlated with an increased growth induced by temperature, whereas the expression of *GH* and *igf1* were responsible for the growth during post-embryonic stages (Gabillard et al., 2005). However, because temperature alone can modulate reaction rates in the organism and oxygen content in the water, it can trigger many other complex physiological responses unrelated to the GH-IGF axis which affect physiology at many levels.

1.4.2. Nutrition

Nutritional status is a critical factor for fish growth. Food is the unique source for energy acquisition and molecules which will serve as the building-blocks for developing and growing tissues. Apart from providing energy, the nutritional status (satiety, food deprivation, fasting) regulates a number of hormonal pathways that will affect body growth in a complex fashion. For example, lack of nutrients normally leads to decreased levels of IGFs and changes muscle metabolism from an anabolic to a catabolic state in which the energy stores within the body are used for the basic maintenance of the organism, involving gene regulation and protein phosphorylation cascades (Glass, 2003, 2005). Nutrition affects most hormonal pathways summarized in section 1.4. For example, food deprivation causes a decrease in circulating thyroid hormones (MacKenzie et al., 1998) and an increase in circulating levels of GH and cortisol (Shimizu et al., 2009; Costas et al., 2010). Nutrient deprivation has been fundamental in discovering the gene and protein networks that are important for the regulation of cell

metabolism in fish (Rescan et al., 2007; Salem et al., 2007; Bower et al., 2008; Bower et al., 2009; Bower and Johnston, 2010a; Fuentes et al., 2011).

1.4.3. Photoperiod

Photoneuroendocrine regulation is a complex physiological response to an external cue mediated by several proteins and enzymes (summarized in section 1.4.5.), and plays an important role in the modulation of somatic growth of fish. Photoperiod effects are extremely pervasive in fish physiology as evidenced by a circadian rhythm of various biological processes in rainbow trout (*Oncorhynchus mykiss*) (Boujard and Leatherland, 1992). The effects of photoperiod manipulation on somatic growth have been reported in the literature by several researchers. Most of these works studied species dwelling in environments which experience a strong seasonality in light conditions over the year, including salmonids. For example, Atlantic salmon (*Salmo salar*) exposed to continuous light periods showed an increased body size, growth rate and plasma level of GH compared to individuals reared under 12: 12h dark: light regimes (Björnsson et al., 2000; Nordgarden et al., 2006). However, juvenile salmon exposed to constant light grow well but do not complete the parr-smolt transformation, in a process mediated by the decreased circulating levels of thyroid hormones, GH and cortisol and local expression of GHr (Stefansson et al., 2007). In another experiment on photoperiod manipulation, melatonin plasma levels were directly negatively related to growth rate levels in rainbow trout without a direct effect on igf1 levels, an important output of the GH pathway (Taylor et al., 2005).

Photoperiod conditions also alter the final fibre number as evidenced in salmon exposed to continuous light which had 23% more muscle fibres in early seawater stages than the group exposed to ambient photoperiod (Johnston et al., 2003). In a recent publication, *pgc1α*/β and the MRF myoD were reported as a clock-controlled gene and suppression of the positive circadian oscillator *clock* resulted in reduction of mitochondrial volume and loss of contractility force, respectively (Andrews et al., 2010). Thus, photoperiod can alter both embryonic and adult muscle physiology through mechanisms that are still under investigation.

1.4.4. Genetics

Each one of the physiological responses to environmental conditions is mediated by a number of proteins, enzymes, transporters, and hormones (i.e., peptides and proteins) or by its products (enzymatic modification of metabolites). It is not surprising, then, that variations in the genetic pool and subtle variations in genomic sequence can elicit differences in biological activity and ultimately physiological responses. These variations can affect different aspects of the genomic sequence. Alterations in either the regulatory, intronic and exonic sequences can lead to differences in gene expression (by modified response *cis*-regulation), alter transcript stability, and the biological activity itself, respectively.

Silverstein (2002) used quantitative genetics to study phenotypic variation of feed intake of channel catfish (*Ictalurus punctatus*) as related to growth differences and hypothesized that a difference of around 40% in phenotypic variance (feed intake in this case) could be attributed to genetic variance. Larsen et al. (2007) studying the gene expression in two populations of European flounders (*Platichthys flesus*) found that a number of genes were differentially expressed between these populations, including components of the somatotropic axis, with possible effects on fitness traits. Maybe the most complete examples of scope for differential biological response elicited by genetic variation comes from the study populations of *Fundulus heteroclitus* living in a range of latitudinal clines which differed in environmental temperature. The researchers found that the activity of lactate dehydrogenase-B (Ldh-B) is important for acclimation and adaptation of this species to different environmental temperatures (Powers and Schulte, 1998). It was hypothesised that Ldh-B activity could be regulated at many levels: post-translational modification (i.e., enzyme phosphorylation and glycosylation), changes in protein sequence, translation rate, mRNA untranslated sequences (mRNA stability), alterations in intronic sequences (transcription), and changes in regulatory DNA sequences (rate of transcription) (Schulte, 2001). Segal et al. (1996) found a high level of variation in the non-coding (regulatory) sequence of the Ldh-B gene between the two populations and this variation resulted in a distinct stress response (Schulte, 2001). Whitehead and Crawford (2006) studied the gene expression pattern of 329 genes of central metabolic pathways in five natural populations of *F. heteroclitus* subjected to different temperature regimens. They found that 13 of the studied genes presented a modulation of expression specifically related to temperature and that this

gene expression varied within and among populations. Furthermore, the difference in expression was related to an adaptive pattern rather than a neutral genetic drift affecting the fitness of the organisms. Nei (2007) also highlighted the importance of changes in both protein-coding and regulatory sequences in phenotypic evolution.

It is, thus, essential to identify and study candidate genes responsible for the phenotypic differences within and among populations. Metabolic and hormonal pathways represent a possible source of genetic differences that could explain partially disparate growth rates among individuals.

1.5. Fish domestication

With the decrease in natural populations of fish and with the growing importance of reducing environmental impacts of human activities, cultured fish is becoming the only acceptable method of fish meat production. A successful fish culture makes use of the available information on the fish biology, encompassing water quality and temperature, embryo and fry rearing, and optimal growth conditions and breeding strategies, including optimal number of parents contributing to offspring as to maintain genetic variation. This results in a change from growing in a highly varying environment in nature to very controlled conditions in hatcheries, with important impacts in embryo and adult physiology and behaviour, collectively known as domestication. Domestication is mediated by the gradual change in the genetic pool of the organisms due to the selective pressures encountered in fish cultures (e.g. absence of predation, selective breeding, and photoperiod and temperature conditions). Common physiological and behavioural responses to domestication include increased feeding rate, decreased stress response and changes in aggression level (Robison and Rowland, 2005). For example, after five generations of selection for fork length of brown trout (*Salmo trutta*) a significant increase in growth rate was recorded in the selected lines owing to the increased feeding rate, with no difference in feed efficiency (Mambrini et al., 2006). In captive fish the phenotypical changes in response to domestication can occur rather faster, depending on the selective pressure when breeding animals for a desired trait. For example, selection for body size of medaka for two generations resulted in lineages with an inversely proportional growth rate to antagonistic behaviour relationship (Ruzzante and Doyle, 1991). Despite the importance of domestication to the aquaculture industry, the genetic variations imposed by captive breeding and rearing are poorly understood. Experimental selection protocols can be particularly valuable to this end, but the long generation time of aquaculture species and high costs of keeping separate lineages for a long time in culture made this approach underexplored. In a recent publication, domestication and GH-transgenesis of coho salmon was found to have similar effects on IGF-axis genes in liver and muscle (Devlin et al., 2009). The zebrafish has emerged as a model for studies of domestication, in which a similar behavioural response was observed between zebrafish and salmonids (Robinson and Rowland, 2005). The advantages of using zebrafish in selection experiments to model domestication are clear, but some are highlighted in that paper.

In addition to being valuable to the aquaculture industry in modelling domestication responses in teleosts, selected lines of zebrafish could provide a unique opportunity to model many other aspects in biology. For example, other model species (e.g. mouse, *Drosophila*, and *C. elegans*) are used to investigate the effects of selection on body composition and longevity. There are many interesting examples in the literature of successful experimental selection on *C. elegans* and *Drosophila* including recent discoveries of genes related to decreased effects of aging on the body phenotype (Jenkins et al., 2004; Sarup et al., 2011). While the mouse model currently fulfils the role of a vertebrate system for experimental selection, the zebrafish might prove valuable in adding more information on genes associated with desirable traits.

1.6. Objectives

- To characterize the transcriptional regulation of the IGF-system in zebrafish skeletal muscle after a period of fasting followed by a satiating meal, using quantitative PCR (qPCR) (Chapter 2);

- To identify genes and pathways involved in the biological process of anabolism and catabolism observed during feeding and fasting, respectively, using a genome-wide microarray (Chapter 2);

- To investigate the presence of circadian patterns of expression of the main core-clock genes in zebrafish skeletal muscle (chapter 3);

- To test the hypothesis that the expression of myogenic regulatory factors, components of the Insulin-like Growth Factor (IGF) system and other selected nutritionally responsive genes in zebrafish skeletal muscle are under control of the circadian clock mechanism (Chapter 3);

- To obtain replicate lineages of zebrafish artificially selected for divergent body size and model the pattern of somatic growth from embryonic to adult stage (Chapter 4);

- To examine the effects of short-term artificial selection for body size on early-life traits of the zebrafish, with special attention to the maternal and embryonic environment (Chapter 4);

- To investigate the effects of short-term artificial selection for body size on the transcriptional response to fasting/refeeding in skeletal muscle of the zebrafish (Chapter 4).

2. Insulin-like growth factor (IGF) signaling and genome-wide transcriptional regulation in fast muscle of zebrafish following a single-satiating meal

2.1. Summary

Male zebrafish (*Danio rerio,* Hamilton) were fasted for 7d and fed to satiation over 3h to investigate the transcriptional responses to a single meal. The intestinal content at satiety (6.3% body mass) decreased by 50% at 3h and 95% at 9h following food withdrawal. Phosphorylation of the insulin-like growth factor (IGF) signaling protein Akt peaked within 3h of feeding and was highly correlated with gut fullness. Retained paralogues of IGF hormones were regulated with feeding, with *IGF-Ia* showing a pronounced peak in expression after 3h and *IGF-IIb* after 6h. *Igf1* receptor (*igf1r*) transcripts were markedly elevated with fasting and decreased to their lowest levels 45min after feeding. *Igf1rb* transcripts increased more quickly than *igf1ra* transcripts as the gut emptied. Paralogues of the insulin-like growth factor binding proteins (IGFBPs) were constitutively expressed, expect for *igfbp1a* and *1b* transcripts, which were significantly elevated with fasting. Genome-wide transcriptional responses were analysed using the Agilent 44k Oligonucleotide microarray and selected genes validated by qPCR. Fasting was associated with the upregulation of genes for the ubiquitin-proteasome degradation pathway, antiproliferative and pro-apoptotic genes. Protein chaperones (*unc45b*, *hspd1*, *hspa5*, *hsp90a.1*, *hsp90a.2*) and chaperone interacting proteins (*ahsa1* and *stip1*) were upregulated 3h after feeding along with genes for the initiation of protein synthesis and mRNA processing. Transcripts for the enzyme ornithine decarboxylase 1 showed the largest increase with feeding (11.5-fold) and were positively correlated with gut fullness. This chapter demonstrates the fast nature of the transcriptional responses to a meal and provides evidence for differential regulation of retained paralogues of IGF signaling pathway genes.

2.2. Introduction

Growth hormone (GH) is synthesized, stored and secreted by specialised cells in the anterior pituitary and plays a central role in controlling feeding behaviour, cell growth, osmoregulation and reproduction in teleosts (Kawauchi and Sower, 2006). GH acts directly on muscle through sarcolemmal receptors and indirectly via the production of insulin-like growth factors (IGFs) in the liver and peripheral tissues which are released into the circulation (Wood et al., 2005a). IGFs are also produced by paracrine pathways and are stimulated by amino acid influx into the muscle (Bower and Johnston, 2010b). In mammals, the IGF system comprises 10 components: 2 hormones (igf1, igf2), two receptors (igf1r, igf2r) and 6 binding proteins (IGFBPs 1-6) (Duan et al., 2010). IGFBPs have distinct physiological roles in development and regulate IGF release to tissues in association with specific proteases (Duan et al., 2010). Binding of igf1 to its receptor activates several downstream signaling cascades including the PI3K/Akt/TOR and MAP kinase pathways that are well conserved in fish and mammals (Engert et al., 1996; Duan et al., 2010). Activation of PI3K/Akt/TOR stimulates a phosphorylation cascade that increases translation and protein synthesis (Engert et al. 1996; Duan et al. 2010) and inhibits protein degradation by the 26S proteasome system (Witt et al., 2005). In the zebrafish (*Danio rerio*, Hamilton), no fewer than 16 components of the IGF system have been described (Maures et al., 2002; Maures and Duan, 2002; Chen et al., 2004; Zhou et al., 2008; Wang et al., 2009; Zou et al., 2009; Dai et al., 2010). The larger number of IGF components in zebrafish compared to mammals reflects a whole genome duplication (WGD) that occurred at the base of teleost evolution (Jaillon et al., 2004). It is thought 15% of the duplicated genes or paralogues from this basal WGD have been retained in extant species (Jaillon et al., 2004). The distinct patterns of tissue expression and transcriptional regulation of many IGF system paralogues observed in zebrafish (Maures et al., 2002; Maures and Duan, 2002; Chen et al., 2004; Zhou et al., 2008; Wang et al., 2009; Zou et al., 2009; Dai et al., 2010) is consistent with either subfunctionalization or neofunctionalization of these genes.

Fasting-refeeding protocols are commonly used to investigate transcriptional regulation in the IGF-system in teleosts following the transition from catabolic to anabolic states (Chauvigne et al., 2003; Salem et al., 2005; Gabillard et al., 2006; Rescan

et al., 2007; Bower et al., 2008). Feeding to satiation after a prolonged fast, results in increased feeding intensity relative to continuously fed controls and a period of compensatory or catch-up growth (Nicieza and Metcalfe, 1997). The transcriptional responses observed in such experiments are dependent on the nutritional state of the fish prior to fasting, particularly the extent of fat stores, the duration of the fast, body size and temperature (Johnston et al., 2011). Fish show diurnal rhythms in feeding behaviour and activity driven by central oscillators in the brain that are synchronised by environmental cycles and co-ordinated with peripheral clock genes regulating metabolism (Davie et al., 2009). In aquaculture, meal times entrain biological rhythms and ready physiological systems in anticipation for processing the food (Sanchez et al., 2009). As a consequence great care should be taken in designing fasting-feeding experiments in order to define all experimental variables including the frequency and timing of feeding in relation to diurnal cycles.

Following the digestion and assimilation of a meal, the organism changes from an overall catabolic to an anabolic state, utilizing the nutrients from the meal to acquire energy and synthesize new molecules, characterizing the postprandial period. Currently there is a lack of studies describing the transcriptional changes during and following a postprandial period in fish, with most studies focusing on the changes in metabolic rate (Clark et al., 2010; Vanella et al., 2010) and plasma level of metabolites following feeding (Eames et al., 2010; Eliason et al., 2010; Wood et al., 2010). In the present chapter the transcriptional regulation in the fast myotomal muscle of male zebrafish in response to a single satiating meal delivered at first light was investigated. Expression of all 16 genes of the IGF-system was investigated by qPCR and supplemented with a genome-wide survey of transcript abundance using the Agilent 44k oligonuclotide microarray. Transcript abundance and the phosphorylation of the signaling protein Akt were determined in relation to the presence of food in the gut as a reference point. The single-meal experimental design potentially provides greater temporal resolution for studying transcriptional responses compared to continuous refeeding where early and late events quickly become confounded. The aim of the chapter was to test the hypothesis that paralogues of IGF-system genes were differentially regulated with feeding and to discover novel genes associated with the fasting and fed states in skeletal muscle.

2.3. Materials and Methods

2.3.1. Fish and water quality

The F5 generation of a wild-caught population of zebrafish (*Danio rerio*, Hamilton) from Mymensingh, Bangladesh, was used in this study. All fish were adult males aged 9 months. Prior to the single meal experiment the fish were maintained in a single 50L tank at 27.6±0.4ºC range and 12:12h dark:light photoperiod and fed bloodworms (Ocean Nutrition™, Belgium) to satiety twice daily for one week. Nitrite (0 ppm), nitrate (10-20 ppm), ammonia (0 ppm) and pH (7.6 ± 0.2) were tested during acclimation and experimental periods using Freshwater Master Test Kit (Aquarium Pharmaceuticals Inc., Chalfont, PA, USA).

2.3.2. The single meal experiment

Two replicate experiments were carried out three months apart with identical environmental conditions and food to account for any tank-to-tank variation in the feeding response. The experimental protocol involved fasting fish for 7 days and then feeding a single meal of bloodworms delivered over a 3h period, after which any uneaten food was removed from the tank by siphoning. In the first replicate experiment 7 fish per time-point were sampled and in the second replicate experiment 6 fish per time-point were sampled at the following times: -156, -24, 0h (prior to the meal), 0.75, 3, 6, 7.5, 9, 11, 24, and 36h (after the meal). The average body mass (g) and standard length (from tip of snout to last vertebrae, in mm) of the fish was respectively 0.46 ± 0.02 and 29.8 ± 0.4 (n = 77) (1st replicate experiment) and 0.53 ± 0.016 and 32.6 ± 0.3 (n = 66) (2nd replicate experiment) (Mean ± SE). Fish were humanely killed by an overdose of ethyl 3-aminobenzoate methanesulphonate salt (MS-222) (Fluka, MO, USA). Fast skeletal muscle was dissected from the dorsal epaxial myotomes, flash frozen in liquid nitrogen and stored at -80ºC prior to total RNA and protein extraction. The digestive tract was dissected and fixed in 4% (m/v) paraformaldehyde for later quantification of intestine content to the nearest milligram. Fixation was necessary to prevent tissue loss during dissection and to achieve an accurate quantification of intestine content. Since the nature of the tissue and food were the same for all samples, any shrinking caused by

fixation should be proportional to the amount of material and was not considered in the interpretation of the results. All experiments and animal handling were approved by the Animal Welfare and Ethics Committee, University of St Andrews and conformed to UK Home Office guidelines.

2.3.3. Protein extraction

Total protein was extracted from fast skeletal muscle from 5 randomly selected fish per time-point in each of the independent experiments. 30mg of tissue was homogenised in Lysing Matrix D (Qbiogene, CA, USA) in a FastPrep® machine (Qbiogene) using 350µL of 25 $mmol.L^{-1}$ MES (2-morpholino-ethanesulfonic acid monohydrate) pH 6.0 containing 1 $mol.L^{-1}$ NaCl, 0.25% (m/v) CHAPS, DNA/RNA nuclease (Invitrogen) and protease inhibitor cocktail (Invitrogen, CA, USA) .

2.3.4. Western blotting

The optimal protein amount to be used for electrophoresis separation and transfer was empirically determined by applying from 10 to 60µg of protein of a reference sample in duplicates and analysing the densitometry of the ponceau S staining (Figure 2.1A,B). TotalLab software (Nonlinear Dynamics, Newcastle upon Tyne, UK) was used to analyse the densitometry of bands from ponceau S staining and western-blots. Protein saturation was observed when more than 30µg of protein was loaded in the gel. The optimal amount was 20µg considering both ponceau S staining linearity (Figure 2.1B) and total protein availability for the experiment. The membranes used for optimal protein loading determination included a reference sample treated with calf intestinal alkaline phosphatase (A2356, Sigma) to confirm that the antibody targeted the phosphorylated moiety of the protein of interest (Figure 2.1C). Actin intensity was better correlated with ponceau S staining when compared to GAPDH (Figure 2.1C) and was used to normalize differences in protein loading. Dephosphorylation of P-AKT significantly decreased its detection by P-AKT specific antibody (Figure 2.1C), while no change in detection was observed for actin antibody in the dephosphorylated sample (Figure 2.1C), confirming the specificity of the P-AKT antibody to the phosphorylated moiety of AKT.

Samples (20µL, containing 20µg of protein) were added to 6µL of a solution containing 5µL of 5-times concentrated protein loading buffer and 1µL 20-times concentrated reducing agent (Fermentas, Vilnius, Lithuania), heated for 5min at 95°C, loaded in NuPAGE® Novex 4-12% Bis-Tris gels (Invitrogen) and ran at 120V. A protein ladder from 10 to 250 kDa (Fermentas) and a reference sample were loaded in all gels to estimate the molecular weight of proteins of interest and serve as a normalization sample, respectively. Proteins separated by electrophoresis were transferred to a PVDF Immobilon-P Transfer Membrane (Millipore, MA, USA) at 25V for 105min. Successful protein separation and transfer were confirmed by Ponceau S staining (Sigma). PVDF membranes were blocked overnight at 10°C using 5% (m/v) non-fat milk (AppliChem, Darmstadt, Germany) prepared in PBS (Sigma) containing 0.1% (v/v) Tween 20 (Sigma). Blocked membranes were incubated overnight at 10°C with the following primary antibodies (IgGs): P-Akt (1:1,000 dilution (v/v), Cell Signaling #4060, MA, USA), Akt (1:1,000 (v/v), Cell Signaling #2966), Actin (1:20,000 (v/v), Sigma A2066), and GAPDH (1:30,000 (v/v), Sigma G9545). Probed membranes were incubated at 20°C for one hour with the secondary antibody against mouse or rabbit IgG conjugated to horseradish peroxidase (both from Sigma and used at 1:60,000 (v/v)). Positive reactions were recorded by exposing Hyperfilm ECL (Amersham, Buckinghamshire, UK) to the membranes after incubation for one minute with ECL Western Blotting Detection Reagents (Amersham) at room temperature. Experimental variations in the electrophoresis and transfer were normalized using a reference sample common to all membranes. The fold-change in phosphorylation of Akt in each time-point was compared to the samples from -159h.

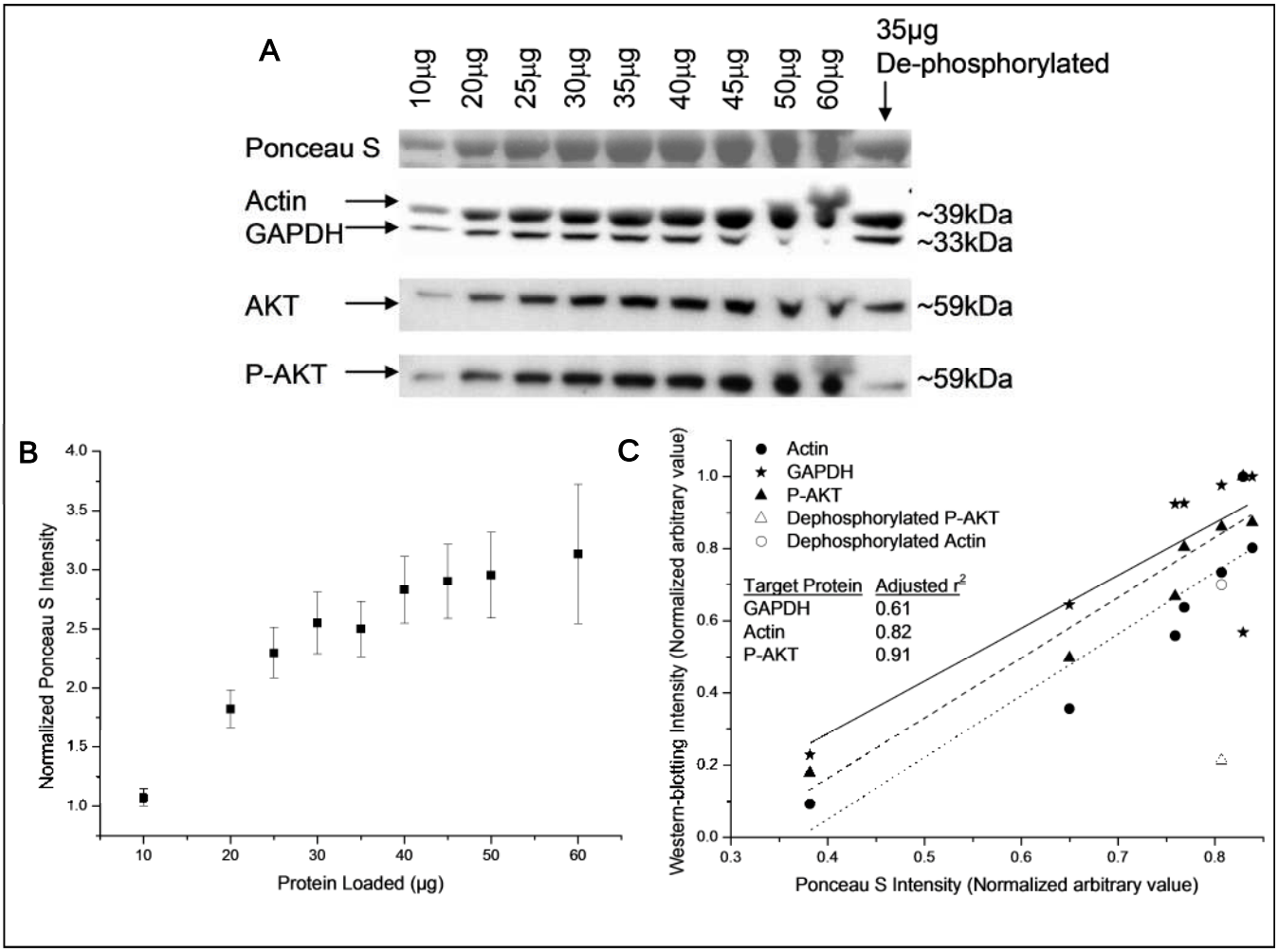

Figure 2.1 – Optimization of protein loading for electrophoresis and western-blotting. Determination of the optimal amount of protein for SDS-PAGE separation and antibody detection linearity by ponceau S staining (A,B) and comparisons of ponceau S staining with western-blotting intensity signals (C). A considerably lower signal was observed for P-AKT after submitting the sample to de-phosphorylation(△) in comparison to the untreated sample (▲).

2.3.5. Total RNA extraction from skeletal muscle and first strand cDNA synthesis

Total RNA was extracted by homogenisation in Lysing Matrix D (Qbiogene) using 1mL of TRI reagent (Sigma) in a FastPrep® machine (Qbiogene). The RNA concentration, 260/280 and 260/230 ratios were measured using a NanoDrop® spectrophotometer (Thermo Fisher Scientific, Loughborough, UK) and were between 1.5-2.0 and >2 respectively. RNA integrity was also checked by agarose gel electrophoresis. A Quantitect Reverse Transcription Kit (Qiagen, Hilden, Germany) was used to produce first strand cDNA from 0.6µg of total RNA following the manufacturer's instructions.

2.3.6. Microarray experiments

Microarray experiments were carried out by an Agilent-certified microarray service provider (Microarray Centre, University Health Network, Toronto, Canada) using the Dual-Mode Gene Expression Analysis Platform (Agilent Technologies) in a 4x44K slide format (Zebrafish (v2) Gene Expression Microarray). RNA from time-points 3h and 6h were hybridized with the RNA from the 0h sample to identify differentially regulated genes in 7d fasted fish following a single satiating meal. The 3h samples coincided with 50% of maximum gut fullness (Figure 2.2). Six phenotypic replicates from each group were used. R version 2.9n.0 with arrayQualityMetrics_2.2.0 and limma_2.18.0 was used for quality analysis of microarray data. Microarray results were also analysed using GeneSpring® v7. The intensities of spots among arrays was normalised using the AQuantile method and intensities were log transformed prior to performing a T-test using the Benjamini & Hochberg method for multiple testing correction (Benjamini and Hochberg, 1995). A list of differentially regulated genes was built by screening against the following criteria: > 2-fold change in expression, B-value statistic > 0 and an adjusted P-value < 0.05. Blast2GO software was used to analyse the gene ontology (GO) terms of the differentially expressed genes. GO enrichment analysis of the annotated genes was performed with the GOSSIP tool using Blast2GO software. The European Bioinformatics Institute Miame ArrayExpress accession number for the microarray experiment is E-MEXP-2887.

2.3.7. Primer design and cloning

Transcript sequences from the Ensembl database (release 55) (www.ensembl.org) were used to design primer pairs for each gene in Table 2.1. Primers were designed using NetPrimer (http://www.premierbiosoft.com/netprimer/index.html, Premier BioSoft, CA, USA). Where possible the primer pairs were designed so that at least one primer spanned an exon-exon boundary (otherwise primers pairs were in different exons), with a T_m close to 60ºC. First strand cDNA from muscle was used as a template to synthesise PCR products for cloning. The PCR reaction mixture contained 1.5 mmol.L^{-1} $MgCl_2$, 1x NH_4 buffer, 0.25µL BioTaq™ DNA polymerase (Bioline, London, UK), 0.2 mmol.L^{-1} dNTP (Promega, WI, USA), 1µL cDNA and 0.5 µmol.L^{-1} of each primer (Invitrogen) and the following thermal cycling conditions were employed: denaturation for 5min at 95ºC followed by 36 cycles of 30s at 95ºC, 30s at 60ºC, and 30s at 72ºC, final elongation of 5min at 72ºC. After agarose gel electrophoresis the products of expected size were extracted and purified using a QIAquick Gel Extraction Kit (Qiagen) and cloned using a StrataClone™ PCR Cloning Kit (Stratagene, CA, USA) according to the manufacturer instructions. Positive clones were picked after 16h of growth at 37ºC in LB-agar plates containing ampicillin (0.1mg/mL) and transferred to 96 well plates containing LB-broth and ampicillin (0.1mg/mL). After 16h of growth at 37ºC colony-PCR was performed to confirm the sequence of the insert using Big Dye terminator sequencing (Applied Biosystems, CA, USA) at the University of Oxford (T3 and T7 primers were used to confirm the sequence in both directions). The clones bearing plasmids with the expected insert were grown in 5mL LB-broth and plasmids were purified using a QIAprep Spin Miniprep Kit (Qiagen). The plasmid concentration, 260/280 and 260/230 ratios were measured using a NanoDrop® instrument and were higher than 1.8 and 2.0, respectively.

Table 2.1 – Sequence and properties of primers used in the experiments of chapter 2. Ensembl gene symbols, forward (f) and reverse (r) primer sequences, product size, product melting temperature (Tm), amplification efficiency (E), linearity of standard curve and Ensembl gene ID are shown.

Ensembl Gene	f/r	Primer 5'-3' sequence	Product Size (bp)	Tm (°C)	E (%)	R^2	Ensembl Gene ID
Reference genes selected from the microarray experiment							
tomm20b	f:	GCTGCTGGCTCAGGGAGACTATG	170	86.2	103.8	0.999	ENSDARG00000044636
	r:	CGCTGACGATACGCTGGCTG					
rpl7a	f:	CCCATTGAGCTGGTGGTGTTCT	216	84.8	96.2	0.999	ENSDARG00000019230
	r:	ACGGATCTCCTCATATCTGTCATTGTA					
lman2	f:	GGATCGCTCCTTTCCATACATTTC	176	81.7	104.7	0.999	ENSDARG00000061854
	r:	CCACCATTATCGTGAGTCTGCCT					
si:ch211-273k1.4 [1]	f:	GCTGTTTTTGTGAAGGAGTGTGGTC	193	82.4	98.5	0.998	ENSDARG00000033259
	r:	TTTCCCAAACAAGCGTCATCTCTG					
Genes up-regulated during fasting selected from the microarray experiment							
odc1	f:	CGACTGTGCCAGCAAAACGG	201	85.7	103.5	1.000	ENSDARG00000007377
	r:	CGGAGAACCAGCTTGGCATTT					
hsp90a.1	f:	TGGCGAACTCAGCGTTTGTG	259	83.3	100.6	0.997	ENSDARG00000010478
	r:	ACGGTGACCTTCTCAATCTTTTTG					
fkbp5	f:	GACACAGTATTTCAAGGCAGGACG	215	84.3	99.2	0.999	ENSDARG00000028396
	r:	CCAGCTCCATTACCTTGTTGCAG					
sae1	f:	GCAAGTGCTTCTGAAGTTTCGC	232	83.6	106.3	0.999	ENSDARG00000010487
	r:	CTGAGACAGCGCCTTGACAATC					
hsp90a.2	f:	CTGGAGAAGAAAGTGGAGAAGGTCA	367	85.4	102.0	0.998	ENSDARG00000024746
	r:	CCTCATCAATGCCTAAGCCCAG					
foxo1a	f:	GCGGGCTGGAAGAACTCAATCA	219	85.1	101.7	0.999	ENSDARG00000063540
	r:	CACCCTGAAGAGCCAGCTTTTTCT					
Genes down-regulated during fasting selected from the microarray experiment							
klf11b	f:	GCCCCAGTCGCCAGTATCTTC	240	86.8	97.8	0.999	ENSDARG00000013794
	r:	GGTTTCTCTCCTGTATGGGTTCTGA					
nr1d1	f:	GAAGGCTGGAACATTTGAGGTC	228	83.3	101.2	0.999	ENSDARG00000033160
	r:	GCAGACACCAGGACGACCG					
cited2	f:	AGCGGAGAGGGGAATGGTAGAC	264	84.8	103.4	0.998	ENSDARG00000030905
	r:	CGGGCAGGCAAGTTTCCATT					
bbc3	f:	GGGACAATTCAGGAACAGAACAGGA	222	86.8	95.2	0.999	ENSDARG00000069282
	r:	GCGGGACGGCATTCCTCTG					
znf653	f:	GCCATCAGCAGTTTCCAGAATCAT	255	81.9	100.7	0.999	ENSDARG00000093469
	r:	CTGATACCCACATATCTCACATTGTAATG					
hsf2	f:	CCTTCTGGGCAAAGTTGAGCTG	194	80.3	100.2	0.997	ENSDARG00000053097
	r:	GCTGCTTGTCTGTGTTTTCTGAATC					
Reference genes selected from the literature							
ef1a	f:	GAGGAGTGATCTCTCAATCTTGAAAC	191	83.8	101.0	0.999	ENSDARG00000020850
	r:	CCCTTGCCCATCTCAGCG					

Table 2.1 (continuation)

Ensembl Gene	f/r	Primer 5'-3' sequence	Product Size (bp)	Tm (°C)	E (%)	R^2	Ensembl Gene ID
Reference genes selected from the literature (continuation)							
rpl13a	f:	AAAATTGTGGTGGTGAGGTGTG	183	81.5	100.3	0.998	ENSDARG00000044093
	r:	GGTTTTGTGTGGAAGCATACCTCT					
Bactin2	f:	CCCAAACCCAAGTTCAGCC	112	83.0	100.5	0.999	ENSDARG00000037870
	r:	GAAGACAGCACGGGGAGCA					
b2m	f:	GGGGAAAGTCTCCACTCCGAAA	166	81.7	102.7	0.997	ENSDARG00000053136
	r:	CAGGTCGGTCTGCTTGGTGTCC					
usp5	f:	GACCCGGAAAACACAGAAGGAG	101	79.5	102.9	0.999	ENSDARG00000014517
	r:	CAAACCCTCCCTCAATACCAATG					
tbp	f:	CCTGCGAATTATCGTTTACGTCTTTT	151	81.7	98.4	0.999	ENSDARG00000014994
	r:	CCCTGTGGAGATGCCAGACCT					
cyp1a	f:	GACCTATTCGGAGCCGGTTTCG	120	82.8	103.7	1.000	ENSDARG00000026039
	r:	CCCGATCTTTTCATCCAATTCTCTTTG					
IGF pathway components							
igf1a [2]	f:	GCATTGGTGTGATGTCTTTAAGTGTA	188	87.1	95.9	1.000	ENSDARG00000094132
	r:	GTTTGCTGAAATAAAAGCCCCT					
igf1b [2]	f:	GGCTTTTACATAGGCAAACCTGGAG	166	84.8	NA	NA	ENSDARG00000058058
	r:	GCAGCACAGATGCAGGGACAT					
igf1ra	f:	GCCCGTGGAGAAGTCTGTGG	154	81.3	98.0	0.999	ENSDARG00000027423
	r:	GTGTGCGAAAGTGTTCCTGGTT					
igf1rb	f:	CACAACTACTGCTCCAAAGAACTGA	238	83.8	94.5	0.999	ENSDARG00000034434
	r:	GCCTGTCTGGAGGTCTGGGA					
igf2a	f:	GAAACACGAACAACGATGCG	346	82.8	91.8	1.000	ENSDARG00000018643
	r:	AGTACTTCACATTTATGGTGTCCTTG					
igf2b	f:	ACAGACAGTTTCGTAAATAAGGTCATAA	236	85.5	97.0	0.999	ENSDARG00000033307
	r:	CAACACTCCTCCACAATCCCAC					
ig2ir	f:	ACCCCTGTCCTCAAGTAACAGAT	176	80.1	99.4	0.998	ENSDARG00000006094
	r:	TTGCACACCGTCAGTACAAAAG					
igfbp1a	f:	ACTGGTGGAACAGGGTCCCT	158	82.1	98.0	1.000	ENSDARG00000014947
	r:	CTAGAGATGATTCGCACTGTTTGATT					
igfbp1b	f:	GCTCATCCAGCAGGGTCCG	151	83.5	101.2	0.999	ENSDARG00000038666
	r:	CGACACACACTGTTTGGCCTTG					
igfbp2a	f:	GGGAAGTCAGCGGTGAGGTG	196	83.0	100.8	0.999	ENSDARG00000052470
	r:	TGCTGGCACTGGCTCTGTTTA					
igfbp2b	f:	GTCAGCAGCACACAGTGGAGAAGTA	188	82.5	99.7	0997	ENSDARG00000031422
	r:	GCTCCTGTTGACACTGGCTCTG					
igfbp3	f:	AATGAATATGGCCCATGTCGT	146	80.9	101.2	0.999	ENSDARG00000014859
	r:	CCTTTGGATGGACTGCACTGT					
igfbp5a	f:	ACAACAAGCTAAGCTCGGTCCA	209	81.0	100.5	0.998	ENSDARG00000039264
	r:	TAGAGGGCTTACACTGTTTGCG					
igfbp5b	f:	GCACCCACCCATTGATCGT	241	82.8	95.3	0.999	ENSDARG00000025348
	r:	CCTTCTGCACGGACCAAATTC					

Table 2.1 (continuation)

Ensembl Gene	f/r	Primer 5'-3' sequence	Product Size (bp)	Tm (°C)	E (%)	R^2	Ensembl Gene ID
IGF pathway components (continuation)							
igfbp6a	f:	CCCTCCGCCTACAGACTATGA	180	83.1	100.7	0.997	ENSDARG00000070941
	r:	GACGAGCGACACTGCTTCCT					
igfbp6b	f:	CGTTGGGGGAGCCCTGCG	201	82.3	96.9	0.998	ENSDARG00000090833
	r:	GAGCCTTTTCCATTTCACCACTGT					
Muscle-specific ubiquitin ligases							
fbxo32	f:	GAGCACCAAAGAGCGTCAT	154	82.8	105.6	0.999	ENSDARG00000040277
	r:	CACTCCACTCAGAGAAGGCAG					
trim63	f:	CCTGGCTTTGAGAGTATGGACC	225	80.1	102.5	0.999	ENSDARG00000028027
	r:	GCCCCTTGCCTCACAGTTAT					
Muscle structural proteins							
tnni2a.4	f:	GCAGACAAGGAGATTGAGGATCTG	199	83.8	101.7	0.998	ENSDARG00000029069
	r:	GTTCTACAGACTCCTCCTTGACCTCC					
mylz2	f:	GGAGAGAAGTTGAAGGGTGCTGAC	154	83.8	103.9	1.000	ENSDARG00000053254
	r:	GATTCTTCATCTCCTCTGCGGTG					

[1] Orthologue of the gene *dis3l2* in various species.

[2] According to Zou et al. (2009) the genes *igf1* and *igf3* annotated in the zebrafish ensembl database V58 are two paralogues of the igf1 gene and should be named igf1a and igf1b, respectively.

2.3.8. Quantitative PCR (qPCR)

All protocols and reporting of qPCR assays adhered to "Minimum Information for Publication of Quantitative Real-Time PCR experiments" guidelines (Bustin et al., 2009). The qPCR reaction mixture contained 7.5µL 2x Brilliant II SYBR® QPCR Low ROX Master Mix (Stratagene), 6µL 40-fold diluted cDNA, 0.25 µmol.L^{-1} each primer and nuclease-free water (Qiagen) to a final volume of 15µL in 96 well plates (Stratagene). The reactions were performed in a Stratagene MX3005P machine (initial activation at 95°C for 10 min, followed by 40 cycles of 30s at 95°C, 30s at 60°C and 30s at 72°C) and the fluorescence results collected after the elongation step (72°C) were recorded by the MxPro software v4.10 (Stratagene). Negative controls were included and ran in duplicate, and contained either all components of the reverse transcription mixture, except reverse transcriptase (no reverse transcriptase control) or water instead of a cDNA template (no template control). After the qPCR a dissociation curve (from 55 to 95°C) was performed to verify the presence of a single peak. The specificity of each qPCR assay was also validated by sequencing transformants for each qPCR product. Absolute copy number of each gene

was calculated based on a standard curve of at least 6 orders of magnitude prepared with the plasmids which was also used to analyse the efficiency of each primer pair (Table 2.1). The threshold of fluorescence (for dRn values) used for determination of the quantification cycle (C_q) was set to 1.0 for all plates to allow for comparison between plates. Comparison between plates was possible after normalization to six samples loaded on all plates.

Six reference genes selected from the literature (*ef1a, rpl13a, bactin2, b2m, usp5, tbp and cyp1a*) and four selected from the microarray experiment (*tomm20b, rpl7a, lman2, dis3l2*) were analysed using Genorm v3.5 (Vandesompele et al., 2002) with M set to <1.5. The two genes with the most stable level of expression across the experimental conditions were *ef1a* and *lman2* (M=0.4). The expression of genes of interest was normalized to the geometric average of the two most stable genes and gene expression was reported as arbitrary units (a.u.).

2.3.9. Data analysis and statistics

All data was analysed for normal distribution and equality of variance. Normally distributed data was analysed using ANOVA followed by Tukey post-hoc tests using PASW Statistics 18 (SPSS Inc., Chicago, Illinois, USA). Kruskal-Wallis non-parametric tests followed by Conover post-hoc tests were used for the data that was not normally distributed using BrightStat software (Stricker, 2008). There was no statistically significant difference in the standard length, body mass, intestine content or normalised gene expression between the two replicate experiments (P>0.05). Therefore, the results from both experiments were combined to facilitate their interpretation, resulting in n=13 per time-point (i.e., 7 fish from the first replicate experiment plus 6 from the second replicate). In order to combine the data from mRNA levels from both experiments, the results of gene expression from the second replicate experiment were normalised to the average value of 7 samples from the first replicate experiment which had been included from the cDNA synthesis step onwards. Correlation of gene expression from both qPCR and microarray experiments was analysed by Spearman's correlation test using PASW Statistics 18 (SPSS Inc.). Clustering of gene expression was performed using PermutMatrix (http://www.lirmm.fr/~caraux/PermutMatrix/EN/index.html).

2.4. Results

2.4.1. Feeding response during the single meal experiment

Fish were continuously fed to satiation and then fasted for 7d prior to feeding a single meal over 3h. Three samples were taken during the fast: -156, -24 and 0h, corresponding to 9h, 144h and 168h after the last food. Only traces of food remained in the gut after 9h of fasting (-156h time-point), corresponding to 0.1% of body mass, with only bile observed with more prolonged fasting (-24 and 0h time-points). The maximum average gut fullness, equivalent to 6.3% of body mass, was observed at 0.75h (45min) after food became available, indicating satiety had been reached. Intestinal contents had decreased by 50% three hours after food was withdrawn and 95% of the food ingested had been assimilated or excreted by 9h (Figure 2.2). No significant statistical difference was observed for either standard length (SL), body mass or condition factor (Table 2.2).

Table 2.2 – Biometry (mean ± standard error, n=7) of fish from the single-meal experiment.

Time (h)	SL*	Body Mass (mg)	Condition Factor (K)
-159	$30.4^{a} \pm 2.6$	$530^{a} \pm 110$	$1.01^{a} \pm 0.11$
-24	$30.6^{a} \pm 2.7$	$460^{a} \pm 120$	$0.87^{a} \pm 0.09$
0	$31.6^{a} \pm 3.6$	$460^{a} \pm 140$	$0.77^{a} \pm 0.07$
0.75	$33.7^{a} \pm 2.6$	$580^{a} \pm 140$	$0.84^{a} \pm 0.04$
3	$30.4^{a} \pm 2.4$	$460^{a} \pm 120$	$0.85^{a} \pm 0.10$
6	$32.1^{a} \pm 4.0$	$550^{a} \pm 180$	$0.88^{a} \pm 0.09$
8	$29.2^{a} \pm 2.8$	$420^{a} \pm 120$	$0.88^{a} \pm 0.06$
9	$31.2^{a} \pm 3.5$	$490^{a} \pm 140$	$0.86^{a} \pm 0.07$
12	$30.8^{a} \pm 3.3$	$480^{a} \pm 140$	$0.86^{a} \pm 0.11$
24	$32.1^{a} \pm 3.9$	$520^{a} \pm 170$	$0.83^{a} \pm 0.08$
36	$31.4^{a} \pm 2.0$	$470^{a} \pm 80$	$0.81^{a} \pm 0.07$

* SL had a strong positive linear correlation with fork length ($FL=1.14\times SL+0.9$, $r^2=0.98$, $p<0.001$) and total length ($TL=1.14\times SL+2.71$, $r^2=0.98$, $p<0.001$); a strong exponential correlation between SL and body mass (BM) was also recorded in this experiment ($BM=0.097\times SL^{2.48}$, $r^2=0.84$, $p<0.001$). Values followed by a different letter means statistically different means (analysed by ANOVA with Tukey post-hoc tests, p=0.05 for both tests).

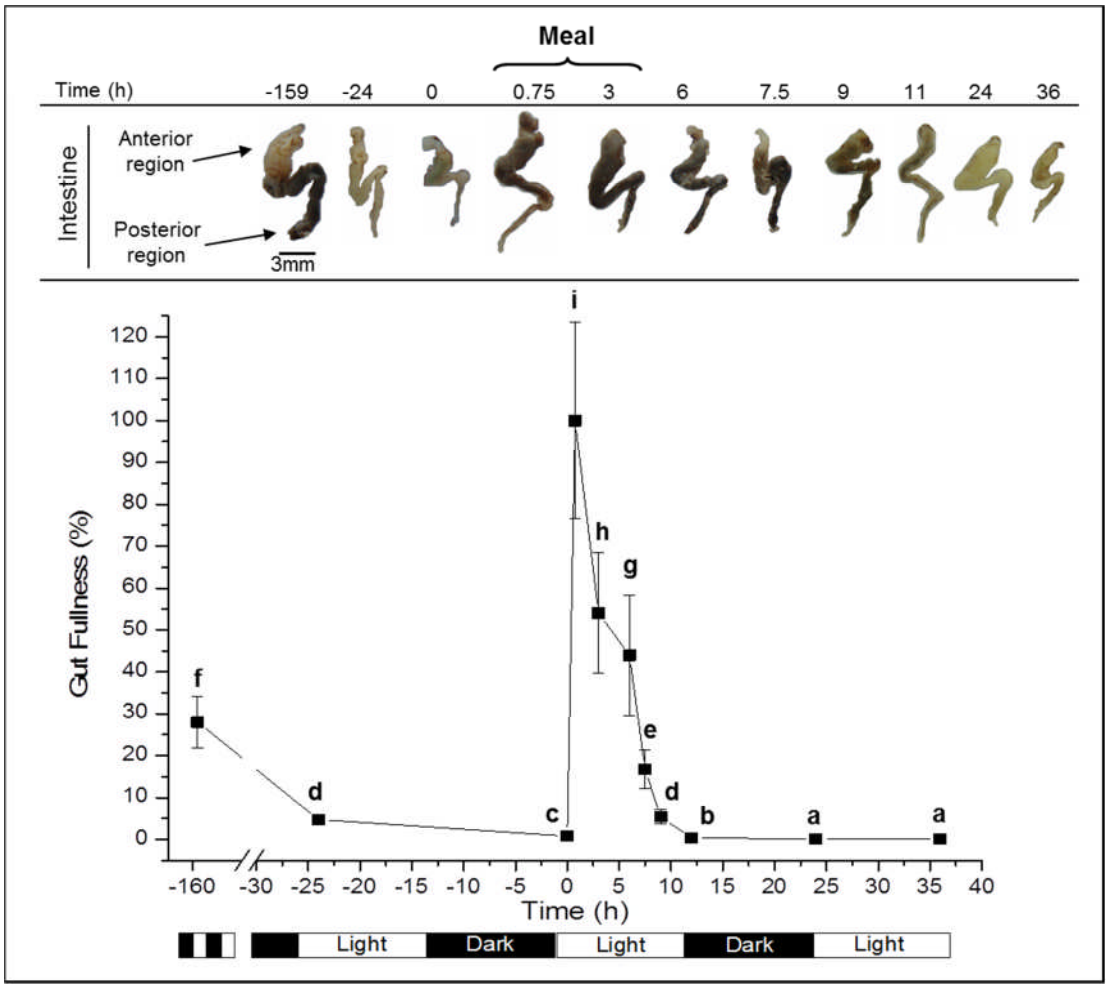

Figure 2.2 – The feeding response of male zebrafish during the course of the single meal experiment. The upper panel shows the micro-dissection of a representative intestine for each sample point. Gut fullness reached a maximum after 45min, indicating satiety. The relative intestinal content (% maximum fullness, lower panel) is shown throughout the experiment together with the dark: light cycle. Values represent Mean ± s.e.m., n = 13 fish per sample. Different letters signify statistically different means at 0.05 significance level.

2.4.2. Phosphorylation of the Insulin-like growth factor (IGF) signaling protein Akt

In fast myotomal muscle the protein Akt showed a marked increase in phosphorylation to peak levels within 3h of the start of feeding and became steadily dephosphorylated as the intestine emptied (Figure 2.3). The level of the protein load control actin and the dephosphorylated AKT did not change significantly over the course of the experiment (Figure 2.3).

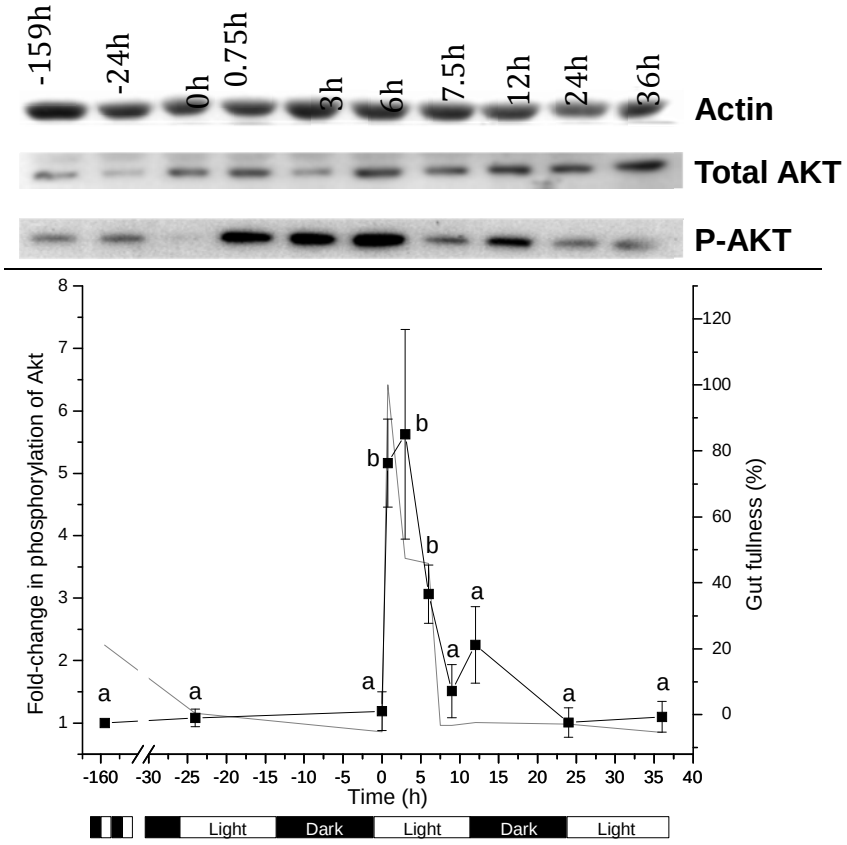

Figure 2.3 – Phosphorylation of the Insulin-like growth factor signaling protein Akt in the fast myotomal muscle of male zebrafish during the course of the single meal experiment (solid squares). Insert shows a representative Western Blot with the P-Akt antibody. The grey line represents the average gut fullness illustrated in Figure 2.2. Values represent Mean ± s.e.m., n = 5 fish per sample. Different letters signify statistically different means at 0.05 significance level.

2.4.3. Transcriptional regulation of the Insulin-like Growth Factor (IGF) system

The expression of all the paralogues of IGF-system genes was determined by qPCR including *igf1*, *igf2*, IGF-receptors and IGF binding proteins. In many cases retained paralogues of IGF system components showed distinct patterns of transcriptional regulation over the course of the experiment. Changes in transcript levels could be directly attributed to feeding since marked responses were largely present in only the first of two light: dark cycles following the meal.

2.4.4. IGF hormones gene expression

Igf1a expression was correlated with, but lagged behind gut fullness showing a distinct peak 3h after the start of feeding ($P<0.05$) (Figure 2.4A). The *igf1b* paralogue was not detected in fast myotomal muscle after 35 cycles of PCR (Figure 2.4D). *Igf2b* expression was also increased following feeding, showing peak expression 3h later than *igf1a* (Figure 2.4B). The *igf2a* paralogue was 3.7 times more abundant than the *igf2b* transcripts at 0h and was constitutively expressed during the experiment with no discernible pattern in relation to feeding (Figure 2.4C-D).

2.4.5. IGF receptors (IGFRs) gene expression

Igf1ra receptor expression increased more than 2.7-fold between 9h and 168h fasting, decreased to its lowest levels 45min after feeding and then showed variable though still depressed expression over the next 36h (Figure 2.5A). *Igf1rb* paralogue expression was inversely related to gut fullness showing a more than 3.3-fold decrease within 45min of feeding, returning to levels not significantly different to fasting after only 12h (Figure 2.5B). *Igf1rb* transcripts were more abundant than *igf1ra* transcripts over the single meal experiment, with 7.4 more copies at the start of feeding (Figure 2.5E). Transcripts of the single retained paralogue of the *igf2* receptor gene showed no consistent changes in expression over the fasting-feeding-fasting cycle (Figure 2.5C).

2.4.6. IGF binding proteins (IGFBPs) gene expression

The two retained paralogues of *igfbp1* (*1a* and *1b*) showed similar changes in expression over the experiment with high levels during prolonged fasting (144-168h), a

marked reduction in transcript abundance within 45min of the start of feeding and variable, but generally low levels over the following 36h (Figure 2.5D,E). Expression of *igfbp1a* was considerably higher than *igfbp1b* over the experiment, with a 12.4 times greater copy number at 0h (Figure 2.5F). The remaining IGF binding proteins (*igfbp2a, b; igfbp3; igfbp5a, b; and IGFBP6a, b*) showed no consistent change in expression in response to a single satiating meal (Figure 2.5G-L).

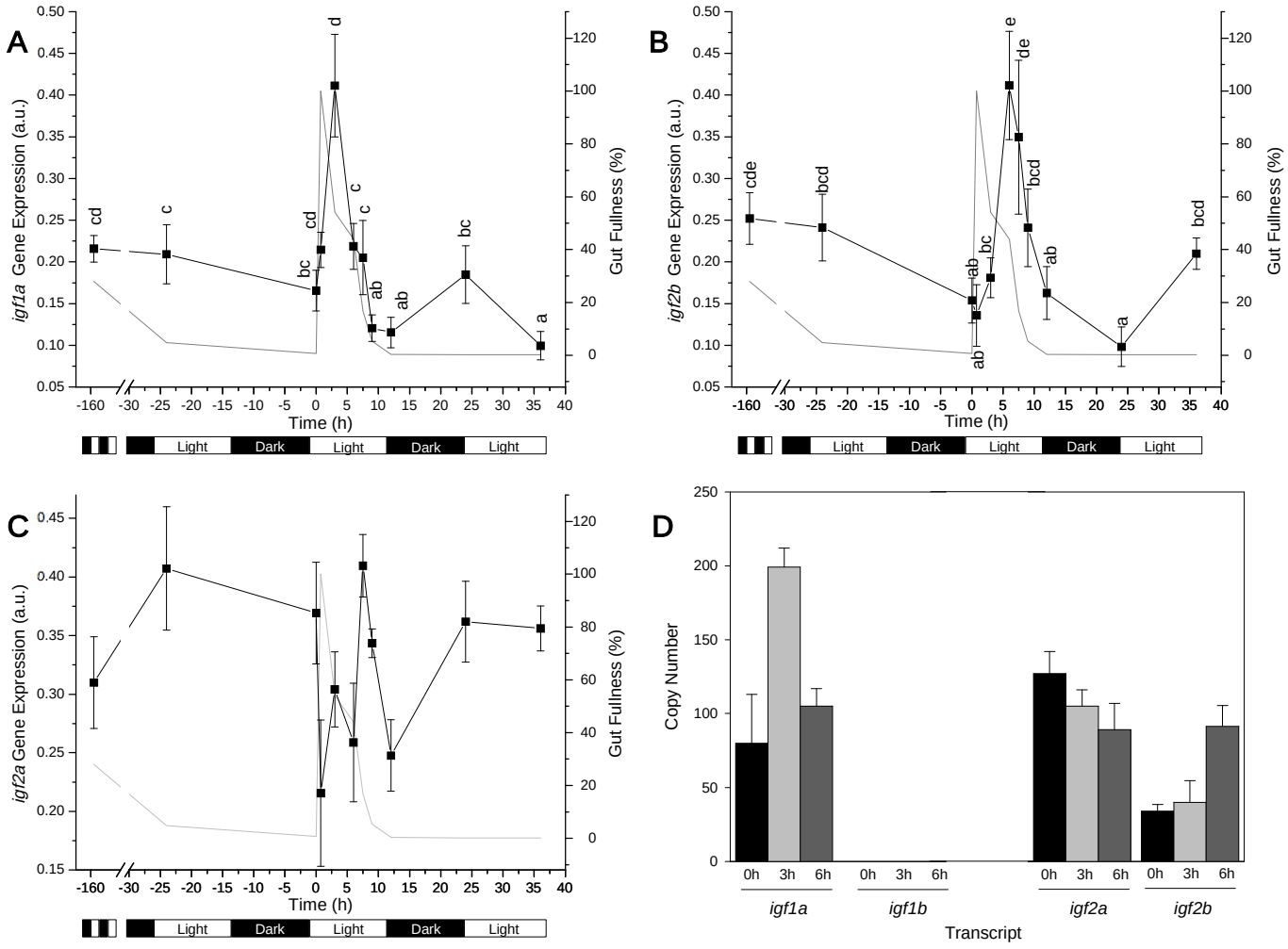

Figure 2.4 – Transcriptional responses of insulin-like growth factor (IGF) system genes in the fast myotomal muscle of male zebrafish during the course of the single meal experiment determined by qPCR (solid squares): Hormone transcripts (A) *igf1a*, (B) *igf2b,* and (C) *igf2a* and (D) copy number of *igf1a*, *igf1b*, *igf2a* and *igf2b*. The grey line represents the average gut fullness illustrated in Figure 2.2. Values represent mean ± s.e.m., n = 13 fish per sample. Different letters signify statistically different means at 0.05 significance level.

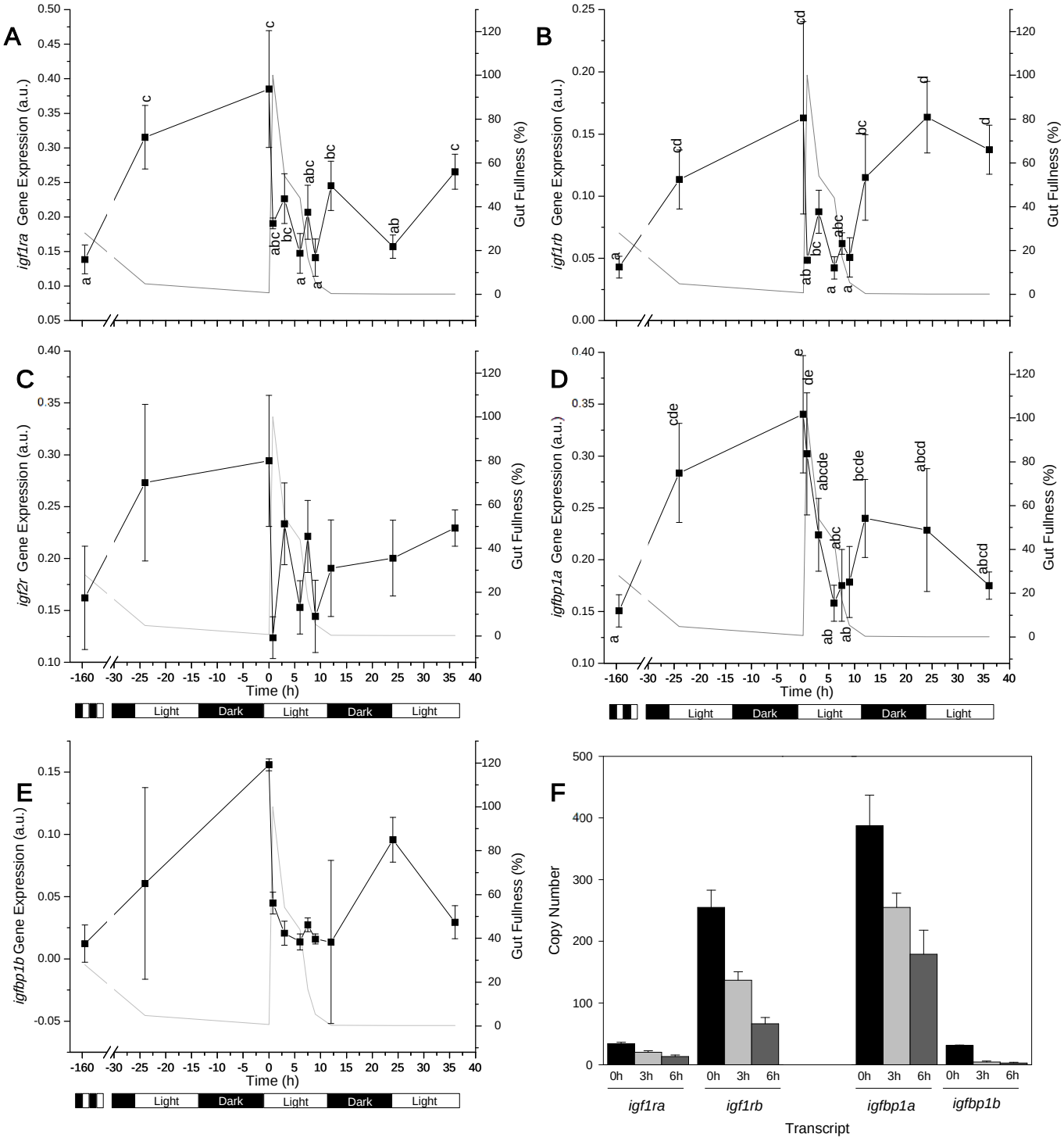

Figure 2.5 – Transcriptional responses of insulin-like growth factor receptor and binding protein genes in the fast myotomal muscle of male zebrafish during the course of the single meal experiment determined by qPCR. IGF receptors (A, B, C), *igfbp1a/b* (D, E), copy number of *igf1ra*, *igf1rb*, *igfbp1a* and *igfbp1b* (F) and transcription level of IGFBPs-2 – 6 (G-M). The grey line represents the average gut fullness illustrated in Figure 2.2. Values represent mean ± s.em., n = 13 fish per sample. Different letters signify statistically different means at 0.05 significance level (see text for details).

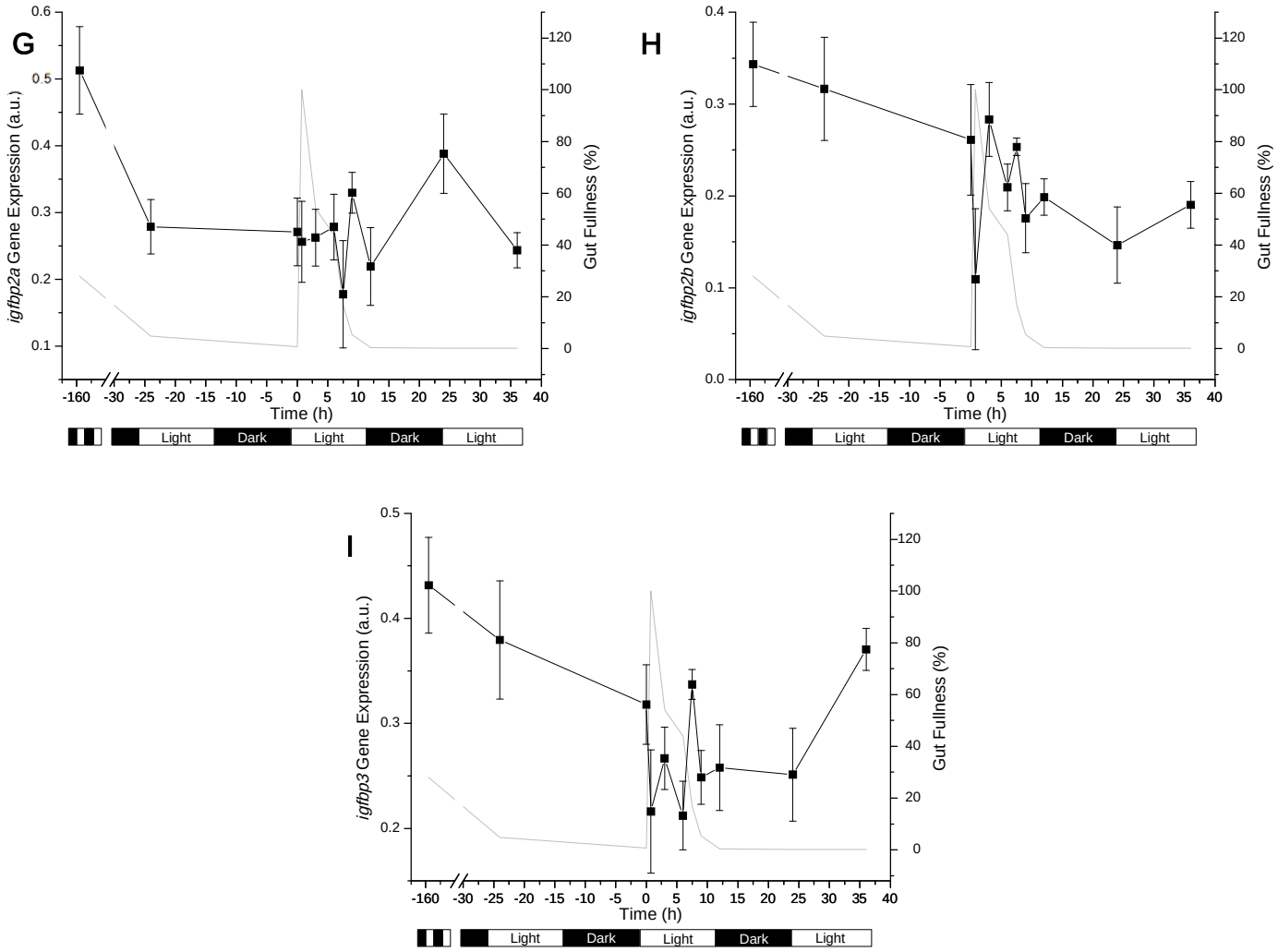

Figure 2.5 (continuation)

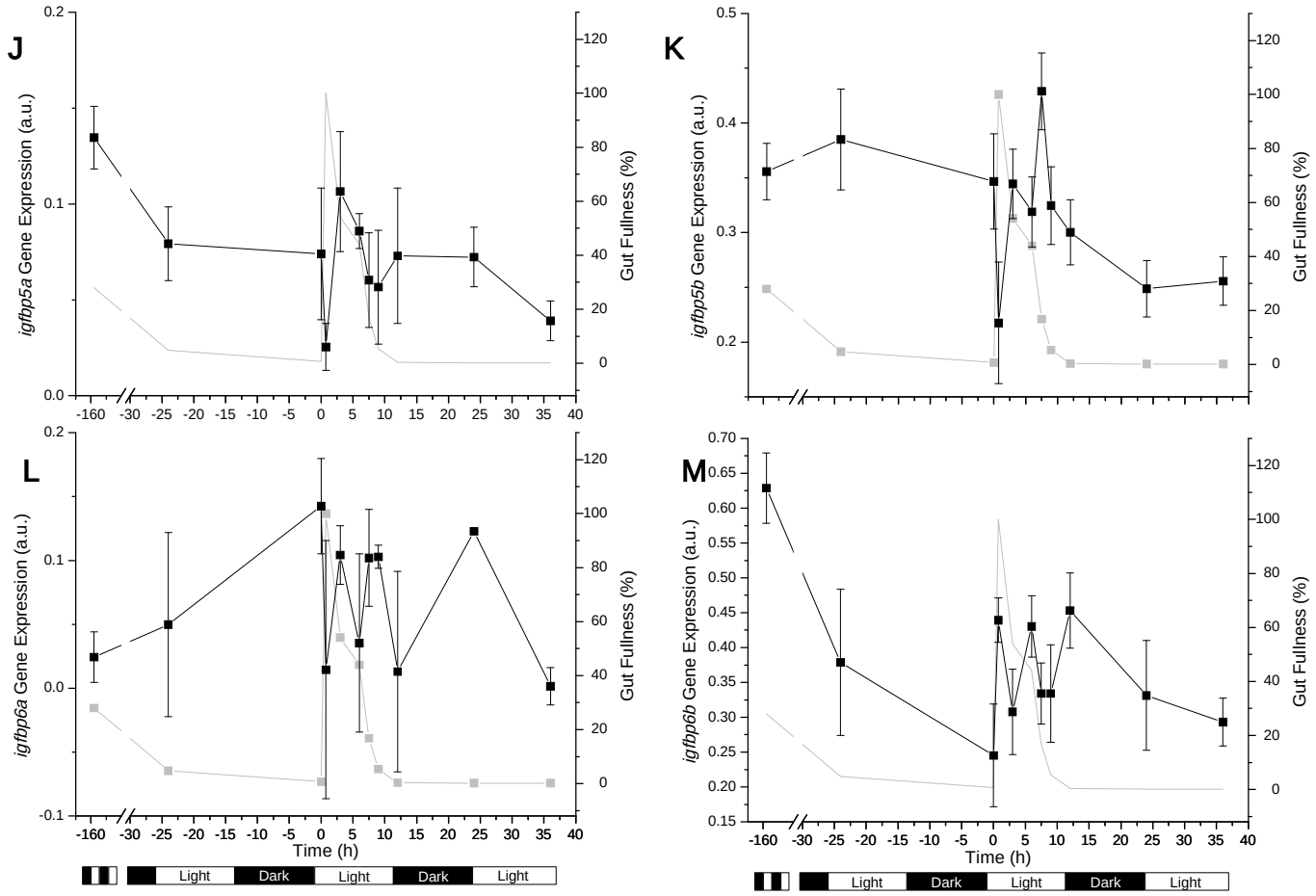

Figure 2.5 (continuation)

2.4.7. Genome-wide changes in gene expression with feeding

In order to identify some nutritionally-responsive candidate genes for further investigation whole genome microarray analysis was performed. Total RNA from maximally fasted fish (0h) was hybridised with RNA from fish sampled 3h and 6h after the initiation of feeding. Genes were considered differentially regulated if they showed a higher than 2.0-fold change in expression, a B value higher than zero, and were significant at the P-value < 0.05 level following correction for multiple comparisons. The hybridisations of fasting and 6h fed samples produced a relatively short gene list and no genes that were not represented in the hybridisation of fasting and 3h fed samples and are not considered further. Fast skeletal muscle from zebrafish fasted for 7d had 56 up-regulated genes (Table 2.3) and 91 down-regulated genes (Table 2.4) compared to fish fed to satiation over 3h. 45 of the up-regulated genes in fasting and 79 of the up-regulated genes with feeding had associated gene ontology (GO) terms. For the genes up-regulated with fasting GO term analysis revealed a significant enrichment of terms associated with catabolic processes, ubiquitin ligase activity and positive regulation of endothelial cell differentiation, including the genes *btg1* and *btg2* which have antiproliferative properties (Winkler, 2010) (full listing in Table 2.5). Analysis of the genes up-regulated with feeding showed enrichment for GO terms such as unfolded protein binding, protein folding, endoplasmic reticulum lumen, protein maturation, chaperone binding, sarcomerogenesis, myosin filament assembly, collagen biosynthesis and regulation of the JAK-STAT cascade (full listing in Table 2.4). The gene showing the largest fold change of 32.2 with fasting (Table 2.3) coded for a novel protein with ~23% identity to the mammalian orthologue of harbinger transposase derived 1 (*harbi1*) which is thought to have nuclease activity (Kapitonov and Jurka, 2004). The list of genes up-regulated with feeding included many chaperone genes (unc45b, *ptges3, serpinh1*), heat shock protein (*hsp90a.1, hsp90a.2, hspd1, hspa5*) and heat shock protein-associated genes (*ahsa1*, *calrl and stip1*) (Table 2.4). Feeding was also associated with enrichment of the interleukin-20 receptor binding GO term (Table 2.5) and increased *il34* expression (Table 2.4).

Table 2.3 – Filtered gene list from the microarray experiment showing transcripts up-regulated with fasting in the zebrafish single meal experiment.

	Gene symbol	Gene description	Fold change (Mean ± SE, n=6)	Adjusted P-value
1	*Novel gene*	Novel gene	32.2 ± 10.4	0.048
2	*zgc:86757*	murf1 (muscle-specific RING finger protein 1)	25.4 ± 7.6	0.022
3	*fbxo32*	(MAFbx) F-box protein 32	17.9 ± 5.7	0.040
4	*pdk2*	Pyruvate dehydrogenase kinase 2	16.9 ± 3.8	0.022
5	*zp2*	Zona pellucida glycoprotein 2.3	13.8 ± 5.6	0.049
6	*h1m*	Linker histone H1M	12.8 ± 4.2	0.049
7	*si:ch211-284a13.1*	Novel protein (Si:ch211-284a13.1)	12.5 ± 2.6	0.022
8	*klf11b*	Kruppel-like factor 11b	11.0 ± 0.7	0.020
9	*zgc:162945*	Hypothetical protein LOC560936	9.8 ± 2.9	0.032
10	*bbc3*	BCL2 binding component 3	9.4 ± 3.1	0.038
11	*si:ch211-63o20.5*	Hypothetical protein LOC566703	9.3 ± 1.6	0.022
12	*ypel3*	Protein yippee-like 3	8.7 ± 2.8	0.037
13	*cited2*	Cbp/p300-interacting transactivator, with Glu/Asp-rich carboxy-terminal domain, 2	8.6 ± 1.8	0.022
14	*nr1d1*	Nuclear receptor subfamily 1, group D, member 1	8.5 ± 1.7	0.023
15	*ccng2*	Cyclin G2	7.6 ± 1.2	0.022
16	*gbp*	Glycogen synthase kinase binding protein	7.6 ± 1.6	0.049
17	*gpr137ba*	G protein-coupled receptor 137ba	7.2 ± 1.8	0.048
18	*si:dkey-42i9.4*	B-cell translocation gene 1-like	6.9 ± 1.1	0.025
19	*zgc:100920*	Hypothetical protein LOC445241	6.6 ± 2.2	0.049
20	*LOC566363*	Mucin 3-like	6.3 ± 2.1	0.049
21	*zgc:55582*	Myomegalin	5.9 ± 1.0	0.028
22	*slc16a9a*	Solute carrier family 16 (monocarboxylic acid transporters), member 9a	5.6 ± 1.2	0.032
23	*rab40b*	RAB40B, member RAS oncogene family	5.4 ± 0.6	0.025
24	*TCEANC*	Transcription elongation factor A (SII) N-terminal and central domain containing	5.4 ± 1.0	0.040
25	*zgc:77714*	Carboxy-terminal domain RNA polymerase II polypeptide A small phosphatase 2	5.3 ± 0.9	0.040
26	*stk11ip*	Serine/threonine kinase 11 interacting protein	5.3 ± 0.6	0.025
27	*btg2*	B-cell translocation gene 2	5.2 ± 1.2	0.049
28	*LOC794083*	Pyruvate dehydrogenase kinase 2-like	5.2 ± 1.1	0.040
29	*vgll2b*	Vestigial like 2b	5.2 ± 1.4	0.047

Table 2.3 (continuation)

	Gene symbol	Gene description	Fold change (Mean ± SE, n=6)	Adjusted P-value
30	*hsf2*	Heat shock factor 2	5.1 ± 0.6	0.023
31	*znf653*	Zinc finger protein 653	5.1 ± 0.8	0.025
32	heca	Headcase homolog	4.8 ± 0.8	0.036
33	per1b	Period homolog 1b	4.5 ± 0.8	0.048
34	zgc:92851	Jun dimerization protein 2	4.4 ± 1.1	0.049
35	pcmtd2	Protein-L-isoaspartate (D-aspartate) O-methyltransferase domain containing 2	4.3 ± 0.6	0.036
36	LOC559993	Similar to THAP domain containing, apoptosis associated protein 1	4.3 ± 0.7	0.042
37	brms1l	Breast cancer metastasis-suppressor 1-like protein	4.0 ± 0.7	0.048
38	usf1	Upstream transcription factor 1	3.9 ± 0.7	0.042
39	ubr1	Ubiquitin protein ligase E3 component n-recognin 1	3.8 ± 0.5	0.040
40	vsg1	Vessel-specific 1	3.7 ± 0.7	0.048
41	si:dkey-86e18.1	Hypothetical protein LOC557342	3.6 ± 0.4	0.040
42	slc25a1	Solute carrier family 25 (mitochondrial carrier; citrate transporter), member 1	3.6 ± 0.6	0.048
43	si:ch73-138e16.8	Hypothetical protein LOC100006084	3.4 ± 0.5	0.049
44	n4bp2	NEDD4 binding protein 2	3.4 ± 0.4	0.040
45	fbxo25	F-box only protein 25	3.4 ± 0.4	0.042
46	ccdc149	Coiled-coil domain containing 149	3.2 ± 0.4	0.050
47	npl	N-acetylneuraminate lyase (NALase)(EC 4.1.3.3)(N-acetylneuraminic acid aldolase)(N-acetylneuraminate pyruvate-lyase)(Sialic acid lyase)(Sialate lyase)(Sialate-pyruvate lyase)(Sialic acid aldolase)	3.2 ± 0.4	0.050
48	zgc:110708	Hypothetical protein LOC553793	3.1 ± 0.4	0.048
49	mtus1a	Mitochondrial tumor suppressor 1 homolog A	3.1 ± 0.4	0.050
50	zgc:171727	Hypothetical protein LOC799470	3.1 ± 0.2	0.040
51	id2b	Inhibitor of DNA binding 2, dominant negative helix-loop-helix protein, b	3.0 ± 0.3	0.048
52	nbr1	Neighbor of BRCA1 gene 1	3.0 ± 0.4	0.048
53	gmcl1	Germ cell-less homolog 1 (Drosophila)	3.0 ± 0.3	0.049
54	LOC799552	Hypothetical protein	2.9 ± 0.2	0.045
55	zgc:163003	Inactive Ufm1-specific protease 1	2.9 ± 0.2	0.047
56	spns1	Protein spinster homolog 1 (Spinster-like protein)	2.8 ± 0.2	0.047

Table 2.4 – Filtered gene list from the microarray experiment showing transcripts up-regulated with feeding in the zebrafish single meal experiment.

	Gene symbol	Gene description	Fold change (Mean ± SE, n=6)	Adjusted P-value
1	*odc1*	Ornithine decarboxylase 1	11.5 ± 2.8	0.022
2	*pptc7*	Protein phosphatase PTC7 homolog	10.5 ± 1.8	0.022
3	*ctsll*	Cathepsin L, like	9.9 ± 3.2	0.027
4	*ddx5*	DEAD (Asp-Glu-Ala-Asp) box polypeptide 5	9.8 ± 3.4	0.038
5	*pdip5*	Protein disulfide isomerase-related protein	9.5 ± 1.9	0.025
6	*si:ch211-76m11.7*	si:ch211-76m11.7	9.0 ± 2.5	0.038
7	*mylk4*	Myosin light chain kinase family, member 4	8.9 ± 3.1	0.040
8	*mfsd2b*	Major facilitator superfamily domain-containing protein 2-B	8.0 ± 1.1	0.022
9	*zgc:110154*	Eukaryotic translation initiation factor 4E-like	7.9 ± 2.0	0.038
10	*fkbp5*	FK506 binding protein 5	7.7 ± 2.2	0.040
11	*rcn3*	Reticulocalbin 3, EF-hand calcium binding domain	7.5 ± 2.3	0.048
12	*dyrk2*	Dual-specificity tyrosine-(Y)-phosphorylation regulated kinase 2	7.5 ± 2.1	0.028
13	*calrl*	Calreticulin like	7.2 ± 2.2	0.049
14	*ahsa1*	AHA1, activator of heat shock protein ATPase homolog 1	7.0 ± 1.2	0.025
15	*eif4a1a*	Eukaryotic translation initiation factor 4A, isoform 1A	6.8 ± 1.3	0.025
16	*klf13l*	Kruppel-like factor 13 like	6.8 ± 1.9	0.049
17	*LOC792864*	Similar to Dual specificity protein phosphatase 13 (Testis- and skeletal-muscle-specific DSP) (Dual specificity phosphatase SKRP4)	6.6 ± 1.5	0.049
18	*slc25a25*	Calcium-binding mitochondrial carrier protein SCaMC-2-A (Small calcium-binding mitochondrial carrier protein 2-A)(Solute carrier family 25 member 25-A)	6.5 ± 1.5	0.049
19	*LOC100332265*	Adaptor-related protein complex 1 associated regulatory protein-like	6.3 ± 1.0	0.025
20	*mid1ip1*	MID1 interacting protein 1	5.9 ± 0.7	0.025
21	*zgc:73230*	Hypothetical protein LOC406311	5.8 ± 0.9	0.032
22	*hsp90a.1*	Heat shock protein HSP 90-alpha 1	5.7 ± 0.6	0.022
23	*ctrl*	Chymotrypsin-like	5.7 ± 1.3	0.045
24	*hsp90a.2*	Heat shock protein 90-alpha 2	5.6 ± 0.7	0.025
25	*foxo1a*	Forkhead box O1 a	5.4 ± 0.7	0.025
26	*zgc:110801*	Protein phosphatase 5, catalytic subunit	5.3 ± 1.6	0.049
27	*zgc:158222*	Adenosylhomocysteinase	5.3 ± 1.0	0.040
28	*syncripl*	Synaptotagmin binding, cytoplasmic RNA interacting protein, like	5.1 ± 1.0	0.045
29	*dnaja4*	DnaJ (Hsp40) homolog, subfamily A, member 4	5.1 ± 0.6	0.025

Table 2.4 (continuation)

	Gene symbol	Gene description	Fold change (Mean ± SE, n=6)	Adjusted P-value
30	*fam69b*	Family with sequence similarity 69, member B	5.0 ± 0.9	0.048
31	*s1pr2*	Sphingosine 1-phosphate receptor 2 (S1P receptor 2)(S1P2)(Sphingosine 1-phosphate receptor Edg-5)(S1P receptor Edg-5)	5.0 ± 1.1	0.048
32	*pias4*	Protein inhibitor of activated STAT, 4	5.0 ± 0.9	0.042
33	*lmnb1*	Lamin B1	5.0 ± 1.2	0.049
34	*ehmt1b*	Euchromatic histone-lysine N-methyltransferase 1b Fragment	4.9 ± 0.3	0.022
35	*smyd1b*	SET and MYND domain containing 1b	4.8 ± 0.8	0.032
36	*LOC100006303*	Novel protein similar to glutaminase (Gls)	4.8 ± 1.2	0.048
37	*hspd1*	Heat shock 60 kD protein 1	4.7 ± 1.0	0.042
38	*slmo2*	Slowmo homolog 2	4.6 ± 1.0	0.048
39	*abcf2*	ATP-binding cassette, sub-family F	4.6 ± 0.9	0.042
40	*zgc:92429*	Hypothetical protein LOC445063	4.6 ± 0.7	0.040
41	*kctd20*	Potassium channel tetramerisation domain containing 20	4.5 ± 0.5	0.026
42	*ppig*	Peptidylprolyl isomerase G	4.5 ± 0.9	0.049
43	*g3bp1*	Ras-GTPase-activating protein SH3-domain-binding protein	4.4 ± 0.9	0.042
44	*slc4a2a*	Solute carrier family 4, anion exchanger, member 2a	4.4 ± 0.4	0.025
45	*LOC100150539*	Novel protein similar to vertbrate adenylate cyclase 9 (ADCY9) Fragment	4.3 ± 0.9	0.050
46	*sulf1*	Sulfatase 1	4.3 ± 0.9	0.048
47	*sae1*	SUMO-activating enzyme subunit 1 (Ubiquitin-like 1-activating enzyme E1A)	4.3 ± 0.5	0.028
48	*zgc:85702*	Hypothetical protein LOC321718	4.2 ± 0.7	0.042
49	*abcb10*	ATP-binding cassette, sub-family B (MDR/TAP), member 10	4.2 ± 0.9	0.048
50	*ranbp1*	RAN binding protein 1	4.1 ± 0.4	0.028
51	*dazap1*	Dazap1 protein Fragment	4.0 ± 0.7	0.049
52	*il34*	Interleukin 34	4.0 ± 0.6	0.040
53	*frzb*	Frizzled-related protein	3.8 ± 0.4	0.037
54	*zgc:113183*	SWI/SNF-related, matrix-associated actin-dependent regulator of chromatin, subfamily a, containing DEAD/H box 1	3.8 ± 0.5	0.041
55	*smarca5*	SWI/SNF related, matrix associated, actin dependent regulator of chromatin, subfamily a, member 5	3.8 ± 0.7	0.049
56	*agr2*	Anterior gradient 2 homolog	3.7 ± 0.5	0.047
57	*zgc:136374*	2'-phosphodiesterase	3.7 ± 0.5	0.040

Table 2.4 (continuation)

	Gene symbol	Gene description	Fold change (Mean ± SE, n=6)	Adjusted P-value
58	*stip1*	Stress-induced-phosphoprotein 1 (Hsp70/Hsp90-organizing protein)	3.7 ± 0.6	0.048
59	*si:ch211-132p20.4*	Sodium-coupled neutral amino acid transporter 2 (Amino acid transporter A2)(System A amino acid transporter 2)(System N amino acid transporter 2)(System A transporter 1)(Solute carrier family 38 member 2)	3.7 ± 0.4	0.038
60	*zgc:172028*	ADP-ribosylation factor 6-like	3.6 ± 0.6	0.048
61	*zgc:153972*	Transmembrane and coiled-coil domain family 1	3.5 ± 0.6	0.049
62	*zgc:153290*	Coiled-coil domain containing 51	3.5 ± 0.5	0.045
63	*zgc:114204*	Golgi transport 1 homolog B	3.5 ± 0.2	0.032
64	*zgc:86751*	Hypothetical protein LOC415227	3.4 ± 0.5	0.048
65	*ppp4cb*	Serine/threonine-protein phosphatase 4 catalytic subunit B (PP4C-B)(EC 3.1.3.16)	3.3 ± 0.5	0.048
66	*LOC558153*	Adaptor-related protein complex 2, alpha 1 subunit-like	3.3 ± 0.4	0.048
67	*cmpk*	UMP-CMP kinase (EC 2.7.4.14)(Cytidylate kinase)(Deoxycytidylate kinase)(Cytidine monophosphate kinase)(Uridine monophosphate kinase)(Uridine monophosphate/cytidine monophosphate kinase)(UMP/CMP kinase)(UMP/CMPK)	3.3 ± 0.5	0.049
68	*si:ch211-253h3.1*	si:ch211-253h3.1	3.3 ± 0.5	0.049
69	*hspa5*	Heat shock 70kDa protein 5	3.3 ± 0.3	0.045
70	*slc38a4*	Solute carrier family 38, member 4	3.3 ± 0.2	0.039
71	*ncl1*	Nicalin-1 Precursor (Nicastrin-like protein 1)	3.2 ± 0.2	0.039
72	*ssrp1a*	Structure specific recognition protein 1a	3.2 ± 0.4	0.044
73	*zgc:153327*	Arginine-rich, mutated in early stage tumors	3.2 ± 0.3	0.041
74	*lamb1*	Laminin, beta 1	3.2 ± 0.3	0.041
75	*zgc:77244*	Potassium channel tetramerisation domain containing 5	3.2 ± 0.5	0.050
76	*zgc:158393*	Hypothetical protein LOC564849	3.2 ± 0.4	0.048
77	*zgc:171630*	Serine (or cysteine) proteinase inhibitor, clade H, member 1	3.2 ± 0.4	0.047
78	*unc45b*	Unc-45 (C. elegans) related	3.1 ± 0.2	0.040
79	*zgc:153981*	Muscle-restricted dual specificity phosphatase	3.1 ± 0.2	0.041
80	*sf3b4*	Splicing factor 3b, subunit 4	3.1 ± 0.4	0.048
81	*thoc6*	THO complex 6 homolog (Drosophila)	3.0 ± 0.4	0.050
82	*pl10*	pl10	3.0 ± 0.3	0.047

Table 2.4 (continuation)

	Gene symbol	Gene description	Fold change (Mean ± SE, n=6)	Adjusted P-value
83	*tram1*	Translocating chain-associating membrane protein 1	3.0 ± 0.3	0.048
84	*zgc:56005*	Oxidative stress induced growth inhibitor 1	3.0 ± 0.3	0.049
85	*prelid1*	PRELI domain containing 1	3.0 ± 0.2	0.044
86	*per2*	Period homolog 2	3.0 ± 0.3	0.048
87	*si:ch211-59d15.5*	YLP motif containing 1	2.8 ± 0.1	0.042
88	*snrnp40*	Small nuclear ribonucleoprotein 40 (U5)	2.8 ± 0.1	0.042
89	*ehd1*	EH-domain containing 1	2.8 ± 0.3	0.048
90	*si:ch211-286m4.4*	Exportin-T (tRNA exportin)(Exportin(tRNA))	2.8 ± 0.2	0.049
91	*alg9*	Asparagine-linked glycosylation 9 protein	2.7 ± 0.3	0.050

Table 2.5 – Enrichment analysis of gene ontology terms for biological processes associated with genes differentially regulated in response to a single-satiating meal using the 44K Agilent zebrafish microarray V2. Only the most-specific terms are shown in the table.

GO Identifier	GO Term	Number of genes differentially expressed	FDR*
	Enriched with fasting		
GO:0043632	modification-dependent macromolecule catabolic process	8	0.031
GO:0045603	positive regulation of endothelial cell differentiation	2	0.052
	Enriched with feeding		
GO:0042026	protein refolding	3	0.004
GO:0051604	protein maturation	3	0.035
GO:0030241	skeletal muscle thick filament assembly	2	0.035
GO:0034619	cellular chaperone-mediated protein complex assembly	2	0.035
GO:0042517	positive regulation of tyrosine phosphorylation of Stat3 protein	2	0.035
GO:0048769	sarcomerogenesis	2	0.035
GO:0046425	regulation of JAK-STAT cascade	3	0.042
GO:0045618	positive regulation of keratinocyte differentiation	2	0.045
GO:0045606	positive regulation of epidermal cell differentiation	2	0.054
GO:0070096	mitochondrial outer membrane translocase complex assembly	2	0.068

* FDR – false discovery rate.

2.4.8. Expression and clustering of candidate nutritionally-regulated genes

A selection of candidate nutritionally-regulated genes comprising 8 genes up-regulated with fasting (*fbxo32, trim63, klf11b, nr1d1, cited2, bbc3, znf653, hsf2*) and 6 genes up-regulated with feeding (*odc1, fkbp5, sae1, foxo1a, hsp90a.1, hsp90a.2*) plus some contractile protein genes (*mylz2 and tnni2a.4*) was further investigated using qPCR. The log fold-change in expression of all the genes assayed by qPCR showed a good correlation with the microarray experiment ($R = 0.79$; $P<0.001$; $n = 76$) (Figure 2.6). Genes from the IGF pathway and those selected from the microarray experiment formed five major clusters (Figure 2.7). Cluster I contained genes up-regulated with feeding, with low levels of expression during prolonged fasting (-24 and 0h) and intermediate levels of expression from 9 to 36h (*igf1a, hsp90a.1, odc1, foxo1a, igfbp6a, igf2b, sae1 and fkbp5*). Cluster II comprised genes that were down-regulated at -159h and from 0.75 to 9h, with upregulation during prolonged (-24 and 0h) and early fasting (12-36h) *(igf1ra, igf2r, igf1rb, fbxo32, trim63, klf11b, bb3 and znf653*). Cluster III contained genes that were only up-regulated with prolonged fasting (144 and 168h) and just after the beginning of feeding (45 min), with low expression at other time points (*tnni2a.4, hsp90a.2, nr1d1, igfbp1a, hsf2 and igfbp1b*). Cluster IV comprised genes with high expression during prolonged fasting, low expression whilst the intestine was full (0.75 to 6h), and intermediate levels of expression from 7.5 to 36h (*igf2a, igfbp3 and cited2*). Cluster V comprised genes with high expression with prolonged fasting, but with intermediate level of expression during feeding and early fasting (*mylz2, igfbp5b, igfbp2b, igfbp5a, igfbp2a, igfbp6b*). Genes pairs that showed strong significant correlations ($R>0.7$, $p<0.05$, $n=126$) were considered candidates for co-regulation of expression. Eight strong positive correlations were found and included *hsf2* versus *nr1d1* ($R=0.83$; $P<0.001$) and *fbxo32* ($R= 0.78$; $P<0.001$); *bbc3* versus *znf653* ($R=0.76$; $P<0.001$) and *klf11b* ($R= 0.75$; $P<0.001$); *fbxo32* versus *trim63* ($R= 0.73$; $P<0.001$); and *bbc3* versus *cited2* ($R= 0.73$; $P<0.001$) and *fbxo32* ($R= 0.72$; $P<0.001$). The only strong negative correlation found was between *odc1* and *bbc3* (Cluster II).

All 8 of the candidate genes up-regulated with fasting in the microarray experiments were validated by qPCR. The expression of the muscle-specific ubiquitin ligases, *MAFbx/Atrogin-1* (annotated with the synonym *fbxo32* in the zebrafish genome assembly) and *MURF1* (annotated as t*rim63*) was highly sensitive to nutritional status. mRNA transcripts for *fbxo32* and *trim63* increased 13.3 and 2.7-fold, respectively,

between 9h and 144h of fasting and were down-regulated by 55% (*fbxo32*) and 77% (*trim63*) in the 45min sample after feeding, with lowest levels observed after 6h (Figure 2.8A, B). Expression of both genes started to increase soon after food was cleared from the intestine and mRNA levels were at 168h fasting levels by 36h after the meal (Figure 2.8A, B).

Four genes (*bbc3*, *cited2*, *znf653* and *klf11b*) had expression patterns that were inversely correlated with gut fullness. Transcript abundances were lowest 45min to 3h after feeding and rapidly increased as the gut emptied (Figure 2.9A-D). *nr1d1* and *hsf2* mRNA levels increased ~130 and ~21-fold between 9h and 144h of fasting, respectively, and were strongly down-regulated with feeding and showed a transient increase in levels 15h after the intestine was empty (Figure 2.9E, F). Three of the selected genes up-regulated with feeding in the microarray experiment showed expression patterns related to gut fullness. *fkbp5* and *odc1* showed a peak of expression coincident with the presence of food in the intestine corresponding to a 5.6 and 17.2-fold increase in transcript abundance relative to maximal fasting values, respectively (Figure 2.10A, B). *sae1* showed a ~6.5-fold increase in expression 6 to 9h after the start of the meal and a steady decline to levels not significantly different from fasting values by 36h (Figure 2.10C).

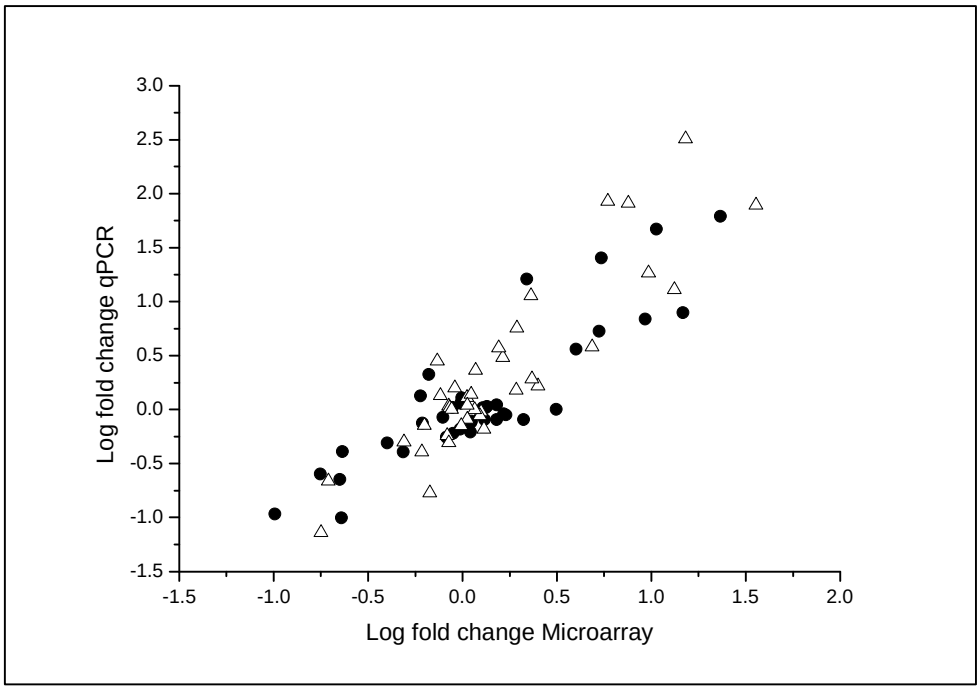

Figure 2.6 – Correlation between log fold changes in mRNA levels of 38 genes from qPCR and microarray experiments from two hybridizations: 0 with 3h (•) and 0 with 6h samples (△) (Spearman's correlation test, n=76, r^2=0.79, p<0.001).

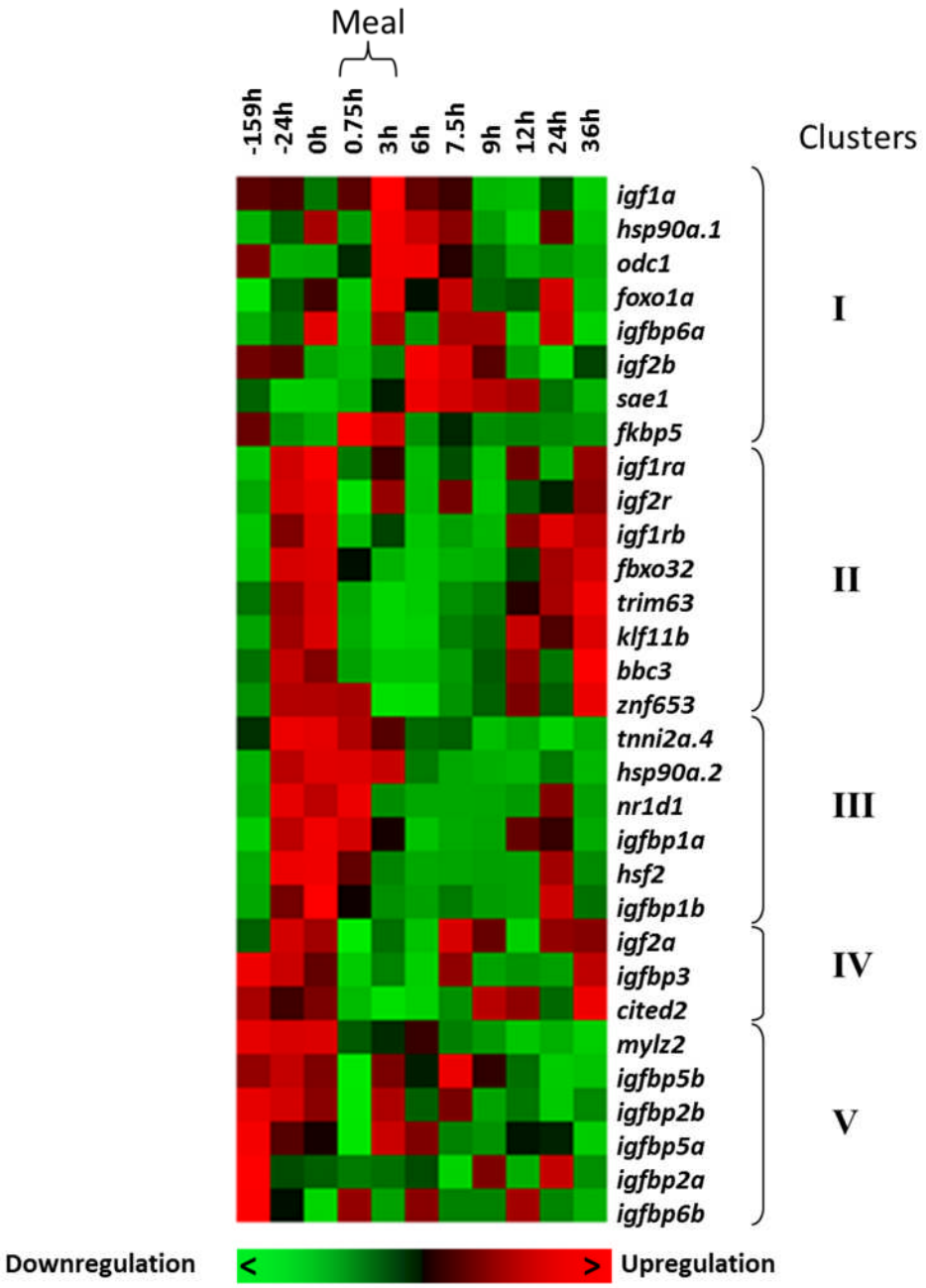

Figure 2.7 – Hierarchical clustering and heat map of Insulin-like growth factor (IGF) system gene transcripts and candidate nutritionally regulated genes identified from microarray experiments over the time course of the single meal experiment. The roman numbers indicate clusters discussed in the text. Rows (mRNA transcripts) in the heatmap are standardised to have mean of zero and standard deviation of one (i.e. standard score normalisation). Red and green shading respectively indicates the highest and lowest expression levels as indicated in the scale bar at the bottom of the figure. Each block represents the average standard-score normalisation for the 13 fish sampled at each time point in the experiment.

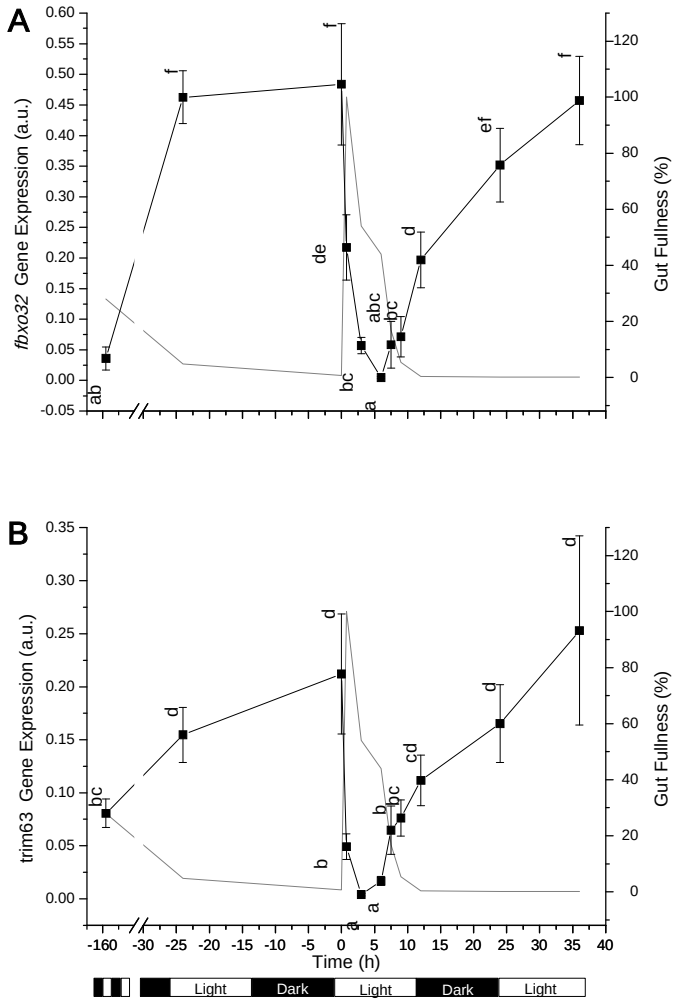

Figure 2.8 – Expression profiles of ubiquitin ligase genes in male zebrafish identified from microarray experiments over the time course of the single meal experiment as determined by qPCR (solid squares): Genes up-regulated during fasting (A) Atrogin 1-MAFbx (*fbxo32*) and (B) Muscle-specific RING finger protein 1 - *MURF1* (*trim63*). The grey line represents the average gut fullness illustrated in Figure 2.2. Values represent mean ± s.e.m., n = 13 fish per sample. Different letters signify statistically different means at 0.05 significance level.

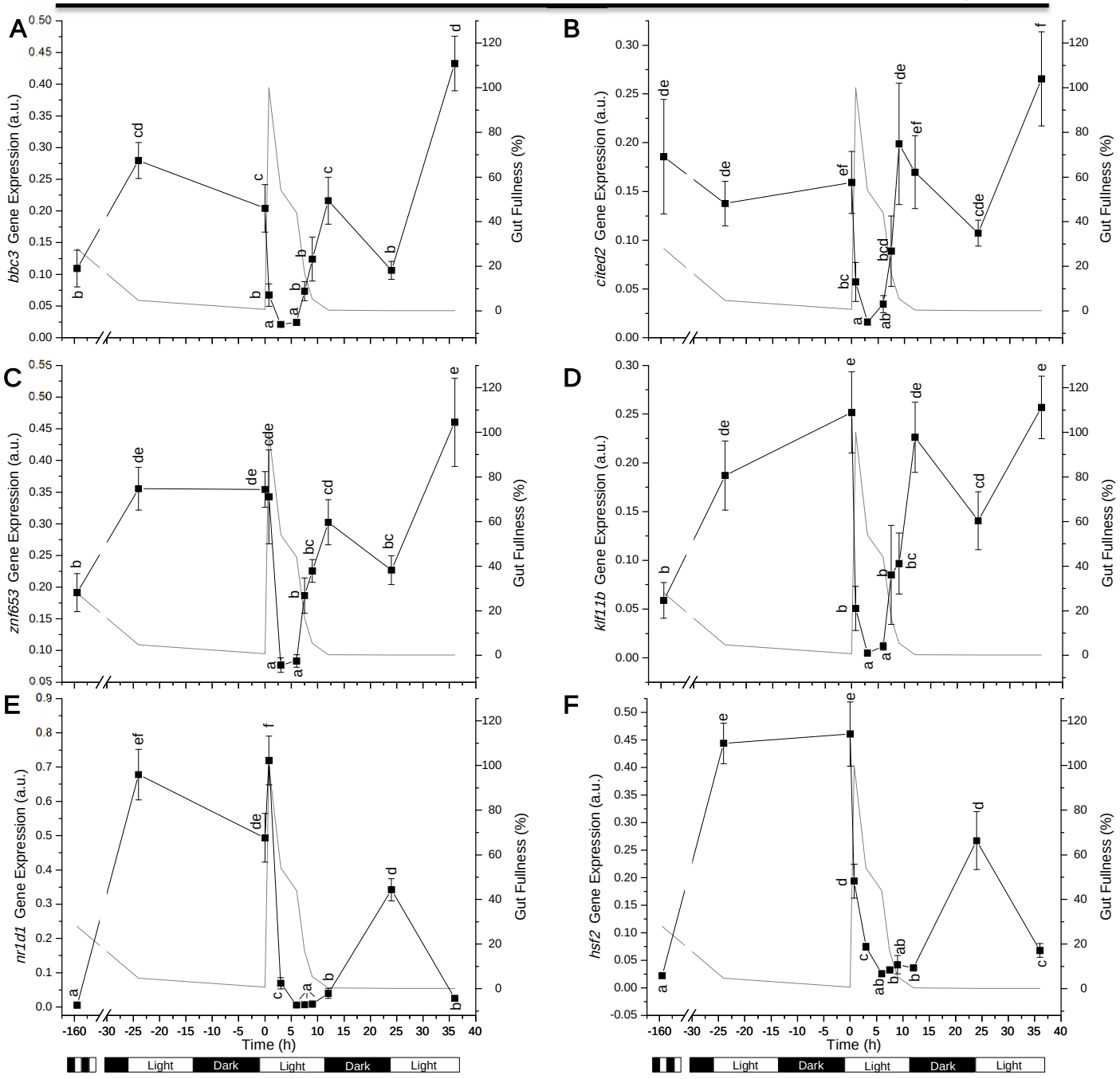

Figure 2.9 – Expression profiles of candidate nutritionally-regulated genes in male zebrafish identified from microarray experiments over the time course of the single meal experiment as determined by qPCR (solid squares): genes up-regulated during fasting: (A) BCL2 binding component 3 (*bbc3*), (B) Cbp/p300-interacting transactivator, with Glu/Asp-rich carboxy-terminal domain, 2 (*cited2*), (C) zinc finger protein 653 (znf653), (D) Kruppel-like factor 11b (*klf11b*), (E) nuclear receptor subfamily 1, group d, member 1 (*nrld1*), and (F) heat shock factor 2 (*hsf2*). The grey line represents the average gut fullness illustrated in Figure 2.2. Values represent Mean ± s.e.m., n = 13 fish

per sample. Different letters signify statistically different means at 0.05 significance level.

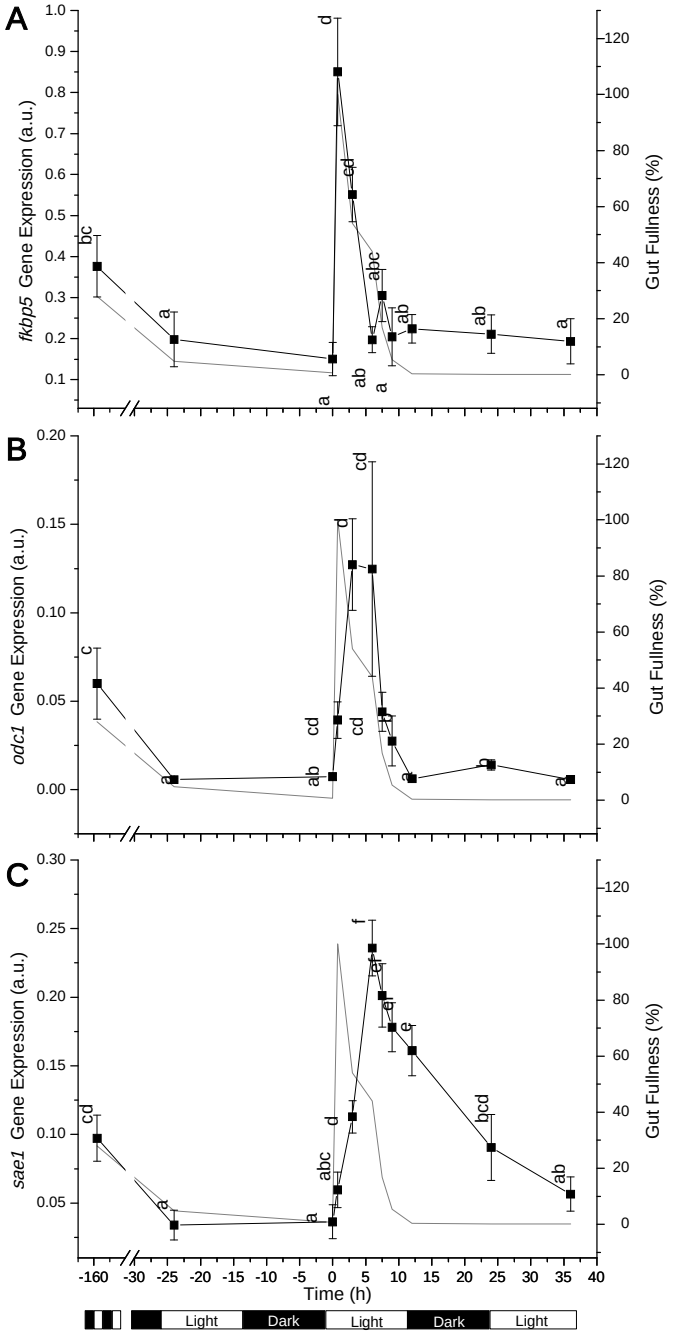

Figure 2.10 – Expression profiles of candidate nutritionally-regulated genes in male zebrafish identified from microarray experiments over the time course of the single meal experiment as determined by qPCR (solid squares): Genes up-regulated with feeding (A) FK506 binding protein 5 (*fkbp5*) (B) Ornithine decarboxylase 1 (*odc1*) and (C) SUMO-activating enzyme subunit 1 (*sae1*). The grey line represents the average gut

fullness illustrated in Figure 2.2. Values represent mean ± s.e.m., n = 13 fish per sample. Different letters signify statistically different means at 0.05 significance level.

2.5. Discussion

2.5.1. Transcriptional regulation of the IGF system

Transit of food through the gastrointestinal system and phosphorylation of the IGF-pathway signaling protein Akt provide a context for interpreting the transcriptional response to a single satiating meal in the absence of information on plasma hormone and amino acid levels in small tropical fishes. In a previous fasting-refeeding study on the rainbow trout, *Oncorhynchus mykiss*, maximum plasma insulin and amino acid levels were recorded 30min and 2.5h after feeding and were quickly followed by phosphorylation of several kinases indicating activation of the TOR signaling pathway (Seiliez et al., 2008). Amino acids and insulin also rapidly increase the level of circulating IGFI in brown trout (Banos et al., 1999). In the present experiments with zebrafish, 50% of the food ingested had been processed and eliminated within 3h after the start of feeding and the gut was empty after 9h (Figure 2.2). Akt showed a significant increase in phosphorylation within 45min, with peak levels at 3h of feeding and became dephosphorylated over a similar time course to the elimination of food from the gut (Figure 2.3). Changes in muscle mRNA levels also mostly took place with a time course of hours and were generally quicker than described in the literature for larger temperate fish species maintained at lower temperatures (Chauvigne et al., 2003; Bower et al., 2008).

The first aim of this chapter was to test the hypothesis that retained paralogues of IGF-system genes were differentially regulated following transition from a catabolic to an anabolic state. Fasting has been shown to result in an upregulation of muscle *igf1* receptors in a number of teleost species and is probably a response to a decrease in circulating IGF hormone levels (Chauvigne et al., 2003; Gabillard et al., 2006; Bower et al., 2008; Bower and Johnston, 2010a). In rainbow trout, prolonged fasting resulted in an upregulation of *igf1ra*, but not *igf1rb* (Chauvigne et al., 2003) whereas in zebrafish both IGFR paralogues were upregulated (Figure 2.5A, B). However, zebrafish *igf1rb* increased more rapidly following gut emptying than *igf1ra* reaching fasting levels >36h and <25h respectively (Figure 2.5A, B), indicating differential regulation of *igf1* receptor

paralogues. Functional characterisation studies of the igf2r in fish are scarce and its role in the response to nutrient levels is not yet clear. In Atlantic salmon, *igf2r* transcripts were significantly upregulated with prolonged fasting and downregulated after 7 days of refeeding (Bower et al., 2008). In this study there was no discernible pattern of transcriptional regulation of *igf2r* over the experiment. Muscle IGF hormone transcript levels showed distinct peaks within a few hours of feeding (Figure 2.4A, B). In the case of *igf1a* peak values were found within 3h of feeding and had declined to fasting levels before the gut was emptied (<5h) (Figure 2.4A). In contrast, *igf2b* transcripts reached a peak 6h after feeding and were not significantly different to fasting levels by 9h (Figure 2.4B). *Igf1b* transcripts were not detected in fast muscle whereas the *igf2a* paralogue was constitutively expressed and showed no consistent change in expression over the fasting-feeding-fasting cycle associated with a single meal. *In vitro* studies with Atlantic salmon (*Salmo salar*) myocytes have shown synergistic effects of insulin, igf1 and amino acids on muscle *igf1* transcript abundance, indicating multiple pathways leading to igf1 transcription (Bower and Johnston, 2010b). In mammals, the binding of IGFs to the igf1r induces its auto-phosphorylation resulting in the activation of several down-stream signal transduction cascades via adaptor molecules such as the insulin receptor substrate 1 (IRS-1) which has multiple tyrosine phosphorylation sites (Duan et al., 2010). Igf1 stimulates growth via effects on protein synthesis (Rommel et al., 2001), myoblast proliferation and differentiation acting through distinct signaling pathways (Ren et al., 2010). The effective concentration of IGFs in the muscle is regulated by 6 IGF-binding proteins (IGFBPs) which are degraded by specific proteases to release the hormone to target sites (Wood et al., 2005a). Evidence, largely from mammals, indicates that IGFBPs can inhibit and/or potentiate IGF actions depending on the cellular context and/or environmental conditions (Duan et al., 2010). In Atlantic salmon, the transition from maintenance to fast growth was associated with a constitutive upregulation of *igfbp4*, a transient increase in *igfbp5.1*, and a downregulation of *igfbp2.1* (Bower et al., 2008). The two retained zebrafish paralogues of *igfbp1* had similar expression in the single meal experiment with high transcript abundance during fasting, a marked reduction in mRNA levels within 45min of feeding and variable, but generally low level of expression over the following 36h (Figure 2.5D). Mammalian studies indicate that in addition to its role as a modulator of igf1 availability, igfbp1 has putative IGF-independent biological activities through

interaction with cell-surface integrins, with putative direct effects on the PI3K/AKT/mTOR pathway (Wheatcroft and Kearney, 2009). There was no evidence for the transcriptional regulation of *igfbp2a*, *b*, *igfbp3*, *igfbp5a, b, igfbp6a* and *b* paralogues with feeding in the present experiments. Although experimental context may explain some of these differences in IGFBP expression it is clear that there are lineage-specific differences in IGF binding protein function and regulation within the teleosts. For example, *igfbp4* is not represented in the current *Danio rerio* genome assembly (http://www.sanger.ac.uk/Projects/D_rerio/) and is probably absent from the zebrafish lineage. These results at least indicate that caution is needed in inferring similar functions of IGFBPs between teleost lineages and certainly between teleosts and mammals. Overall the conclusion is that following WGD some of the retained paralogues of IGF-system genes show differential transcriptional regulation with fasting and refeeding in skeletal muscle, but that complex patterns of regulation have evolved between and within lineages.

2.5.2. Genome-wide transcriptional regulation with catabolic to anabolic transition

Microarray experiments provided a snapshot of the fast muscle transcriptome during fasting and at the point IGF transcripts reached their maximum abundance following feeding. The screening criteria used to build lists of differentially regulated genes were apparently robust since all 14 genes tested were validated by qPCR and were well correlated (R=0.79, Figure 2.6). Fasting in zebrafish (Figure 2.8A, B) and Atlantic salmon (Bower et al., 2008; Bower and Johnston, 2010a) is associated with a large increase in the abundance of E3 ubiquitin ligases *MURF1* and *atrogin-1/MAFbx* transcripts. In mammals, the ubiquitin substrate recognition system has been implicated in specific degradation of myoD (Tintignac et al., 2005; Finn and Dice, 2006) and other promyogenic transcription factors (Finn and Dice, 2006). Two substrate recognition components of the ubiquitin ligase system, F-box only protein 25 (*fbxo25*) and RAB40B, member RAS oncogene family (*rab40b*), were also highly up-regulated with fasting in zebrafish fast muscle (Table 2.3). Two genes with putative roles in autophagy were found to be up-regulated during food deprivation [microtubule-associated protein 1 light chain 3 beta (*map1lc3b*) and neighbour of BRCA1 gene (*nbr1*)] (Table 2.3). It is known that myofibrillar proteins are degraded to provide a source of

amino acids for energy metabolism during prolonged fasting in teleosts (Johnston and Goldspink, 1973). However, the relative importance of the ubiquitin-proteasome degradation pathway, autophagy and other classes of proteases in mediating protein breakdown during normal protein turnover and short periods of fasting remains to be established. Cell cycle arrest and apoptosis also seems to be an important response in adapting to periods of limited energy supply in zebrafish as evidenced by the upregulation of antiproliferative protein gene transcripts [B-cell translocation gene 1 and 2 (*btg1* and *2*), THAP domain-containing protein 1 (*thap1*) and pro-apoptotic genes (*bbc3* and *klf11b*)] (Table 2.3).

Transition to an anabolic state 3h after the meal resulted in major changes in the muscle transcriptome. Feeding was associated with the upregulation of transcripts for chaperone proteins (*unc45b, ppig, pdip5, dnaja, stip1*) including various heat shock proteins and associated proteins (*hsp90a.1*, *hsp90a.2*, *hsdp1*, *hspa5*) (Table 2.4). Molecular chaperones are essential for both the folding and maintenance of newly translated proteins and the degradation of misfolded and destabilized proteins (Zhao and Houry, 2007). In zebrafish, the chaperones hsp90a and unc45 are coregulated and involved in the folding of the globular head of myosin during myofibrillargenesis, associating with the Z line once myofibrillar assembly is completed (Etard et al., 2008). The sequencing of subtractive cDNA libraries from fast skeletal muscle of Atlantic salmon fed either maintenance or satiating rations also revealed that expression of chaperone proteins indicative of unfolded protein response (UPR) pathways such as *dnaj4, hspa1b, hsp90a* and *chac1* was an early response to increased food intake and growth (Bower and Johnston, 2010a). Accumulation of unfolded proteins can occur when the amounts of newly synthesised proteins exceeds that of the protein folding capacity of the endoplasmic reticulum (Okada et al., 2002). Taken together these results indicate that an increase in protein chaperone gene expression and activation of UPR pathways is a general response of teleost skeletal muscle following the transition from a catabolic to anabolic state.

The largest increase in transcript abundance found with feeding was for the gene coding the enzyme ornithine decarboxylase 1 (*odc1*) (11.5-fold). Ornithine decarboxylase, a key metabolic enzyme of the polyamine biosynthesis pathway, also showed an increase in activity after feeding in fasted rat tissues (Moore and Swendseid, 1983). Polyamines have a number of biological functions including cell growth and

apoptosis and act in a concentration-dependant manner (Larqué et al., 2007). The anabolic state was associated with enrichment of GO terms for mitochondrial translocase activity, initiation of protein synthesis [e.g. eukaryotic translation initiation factor 4A isoform 1A (*eif4a1a*), dual-specificity tyrosine-(Y)-phosphorylation regulated kinase 2 (*dyrk2*)] and mRNA processing, maturation and export protein genes [e.g. DEAD (Asp-Glu-Ala-Asp) box polypeptide 5 (*DDX5*) and small nuclear ribonucleoprotein 40 (U5) (*snrnp40*)]. Furthermore, *pias4* and *sae1*, which are involved in the post-translational conjugation of SUMO (small ubiquitin-like modifier) to target proteins, were up-regulated with feeding. Sumoylation of proteins may affect their stability, localization and activity (Geiss-Friedlander and Melchior, 2007). In contrast to the ubiquitin-conjugated proteins, sumo-conjugated proteins are not targeted for degradation and indeed sumoylation may function as an antagonist pathway to the ubiquitin-proteasome pathway (Desterro et al., 1998; Hay, 2005).

Feeding was also associated with significant changes in the expression of genes that may function as epigenetic switches coding for proteins that modify chromatin structure and alter the expression of suites of other genes. For example, SET and MYND containing protein 1b (*smyd1b*) transcripts increased 4.8-fold between the fed and fasted states (Table 2.4). Smyd1 functions as a transcriptional repressor in mouse cardiac muscle (Gottlieb et al., 2002) and is required for normal skeletal muscle development in zebrafish (Tan et al., 2006). In the present study feeding also resulted in a 4.9-fold increase in transcript abundance for the euchromatic histone-lysine N-methyltransferase 1b fragment gene (*ehmt1b*). The human orthologue of ehmt1b was found to be part of the E2F6 complex and is probably involved in the silencing of MYC- and E2F-responsive genes (Ogawa et al., 2002), and is thought to play a role in G0/G1 cell-cycle transition.

The recruitment and hypertrophy of fast myotomal muscles in zebrafish was shown to be typical of teleosts (Johnston et al., 2009). The present study also demonstrates the utility of the zebrafish for mechanistic studies on the regulation of growth signalling pathways in teleost muscle providing the advantages of a sequenced genome, commercially available molecular resources and low husbandry costs due to the small body size. However, caution should be applied in extrapolating all results from model to aquaculture fish species in the light of evidence for lineage-specific patterns of paralogue retention (Macqueen and Johnston, 2008a, 2008b) and IGFBP gene

expression (this chapter). The single meal paradigm also provides an interesting alternative to the use of continuous feeding regimes to investigate transcriptional regulation during the transition from a catabolic to an anabolic state.

3. Circadian expression of clock and putative clock-controlled genes in skeletal muscle of the zebrafish

3.1. Summary

To identify circadian patterns of gene expression in skeletal muscle, adult male zebrafish were acclimated for two weeks to a 12:12h light:dark photoperiod and then exposed to continuous darkness for 86h with *ad libitum* feeding. The increase in gut food content associated with the subjective light period (SLP) was much diminished by the third cycle enabling feeding and circadian rhythms to be distinguished. Expression of zebrafish paralogues of mammalian positive regulators of the circadian mechanism (*bmal1*, *clock1* and *rora*) followed a rhythmic pattern with a ~24h periodicity. Peak expression of *rora* paralogues occurred at the beginning of the SLP [Zeitgeber time (ZT)07 and ZT02 for *roraa* and *rorab*] whereas the highest expression of *bmal1* and *clock* paralogues occurred 12h later (ZT13-15 and ZT16 for *bmal* and *clock* paralogues). Expression of the negative oscillators *cry1a, per1a/1b, per2, per3, nr1d2a/2b,* and *nr1d1* also followed a circadian pattern with peak expression at ZT00-02. Expression of the two paralogues of *cry2* occurred in phase with *clock1*. Duplicated genes had a high correlation of expression except for paralogues of *clock1*, *nr1d2* and *per1*, with *cry1b* showing no circadian pattern. The highest expression difference was 9.2-fold for the positive regulator *bmal1b* and 51.7-fold for the negative oscillator *per1a*. Out of 32 candidate clock-controlled genes, only *myf6, igfbp3, igfbp5b and hsf2* showed circadian expression patterns. *Igfbp3*, *igfbp5b* and *myf6* were expressed in phase with *clock1* and had an average of 2-fold change in expression from peak to trough whereas *hsf2* transcripts were expressed in phase with *cry1a* and had a 7.2 fold-change in expression. The changes in expression of clock and clock-controlled genes observed during continuous darkness were also observed at similar ZTs in fish exposed to a normal photoperiod in a separate control experiment. The role of circadian clocks in regulating muscle maintenance and growth are discussed.

3.2. Introduction

Teleost fish show pronounced circadian rhythms of foraging behaviour and locomotor activity that are driven by central oscillators in the brain, synchronised by light cycles (del Pozo et al., 2011), and modulated by a variety of environmental cues including temperature (Lahiri et al., 2005) and food availability (Sanchez et al., 2009; Sanchez and Sanchez-Vazquez, 2009). The rhythm and period of circadian biological processes are driven by a complex molecular clock machinery which is highly conserved across the animal kingdom. Knowledge about basic clock mechanisms and functions are largely derived from studies in Drosophila (Plautz et al., 1997; Peschel and Helfrich-Forster, 2011) and mice (Ripperger et al., 2011), with increasing interest in the zebrafish model (*Danio rerio*) [reviewed in (Vatine et al., 2011)]. The molecular clock involves transcription-translation and post-translational feedback loops, for example in mammals the transcription factor bmal1 forms a dimer with another PAS domain protein, clock, to activate *period* (per1 and per2) and *cryptochrome* (cry1 and cry2) genes (Ripperger et al., 2011). Per and cry proteins are translocated into the cell nucleus where they inhibit their own transcription. Secondary feedback loops involving the *rora* (transcriptional activator of *bmal1*) and *rev-erbα* genes (*nr1d1*, transcriptional repressor of *bmal1*) act to stabilise the clock mechanism whereas post-translational modifications of the per-cry dimer are required to set the period of the rhythm (Takahashi et al., 2008). In mice, light information received by the eyes travels to the suprachiasmatic nucleus which synchronizes the central and peripheral molecular clocks in a hierarchical manner [cf. (Ripperger et al., 2011)], i.e. peripheral clocks are entrained and synchronized to the central pacemaker. Studies in the teleosts have demonstrated that the pineal gland is the central photoreceptive organ, which contains intrinsic circadian oscillators that drive the rhythmic secretion of melatonin in response to light input [cf. (Cahill, 2002; Falcon et al., 2011)]. The role of the pineal as a hierarchical master clock in fish has been under discussion since observations that dissected zebrafish peripheral tissues (heart and kidney) and cells in cultures can be directly entrained by light and show a robust circadian rhythm (Whitmore et al., 1998). There is a growing body of information on zebrafish genes whose expression is inducible by light (Tamai et al., 2007; Vatine et al., 2009; Weger et al., 2011). Of particular interest is the observation that two main oscillators of the circadian rhythm namely *per2* and *cry1a* are inducible by light and that

deletion or mutation of the light responsive elements from the promoter of these genes cause disruption of the clock mechanism (Tamai et al., 2007; Vatine et al., 2009). Thus, the peripheral clock mechanism in fish has some similarities with that in *Drosophila*, which is directly responsive to light (Plautz et al., 1997). However, it remains to be determined whether enough light reaches the internal organs of adult zebrafish to render them photoreceptive and photoresponsive, and how the putative *in vivo* peripheral entrainment to light interacts with the neuroendocrine signals from the pineal.

Microarray studies have identified several hundred genes with circadian patterns of expression in mouse liver and skeletal muscle (Miller et al., 2007). Genes that are under control of the clock mechanism are referred to as clock controlled genes (CCGs), which are responsible for the integration between the clock mechanism and other physiological pathways, and ultimately orchestrate the biological output of the circadian pathway. For example, the positive oscillator of the stabilizing loop *nr1d1* has been shown to play an important role in the genomic recruitment of histone deacetylase 3 (*hdac3*) in mouse liver (Feng et al., 2011). Hdac3 functions in lipid homeostasis and absence of *nr1d1* caused impaired lipid metabolism with subsequent changes in the phenotype of the liver (Feng et al., 2011). The clock mechanism is also important for the physiology of other peripheral tissues and has been shown to play a pivotal role in maintaining muscle phenotype in the mouse (Andrews et al., 2010). In this tissue, the *clock* gene controls the expression of *myoD*, a member of the myogenic regulatory factor family, which functions in muscle determination and differentiation (McCarthy et al., 2007; Andrews et al., 2010). The absence of a functional clock mechanism in this tissue led to reduced force generation and reduced mitochondrial volume, mediated by the CCGs *myoD* and *pcg1a/β* respectively (Andrews et al., 2010).

Zebrafish have many advantages as a model system for investigating circadian clocks, including transparent embryos which facilitate the imaging of fluorescent reporter genes *in vivo* and the ease of performing large-scale forward genetic screens (Vatine et al., 2011). *Danio* is a diurnal fish that is mostly active during the subjective light phase of the photoperiod, with clear differences in locomotor activity and spawning behaviour between the dark and light phases (Hurd et al., 1998; Blanco-Vives and Sanchez-Vazquez, 2009). Teleost fish underwent whole genome duplication early in their evolution, and subsequent differential patterns of gene loss have resulted in lineage-specific differences

in the paralogues retained (Wang, 2008b). For example, the zebrafish and Tiger pufferfish (*Takifugu rubripes*) have three *clock* genes whereas the stickleback and Japanese Medaka fish have two (Wang, 2008b). Additional copies of *bmal1*, *cry1*, *cry2*, *per1*, *rora,* and *rev-erbβ* (*nr1d2*) genes have also been described for zebrafish (Kobayashi et al., 2000; Flores et al., 2007; Wang, 2008a; Wang, 2009). The expression pattern of the main oscillators of the circadian rhythm in zebrafish have been investigated in the retina, brain, pineal gland, and Z3 cell line [reviewed in (Vatine et al., 2011)].

The main objective of the present chapter was to provide a detailed description of the expression of 17 clock genes and their paralogues in zebrafish skeletal muscle. Circadian patterns of expression were determined in relation to the subjective light cycle in fish exposed to 3-4 cycles of continuous darkness. Using qPCR and a robust normalisation strategy, the hypothesis that the expression of myogenic regulatory factors, components of the insulin-like growth factor (IGF) system and other selected nutritionally responsive genes in skeletal muscle is under control of the circadian clock mechanism was also investigated.

3.3. Materials and Methods

3.3.1. Fish and water quality

The F8 generation of a wild-caught population of zebrafish [*Danio rerio* (Hamilton 1822)] from Mymensingh, Bangladesh was used. All fish were adult males aged 10 months [total length (TL) = 38.1 ± 0.2mm and body mass (BM) = 496 ± 8mg (mean ± s.e.m, N=130)]. The source colony and experimental animals were kept in a stand-alone freshwater circulating system, which included a UV water sterilising device and biological, chemical and particle filters. Nitrite (0 ppm), nitrate (10-20 ppm), ammonia (0 ppm) and pH (7.6 ± 0.2) were tested during acclimation and experimental periods using a Freshwater Master Test Kit (Aquarium Pharmaceuticals Inc., Chalfont, PA, USA). All experiments and animal handling were approved by the Animal Welfare and Ethics Committee, University of St Andrews and conformed to UK Home Office guidelines.

3.3.2. The circadian rhythm experiment

140 male fish from the same breeding stock were transferred to 4 separate tanks (N=35 per tank, 50L freshwater) maintained at 27.6 ± 0.3ºC range, in a 12:12h light:dark photoperiod and fed bloodworms (Ocean Nutrition™, Belgium) to satiety twice daily. Fish were acclimated for 2 weeks in the experimental tanks under the same environmental conditions as the source colony. The lights were switched-off at the beginning of a light cycle (10a.m.) to start the experiment (referred to as cycle 1: time 0h, C1:ZT00) and continuous darkness was maintained for 86h, corresponding to three complete light-dark cycles of the acclimation period (Figure 3.1). 10 fish were randomly sampled from one of the 4 tanks every 4h from C2:ZT02 to C4:ZT02, resulting in 13 time-points (N=130 fish), using a very dim torch-light directed to the floor. The fish were not disturbed during sample collection as no sudden change in activity was observed. After collection at each time-point additional bloodworms were offered to the fish to make sure food was available at all times across the experiment. This experimental design reduced the possibility of stress due to excessive handling since each tank was disturbed only every 16h. In addition, no maintenance was necessary for the duration of the acclimation and experimental periods due to the automatic filtration system which prevented the creation of external cues to which the fish could respond. The fish were killed by an overdose of

ethyl 3-aminobenzoate methanesulphonate salt (MS-222) (Fluka, St Louis, MO, USA) and had their TL and BM measured. Condition factor was calculated as K=[(BM/100)/(TL/10)^3]. Fast skeletal muscle was dissected from the dorsal epaxial myotomes, flash frozen in liquid nitrogen and stored at -80ºC prior to total RNA extraction. The digestive tract was dissected and fixed in 4% (m/v) paraformaldehyde for later quantification of intestine content to the nearest milligram. A control experiment under normal 12:12h light: dark photoperiod was performed eight months later using the F9 generation of fish, which were 11 months old. In this experiment the fish were collected at two time-points (ZT02 and ZT14) after two weeks of acclimation under the same environmental conditions as the continuous dark experiment. These time-points were chosen to confirm that either the maximum or minimum of expression observed in skeletal muscle under continuous darkness photoperiod also occurred under the normal 12:12h light:dark photoperiod. The sampling and data collection were as described for the continuous darkness experiment. Total RNA extraction and first strand cDNA synthesis were as described in section 2.3.5.

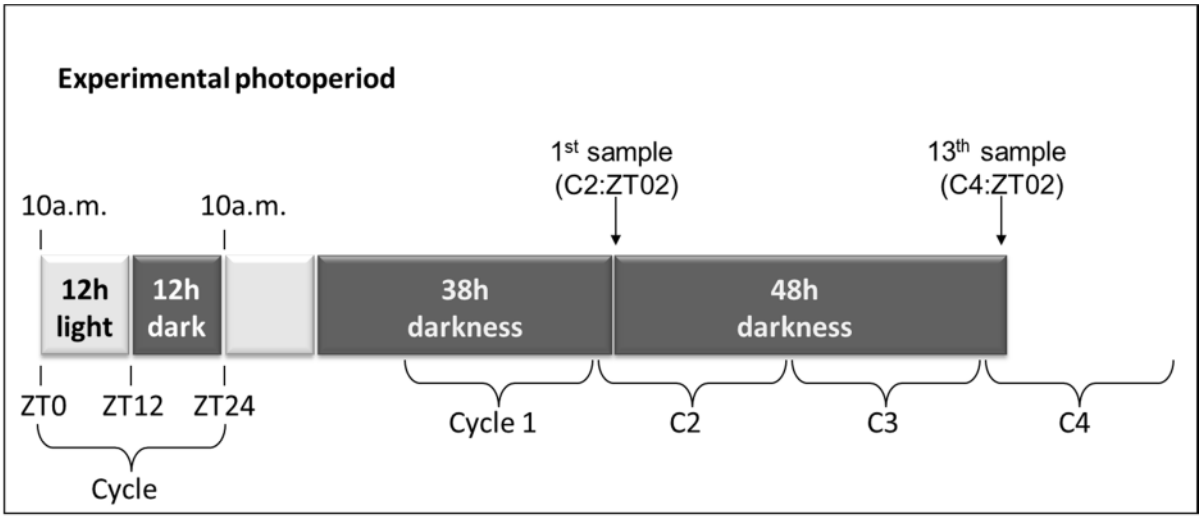

Figure 3.1 – Experimental design of the continuous darkness photoperiod experiment: male fish from the source colony of zebrafish (N=140), kept at 27.6±0.3ºC range in a 12:12h light:dark photoperiod and fed bloodworms twice daily, were transfered to four separate tanks with the same environmental conditions as the source colony (N=35 fish per tank). After two weeks of acclimation, 10 fish were randomly collected after 38h in continuous darkness every 4h for 48h until 86h of continuous darkness, resulting in 13 time-points (N=130 fish). Condition factor, gut food content and gene expression in skeletal muscle (by qPCR) were determined for each fish. A complete 12:12h light: dark is considered one cycle and times from ZT0 to ZT12 and ZT12 to ZT24 represent the subjective light and dark period of the cycle, respectively.

3.3.3. Primer design and screening for circadian expression by qPCR

Primer pairs were designed for 16 genes described as core-clock genes in other vertebrate models and tissues (*bmal1a, bmal1b, clock1a, clock1b, cry1a, cry1b, cry2a, cry2b, per1a, per1b, per2, per3, roraa, rorab, nr1d2a, and nr1d2b*), and 4 myogenic factors genes (*myoD, myog, myf5, and myf6*) as described in section 2.3.7 (Table 3.1). Previously validated primer pairs for 15 genes of the IGF pathway (*igf1a, igf2a, igf2b, igf1ra, igf1rb, igf2r, igfbp1a, igfbp1b, igfbp2a, igfbp2b, igfbp3, igfbp5a, igfbp5b, igfbp6a, and igfbp6b*), 2 ubiquitin ligases genes (*MAFbx and trim63*), and 12 nutritionally responsive genes [*odc1,*

hsp90a.1, fkbp5, sae1, hsp90a.2, foxo1a, klf11b, nr1d1 (known to be a circadian oscillator) , *cited2, bbc3, znf653, and hsf2*) were also used (Table 2.1).

The qPCR reagents and conditions were as described in section 2.3.8. and followed the MIQE guidelines (Bustin et al., 2009). After the qPCR a dissociation curve (from 55 to 95ºC) was performed to verify the presence of a single peak. The specificity of each qPCR assay was also validated by directly sequencing the qPCR products in both directions. The efficiency of each primer pair was calculated by the LinReg software (Ruijter et al., 2009) (Table 3.1) and used to calculate arbitrary mRNA copy numbers. Four reference genes [*ef1a, bactin2, lman2* (Table 2.1), and *gapdh* (Table 3.1)] were analysed using Genorm v3.5 (Vandesompele et al., 2002) with M set to <1.5. The two genes with the most stable level of expression across the experiment were *ef1a* and *bactin2* (M=0.3). The expression of genes of interest was normalized to the geometric average of the two most stable genes and gene expression was reported as arbitrary units (a.u.).

Genes were screened for circadian expression using pools containing equal amounts of cDNA from 10 fish per time-point. Transcript levels were analysed using the ARSER algorithm (Yang and Su, 2010) with period window of 20-28h and a false discovery rate (FRD) set to 0.05 (Benjamini and Hochberg, 1995). Individual reactions were carried out for all genes that passed these screening criteria for rhythmic expression plus *cry1b* and *nrld2a* (two genes paralogous to core-clock genes). The screening step was robust since: (a) the results of mRNA levels calculated by the screening and individual reactions were highly correlated (Spearman's correlation test, N=500, R=0.85, p<0.001); and (b) periodicity parameters calculated by the ARSER algorithm using the results from the individual reactions resulted in values very similar to those calculated for the screening reactions.

3.3.4. Data analysis and statistics

All data was analysed for normal distribution and equality of variance. Normally distributed data was analysed using ANOVA followed by Tukey post-hoc tests using PASW Statistics 18 (SPSS Inc., Chicago, Illinois, USA). Kruskal-Wallis non-parametric tests followed by Conover post-hoc tests in BrightStat software (Stricker, 2008) were used for the data that was not normally distributed. Hierarchical clustering of gene expression and heat-maps were produced using PermutMatrix

(http://www.lirmm.fr/~caraux/PermutMatrix/EN/index.html). Correlation of mRNA levels between genes was analysed by Spearman's correlation test in SPSS.

Table 3.1 – Sequence and properties of primers used in the experiments of chapter 3. Ensembl gene symbols, forward (f) and reverse (r) primer sequences, product size, product melting temperature (Tm), calculated efficiency (E) and Ensembl gene ID are shown.

Ensembl Gene symbol	f/r	Primer 5'-3' sequence	Product Size (bp)	Tm (°C)	E	Ensembl Gene ID
		Reference gene				
gapdh	f:	TAACGGATTCGGTCGCATTG	226	83.6	105.3	ENSDARG00000043457
	r:	GGCTGGGTCCCTCTCGCTA				
		Core circadian genes				
per1b	f:	CCTCCTGAGTCAGATATCGTAATGG	324	85.0	96.2	ENSDARG00000012499
	r:	GCAGCGCACACCTCTTGATAA				
per1a	f:	GTTCGAACGAGTCCGCTAAATG	256	85.3	99.6	ENSDARG00000056885
	r:	TGTCATTGGTTTCCTGGGCTT				
per2	f:	GTGGAGAAAGCGGGCAGC	252	87.4	95.9	ENSDARG00000034503
	r:	GCTCTTGTTGCTGCTTTCAGTTCT				
per3	f:	CCACAGCCTGAGTCCGAAGTC	300	87.8	98.0	ENSDARG00000010519
	r:	CCCCTCTGTGATGTGAATGTGC				
roraa	f:	GCATGTCACGTGACGCGGT	424	87.1	96.1	ENSDARG00000031768
	r:	TGGGCCAGATGTTCCAACTCA				
rorab	f:	AGCATTGGGCTGTGATGATCTT	241	82.8	96.5	ENSDARG00000001910
	r:	ACAGACAAGCTTAGTTAGAATTCCCTC				
nr1d1	f:	GAAGGCTGGAACATTTGAGGTC	228	83.3	104.2	ENSDARG00000033160
	r:	GCAGACACCAGGACGACCG				
nr1d2a	f:	CATGTCAAGAGACGCCGTGC	478	87.0	96.1	ENSDARG00000003820
	r:	GGGACAAACCAGATGTGCTCG				
nr1d2b	f:	GCACCTGGTCTGCCCGA	207	83.8	100.5	ENSDARG00000009594
	r:	CGGACCACCAGCACCTCA				
clock1a	f:	GGTTCAAGGACAGGGTTTACAGATG	280	87.3	100.0	ENSDARG00000011703
	r:	GGTCGACCTCTGAGACTGCTGG				
clock1b	f:	GAGAGTACAGGGACCTCAGATGATC	268	85.6	96.1	ENSDARG00000003631
	r:	ATACACAGGACCGCACTGAGTTAC				

Table 3.1 (continuation)

Ensembl Gene symbol	f/r	Primer 5'-3' sequence	Product Size (bp)	Tm (°C)	E	Ensembl Gene ID
		Core circadian genes (continuation)				
bmal1a	f:	GTCACAGACAAGTGCTACAGATGCG	261	82.1	102.5	ENSDARG00000006791
	r:	TCCCTCCGCCATCTCCTGA				
bmal1b	f:	TGACGGCTCAGGGAAAACC	305	86.1	99.3	ENSDARG00000035732
	r:	GAGAATTGTCACTTAAAATGGAGCTG				
cry1b	f:	CTACAGGAAGGTAAAGAAGAACAGCA	340	85.3	92.6	ENSDARG00000011583
	r:	CAACAACTCCTCAAACACCTTCAT				
cry1a	f:	CTACAGGAAGGTCAAAAAGAACAGC	334	87.1	99.1	ENSDARG00000045768
	r:	CTCCTCGAACACCTTCATGCC				
cry2a	f:	GGACCAATACACCAGCACCAG	245	83.6	99.7	ENSDARG00000069074
	r:	CAGCAAGTGTCCTGCCATGTC				
cry2b	f:	ATCGTCTTATACAGGGGTCAGGAG	287	87.3	98.9	ENSDARG00000091131
	r:	CTTCCCGCCTCTCGTTGTC				
		Myogenic regulatory factors				
myoD	f:	CGTCCACCAACCCGAACC	270	82.8	102.9	ENSDARG00000030110
	r:	TCCGTGCGTCAGCATTTGG				
myog	f:	ACATACTGGGGTGTCGTCCTCTA	209	86.5	97.92	ENSDARG00000009438
	r:	CCACTGGAGTCGCCTCTGTT				
myf5	f:	CAGAGAGCATGGTTGACTGCAAC	243	83.3	96.44	ENSDARG00000007277
	r:	TTGGACTGTCTGGAGAACTGCAC				
myf6	f:	CAACGAAGCTTTTGACGCG	291	83.8	92.44	ENSDARG00000029830
	r:	AACACGGCTCCTTCTCTATGACC				

3.4. Results

3.4.1. Feeding behaviour

Fish continued to eat during the experiment, but showed a marked change in feeding behaviour between C2 and C3, resulting in a decoupling of feeding activity from the light: dark cycle of the acclimation period. Gut food content (% body mass) was ~1.5 at C2:ZT02, increased to ~3.7 at C2:ZT10 and then declined to 0.8 at C2:ZT22. The food content of the gut only showed modest increase to ~1.4 during what would have been the light period of C3, declining to ~0.3 at C4:ZT02, indicating a marked reduction of foraging behaviour (Figure 3.2A). In the control experiment, a very similar pattern was observed with an increase of ~2-fold in gut food content from ZT02 (1.1%) to ZT14 (2.1%) under a 12:12h light: dark photoperiod (Figure 3.2A). No clear pattern was observed for condition factor among the time-points over the experiment (Figure 3.2B).

3.4.2. Non-circadian gene expression in skeletal muscle

25 out of 32 of the non-clock genes screened showed no evidence for circadian patterns of expression (*sae1, odc1, hsp90a.2, klf11b, foxo1a, fkbp5, cited2, bbc3, znf653 MAFbx, myf5, myoD*, *myogenin, igf1a, igf2a, igf2b, igf1ra, igf1rb, igf2r, igfbp1a, igfbp1b, igfbp2a , igfbp2b, igfbp5a, and igfbp6b)* (Figure 3.3). In addition, *trim63*, *hsp90a.1*, and *igfbp6a* passed the screening criteria, but failed to show strong evidence for circadian expression based on the individual reactions (adjusted-r^2 lower than 0.3 and FDR higher than 0.07). *Cry1b* was the only zebrafish paralogue of a core-clock gene that had a non-circadian pattern of expression (Figure 3.3).

The transcription levels of some genes were significantly correlated with the food content in the gut. Transcripts of *igf1rb, MAFbx, bbc3, igf1ra, igfbp5a,* and *igf2b* were negatively correlated (Spearman's correlation < -0.5, $P<0.05$) whereas *odc1, igf2a, igfbp2b,* and *sae1* were positively correlated with gut food content (Spearman's correlation > 0.5, $P<0.05$).

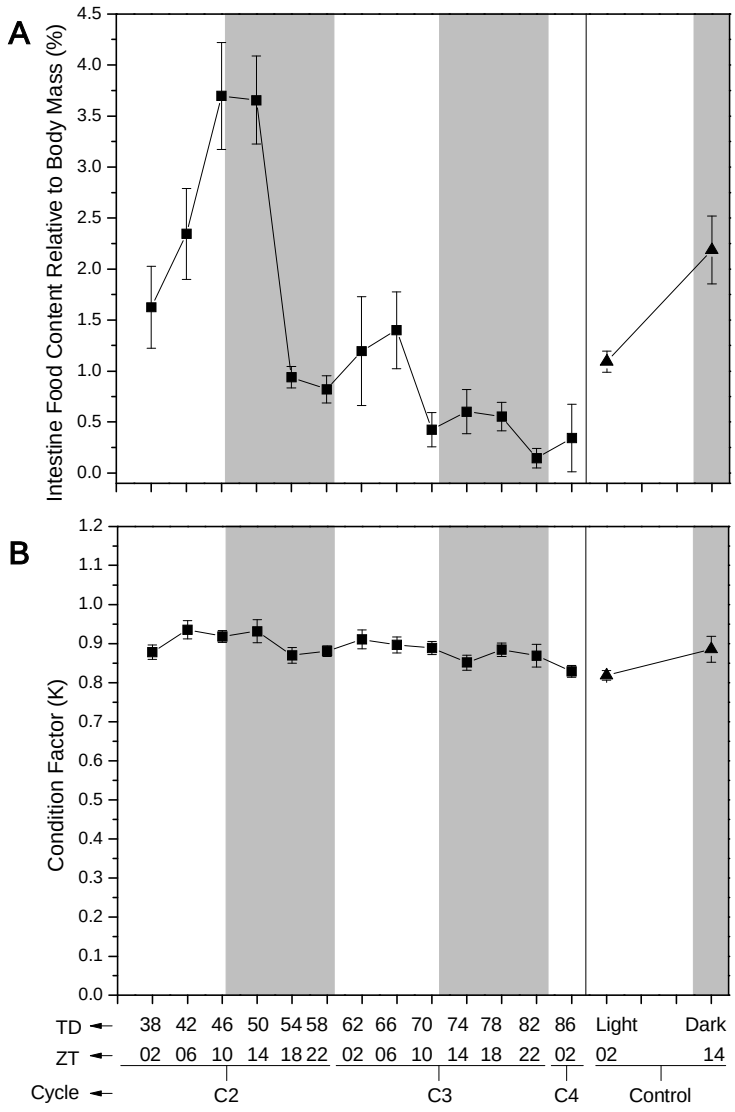

Figure 3.2 - Intestine food content relative to body mass (A) and condition factor (B) over the 48h of the photoperiod experiment. Fish kept in a 12:12h light:dark photoperiod for two weeks were exposed to complete darkness and condition factor and food content was calculated for 10 fish every 4h until 86h of continuous darkness. The subjective light and dark periods of the photoperiod are represented by white and gray background respectively. Values are mean ± s.e.m., N=10 fish per time-point. Different letters represent statistically different means ($P<0.05$). TD and ZT in the X-axis stands for "time in continuous darkness" and "Zeitgeber time", respectively.

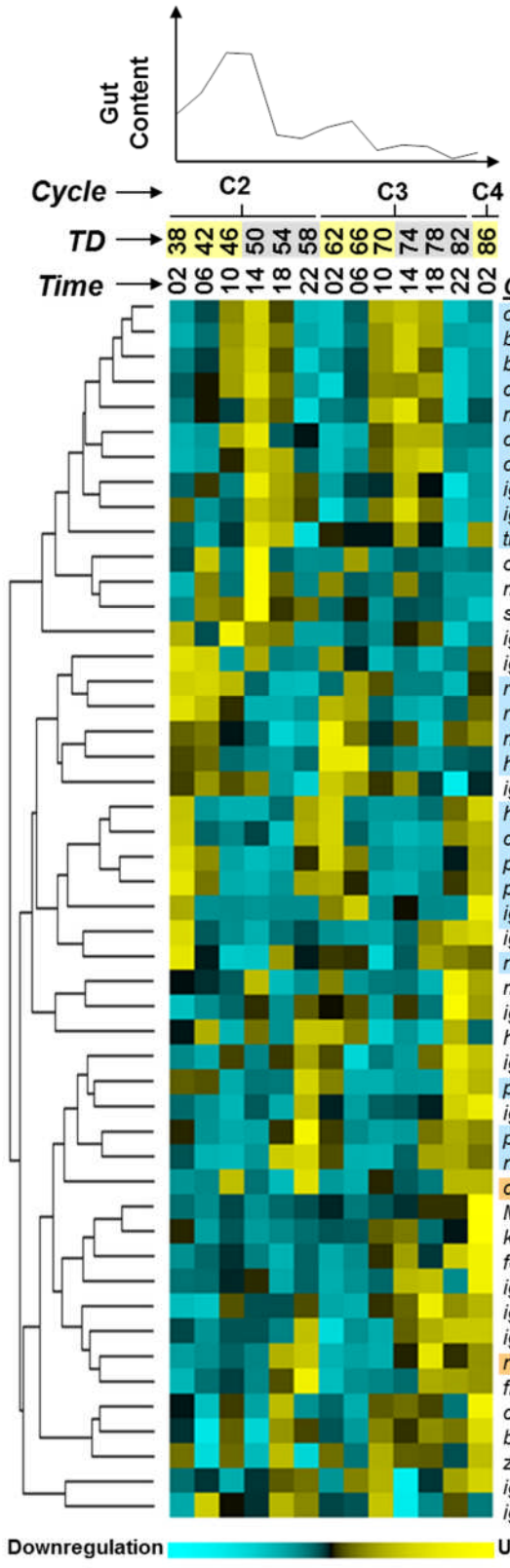

Periodicity parameters calculated by the ARSER algorithm

Gene	Period	Phase	Adjusted r^2	FDR
cry2a	24	13.5	0.88	0.000
bmal1b	24	13.3	0.97	0.000
bmal1a	24	13.2	0.84	0.000
clock1b	24	12.8	0.76	0.002
myf6	23	14.0	0.63	0.010
cry2b	26	11.8	0.75	0.002
clock1a	24	15.6	0.93	0.000
igfbp3	21	19.1	0.63	0.010
igbp5b	21	20.2	0.88	0.000
trim63	20	18.3	0.45	0.050
odc1	23	12.3	-0.05	0.579
myf5	23	15.2	0.16	0.252
sae1	27	11.5	0.23	0.180
igfbp2b	29	6.1	0.21	0.199
igf1a	24	2.6	0.24	0.179
roraa	24	7.3	0.59	0.014
rorab	25	2.7	0.84	0.000
myog	23	6.2	0.45	0.050
hsp90a.1	26	1.1	0.47	0.046
igf2a	26	5.3	0.24	0.179
hsf2	25	23.3	0.80	0.001
cry1a	25	24.3	0.68	0.005
per3	25	0.9	0.90	0.000
per1b	24	1.2	0.90	0.000
igfbp6a	26	25.4	0.44	0.050
igfbp1b	20	7.0	0.22	0.190
nr1d2b	22	3.7	0.60	0.013
myoD	18	16.8	0.07	0.364
igfbp1a	19	14.1	0.10	0.343
hsp90a.2	23	3.3	0.29	0.133
igf2b	28	15.2	0.35	0.096
per2	24	23.4	0.59	0.013
igf1br	24	23.7	0.34	0.098
per1a	23	22.8	0.62	0.010
nr1d1	28	15.9	0.88	0.001
cry1b	20	12.0	-0.12	0.753
MAFfbx	24	2.8	0.06	0.378
klf11b	24	4.5	0.07	0.364
foxo1a	21	11.5	-0.06	0.609
igf2r	24	12.3	-0.16	0.870
igf1ar	30	7.5	0.42	0.059
igfbp6b	24	20.3	0.09	0.361
nr1d2a	24	19.3	0.41	0.060
fkbp5	29	13.8	0.18	0.231
cited2	22	16.9	-0.19	0.959
bbc3	26	19.4	-0.09	0.666
znf653	19	2.7	0.02	0.446
igfbp5a	28	20.2	0.07	0.364
igfbp2a	24	3.6	-0.19	0.959

Figure 3.3 – legend on next page

Figure 3.3 – Heatmap and periodicity parameters calculated for the screening reactions of the photoperiod experiment. The upper left panel shows the gut content relative to body mass over the 48h of the photoperiod experiment (the subjective light and dark period of the photoperiod are represented by numbers with yellow and gray background, respectively). TD and ZT in the X-axis stands for "time in continuous darkness" and "Zeitgeber time", respectively. The heatmap shows the hierarchical clustering (McQuitty's method) of normalized mRNA levels for each transcript over the continuous darkness photoperiod – mean equals to zero and standard deviation equals to 1. Shades of yellow represent upregulation and shades of cyan represent downregulation. Each block represents the mean of duplicate qPCRs of a pool containing cDNA from 10 fish. Some of the periodicity parameters calculated by the ARSER algorithm are shown on the right (period window set to 20-28h). FDR stands for false discovery rate.

3.4.3. Expression of core clock genes in skeletal muscle

The expression of zebrafish paralogues of the positive oscillators of the circadian mechanism (*bmal1* and *clock1*) and the transcription activator of *bmal1* (*rora*) followed a circadian pattern in skeletal muscle. The 2 paralogues of *bmal1* and *clock1* were expressed in phase with each other showing peak expression at ZT14 (Figure 3.4A-D). *bmal1a* and *bmal1b* showed an 8.5-fold change in expression between maximum and minimum values (Figure 3.4A,B). In contrast, *clock1a* was more responsive to the light: dark cycle than *clock1b* showing a 6.0- and 2.2-fold change in expression respectively (Figure 3.4C,D). The highest expression of the two paralogues of the *rora* gene (*roraa* and *rorab*), known to activate *bmal1* in mammals, occurred in a different phase from *bmal1* and *clock1*, with an ~4.5-fold change in expression of both paralogues between maximum (at ZT02) and minimum (Figure 3.4E,F).

With the exception of *cry1b,* the expression of the negative oscillators determined in this study *(cry1a, cry2a, cry2b, per1a, per1b, per2, per3, nr1d1, nr1d2a and nr1d2b)* followed a circadian pattern. Expression of *cry1a* gene peaked at ZT02 (~4.0-fold upregulation) (Figure 3.5A). In contrast to the expression of *cry1a*, the expression of the two paralogues of the *cry2* gene (*cry2a* and *cry2b*) occurred in phase with *bmal1* and *clock1*, with both paralogues showing similar amplitude of expression in relation to the photoperiod (Figure 3.5B,C).

The transcript levels of all four *per* genes assayed (*per1a*, *per1b*, *per2*, and *per3*) occurred in phase with the negative oscillator *cry1a*. A small shift in the phase of expression was observed among the *per* genes: *per1b* and *per3* mRNA levels were at their highest four hours later than the peak expression of *per1a* and *per2* genes (Figure 3.5D-G). The fold-change in transcription level of the *per1a* (~51.7-fold) and *per3* (~23-fold) were among the highest of all circadian genes studied (Figure 3.5D,G).

Expression of the nuclear receptors genes *nr1d1*, *nr1d2a*, and *nr1d2b*, which belong to the negative loop of transcriptional regulation of the circadian rhythm in mammals, also occurred in phase with expression of the *cry1a* gene (Figure 3.6A-C). Peak expression of *nr1d1* was ~47-fold higher than its lowest expression (Figure 3.6A). A relatively weak, but significant, negative correlation was found between the expression of this gene and food gut content (R=-0.56, P=0.040). The maximum change in expression of *nr1d2a* (~7.3-fold) was significantly higher than for *nr1d2b* (~2.3-fold) (Figure 3.6B,C).

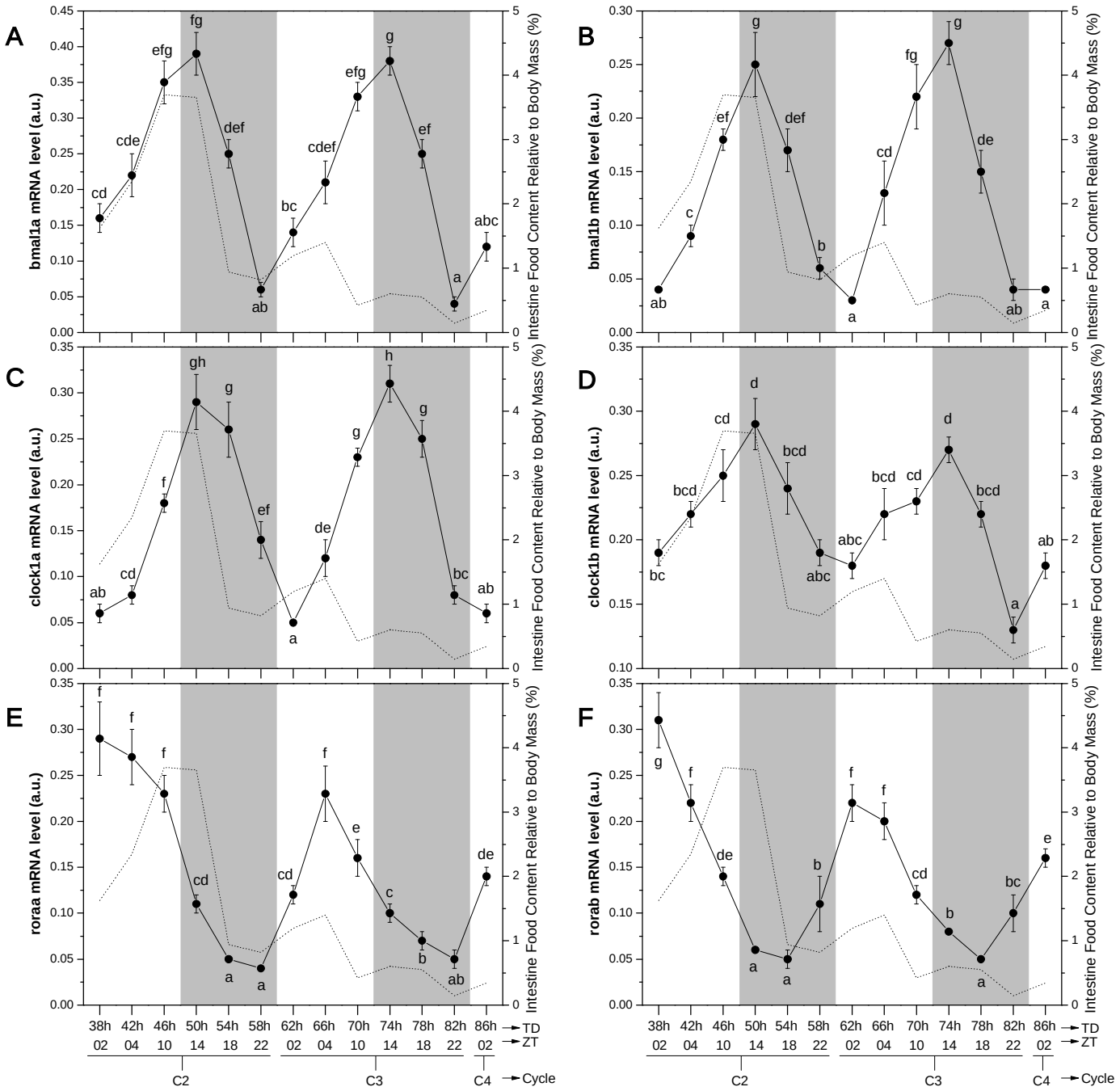

Figure 3.4 - Expression profile of zebrafish orthologues of genes known to be positive regulators of the circadian pathway in mammals. The subjective light and dark periods of the photoperiod are represented by white and gray background respectively. Transcript levels of the paralogues (A) *bmal1a*, (B) *bmal1b*, (C) *clock1a*, and (D) *clock1b* were highest during the beginning of the subjective nigh period. Conversely, transcription of the (E) *roraa* and (F) *rorab* paralogues was highest during the subjective light phase. Values are mean ± s.e.m., N=10 fish per time-point. Different letters represent statistically different means ($P<0.05$). TD and ZT in the X-axis stands for "time in continuous darkness" and "Zeitgeber time", respectively. The dashed lines represent the intestine food content.

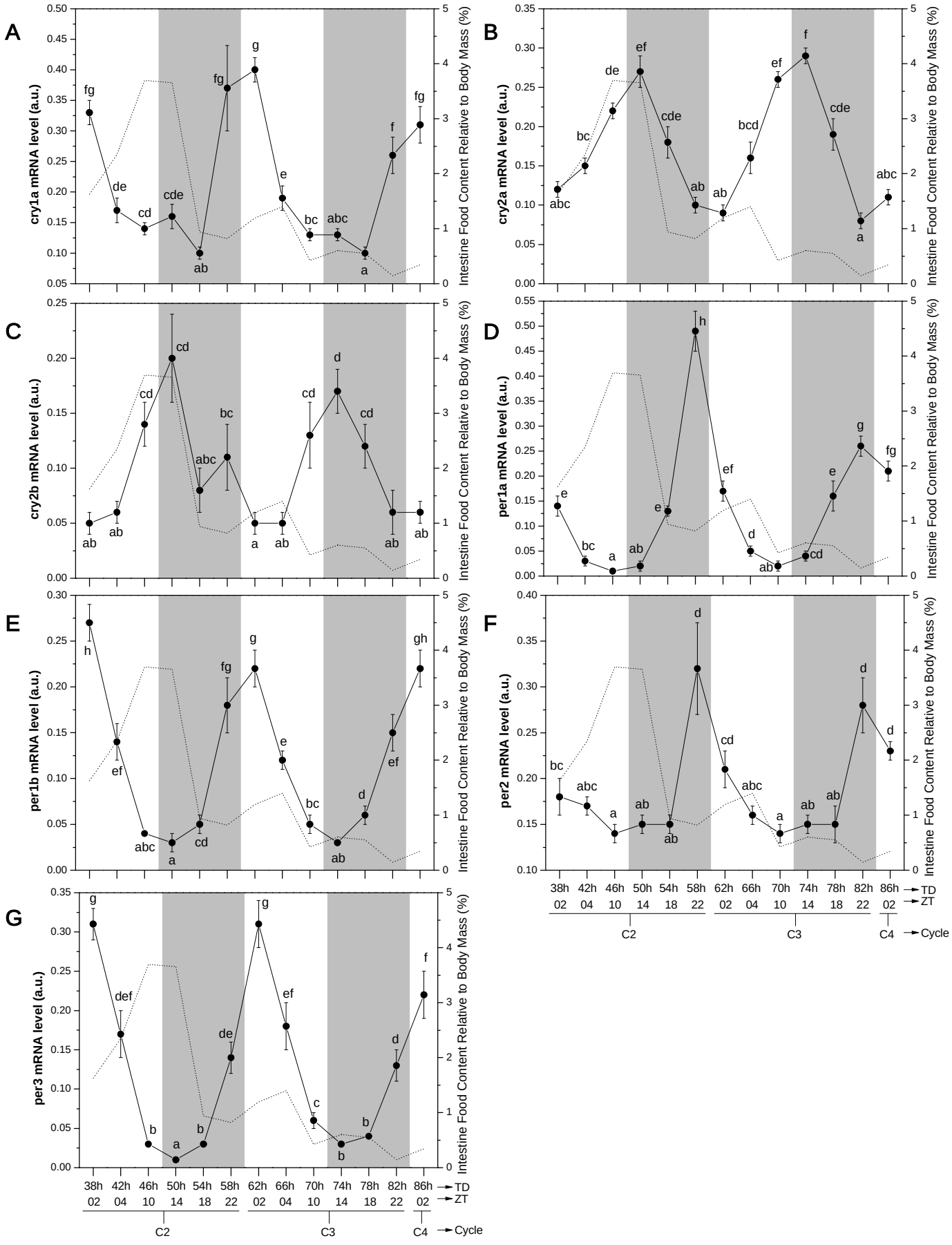

Figure 3.5 – legend on next page.

Figure 3.5 - Expression profile of zebrafish orthologues of genes known to be negative regulators of the circadian pathway in mammals. The subjective light and dark periods of the photoperiod are represented by white and gray background respectively. At the beginning of the subjective dark phase of the photoperiod the expression of (A) *cry1a* was at its lowest while expression of (B) *cry2a*, (C) *cry2b* was at its highest. Expression of the *per* genes was very similar, with (D) *per1a* and (F) *per2* highest expression occurring four hours earlier than expression of (E) *per1b* and (G) *per3*. Values are mean ± s.e.m., N=10 fish per time-point. Different letters represent statistically different means ($P<0.05$). TD and ZT in the X-axis stands for "time in continuous darkness" and "Zeitgeber time", respectively. The dashed lines represent the intestine food content.

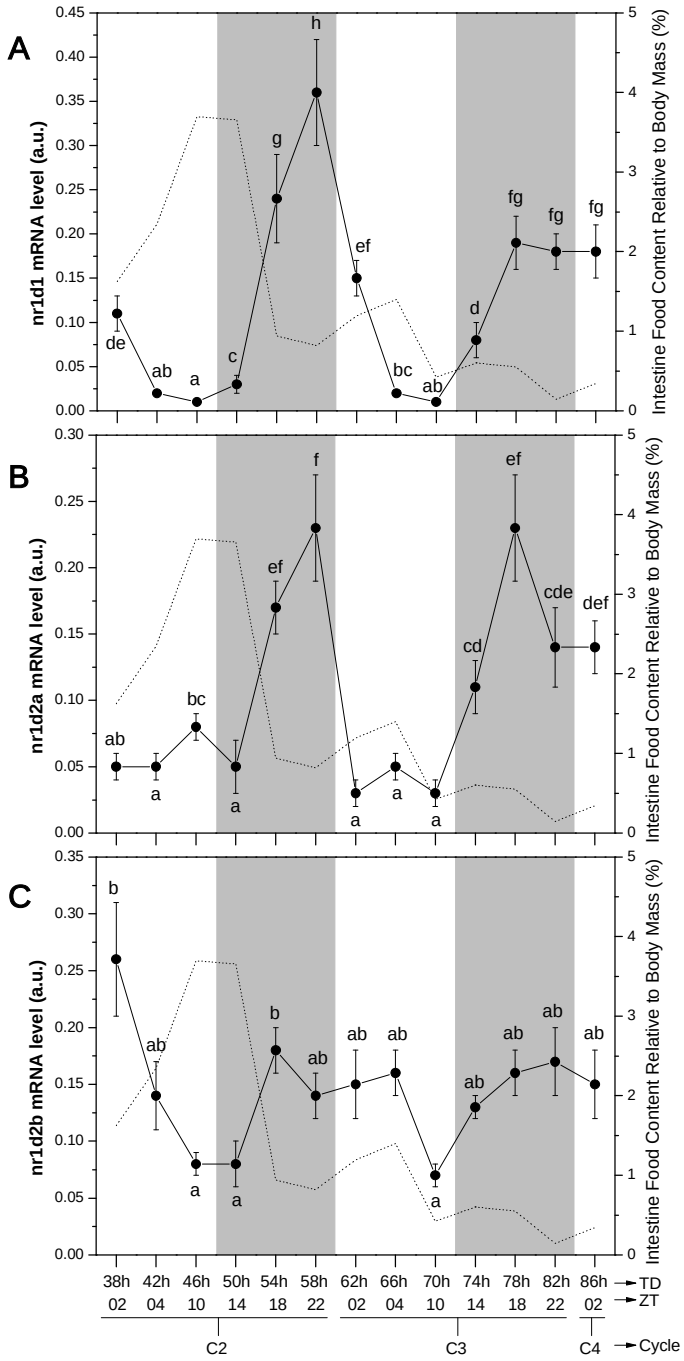

Figure 3.6 - Expression profile of zebrafish orthologues of the nuclear receptor subfamily D, known to be negative regulators of the circadian pathway in mammals. The subjective light and dark periods of the photoperiod are represented by white and gray background respectively. Expression of (A) *nr1d1*, (B) *nr1d2a*, and (C) *nrd1d2b* occurred in phase with one another, but the *nr1d2a* paralogue seems to be more responsive to changes in photoperiod than the *nr1d2b* paralogue. Values are mean ± s.e.m., N=10 fish per time-point. Different letters represent statistically different means ($P<0.05$). TD and ZT in the X-axis stands for "time in continuous darkness" and "Zeitgeber time", respectively. The dashed lines represent the intestine food content.

3.4.4. Putative clock-controlled genes

Expression of two IGF-binding proteins (*igfbp3* and *igfbp5b*) and one myogenic regulatory factor (*myf6*) occurred in phase with the paralogues of the positive oscillators *bmal1* and *clock1*, with an average of ~2.0-fold regulation (Figure 3.7A-C). Expression of the heat shock transcription factor 2 gene (*hsf2*) occurred in phase with *cry1a* and other genes that belong to the negative arm of the transcriptional regulation network of the circadian rhythm (Figure 3.7D). Transcripts of this gene were ~7.0-fold higher at ZT02 than ZT14 (Figure 3.7D).

3.4.5. Expression of circadian genes and CCGs under 12: 12h light: dark photoperiod

The pattern of gene expression in skeletal muscle under a normal photoperiod was similar to the one observed under a continuous darkness condition (Spearman's correlation coefficient = 0.699, P<0.001). However, the amplitude of expression between the light and dark periods was higher in skeletal muscle subjected to a normal photoperiod when compared to the continuous darkness expression (Figure 3.8).

3.4.6. Gene clustering and correlation analysis

The 20 genes found to have a circadian rhythm of expression could be grouped in two major clusters (Figure 3.9). Cluster I comprises genes with peak expression around the middle of the subjective dark photoperiod and included *bmal1a, bmal1b, cry2a, clock1b, myf6, clock1a, cry2b, igfbp3, and igfbp5* (Figure 3.9). Transcript level of paralogue genes in this cluster were highly positively correlated, the two paralogues of the *bmal1* gene had the highest correlation coefficient (R=0.92, P<0.001), followed by the paralogues for the *clock* gene (R=0.84, P<0.001) and lowest correlation was found for the two paralogues of the *cry2* gene (R=0.76, P=0.002) (Table 3.2). Genes with peak expression during the last time-point of the subjective dark photoperiod and the two time-points from the subjective light photoperiod were grouped in cluster II (*cry1a, hsf2, per1b, per3, nr1d2b, roraa, rorab, nr1d1, per1a, per2, nr1d2a*) (Figure 3.9). In this cluster, only the paralogues of the *rora* gene had highly significant positive correlation in mRNA levels (R=0.79, P=0.001) (Table 3.2). Weak, but statistically significant, negative correlations were found between gut food content and transcription level of *per1a* (R=-

0.57, P=0.040) and *nr1d1* (R=-0.56, P=0.040). No significant positive correlation was found between the expression of circadian genes and gut food content.

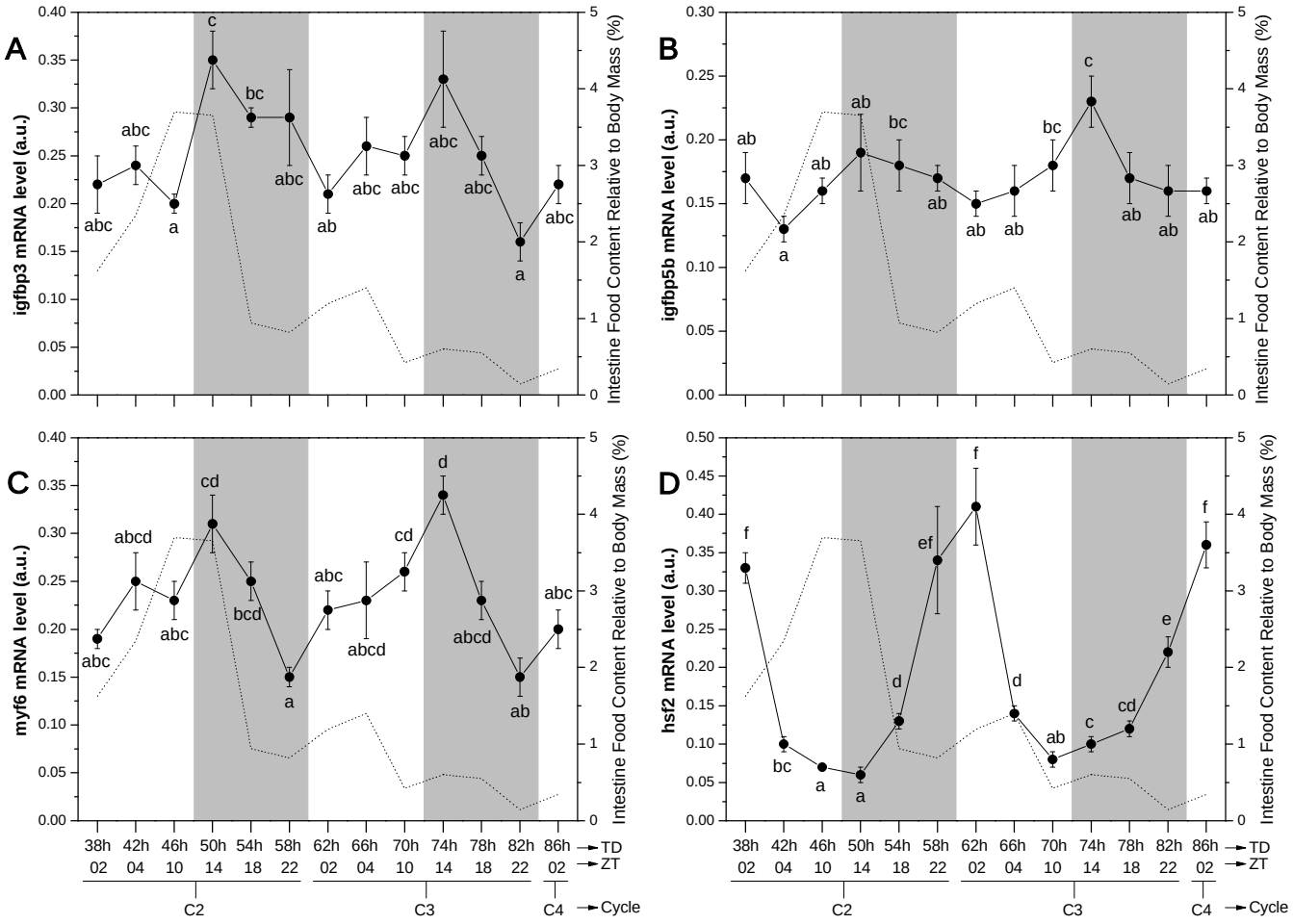

Figure 3.7 - Expression profile of putative zebrafish clock-controlled genes. The subjective light and dark periods of the photoperiod are represented by white and gray background respectively. Expression of (A) *igfbp3*, (B) *igfbp5b*, and (C) *myf6* occurred in phase with one another and with known positive oscillators of the circadian rhythm Expression of (D) *hsf2* was at its highest at the beginning of the light phase of the photoperiod, in phase with known negative oscillators of the circadian rhythm. Values are mean ± s.e.m., N=10 fish per time-point. Different letters represent statistically different means (P<0.05). TD and ZT in the X-axis stands for "time in continuous darkness" and "Zeitgeber time", respectively. The dashed lines represent the intestine food content.

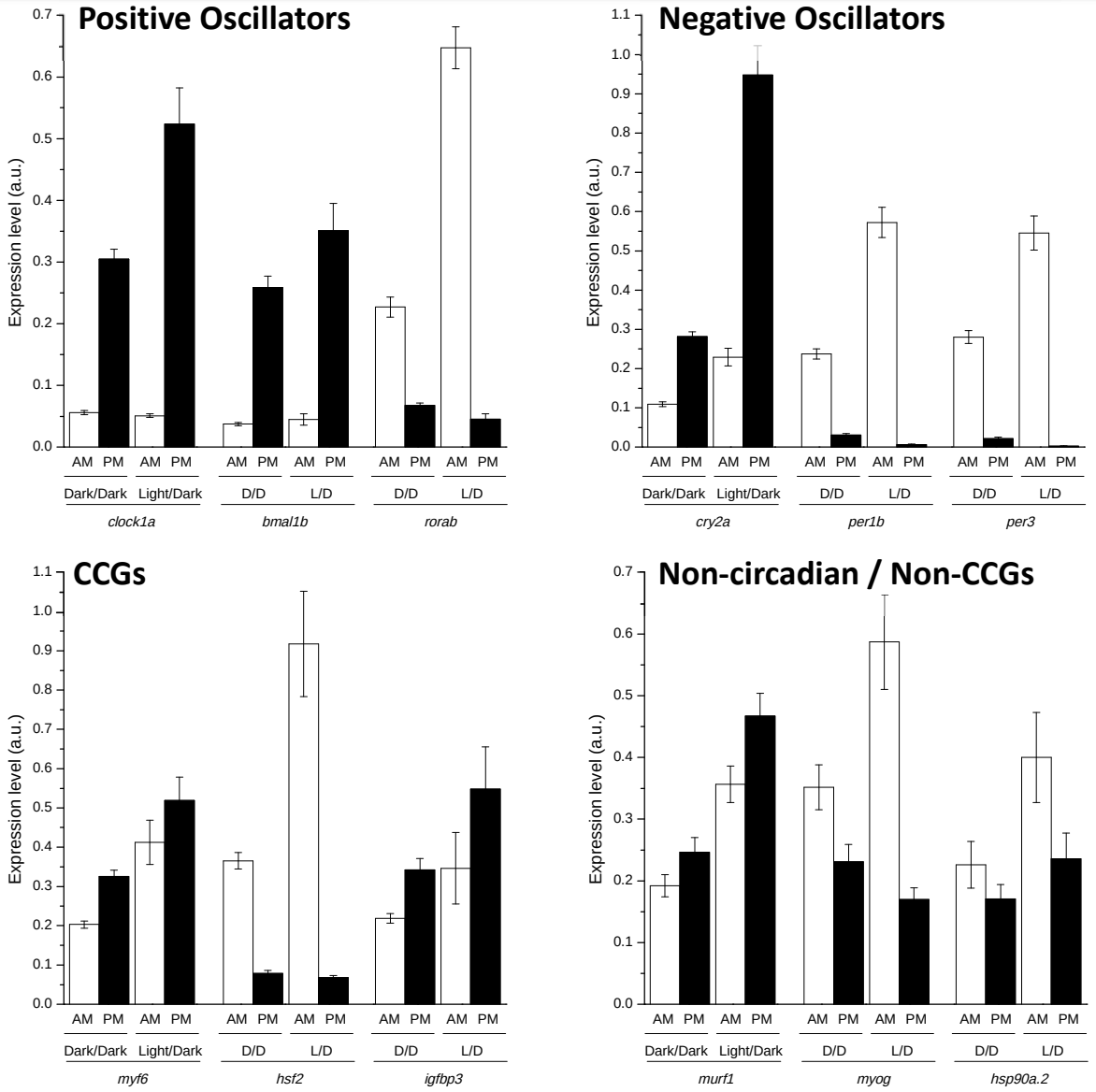

Figure 3.8 – Comparison gene expression during continuous darkness and 12: 12h light: dark photoperiods. AM and PM refers to ZT02 (two hours after lights on) and ZT14 (two hours after lights off), respectively. Results of intestine content from the C2ZT02 and C2ZT14 from the continuous darkness were compared to the two time-points of the control experiment (A) (N=10 per time-point per experiment). The results of gene expression from the time-points 38, 62 and 86h of darkness were averaged and considered as the result of ZT02 (AM) of the continuous darkness experiment (N=30) whereas the averaged results of time-points 50 and 74h of darkness were considered the ZT14 (PM) (N=20) and compared to the two time-points of the control experiment (N=10 per time-point). Columns and error bars represent average and s.e.m., respectively. The pattern of gene expression in skeletal muscle under a normal photoperiod was similar to the one observed under a continuous darkness condition (Spearman's correlation coefficient=0.699, P<0.001)

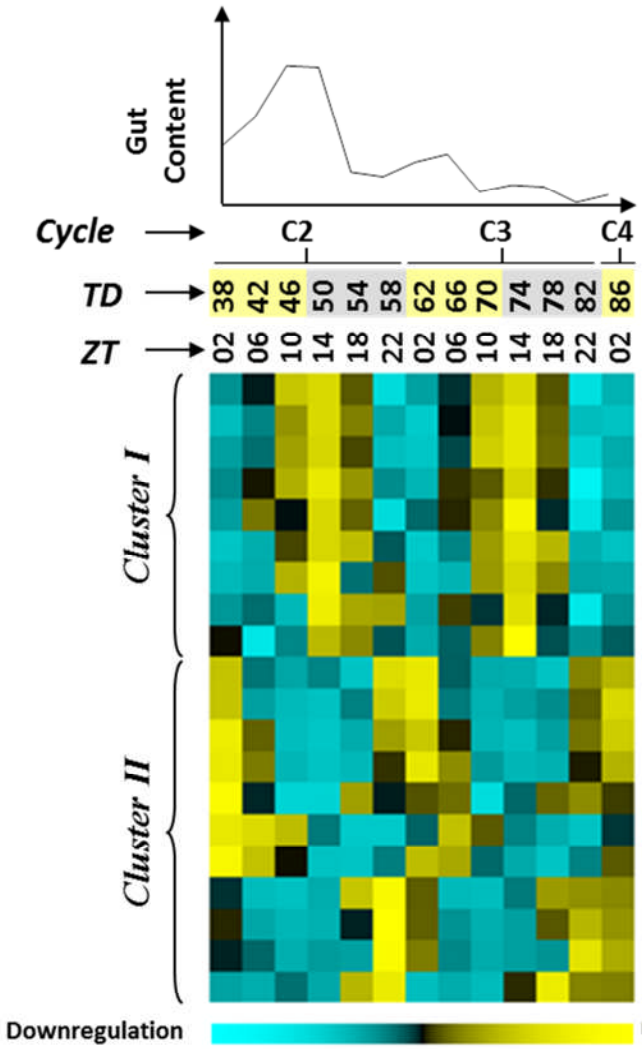

Periodicity parameters calculated by the ARSER algorithm

Gene	Period	Phase	Adjusted r^2	q-value	FDR
bmal1a	23.5	13.1	0.89	0.000	0.000
bmal1b	22.7	15.1	0.97	0.000	0.000
cry2a	23.1	14.1	0.92	0.000	0.000
clock1b	22.3	15.7	0.83	0.000	0.000
myf6	23.3	13.3	0.60	0.001	0.010
clock1a	22.7	16.5	0.98	0.000	0.000
cry2b	23.8	14.3	0.75	0.000	0.002
igfbp3	20.1	0.5	0.54	0.002	0.017
igfbp5b	20.2	0.3	0.73	0.000	0.002
cry1a	26.1	22.9	0.71	0.000	0.003
hsf2	25.8	22.9	0.80	0.000	0.001
per1b	24.2	1.1	0.92	0.000	0.000
per3	25.1	0.2	0.89	0.000	0.000
nr1d2b	22.4	2.3	0.55	0.002	0.017
roraa	24.0	6.4	0.64	0.001	0.007
rorab	24.8	2.2	0.82	0.000	0.000
nr1d1	24.0	21.2	0.69	0.000	0.003
per1a	24.0	22.3	0.58	0.001	0.012
per2	24.3	23.1	0.51	0.002	0.022
nr1d2a	23.9	19.6	0.47	0.003	0.032

Figure 3.9 – Heatmap and periodicity parameters calculated for the individual reactions of the photoperiod experiment. The upper left panel shows the gut content relative to body mass over the 48h of the photoperiod experiment (the subjective light photoperiod are represented by numbers with yellow background and the dark photoperiod by gray background). TD and ZT in the X-axis stands for "time in continuous darkness" and "Zeitgeber time", respectively. Expression of genes that passed the screening step was quantified by qPCR for each individual fish in relation to the photoperiod. The heatmap shows the hierarchical clustering (McQuitty's method) of normalized mRNA levels for each transcript over the complete darkness photoperiod – mean equals to zero and standard deviation equals to 1. Shades of yellow represent upregulation and shades of cyan represent downregulation. Each block represents the mean of mRNA level of 10 fish quantified by qPCR. Some of the periodicity parameters calculated by the ARSER algorithm are shown on the right (period window set to 20-28h). FDR stands for false discovery rate.

Table 3.2 – Significant positive and negative Spearman's correlation of gene expression over the photoperiod experiment. Only correlations higher than 0.75 are shown.

Positive Correlations				Negative Correlations			
Genes		Spearman's Correlation	p-value	Genes		Spearman's Correlation	p-value
bmal1a	*clock1b*	0.96	0.000	*bmal1b*	*per1b*	-0.94	0.000
bmal1a	*cry2a*	0.96	0.000	*clock1a*	*per3*	-0.92	0.000
bmal1b	*cry2a*	0.96	0.000	*bmal1a*	*per2*	-0.90	0.000
bmal1b	*clock1b*	0.95	0.000	*hsf2*	*bmal1b*	-0.90	0.000
clock1b	*cry2a*	0.94	0.000	*clock1b*	*per1b*	-0.90	0.000
clock1a	*bmal1b*	0.92	0.000	*clock1a*	*per1b*	-0.90	0.000
bmal1a	*bmal1b*	0.92	0.000	*bmal1a*	*per1b*	-0.89	0.000
hsf2	*per1b*	0.91	0.000	*bmal1a*	*hsf2*	-0.89	0.000
hsp90a.1	*rorab*	0.90	0.000	*bmal1a*	*per1a*	-0.88	0.000
per3	*per1b*	0.90	0.000	*cry2b*	*per3*	-0.88	0.000
bmal1a	*myf6*	0.89	0.000	*cry2a*	*per1b*	-0.88	0.000
hsf2	*per1a*	0.88	0.000	*igf2a*	*nr1d2a*	-0.87	0.000
cry2b	*clock1a*	0.87	0.000	*per2*	*cry2a*	-0.87	0.000
cry2a	*myf6*	0.86	0.000	*hsf2*	*cry2a*	-0.87	0.000
per1a	*per2*	0.85	0.000	*clock1b*	*per2*	-0.87	0.000
clock1a	*cry2a*	0.85	0.000	*hsf2*	*clock1b*	-0.85	0.000
clock1b	*myf6*	0.85	0.000	*cry2b*	*per1b*	-0.85	0.000
clock1a	*clock1b*	0.84	0.000	*per1a*	*clock1b*	-0.84	0.000
per1a	*nr1d1*	0.84	0.000	*bmal1b*	*per2*	-0.84	0.000
cry2b	*bmal1b*	0.84	0.000	*clock1a*	*cry1a*	-0.83	0.000
per3	*rorab*	0.84	0.000	*per3*	*bmal1b*	-0.83	0.000
hsp90a.1	*per3*	0.82	0.001	*per1a*	*cry2a*	-0.81	0.001
bmal1b	*myf6*	0.82	0.001	*per1a*	*myf6*	-0.81	0.001
hsp90a.1	*cry1a*	0.82	0.001	*hsp90a.1*	*clock1a*	-0.80	0.001
cry1a	*per2*	0.81	0.001	*per1b*	*myf6*	-0.80	0.001
per2	*per1b*	0.81	0.001	*bmal1b*	*cry1a*	-0.80	0.001
hsf2	*per2*	0.81	0.001	*clock1a*	*rorab*	-0.79	0.001
rorab	*roraa*	0.80	0.001	*cry2b*	*hsf2*	-0.78	0.002
per3	*cry1a*	0.80	0.001	*cry1a*	*cry2a*	-0.78	0.002
bmal1a	*clock1a*	0.79	0.001	*per1a*	*bmal1b*	-0.76	0.002
igf1a	*hsp90a.1*	0.79	0.001	*per3*	*clock1b*	-0.76	0.002
cry1a	*per1b*	0.78	0.002	*hsf2*	*myf6*	-0.76	0.002
hsf2	*per3*	0.77	0.002	*nr1d1*	*roraa*	-0.76	0.002
cry2b	*cry2a*	0.76	0.002	*cry2b*	*hsp90a.1*	-0.76	0.003
igfbp3	*clock1a*	0.76	0.002	*per2*	*myf6*	-0.76	0.003
igf2a	*roraa*	0.76	0.003	*hsf2*	*clock1a*	-0.76	0.003

3.5. Discussion

Danios show an endogenous circadian nocturnal feeding behaviour when under a 12: 12h light: dark photoperiod (del Pozo et al., 2011). In the present study, however, continuous darkness led to an inhibition of the feeding response by the third subjective light cycle, as evidenced by direct observation of the food present in the gut, enabling the transcriptional responses due to feeding and circadian rhythmicity to be distinguished. Feeding activity in teleosts initiates well characterised transcriptional responses (Rescan et al., 2007; Bower et al., 2008; Amaral and Johnston, 2011). Transcripts for the ubiquitin ligase *MAFbx*, insulin-like growth factor-1 receptors (*igf1ra*, *igf1rb*) and the mitochondrial pro-apoptotic BCL2 binding protein component 3 (*bbc3*) were inversely correlated with gut food content (Figure 3.3) as previously reported (Amaral and Johnston, 2011). In contrast, transcripts for ornithine decarboxylase (*odc1*) and sumo-activating enzyme (*sae1*), previously shown to be positively correlated with gut food content (Amaral and Johnston, 2011), had peak expression during the subjective light phase of the 2nd diurnal cycle and reduced expression throughout the whole of the 3rd diurnal cycle (Figure 3.3).

3.5.1. Expression of core-clock genes in zebrafish skeletal muscle

Bmal1 and clock are considered the central oscillators of the circadian mechanism due to their ability to bind to E-box elements and activate the transcription of most of the core-clock genes (Figure 3.10). In zebrafish skeletal muscle the expression of the respective paralogues of the two positive oscillators (*bmal1a*, *bmal1b*, *clock1a* and *clock1b*) clustered together (Figure 3.9) and were highly correlated (Table 3.2). The results of the present study are very similar to the expression pattern described in organs that are considered central pacemakers of the zebrafish clock mechanism (Whitmore et al., 1998; Cermakian et al., 2000).

Period proteins (per 1, 2 and 3) together with the cryptochrome proteins 1 and 2 are responsible for the negative loop of the circadian mechanism (Vatine et al., 2011). In addition, period proteins have been shown to be important for maintaining the pace of the clock machinery (Hastings et al., 2007; Vatine et al., 2009). Among the *period* genes assayed in cultured zebrafish cells only *per2* expression was inducible by light (Tamai et al., 2007) (Figure 3.10). In skeletal muscle of the zebrafish *per1a* and *per2* showed peak expression at the end of the subjective dark period (ZT22) whereas *Per1b* and *Per3*

showed highest expression at the start of the light period (ZT02) (Figure 5D-G). Interestingly, expression of *per3* in the zebrafish skeletal muscle was similar to that found in Z3 zebrafish cells (Pando et al., 2001) and in the retina and optic tectum of the nocturnal flatfish *Solea senegalensis* (Martín-Robles et al., 2011), with highest expression at around ZT02 (Figure 5G). The observation that diurnal and nocturnal fish have the same pattern of expression in central and peripheral tissues might be valuable in investigating its function.

The paralogues of both *cry1* and *cry2* have been demonstrated to inhibit bmal: clock-directed transcriptional activation (Vatine et al., 2011). *Cry1a* is considered to act on the core clock machinery and was the only transcript from the *cryptochrome* genes whose expression was induced by light in zebrafish cell cultures (Tamai et al., 2007) (Figure 3.10). The expression of *cry1a*, *cry2a* and *cry2b* in skeletal muscle (Figure 5A-C) were similar to that described in the eye and brain of the zebrafish (Kobayashi et al., 2000), considered central organs of the circadian mechanism. The difference in phase of expression of *cry1a* and paralogues of the *cry2* in the muscle were as previously described in the eye and brain (Kobayashi et al., 2000), with peak expression of *cry1a* occurring at ZT02 and *cry2* paralogues at ZT14. Expression of *cry1b* in the muscle (Figure 3.3), however, did not follow the circadian pattern described for the central organs (Kobayashi et al., 2000). Furthermore, *cry2* genes in zebrafish (Figure 5B,C) and mouse muscle are expressed in anti-phase (McCarthy et al., 2007). In the current model of the circadian clock in the zebrafish cry1 and cry2 proteins forms hetero-dimers that translocate to the nucleus where they inhibit the bmal:clock-dependent transcriptional activation (Vatine et al., 2011). In the skeletal muscle, however, the cry1b might not be part of the pool of cry proteins available to form dimers with per proteins (Figure 3.10).

The *nr1d1*, *nr1d2* and *ror* genes code for nuclear receptors involved in the stabilizing loop of the circadian clock mechanism (Emery and Reppert, 2004; Vatine et al., 2011) (Figure 3.10). The *rev-erb*α and β receptors, coded by the zebrafish *nr1d1* and *nr1d2* respectively, are considered constitutive transcriptional repressors of *bmal1* whereas *ror* genes are transcriptional activators of *bmal1* (Guillaumond et al., 2005) (Figure 3.10). In addition, *nr1d1* has been recently suggested to act as a transcriptional repressor for the *bmal1* partner, *clock* (Crumbley and Burris, 2011), regulating the transcription of both positive main oscillators of the circadian mechanism (Figure 3.10). In zebrafish skeletal muscle, the expression of *nr1d2* and *rora* clustered together with

cry1a (Figure 3.9). However, *nr1d1*, *nr2d2a* and *nr2d2b* transcripts levels peaked at the end of the subjective dark period (ZT22) while transcripts of *roraa* and *rorab* were at their highest levels at the beginning of the subjective light period (ZT02-04) (Figure 3.9). This small difference in phase of expression of the two components of the stabilizing loop might reflect their tight control of regulation over the circadian mechanism which is reflected in the activation/repression of *bmal1* and *clock1* expression. In addition to their role in regulation of circadian rhythm, these genes are known transcription factors for genes involved in lipid metabolism (Duez and Staels, 2008). In the present study, a negative correlation was found between expression of *nr1d1* in skeletal muscle and gut food content in accordance with previous findings (Amaral and Johnston, 2011). It is plausible that *nrld1* may play a role in integrating circadian and metabolic rhythms in skeletal muscle.

3.5.2. Expression of putative clock-controlled genes in zebrafish skeletal muscle

In the zebrafish, the insulin-like growth factor pathway is comprised of four ligands (igf1a, igf1b, igf2a and igf2b), their respective receptors (igf1ar, igf1br and igf2r) and nine igf-binding proteins (igfbp1a, igfbp1b, igfbp2a, igfbp2b, igfbp3, igfbp5a, igfbp5b, igfbp6a and igfbp6b). Interaction between the ligands and igf1-receptors ultimately leads to tissue growth, with the binding proteins playing important roles in regulating the concentration of the ligands in the plasma and their release in target tissues. A previous work has shown that *igf1a* and *igf2b* are upregulated during feeding while *igf1ra*, *igf1rb*, *igfbp1a* and *igfbp1b* are upregulated during fasting (Amaral and Johnston, 2011). In the present study, expression of two insulin-like growth factor binding proteins genes (*igfbp3* and *igfbp5b*) was rhythmic and peaked at the onset of the dark phase (ZT14), in phase with the positive oscillators *bmal1* and *clock1* (Figure 3.9). Changes in mRNA expression have been shown to be propagated to the protein level in hundreds of genes in another teleost, *Fundulus heteroclitus* (Rees et al., 2011). Thus, large changes in transcript levels are likely to be reflected in protein levels with effects on biological functions. Over-expression, knockdown and knockout systems have been previously employed to study the biological importance of the igf-binding proteins in skeletal muscle [reviewd in (Duan et al., 2010)]. Most circulating IGF in the plasma is found to be conjugated to igfbp3, and this binding protein serves as a modulator of the IGF action in target tissues by prolonging hormone half-life (Firth and Baxter, 2002; Yamada and Lee, 2009). Igfbp3 also has IGF-

independent actions in inhibiting cell proliferation in cancer lines (Yamada and Lee, 2009). Igfbp5 is known to play a crucial role in muscle growth and differentiation [reviewed in (Duan et al., 2010)] and circadian expression of this growth-related gene has been previously reported in the skeletal muscle of mouse (Miller et al., 2007). Given the importance of igfbp3 and igfbp5 in the growth axis and the involvement of the clock pathway in the cell cycle a plausible hypothesis is that the cyclic expression of these two IGF binding proteins is related to the local regulation of cell-cycle and growth.

Myogenic regulatory factors (myoD, myf5, myf6 and myogenin) (MRFs) are a class of helix-loop-helix transcription factors that play a pivotal role in myogenesis (Hinits et al., 2007; Chen and Tsai, 2008; Chong et al., 2009). *Myf6* (also known as MRF4) was shown to function in myogenic determination and differentiation in myf5:myoD double knockout mouse (Kassar-Duchossoy et al., 2004). Myf6 was found to play an important role in muscle fibre alignment in zebrafish embryos, using the morpholino technique to knockdown two splice-variants of *myf6* transcripts (Wang et al., 2008). In the present study, the expression of myf6 was not correlated with food intake in C3, but it did exhibit a circadian expression pattern peaking in phase with *bmal1* and *clock1* at the beginning of the subjective dark period (Figure 3.7C). Similar circadian patterns of *myf6* expression were reported previously in skeletal muscle of the horse, a mammalian species with higher physical activity during daylight hours (Martin et al., 2010). In the mouse, *myoD* is a direct target of clock and bmal, which bind in a rhythmic fashion to the core enhancer in the *myoD* promoter (McCarthy et al., 2007; Andrews et al., 2010). Clock$^{\Delta 19}$ and Bmal1$^{-/-}$ mutants showed similar phenotypes to myoD$^{-/-}$ mutants with reduced force generating capacity relative to wild-types due to a disruption of myofilament organisation (Andrews et al., 2010). In contrast, no evidence was found for circadian expression of myoD in zebrafish (Figure 3.3). It is plausible that the well-known redundancy of MRFs may have resulted in lineage-specific differences in their regulation by clock genes. A plausible hypothesis would be that the rhythmic expression of *myf6* in zebrafish muscle parallels that described for *myoD* in mouse muscle, with potential effects on the maintenance of myofibrillar structure.

The rhythmic expression of the chaperone transcriptional regulator *hsf2* was previously described in the pineal tissue of chicken (Hatori et al., 2011) and zebrafish larvae (Weger et al., 2011). The expression of two chaperone genes (*hsp90a.1* and *hsp90a.2*) in zebrafish skeletal muscle showed no discernible pattern of periodicity with

respect to photoperiod, while expression of *hsf2* was rhythmic and peaked at onset of lights on, in phase with the negative oscillator *cry1a* (Figures 3.3 and 7D). The role of *hsf2* as a clock-controlled gene in the circadian output is not known, but evidence from experiments with chicken point to the activation of specific stress-response factors in response to light (Hatori et al., 2011). In zebrafish larvae expression of *hsf2* was concomitant with expression of genes involved in the response of oxidative stress and chaperone genes (Weger et al., 2011). Exposure to light is known to cause oxidative stress through production of hydrogen peroxide in zebrafish cells (Hirayama et al., 2007; Hirayama et al., 2009) with subsequent activation of stress-responsive genes, including the (6-4) pyrimidine-pyrimidone dimer DNA photolyase involved in DNA repair (Hirayama et al., 2009). The production of hydrogen peroxide and subsequent activation of stress-responsive genes and the MAPK signalling pathway has recently been considered one of the potential mechanisms that render peripheral tissues to be photoreceptive and photoresponsive, since these events regulate transcription of *cry1a* in the zebrafish with noticeable effects on the circadian mechanism (Hirayama et al., 2007; Hirayama et al., 2009; Vatine et al., 2011).

In the present chapter the expression of the main oscillators of the clock mechanism in the skeletal muscle of the zebrafish was characterized (Figure 3.10). Most of these genes had a similar expression pattern to that described for the central organs (retina and brain) of the circadian mechanism [reviewed in (Vatine et al., 2011)]. In addition, evidence is provided that differences exist in the responsiveness of *clock1* and *nr1d2* paralogues to circadian stimuli and the loss of a circadian rhythm for *cry1b* in skeletal muscle. Finally, gene expression of two igf-binding proteins (*igfbp3* and *igfbp5b)* and a myogenic regulatory factor (*myf6*) involved in IGF-mediated growth and terminal muscle differentiation in fish, respectively, were identified as clock-controlled gene in zebrafish skeletal muscle. This finding points to an important physiological role of the clock mechanism in regulating muscle mass homeostasis through integration with the IGF pathway and MRFs. These studies provide a foundation for investigating the integration of the clock system with physiological processes in teleosts. In addition, the finding that the circadian expression of many genes in this peripheral tissue is similar to those described for organs considered central photoreceptive and pacemakers of the circadian mechanism is valuable for future investigations on the hierarchy of the systemic clock, i.e.,

the integration between the neuroendocrine signals from the pineal, the central pacemaker organ, and peripheral clocks in fish.

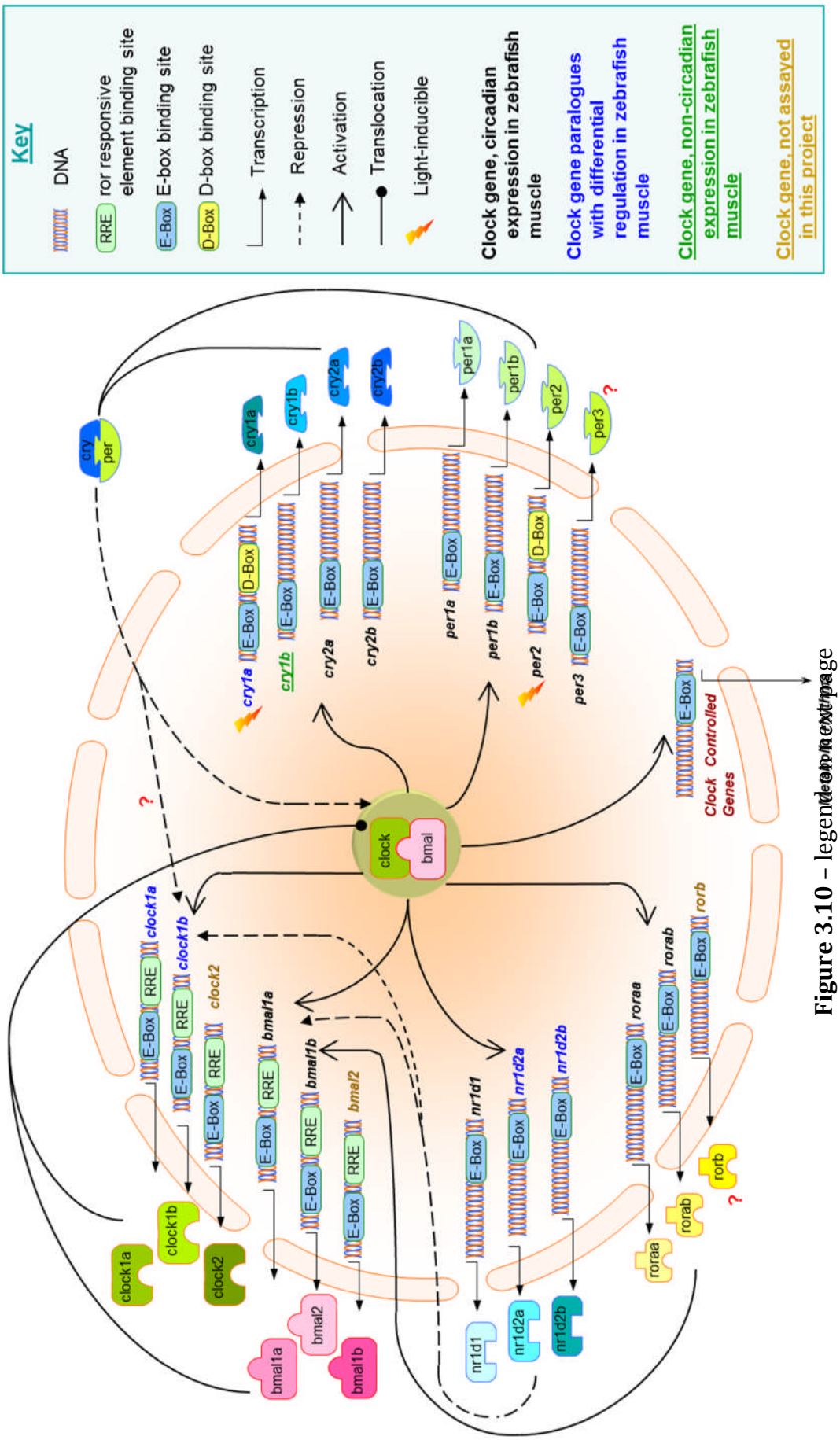

Figure 3.10 – legend in next page

Figure 3.10. Diagram of the molecular circadian mechanism in the zebrafish. *Bmal* and *clock* genes are considered the central oscillators of this pathway due to their ability to modulate the expression of the remaining components through a transcription-translation regulation mechanism. In the zebrafish bmal1a, bmal1b, bmal2, clock1a, clock1b and clock2 form heterodimers in the nucleus and activate the expression of period (*per*) and cryptochrome (*cry*) genes. The expression of *bmal1a, bmal1b, clock1a* and *clock1b* were highly correlated in skeletal muscle and occurred in phase with each other. From the four cry genes investigated in this study, only *cry1b* did not follow a circadian expression. Per and cry proteins are components of the negative arm of the circadian pathway due to their ability to form dimers in the cytoplasm, translocate to the nucleus and represses the activation of expression by bmal: clock heterodimers. In mammals, after translocation to the nucleus the cry protein dissociates from the cry: per complex and directly represses the expression of *clock*. The expression of the negative oscillators *per* and *cry* in skeletal muscle of the zebrafish followed a circadian pattern that is very similar to the one described for organs considered master regulators of the circadian rhythm (retina and brain). Similarly, the expression of *roraa*, *rorab*, *nr1d1*, *nr1d2a* and *nr1d2b* followed a circadian rhythm of expression in zebrafish skeletal muscle. In the present experiment, the circadian expression in response to the photoperiod from the gene expression was distinguished from expression due to rhythmic feeding. This diagram was produced based on the recent review on the zebrafish clock mechanism (Vatine et al., 2011), on the information on the circadian pathway for mammals from Applied Biosystems (http://www5.appliedbiosystems.com/tools/pathway/), and on the results of the present study.

4. Experimental selection of zebrafish for body size at age: effects on early-life history traits and gene expression in skeletal muscle

4.1. Summary

In the present study the short generation time of the zebrafish (*Danio rerio*) was exploited to investigate the effects of selection for body size at age on early life-history traits and on the transcriptional response to a growth stimulus in skeletal muscle of adult fish. A wild-derived population of zebrafish was subjected to four rounds of artificial selection to produce fish divergently selected for small (S-lineage) and large body size (L-lineage) at 90 days post-fertilization. A third lineage was produced in which fish were not selected (U-lineage). Standard length and body mass of fish from the L-lineage was 5.1 and 15.7% higher than fish from the U-lineage and 12.3 and 41.9% higher than fish from the S-lineage. Egg volume from the S-lineage was 5.9% smaller with 4.5% less yolk than the other lineages. The levels of a limited number of maternal transcripts in the 2-4 cell stage embryos were affected by the artificial selection. For example, eggs from the L-lineage showed higher transcript levels for *igf1b*, *igf2a*, *GH-receptors*, *igf1ar* and *igf2r*. Larvae from the L-lineage were significantly larger, but survivorship at the end of the first month was not affected by the selection regimen. The pattern of expression of 11 nutritionally-responsive genes and 8 genes from the insulin-like growth factor pathway was similar in skeletal muscle of adult fish from S- and L-lineages in response to fasting and refeeding. However, 9 (*igf1a, igf2a, igf1ar igf1br, igf2r, igfbp1a, igfbp1b, klf11b* and *myod*) of the 32 genes studied showed a significantly different response to either fasting or refeeding between the S- and L-lineages. This difference in expression could not be explained by different levels of acquired nutritional energy since the two lineages showed a very similar feed intake. The change in expression also seems to be directional according to the observed phenotype. For example, fish from the L-lineage showed higher expression of *igf1a* (constitutive expression) and igf1 receptors (mainly during satiation periods) whereas fish from the S-lineage showed higher constitutive expression of *igbp1a/b* transcripts.

4.2. Introduction

Somatic growth is a very complex trait since it involves all metabolic pathways that control energy acquisition (food ingestion) and energy expenditure (food assimilation, locomotion, reproduction, and maintenance of the existing body mass). Endocrine pathways play a crucial role in orchestrating the energy utilization in these different biological processes. Thus, inheritable variations in the gene and regulatory sequence of genes of endocrine pathways are good candidates for explaining differences in growth trajectory within and between populations. Experimental selection of model organisms like *C. elegans*, *Drosophila* and mice has been proved a valuable tool for the investigation of molecular mechanisms underlying changes in phenotype (e.g. thermal tolerance, body composition and longevity). For example, body fat and growth rate of mice have been correlated to leptin and growth hormone (GH) genes using lineages divergently selected for voluntary locomotor activity (Girard et al., 2007) and body composition (Bunger and Hill, 1999), respectively.

In fish, experimental selection has been mainly used to investigate the effects of domestication on behaviour and growth, the latter being an important consideration in commercial fish culture. For example, after 16 generations of selection for rapid growth, domesticated coho salmon (*Oncorhynchus kisutch*) grew faster than unselected strains with satiation feeding, possibly due to the higher feed intake and feed conversion efficiency (Neely et al., 2008). However, changes in phenotype due to high experimental selection pressure can occur rather faster as evidenced by a change in behaviour after four generations of selection for growth rate in Atlantic silverside (*Menidia menidia*), when a higher feed intake was recorded for the selected lineage (Lankford et al., 2001; Chiba et al., 2007). More recently, experimental selection has been used as a tool to investigate the molecular mechanisms underlying the physiological changes leading to different phenotypes of selected lines. In many cases, the GH-IGF pathway is investigated as the main underlying endocrine mechanism of differences in growth observed between selected lineages due to the direct and indirect anabolic effects of GH. The indirect effects of GH are mainly realised by the IGF pathway, in which igf1 and igf2 are the ligands. Binding of the IGF ligands to igf1r leads to phosphorylation of the PI3K/AKT/mTOR pathway which is responsible for the activation of expression of growth-related genes and repression of transcription of genes that function in protein

degradation, resulting in the anabolic effects of IGF (Rommel et al., 2001). However, binding of IGFs to igf2r results in lysosomal degradation of the ligand and is probably a mechanism of regulating the concentration of circulating IGFs (Lau et al., 1994; Wang et al., 1994). The availability of circulating IGFs and its binding to the respective receptors is also regulated by the IGF-binding proteins (IGFBPs) (Wood et al., 2005a). Thus, changes in the GH-IGF axis might explain some of the effects of domestication observed in selective breeding programs in fish culture. For example, channel catfish (*Ictalurus punctatus*) selected for fast growth for two generations had lower plasma cortisol levels and higher muscle *igf2* mRNA than fish selected for slow growth, leading to the conclusion that the differences in growth were partially explained by the GH-IGF and stress axis (Peterson et al., 2008). A microarray experiment comparing wild-type coho salmon with a GH-transgenic and domesticated fish (12 generations) found that transcriptional responses were similar in the two latter strains compared to the wild-type fish, leading to the hypothesis that domestication affected similar downstream components as in GH-transgenic fish (Devlin et al., 2009). Changes in the components of the GH-IGF axis can also explain decreased growth phenotypes. For example, the investigation of the transcriptional responses to fasting and feeding in five dwarf populations compared to two generalist populations of Arctic charr (*Salvelinus alpinus*) reported a higher expression of *igfbp4* and lower expression of *mTOR* and *4e-bp-1* (two proteins that regulate protein synthesis) in the dwarf populations, leading to the conclusion that parallel adaptive changes in gene expression occurred in the dwarf populations (Macqueen et al., 2011).

The zebrafish (*Danio rerio*) is an excellent model for experimental selection due to its short generation time, available knowledge on its development and physiology, and extensive available molecular tools. In addition, the transcriptional regulation of the IGF system in skeletal muscle have been recently characterized in the zebrafish (Amaral and Johnston, 2011). The aims of this chapter were to produce zebrafish lineages artificially selected for divergent body size and to investigate the effect of the experimental selection on some early life-history traits of embryo and larval stages. In addition, the hypothesis that the transcriptional regulation in skeletal muscle in response to a growth stimulus differs between zebrafish lineages selected for divergent body size was tested. To this end expression levels of transcripts from the IGF axis,

nutritionally-responsive genes and myogenic regulatory factors was investigated in adult fish from the artificially selected lineages in response to fasting and refeeding.

4.3. Materials and methods

4.3.1. Fish husbandry and artificial selection for body size

The study was conducted on the F3 generation of wild-caught zebrafish (*Danio rerio*, Hamilton) from Mymensingh, Bangladesh (27 males and 28 females). Fish were reared in 10L tanks at 27^{o}C ± 0.3^{o}C (range) under a 12h light: 12h dark photoperiodic regime in a filtered freshwater recirculation system and fed to satiation twice daily with bloodworms. Replicated unselected (U), small (S) and large (L) lineages were bred from a random selection of 18-19 fish per lineage (sex ratio ~1 female: 1 male) derived from the founder population (Table 4.1). All breeding was conducted at ~120 days post-fertilization (dpf) when fish were sexually mature. Briefly, for each lineage previously separated, male and female fish were introduced into a breeding tank and eggs were collected each morning for 3 days. Eggs were immediately cleaned and maintained in glass tanks (1L) under the same environmental conditions as the main recirculation system. After 7dpf the larva were fed ZM-100 (Fish Food Ltd., Hampshire, UK) and microworms. 50% of the water was changed twice daily until 30dpf, when fish were transferred to the main recirculation system and fed to satiation with ZM-200 (Fish Food, Hampshire, UK) and bloodworms (Ocean Nutrition™, Belgium) twice daily. Three rounds of artificial selection were conducted based on body size at ~90dpf (see Table 4.1). For the S-lineage, fish with standard lengths (SL) (tip of snout to last vertebrae) greater than 75% of the mean SL for the population were removed from the breeding population at each generation. The L-lineages were generated by removing fish with SLs less than 125% of the mean SL for the population. A third line was produced in which fish were not selected (U-lineage) (Figure 4.1A). The percentage of each lineage selected for breeding in the next generation was 46-52% (L-lineage), 63-75% (S-lineage) and 100% (U-lineage) and this had little impact on the sex ratio of the populations. The number of fish used to produce the 2nd, 3rd and 4th generations ranged from 24 to 78 per replicated lineage (Table 4.1). As part of routine husbandry procedures SL, fork length (FL), total length (TL), maximum body depth (H) and body mass (BM) were measured periodically to access the growth and health of all populations in the colony.

Table 4.1 – Number of individuals in the zebrafish populations from each generation produced during this study. (dpf: days post-fertilization)

	Lineages					
Parents	S-Lineage		U-Lineage		L-Lineage	
Number of Fish	18		19		18	
First Generation (G1)	S1.G1	S2.G1	U1.G1	U2.G1	L1.G1	L2.G1
Age at Selection (dpf)	96	87			96	89
Number of Fish Before Selection	24	32	57	35	46	78
Fish Selected	15	22	57	35	23	36
Second Generation (G2)	S1.G2	S2.G2	U1.G2	U2.G2	L1.G2	L2.G2
Age at Selection (dpf)	90	108			86	109
Number of Fish Before Selection	35	34	35	42	46	117
Fish Selected	26	24	35	42	26	55
Third Generation (G3)	S1.G3	S2.G3	U1.G3	U2.G3	L1.G3	L2.G3
Age at Selection (dpf)	96	101			107	117
Number of Fish Before Selection	36	39	48	38	78	60
Fish Selected	27	26	48	38	43	31
Fourth Generation (G4)	S1.G4	S2.G4	U1.G4	U2.G4	L1.G4	L2.G4
Age at Selection (dpf)	95	90			96	91
Number of Fish Before Selection	38	35	36	39	38	37
Fish Selected	38	35	36	39	38	37
Fifth Generation (G5)	S1.G5	S2.G5	U1.G5	U2.G5	L1.G5	L2.G5
Age at Selection (dpf)	166	163	165	165	164	164
Number of Fish Before Selection	56	52	43	47	64	68
Fish Selected	30	30	43	47	30	30

4.3.2. Early life-history traits of zebrafish egg and larva

Embryos from the 4th generation of artificial selection were collected in the first hour after fertilization and photographed using an AxioCam CCD camera (Zeiss, Göttingen, Germany) and a Leica Wild M3Z stereo microscope (Leica, Heerbrugg, Switzerland) at 10x magnification. Egg and yolk size were calculated by measuring the ferret diameter of 100 eggs and their yolk, respectively, from three different spawns from each lineage, using ImageJ V. 1.42i software (National Institutes of Health, Bethesda, MD, USA). Deformities in the animal pole representing developmental abnormalities were also recorded. The embryos were then reared in glass bowls as described above until 30dpf,

and the mortality was checked twice per day. The TL of 50 larva from each lineage was measured at 6dpf, corresponding to the time when the yolk was almost completely assimilated and the larvae were free swimming.

4.3.3. Quantitative PCR (qPCR) of maternal transcripts

Maternal transcript levels were measured by qPCR in the 4th generation of selection using 12 replicates of 60 embryos per lineage using SYBR II chemistry (Stratagene, La Jolla, CA, USA). Embryos at the 2-4 cell stage were collected at 1 h after fertilization and snap frozen in liquid nitrogen for total RNA extraction using Tri-reagent (Sigma, St Louis, MO, USA) and subsequent first strand cDNA synthesis using a Quantitect Reverse Transcription Kit (Qiagen, Hilden, Germany). cDNA at 40-fold dilution were used as working solutions. Primer pairs for the 16 known genes of the IGF system in the zebrafish (Table 2.1) and myogenic regulatory factors (MRFs) (Table 3.1) were as described previously. New primers were designed to amplify "fecundity genes" (*bmp15* and *gdf9*) and their receptors (*bmpr1aa*, *bmpr1ab*, *bmpr1ba*, *bmpr1bb*, *bmpr2a*, *bmpr2b*), and growth hormone and its receptors (*ghra* and *ghrb*) (Table 4.2). qPCR procedures were compliant with MIQE guidelines (Bustin et al. 2009) and have been described in detail previously (section 2.3.8). In order to establish the best normalization strategy, the expression of 13 reference genes (Table 2.1) were analysed across lineages using Genorm v3.5 (Vandesompele et al., 2002) with M set to <1.5. qPCR efficiency was calculated using LinRegPCR V. 12.5 software (Heart Failure Research Center, Amsterdam, Holland) (Table 4.2). Transcripts levels expressed in arbitrary units were calculated using the mean efficiency of 72 reactions with posterior normalization to the level of the two most stable reference genes (*tomm20b* and *ef1a*, M=0.129). The specificity of each qPCR assay was validated by direct sequencing of the PCR product.

Table 4.2 – Sequence and properties of primers used in chapter 4. Ensembl gene symbols, forward (f) and reverse (r) primer sequences, product size, efficiency (E) product melting temperature (Tm) and Ensembl gene ID are shown.

Ensembl Gene symbol	f/r	Primer 5'-3' sequence	Product Size (bp)	E	Tm (°C)	Ensembl Gene ID
		"Fecundity genes" and their receptors				
bmp15	f:	GCCCGGTCTGAGACTCTGC	334	103.4	84.6	ENSDARG00000037491
	r:	CTGAAGATCACTTGATGTTGGGAG				
gdf9	f:	TCAAGCAAAACAGAGAATTCTTCATG	239	104.5	83.5	ENSDARG00000003229
	r:	GTGATGGACGCGGAAGCTG				
bmpr1aa	f:	TGGACTCCCTCTGCTGGTGC	224	104.0	83.5	ENSDARG00000019728
	r:	CAGCAGCGATAAAGCCGAGTA				
bmpr1ab	f:	GCTCCCCCTGCTGGTTCA	222	108.1	83.5	ENSDARG00000045097
	r:	TCTGCAGCTATGAAGCCGAGT				
bmpr1ba	f:	GCCGTCAAGTTCATCAGCGA	198	116.4	83.5	ENSDARG00000005600
	r:	TATACCTCCGGTGACGCAGC				
bmpr1bb	f:	GAACATACTGGGCTTCATCGCA	309	100.4	87.6	ENSDARG00000031219
	r:	CTGATGAACTTGACAGCGAGGC				
bmpr2a	f:	GCAAACAACAACAACAGCAATAACA	313	96.5	86.6	ENSDARG00000011941
	r:	CGACAGACCTGCCTCCTAGTAATG				
bmpr2b	f:	CAGTGAGGTGGGCACGATCC	306	96.4	86.0	ENSDARG00000020057
	r:	AGAGAGCGCACAGCCAGGC				
		Growth Hormone and its receptors				
gh1	f:	AAAAATGATTAACGACTTTGAGGAA	116	88.7	84.1	ENSDARG00000038185
	r:	CTTTTCCCGTCGGCGTCT				
ghra	f:	CTCCCAGCAGCAGAGGTTGATG	216	95.7	81.9	ENSDARG00000054771
	r:	GAATTCTTCTTATCTGCAGGATCGTC				
ghrb	f:	GAAAAGGATCCAAAGAAAACTTACGG	196	96.0	78.2	ENSDARG00000007671
	r:	CTACAGGTGGGTCTGGAAACACAATA				

4.3.4. Fasting-refeeding experiment

Fish from G5 were used to investigate the effect of the artificial selection on the transcriptional response to nutrient levels in the skeletal muscle. Two replicates from the S- and L-lineages were reared to adult stage in the conditions described in section 4.3.1, population densities during development were the same for all replicates (N~160 fish per tank). At 9 months of age, 50 male fish were randomly collected from each lineage and transferred to a separate tank, where they were fed bloodworms to satiety twice daily for two weeks (acclimation period). Food was withdrawn and, after one week of fasting, feeding was resumed. 6 fish from each lineage were collected at -170h (just before the fasting period), 0h (just before refeeding the fish), 1, 3, 6, 24 and 48h after resuming the feeding (Figure 4.1B). The feeding schedule after the 0h time-point was the same as during the acclimation period. Fish were killed by an overdose of ethyl 3-aminobenzoate methanesulphonate salt (MS-222) (Fluka, St Louis, MO, USA) and had their TL and BM measured. Fast skeletal muscle was dissected from the dorsal epaxial myotomes, flash frozen in liquid nitrogen and stored at -80^{o}C prior to total RNA extraction. The digestive tract was dissected and fixed in 4% (m/v) paraformaldehyde for later quantification of intestine content to the nearest milligram. The transcription levels of the 15 genes of the IGF system, 2 ubiquitin ligases, 12 known nutritionally responsive genes (Table 2.1), and the 4 myogenic regulatory factors (Table 3.1) in skeletal muscle were measured by qPCR. Total RNA extraction, first strand cDNA synthesis and dilution, and qPCR procedures were as described in the sections 2.3.5 and 2.3.8.

4.3.5. Statistical analysis and data transformation

Growth patterns were modelled using Growth II software (Pisces Conservation Ltd., New Milton, UK). The data on size at age of the different lineages were fitted to six growth models (von Bertalanffy, exponential, 3 parameters Gompertz, 3 parameters logistic, 4 parameters Gompertz and 4 parameters logistic) and the one with the lowest Akaike Information Criterion and Schwarz Criterion was chosen. To facilitate the interpretation of the relation between SL and BL in the different populations, these measurements were transformed by raising to the power 0.33 and log transformation respectively. A general linear model (GLM) was used to test the effect of selection on the

proportionality among body size measurements (SL, FL, TL, H, and BM) using PAWS Statistics 18 software (SPSS Inc., Chicago, Illinois, USA). T-test in Paws Statistics (SPSS Inc.,) was used to compare the body size at age between sexes. The chi-square test in R V. 2.10.0 software was used to analyse the sex-ratio among the zebrafish populations at sexual maturity. All data were tested for equality of variance and normal distribution, and ANOVA followed by Tukey post-hoc test using PAWS Statistics 18 software (SPSS Inc.,) or Kruskal-Wallis followed by Conover post-hoc test using Brightstat (Stricker, 2008) was employed to analyse normally distributed and non-normally distributed data, respectively. Bonferoni-corrected p-values lower than 0.05 were considered statistically significant for gene expression data from the maternal transcripts and fasting-refeeding experiments. Data from genes with similar expression between the S- and L- lineage for all time-points of the fasting and refeeding experiment were combined to produce a heatmap of gene expression independent of fish lineage. The heatmap was produced using the PermutMatrix software (http://www.lirmm.fr/~caraux/PermutMatrix/EN/index.html), with gene expression normalized for rows and McQuitty's method used for hierarchical clustering.

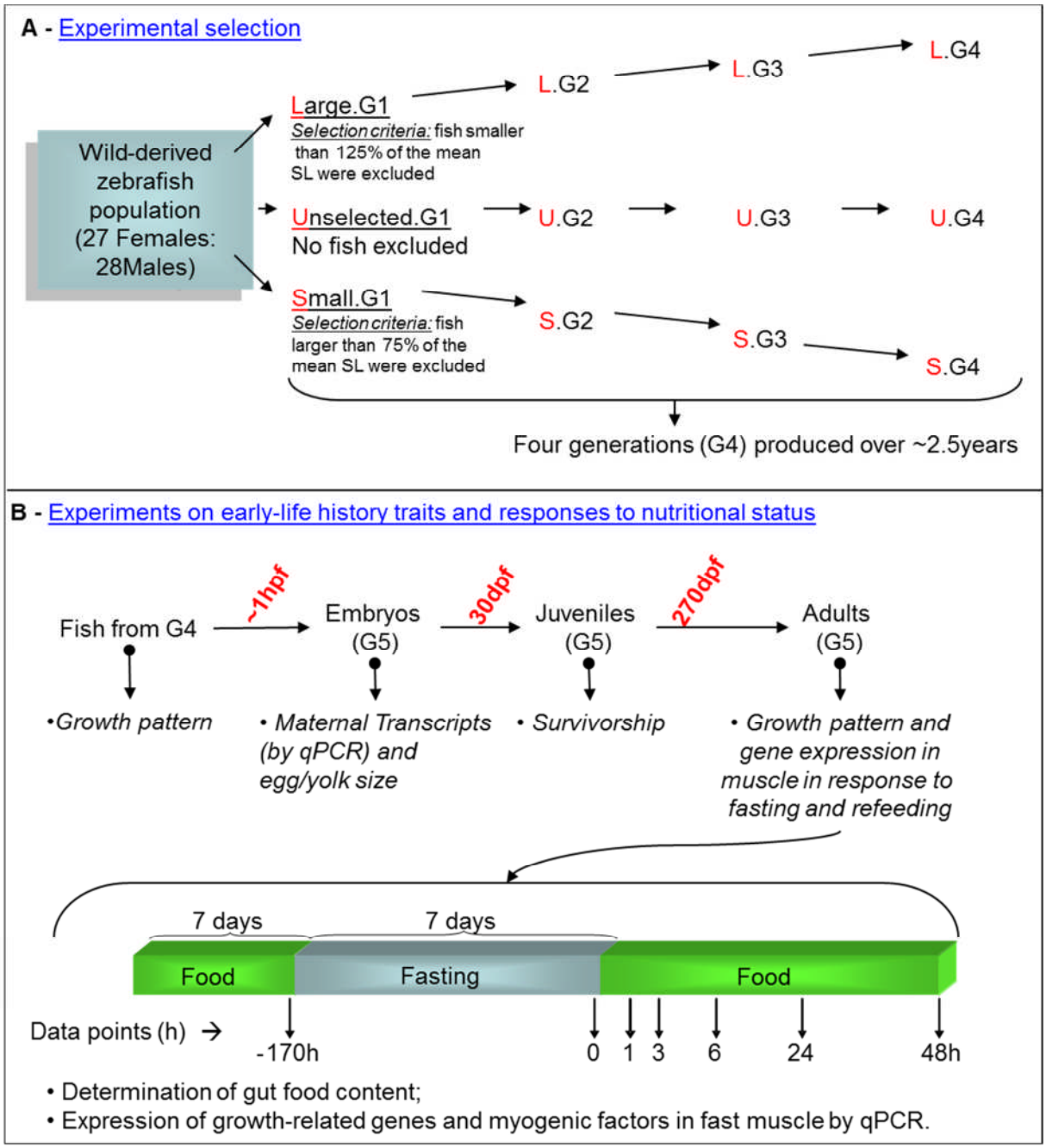

Figure 4.1 – Experimental design for artificial selection (A) and fasting and refeeding protocols (B). Fish from a wild-derived population of zebrafish were separated according to size and used to produce four generations of fish divergently selected for small (S-lineage), unselected (U-lineage) and large body size (L-lineage). Eggs and embryos from G5 were used to investigate the effects of selection for body size on early life-history traits and maternal transcripts levels. Adult fish from G5 were used to investigate the effects of selection for body size on the transcription level of genes of interest in skeletal muscle in response to fasting and refeeding. The growth pattern from embryo to adult stage was determined for fish from G4 and G5.

4.4. Results

4.4.1. Effects of selection for body size on growth pattern

Average SL for fish from the fourth generation of the S-lineage was 2% lower when compared to the founding population (an average of 0.6% loss in SL per generation), while an average increase of 10% in SL was recorded for fish from the L-lineage in the fourth generation (gain in SL of 3.3% per generation). The relationship between various measures of body length (SL, FL, TL and H) and BM were independent of sex and lineage (GLM, $p>0.05$). However, a significant difference in body size at age between sexes was observed, with females having a larger body size than males in all lineages. The sex-ratio of adult fish among the replicate populations from each lineage was close to 1:1 (chi-square test, p-value=0.6). This allowed for the comparison of the body size and growth rate of the lineages without considering sex as a confounding variable. Based on the Akaike Information Criterion (AIC), which measures the closeness of the experimental points to the model, the best model for growth was a 4 parameter Gompertz equation (Figure 4.2). In this model SL follows a sigmoid curve with an inflection point (when growth rate starts to decrease) at 1/3 of age of when the fish reach the predicted maximum body size. There was a statistically significant difference in body size at age among the three different populations observable from 120dpf (Figure 4.3A). Body size measurements between the replicates of a given lineage were not statistically different when adult stage was reached and therefore were pooled to facilitate the interpretation of results (Figure 4.3A, insert). Fish from the L-lineages reached a maximum standard length of 32.9mm at 390dpf, which corresponded to 6.8 and 12.3% larger SLs than fish from U- and S-lineages (Figure 4.3A). These differences of body size at age between the two selected lines from G4 are in accordance with the change in SL per generation (~12%, described in the first sentence of this section). The average BM of the L-lineages (0.521g) was 22.8 and 41.9% greater than the U- and S-lineages at 390dpf (Figure 4.3C). The data on body size at age allowed only for the calculation of the average growth rates from each lineage which were 0.194, 0.181, and 0.173 mm/d for the L-, U-, and S-lineage, respectively, during the exponential phase of growth between 6 and 120 dpf.

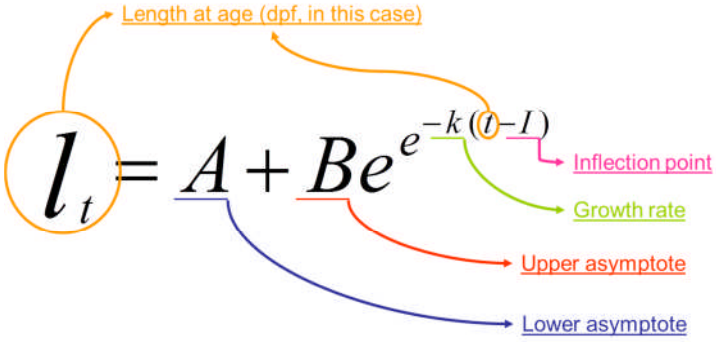

Figure 4.2 – 4 parameters – Gompertz growth equation.

4.4.2. Effects of selection for body size on early life-history traits of zebrafish

The production of eggs per breeding batch in the 4th generation was 5-times greater in the L- than the S-lineages (Table 4.3). Eggs from the S-lineages had a small (5.7%) but significantly reduced diameter than eggs from the L-lineages, corresponding to 18% less yolk (Table 4.3). Three waves of mortality were observed in all lineages peaking at <24h (embryos), 2-4d (yolk-sac larvae) and 8-15d (free swimming larvae). The embryos from L-lineage had the highest rates of deformity and mortality in both first (~12%) and second waves (40%), followed by the U- and S-lineages (Table 4.3). In the third wave, however, this scenario was reversed, with the S-lineage having the highest mortality (~64%) when compared to the other lineages. At the end of the juvenile stage these differences in mortality seem to have been equalized since the survival rate at 30dpf was around 30% for all three lineages (Table 4.3). The average TL of larvae at 6dpf just prior to complete yolk absorption was ~3.7, 3.6, and 3.4mm for the L-, U-, and S-lineages (Table 4.3).

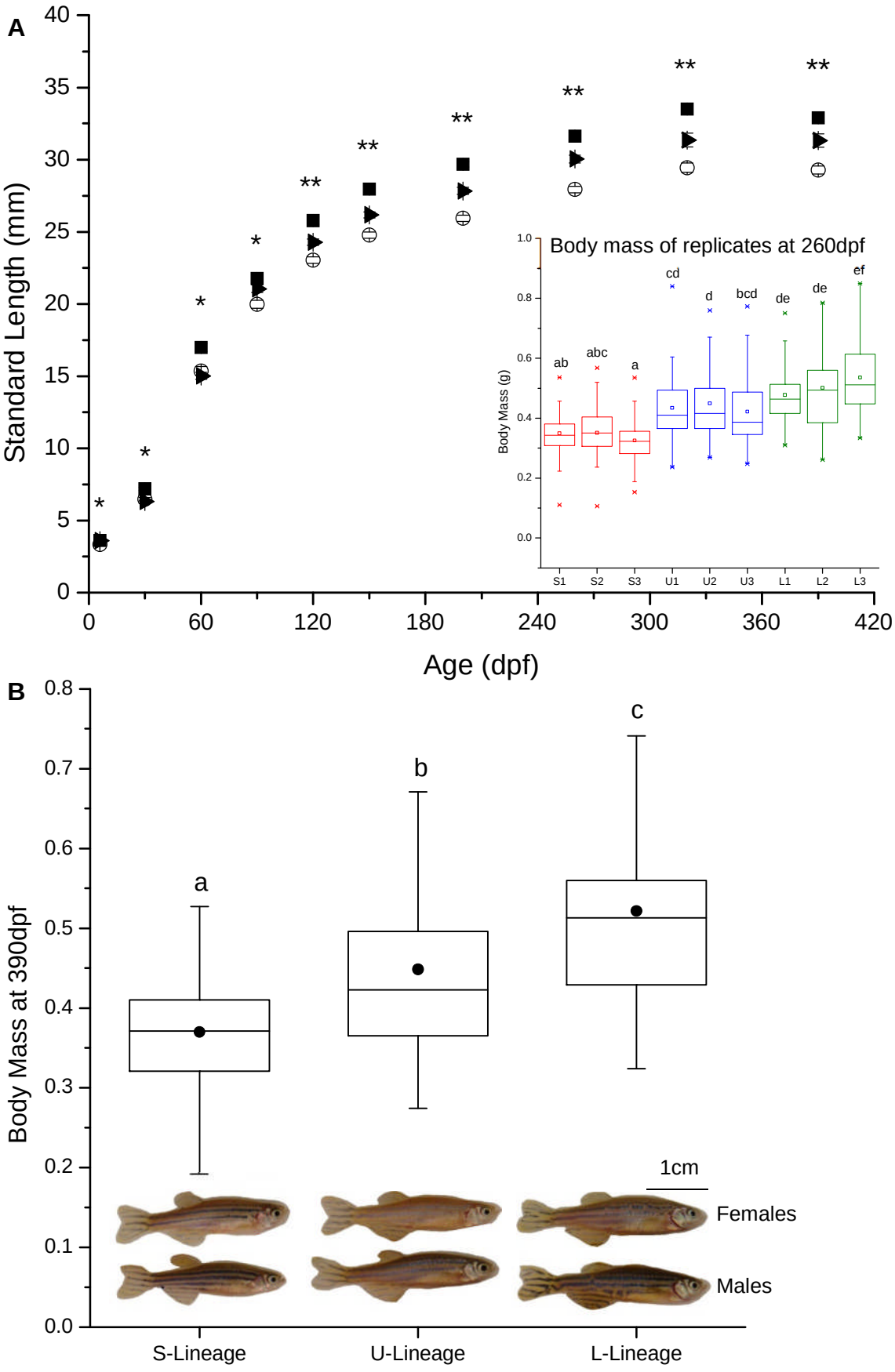

Figure 4.3 – legend on next page.

Figure 4.3 – Growth curve from 6 to 390dpf and body mass at 390dpf of the selected zebrafish lineages. (A)Standard length of zebrafish from S- (○), U- (►) and L-lineages (■) after three rounds of selection for body size (A), symbols and error bars represent mean and s.e.m., respectively. One asterisk above data-points means significant statistical difference in at least one population in comparison to the others at the same age; two asterisks means that the body size of the three lineages are different at the same age (ANOVA followed by post-hoc Tukey test with p-value set to 0.05). (A, insert) body mass at 260dpf of the three replicates lineages of zebrafish. (B) Body mass of zebrafish lineages at 390dpf, ● represents the average body mass and different letters above the box-plot means significant statistical difference (ANOVA followed by post-hoc Tukey test with p-value set to 0.05). Males and females representatives of the average body size at 390dpf of each lineage are shown in the bottom panel (C).

Table 4.3 – Effects of four rounds of artificial selection for body size at age on early life-history traits of eggs and larvae. Values given are average ± s.d.m., different superscript letters across the lineages means statistically significant difference in early-life traits among the zebrafish lineages.

Early-life trait in chronological order	Zebrafish Lineage		
	S-lineage	U-lineage	L-lineage
Eggs per spawning	389 ± 49 ^{a}	1,045 ± 153 ^{a}	1,956 ± 591 ^{b}
Yolk diameter (mm)	0.63 ± 0.02 ^{a}	0.65 ± 0.02 ^{b}	0.66 ± 0.02 ^{c}
Egg diameter (mm)	1.10 ± 0.05 ^{a}	1.18 ± 0.04 ^{b}	1.17 ± 0.03 ^{b}
Embryos with developmental deformities (%)	0.9 ± 0.3 ^{a}	3.6 ± 0.1 ^{b}	12.8 ± 1.1 ^{c}
Mortality from 2 to 6dpf (%)	5.0 ± 0.4 ^{a}	18.0 ± 1.8 ^{b}	40.0 ± 0.9 ^{c}
Total length of larvae at 6dpf (mm)	3.42 ± 0.13 ^{a}	3.56 ± 0.14 ^{b}	3.67 ± 0.14 ^{c}
Mortality from 7 to 30dpf (%)	64.0 ± 2.9 ^{a}	47.0 ± 0.2 ^{b}	32.0 ± 4.8 ^{c}
Survival rate at 30dpf (%)	29.0 ± 4.3 ^{a}	33.0 ± 0.7 ^{a}	28.0 ± 3.3 ^{a}

4.4.3. Effects of selection for body size on maternal transcripts

Growth hormone (GH) mRNA was 1.4 and 1.9-fold higher in eggs from the U- than the S and L-lineages respectively (Figure 4.4). In contrast, *igf1a* transcripts were 1.4-fold more abundant in eggs from the L-lineage than both the S- or U-lineages and *igf1a* transcripts were not detected (Figure 4.4). *Igf2a* and *Igf2b* transcripts were also significantly higher in the L- than either the U- or S- lineages (Figure 4.4). Strikingly, *igf2a* mRNA was 5.6-times more abundant in the L-lineage than the other lineages ($P<0.01$). Four of the five IGF and GH receptors (*ghra, ghrb, igf1ar* and *igf2r*) were similarly higher in the L- than S-lineages by an average of 1.4-fold whereas there was no difference in *igf1br* transcripts between lineages (Figure 4.5). Transcripts of *igfbp2a*, *igfbp5b*, and *igfbp6b* were not detected at the developmental stage studied. *Igfbp1a* and *igfbp3* were 46 and 29% higher whereas *igfbp1b* was 5-fold lower in the L- than the U- or S-lineages respectively. *Igfbp6a* mRNA increased in the series, U- > L- > S-lineage (Figure 4.6).

Transcription factors from the Myogenic Regulatory Family (MRF) function in directing the fate of embryonic cells to myogenic cells and in differentiation in a later stage. Transcripts from three MRFs were detected in fertilized eggs of the zebrafish, while *myog* was not detected. mRNA levels were higher in the L-lineage than in either the U- or S-lineages for myoD (2.5-fold), myf5 (1.4-fold) and myf6 (1.4-fold) (Figure 4.7).

In mammals the transcription level of *bmp15*, *gdf9* and their receptors were found to correlate well with fecundity, and are also known as "fecundity genes". The increase in egg production by the L-lineage of zebrafish could not be explained by the expression of the ligands *bmp15* and *gdf9* since there was no statistically significant difference in the levels of the transcripts for *bmp15, gdf9*, in the eggs of the selected lineages (Figure 4.8). In contrast, *bmpr1aa* and *bmpr1bb* transcripts were 1.4-fold higher in the L- than the S-lineages. A very small but significant difference was observed for transcripts of *bmpr1ab* in the U-lineage when compared to both S- and L-lineages (around 6% higher). In the case of *bmpr2b,* transcript levels increased in the series S- > L- > U-lineages across a 6-fold range of abundance, while no difference was recorded for *bmpr1ba* and *bmpr2a* transcripts (Figure 4.8).

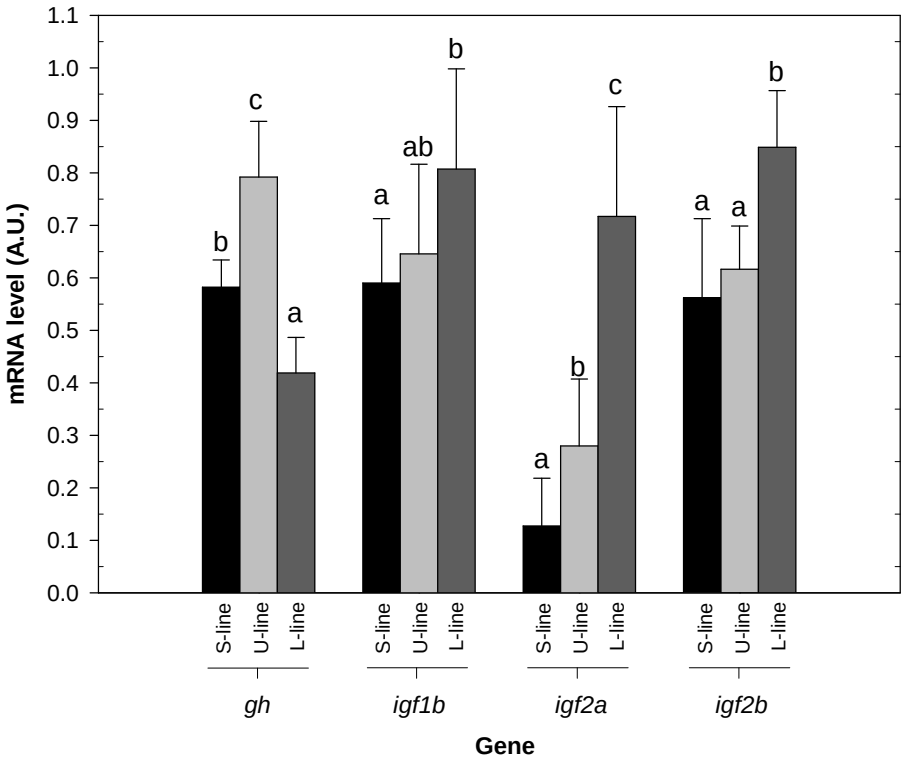

Figure 4.4 – Maternal transcripts of growth hormone and insulin-like growth factors in zebrafish embryos from S-(black bars), U-(light-gray bars) and L-lineages (dark-gray bars). Data-points and error bars represent mean and s.e.m. (n=12), respectively. Different letters above columns of the same gene means statistically significant difference (Kruskal-Wallis followed by post-hoc Conover test with Bonferoni correction for multiple comparisons, $P<0.05$).

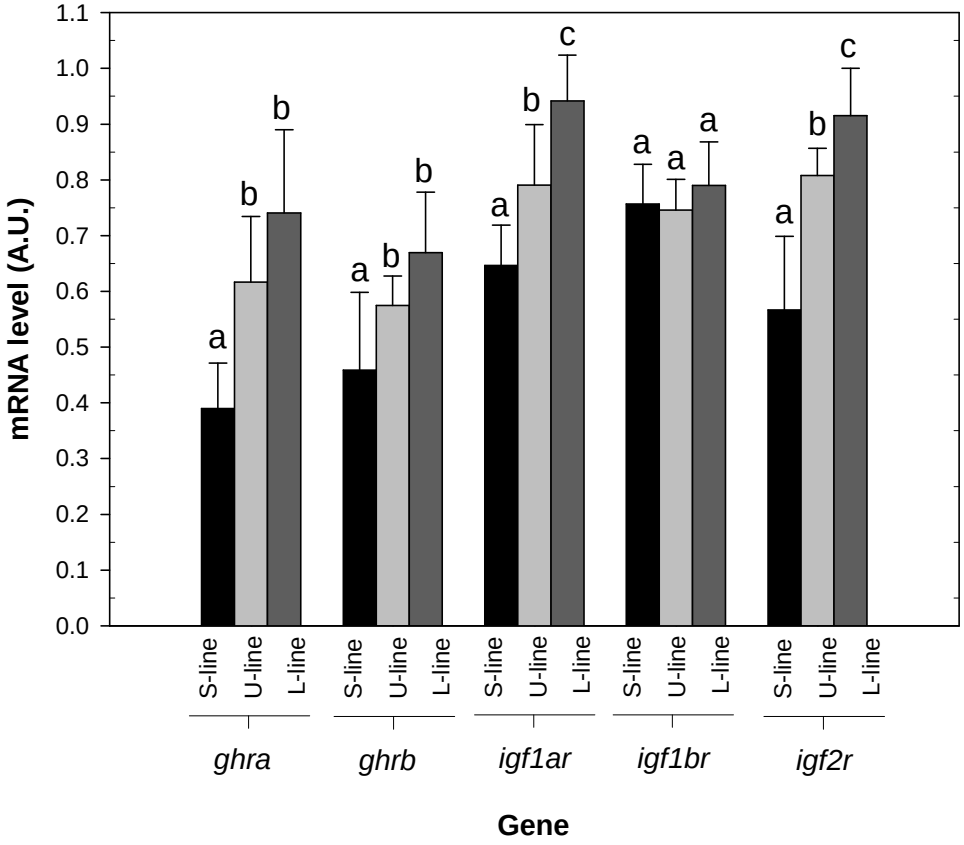

Figure 4.5 – Maternal transcripts of receptors of growth hormone and insulin-like growth factors in zebrafish embryos from S-(black bars), U-(light-gray bars) and L-lineages (dark-gray bars). Data-points and error bars represent mean and s.e.m. (n=12), respectively. Different letters above columns of the same gene means statistically significant difference (Kruskal-Wallis followed by post-hoc Conover test with Bonferoni correction for multiple comparisons, $P<0.05$).

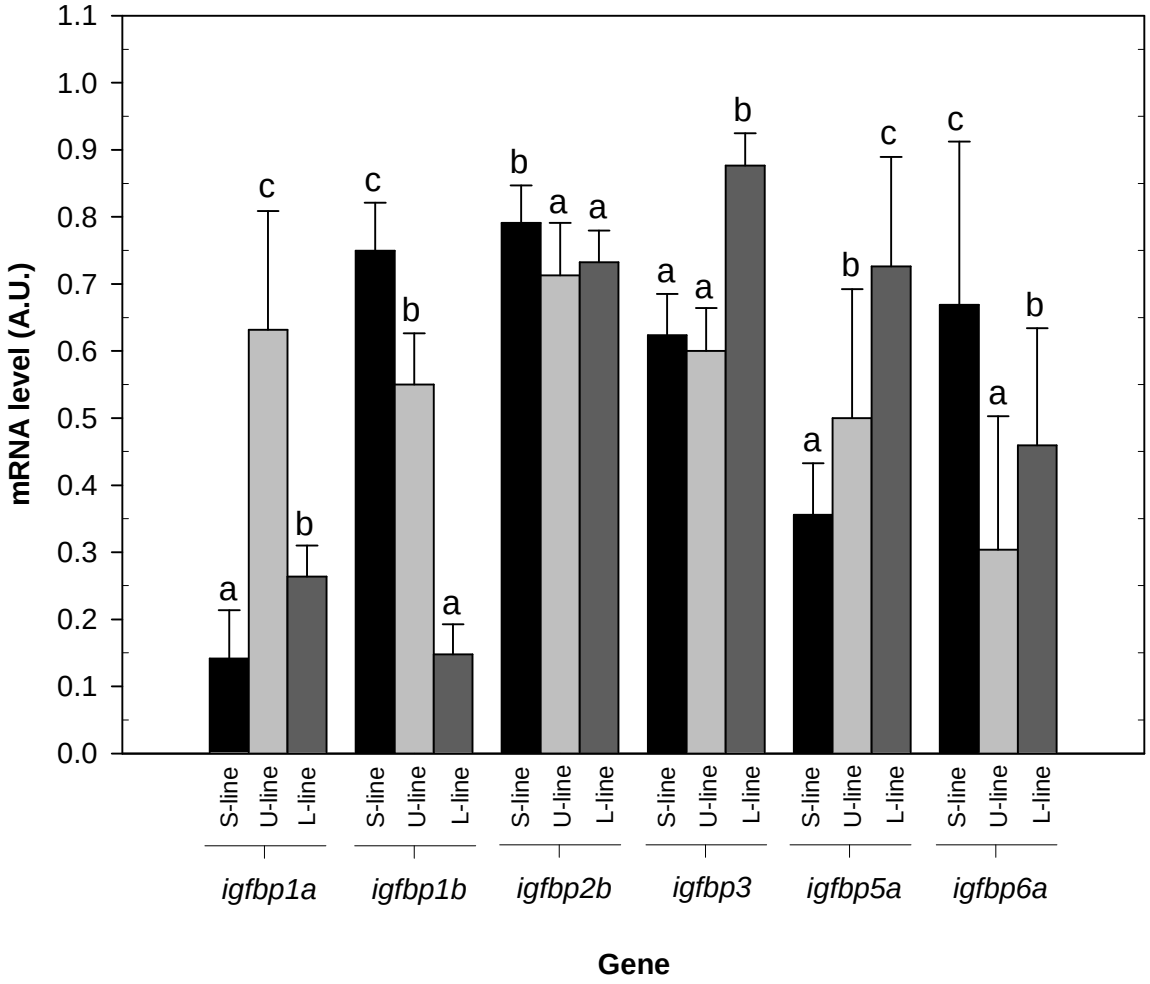

Figure 4.6 – Maternal transcripts of insulin-like binding proteins in zebrafish embryos from S-(black bars), U-(light-gray bars) and L-lineages (dark-gray bars). Data-points and error bars represent mean and s.e.m. (n=12), respectively. Different letters above columns of the same gene means statistically significant difference (Kruskal-Wallis followed by post-hoc Conover test with Bonferoni correction for multiple comparisons, $P<0.05$).

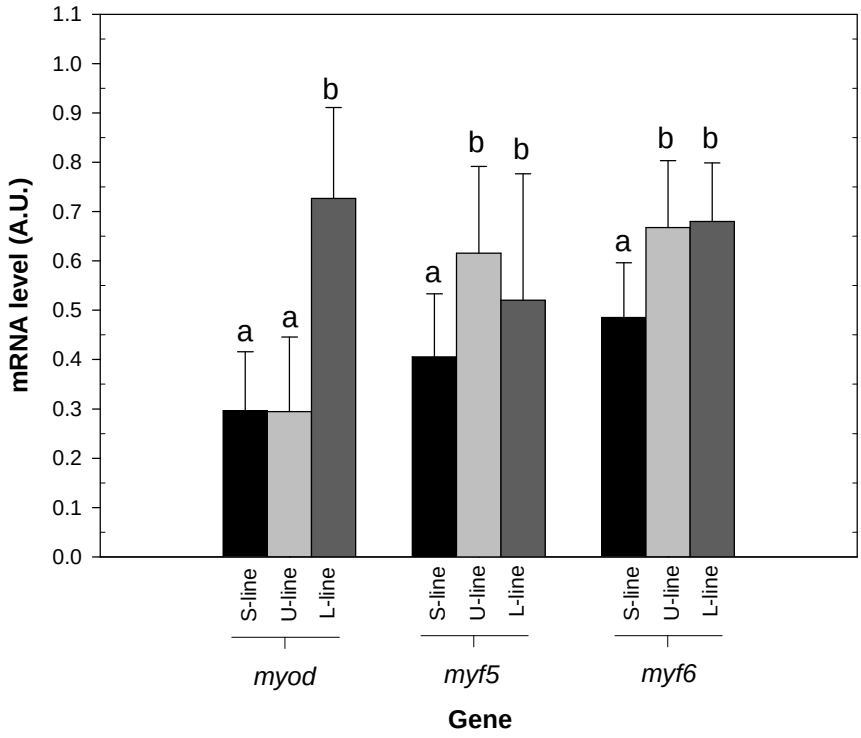

Figure 4.7 – Maternal transcripts of myogenic regulatory factors in zebrafish embryos from S-(black bars), U-(light-gray bars) and L-lineages (dark-gray bars). Myogenin transcripts were not detected in the zebrafish embryo at this stage. Data-points and error bars represent mean and s.e.m. (n=12), respectively. Different letters above columns of the same gene means statistically significant difference (Kruskal-Wallis followed by post-hoc Conover test with Bonferoni correction for multiple comparisons, $P<0.05$).

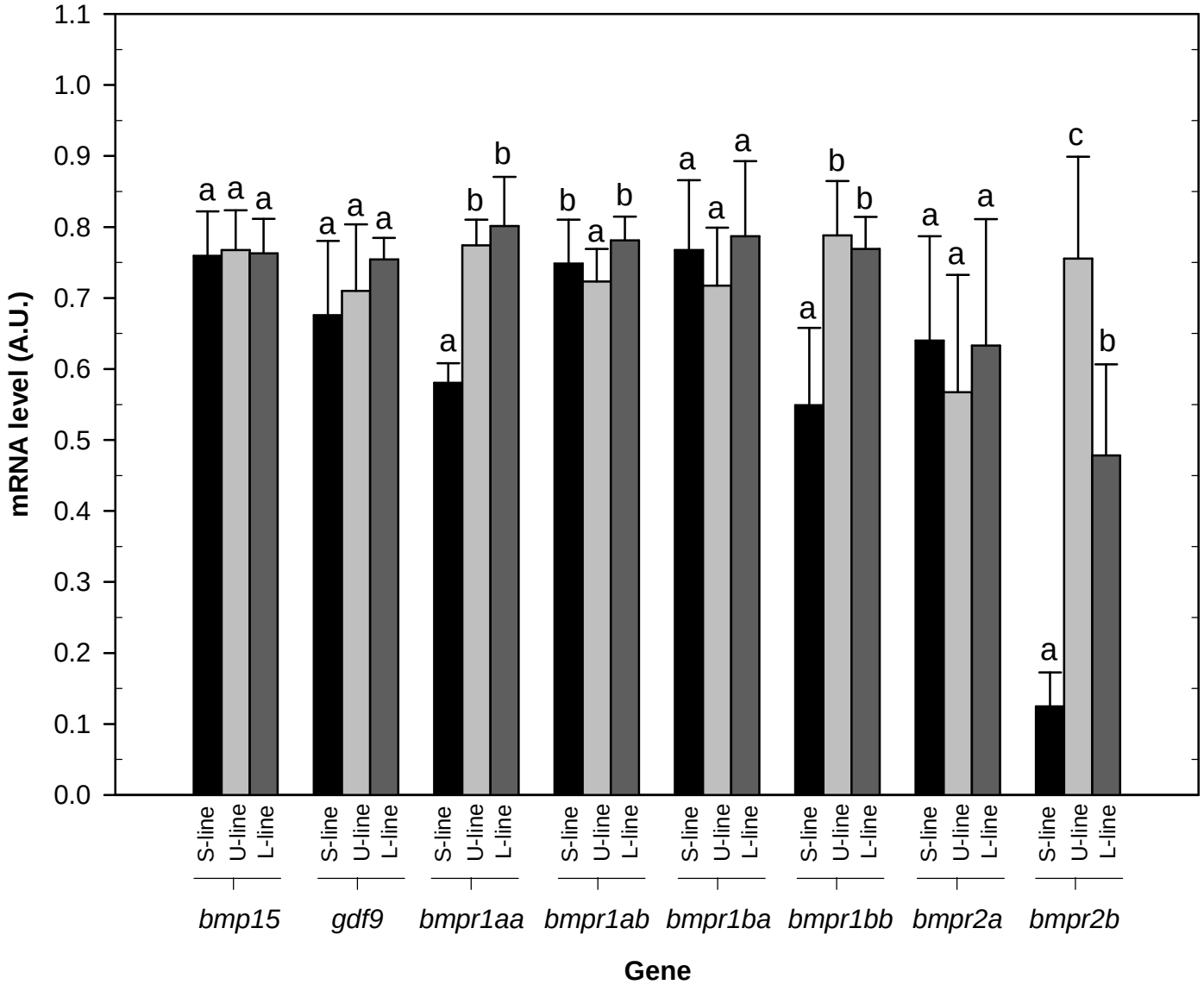

Figure 4.8 – Maternal transcripts of "fecundity genes" and their receptors in zebrafish embryos from S-(black bars), U-(light-gray bars) and L-lineages (dark-gray bars). Data-points and error bars represent mean and s.e.m. (n=12), respectively. Different letters above columns of the same gene means statistically significant difference (Kruskal-Wallis followed by post-hoc Conover test with Bonferoni correction for multiple comparisons, $P<0.05$).

4.4.4. Effects of selection for body size on muscle gene expression in adults

The S- and L-lineages had a similar feeding response across the fasting and refeeding experiment, with no noticeable difference between the two lineages. The gut food content decreased from 1.4 (% of body mass) at -170h to 0% after 7d of fasting. After feeding was resumed the gut food content increased to 4.0, 3.3, and 4.0% at 1, 3 and 6h respectively. At 24 and 48h the gut food content was similar to that found before the fasting period (~1% of body mass), indicating fasting resulted in a transient increase in food intake following refeeding (Figure 4.9).

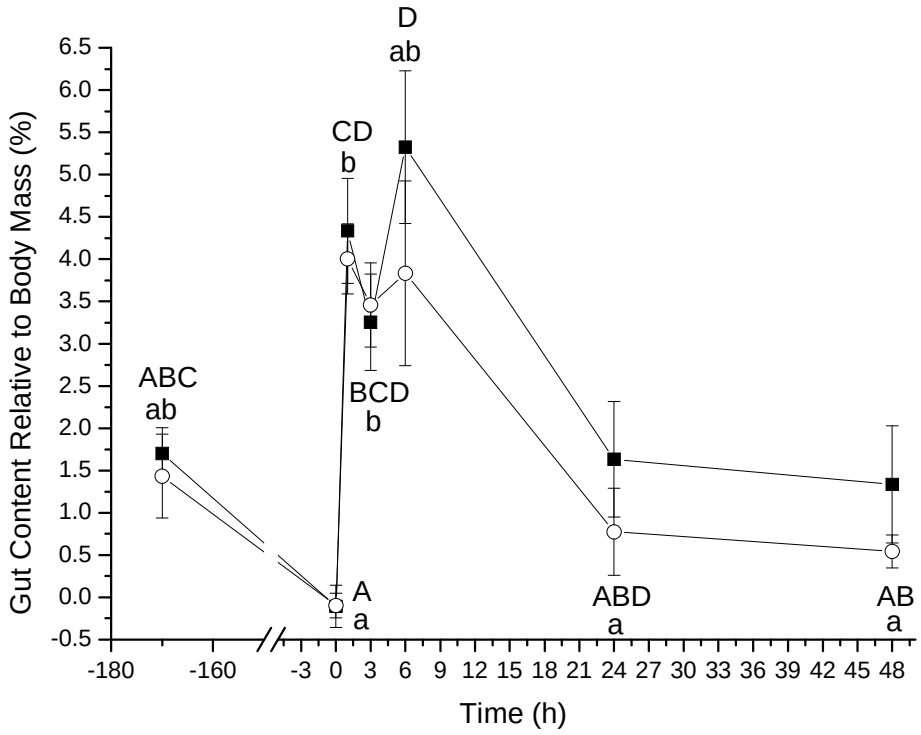

Figure 4.9 – Gut food content of S- (○) and L-lineages (■) in response to fasting and refeeding. Symbols and error bars represent mean and s.e.m., respectively, N=6 fish per lineage per time-point. Different letters above symbols represent statistically different means among time-points for the S- (lowercase letters) and L-lineages (uppercase letters), at $P<0.05$. The gut food content was similar between the two lineages at every time-point at $P<0.05$.

The expression of 8 out of 15 genes from the IGF system was very similar in the S- and L-lineages in response to the fasting and refeeding experiment. Similarly, no significant difference was observed for 11 out of 12 other nutritionally-responsive genes and the 2 ubiquitin ligases [*mafbx* and *trim63 (murf1)*] in the two lineages. The transcript levels of these genes in relation to the gut food content (Figure 4.10A) were comparable to that reported previously (Amaral and Johnston, 2011).

The expression levels of three MRFs (*myogenin*, *myf6* and *myf5*) were similar in both S- and L-lineages, with no discernible pattern of expression for *myf6* and *myogenin* in response to fasting and refeeding (Figure 4.10C,D). In contrast, a small downregulation of *myf5* was observed from 0 to 1h (fasting period), with a subsequent upregulation from 6 to 48h after feeding was resumed (Figure 4.10B). From the 33 genes assayed only 9 (*igf1a, igf2a, igf1ar, igf1rb, igf2r, igfbp1a, igfbp1b, myoD* and *kruppel like factor 11b – klf11b*) showed a significant degree of variation in expression between the S- and L-lineages. In all cases the artificial selection regime modified the responsiveness of the transcriptional regulation in relation to the nutrient level but not the pattern of expression. The constitutive expression of the ligand *igf1a* was around 1.5-fold higher in the L-lineage across the experiment, with a 2-fold higher expression during 6 and 48h after resuming the feeding (Figure 4.11A). Conversely, only a transient but significant difference in expression of *igf2b* was observed during the fasting period, with 22% fewer transcripts detected in the L- compared to the S-lineage during the fasting period (Figure 4.11B).

The artificial selection regime also affected the expression of all three receptors of the IGF system. However, the expression of *igf1ar* was only slighty affected by artificial selection, with a 1.5-fold higher expression in the L-lineage as the only difference in expression of this gene across the experiment between the two lineages (Figure 4.11C). The expression of *igf1br* was 2-fold higher in the L-lineage during the fasting period (0 and 1h). Interestingly, this scenario was reversed during the refeeding period when the transcript levels were around 40% less in the L-lineage from 24 to 48h (Figure 4.11D). On the other hand, the constitutive expression of *igf2r* was 1.5-fold higher on average in the L-lineage at all time-points (Figure 4.11E). Transcript levels of this gene gradually increased as the gut emptied and a very gradual downregulation was observed during the refeeding period for both lineages (Figure 4.11E).

The constitutive level of expression of both *igfbp1a* and *igfbp1b* was around 30% less in the L-lineage across the experiment (Figure 4.12A,B). The biggest difference was observed at 0h for the *igfbp1b* transcript (50% fewer transcripts in the L-lineage).

Transcription of myoD was regulated by nutrient levels and differed between selected lines, with a single peak of expression at 1h after refeeding was resumed, when ~1.7-fold more transcripts were detected in skeletal muscle of the S-lineage (Figure 4.12C).

Kruppel-like factor 11b (*klf11b*) was the only nutritionally-responsive gene with differential expression between the S- and L-lineages, with twice as much transcripts detected in the L-lineage during prolonged fasting (Figure 4.12D).

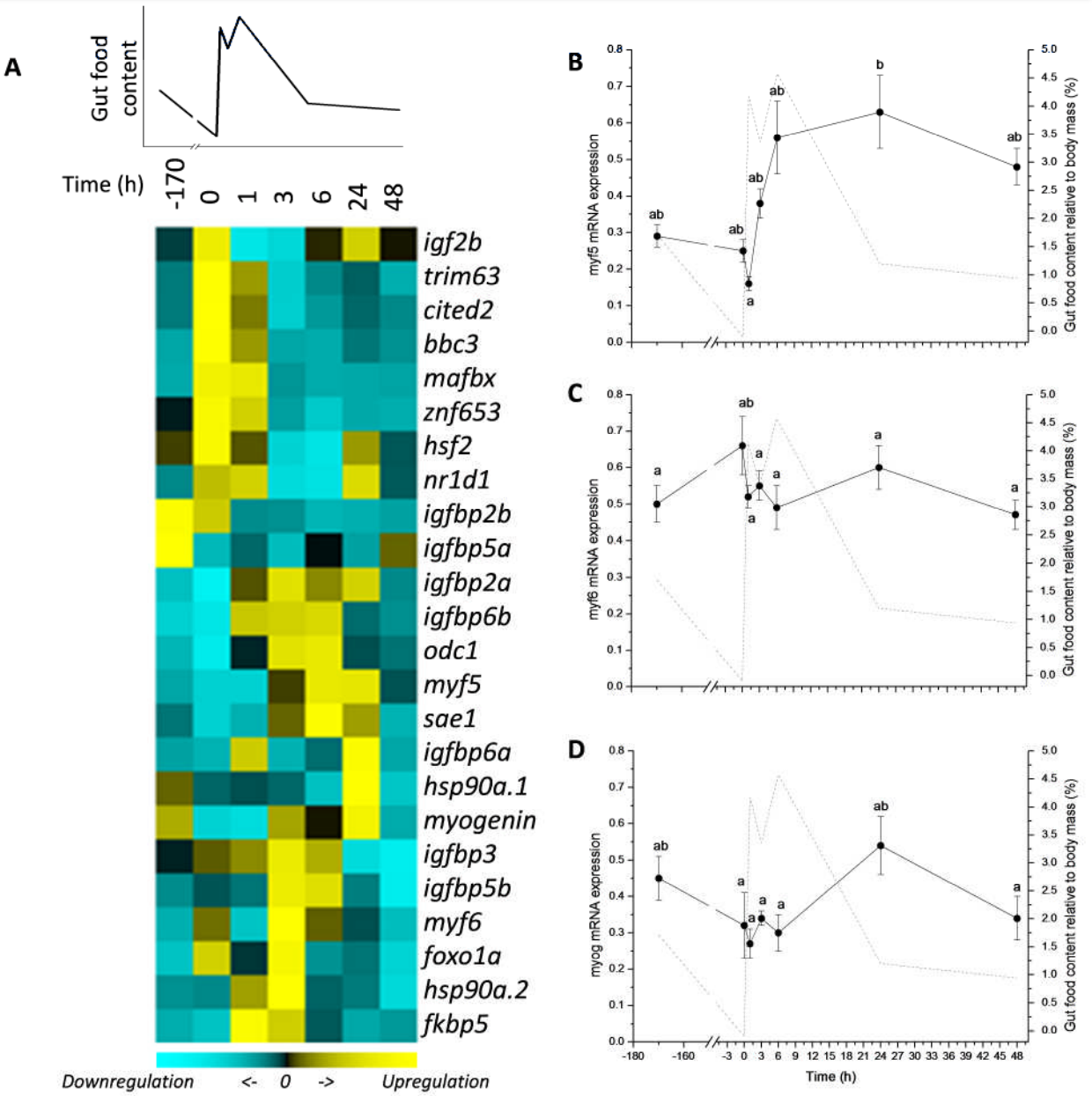

Figure 4.10 – Transcription levels that were similar for the S- and L-lineages were averaged to produce a heatmap of gene expression in response to fasting and refeeding independent of fish lineage (A). The heatmap shows the hierarchical clustering (McQuitty's method) of normalized mRNA levels across the fasting and refeeding periods – mean equals to zero and standard deviation equals to 1. Shades of yellow represent upregulation and shades of cyan represent downregulation. Each block represents the mean of mRNA level of 12 fish quantified by qPCR. The expression of *myf5* (B), *myf6* (C) and *myogenin* (D) in response to nutrient levels were similar for both lineages, with only *myf5* displaying a discernible pattern of expression in response to nutrient levels. Dashed lines in the graphs represent the gut food content and different means are represented by different letters above symbol ($P<0.05$).

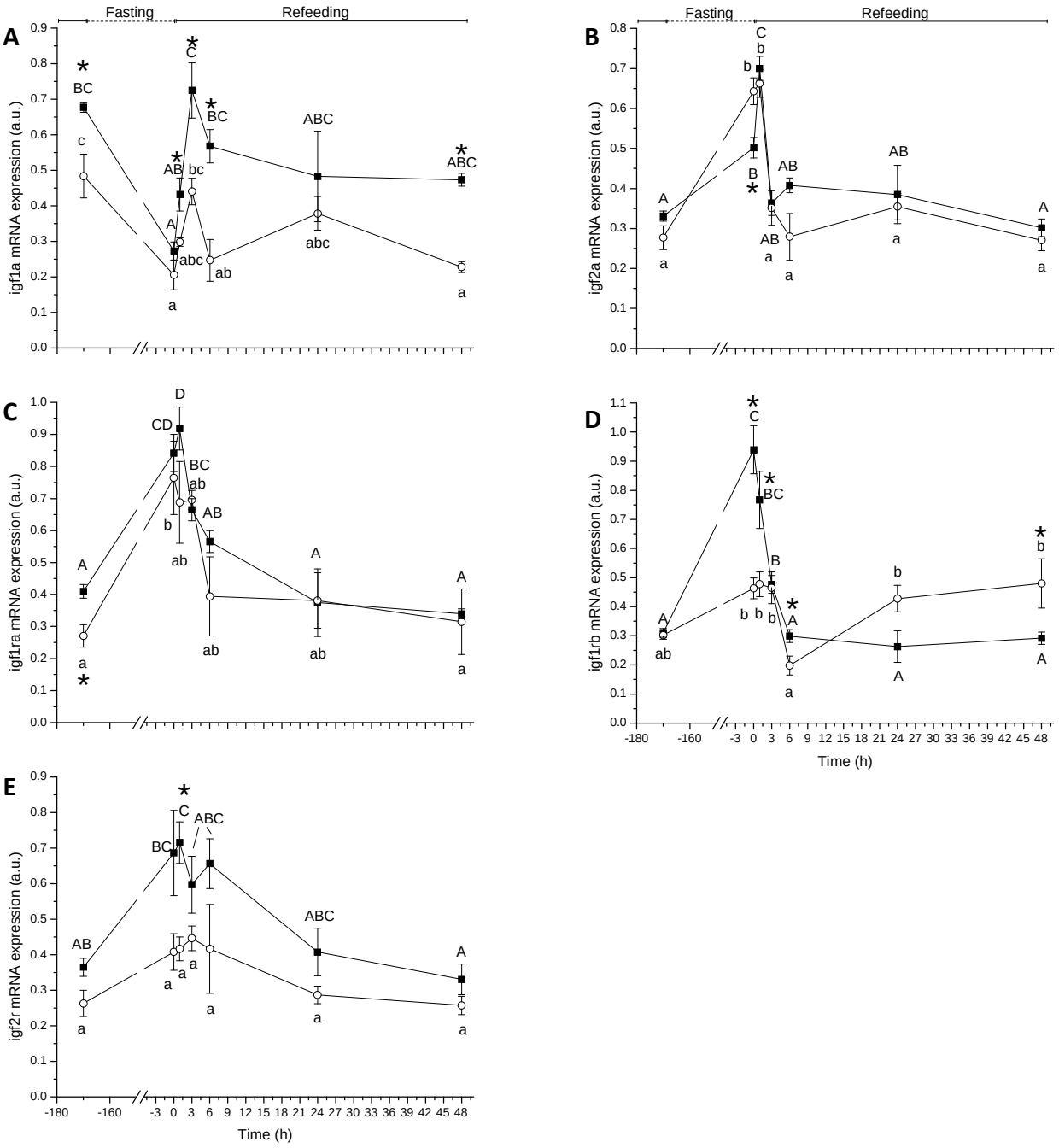

Figure 4.11 – Differential level of expression of the ligands *igf1a* (A) and *igf2a* (B), and IGF receptors *igf1ar* (C), *igf1br* (D) and *igf2r* (E) between the S- (○) and L-lineages (■) in response to fasting and refeeding. Symbols and error bars represent mean and s.e.m, respectively, N=6 fish per time-point per lineage. Different uppercase (L-lineage) and lowercase (S-lineage) letters represent statistically significant means among the time-points of the same lineage ($P<0.05$). Asterisks represent statistically different means between the S- and L-lineages at the same time-point ($P<0.05$). The solid line on the top denotes the acclimation and refeeding periods whereas the fasting period is represented by a dashed line.

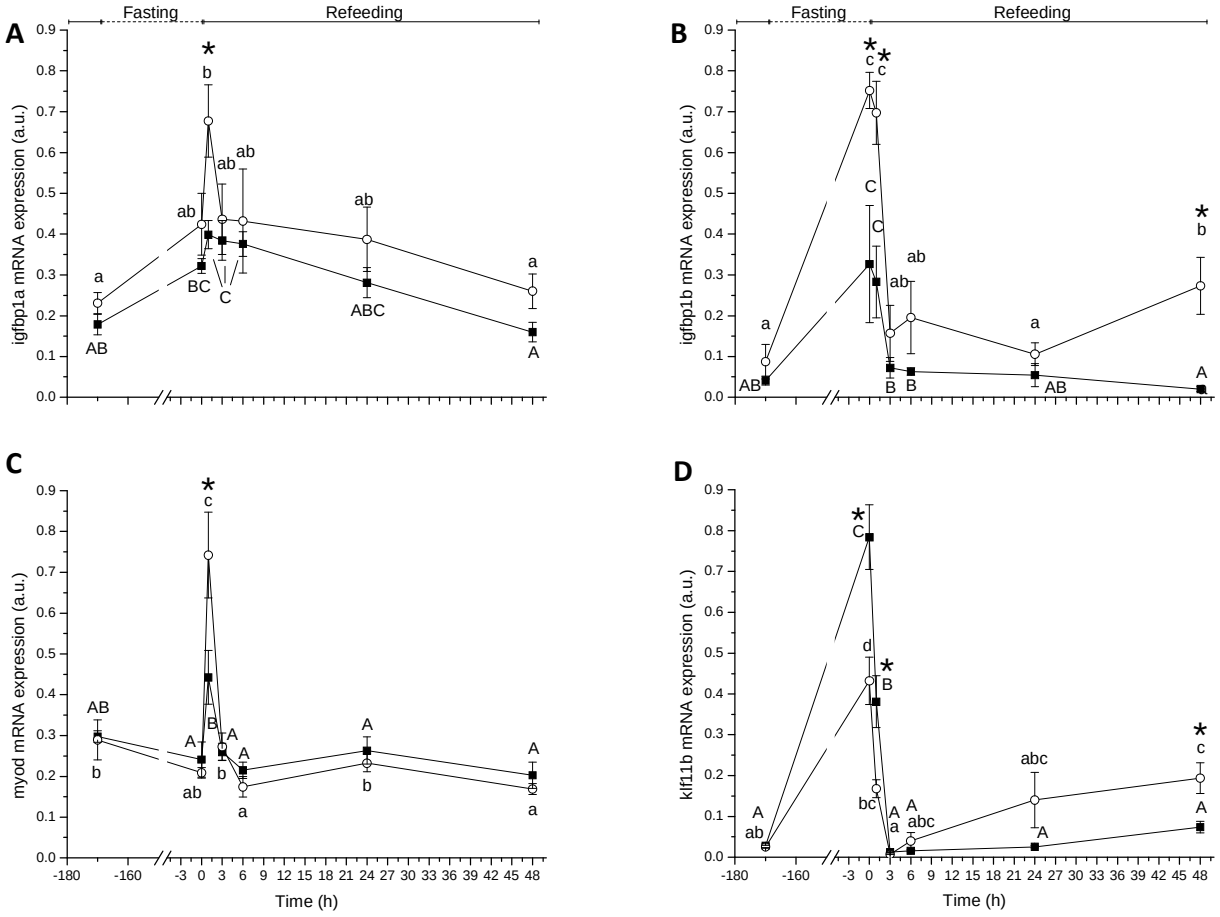

Figure 4.12 – Differential level of expression of the IGF binding proteins *igfbp1a* (A) and *igfbp1b* (B), the myogenic regulatory factor *myoD* (C), and the kruppel-like factor 11b (*klf11b*, D) between the S- (○) and L-lineages (■) in response to fasting and refeeding. Symbols and error bars represent mean and s.e.m, respectively, N=6 fish per time-point per lineage. Different uppercase (L-lineage) and lowercase (S-lineage) letters represent statistically significant means among the time-points of the same lineage ($P<0.05$). Asterisks represent statistically different means between the S- and L-lineages at the same time-point ($P<0.05$). The solid line on the top denotes the acclimation and refeeding periods whereas the fasting period is represented by a dashed line.

4.5. Discussion

After three rounds of experimental selection, the L-lineage of zebrafish showed increased growth rate and final body size when compared to U- and S-lineages. This change in body size seems to have affected the physiology of this fish at many levels. For example, larger fish produced more and larger eggs containing more yolk, which probably explains the larger body size of larvae at yolk absorption stage. Deposition of maternal transcripts was also affected by the selective breeding as evidenced by higher levels of IGFs, and GH and IGF receptors in fertilized eggs from the L-lineage compared to the S-lineage. The experimental selection also affected the transcription of a limited number of genes from the IGF-pathway in skeletal muscle of adult fish in response to a growth-stimulus, including the IGFs, IGF receptors and the nutritionally-responsive *igfbp1*, without significantly affecting the feeding intake. These findings point to a directional and differential regulation of transcript deposition in eggs and transcription in adult muscle that could contribute to the observed differences in growth with selection. The changes in the IGF pathway observed in zebrafish selected for larger body size are similar to those observed in domesticated and GH-transgenic rainbow trout (Devlin et al., 2009).

A considerably higher number of embryos were produced by the L- as compared to the S-lineage (Table 4.3), using the same numbers of fish and sex ratio per spawning. This difference in embryo production could be simply due to the differences in body mass since a strong positive relationship was previously described between body mass and egg production in the zebrafish (Forbes et al., 2010). This difference in egg production could also be due to a higher number of females ready to lay eggs which could be investigated in the future by single-pair breeding experiments. In a previous work the yolk volume of zebrafish embryos was experimentally manipulated and a clear effect of yolk volume on larvae body size was found (Jardine and Litvak, 2003). The larger body size of larvae from the L-lineage (Table 4.3) could be partially explained by the higher amount of energy available for development and growth (yolk content).

During oocyte maturation, maternal transcripts are deposited in the oocyte and are detectable until ~6hpf with varying degrees of degradation (Pelegri, 2003; Mathavan et al., 2005; Tadros and Lipshitz, 2009). The maternally-deposited mRNA are necessary for normal embryo development prior to zygotic activation (Pelegri, 2003; Dosch et al., 2004; Lubzens et al., 2010), but are also thought to partially serve as

nutritional reserves (Hunter et al., 2010). Research in this area tends to focus on observation of developmental abnormalities in zebrafish embryos triggered by chemical mutations by exposing the parents to N-ethyl-N-nitrosurea, which causes random point mutations. Although important, this approach lacks the power to investigate the changes in deposition of non-lethal transcripts, which could have milder but important and persistent effects on fitness. For example, the morpholino knockdown technology has been used to specifically and transiently block the maternal transcripts of the estrogen receptor 2a, which affected the development of the zebrafish embryo and larvae (Celeghin et al., 2011). An earlier research also showed that maternally deposited transcripts of *radar*, a TGF-β signalling molecule, is essential for the ventral fate of cells during development with loss-of-function causing lethal dorsalized phenotypes (Sidi et al., 2003). Thus, it is possible that variation in maternal mRNA deposition between families of fish is a trade-off in egg quality, with permanent effects on early life-history traits. The levels of most of the transcripts investigated in the present work have been recently reported to belong to gene clusters with very little changes between the 1- and 512-cell developmental stages in the zebrafish embryo as assayed by RNA-seq (Vesterlund et al., 2011).

The level of transcription of genes involved in fertilization (*gdf9*, *bmp15* and bmp-receptors), growth (GH-IGF axis) and myogenesis (MRFs) was investigated. No difference was observed in maternal deposition of *gdf9* and *bmp15* transcripts among the three selected lineages. These two genes are closely related members of the TGF-β superfamily with important roles in oocyte maturation in the zebrafish (Liu and Ge, 2007; Peng et al., 2009), and are thought to be involved in ovulation and fecundity. A previous work found no correlation between *gdf9* and *bmp15* levels in mature oocytes and fecundity in zebrafish populations fed four different diets (Forbes et al., 2010). It is possible, however, that ovulation and fecundity are not solely regulated at the ligands but also at the receptor level. For example, polymorphisms in *bmpr1b* correlated well with distinct prolificacy phenotypes in sheep (Chu et al., 2011). However, g*df9* and *bmp15* are not the only ligands that bind to BMP receptors, in fact these receptors are capable of recognizing and binding a number of ligands from the TGF-β family (Koenig et al., 1994; Penton et al., 1994).

The present work shows that deposition of some paralogues of the receptors for BMPs was differentially regulated among the three selected lineages, with the L-lineage

having significantly more transcripts of *bmpr1aa*, *bmpr1ba* and *bmpr2b* (Figure 4.8). Embryos from the L-lineage had more transcripts of three IGF ligands (*igf1b*, *igf2a*, *igf2b* – Figure 4.4), growth hormone receptors (*ghra* and *ghrb* – Figure 4.5) and two IGF receptors (*igf1ar* and *igf2r* – Figure 4.5) than the S-lineage. There is no information available on the effect that change in levels of these maternal transcripts might cause on zebrafish development, but experiments with morpholinos in zebrafish embryos revealed the importance of *igf1* receptors for the normal development of the embryo (Schlueter et al., 2007). Information on the effect of knockdown of *igf2r* is currently lacking. A differential deposition of *igbp1a* and *igfbp1b* in the selected lineages was observed, with *igfbp1* lower in S- than L-lineages, while the opposite was observed for *igfbp1b* (Figure 4.6). Subfunction partitioning between these two *igfbp1* transcripts in the zebrafish has been reported before, with overexpression of either binding protein causing developmental retardation (Kamei et al., 2008). However, care must be taken when interpreting these results since there is no experimental evidence that the different growth phenotypes obtained here are caused by changes in maternal deposition of these transcripts.

Variations in the regulatory sequence of genes is an important mechanism that can result in phenotypic variation and evolution (Nei, 2007). In this case, variations in the regulatory sequence would cause changes in expression of the affected gene, with a quantitative effect on biological processes upstream of gene expression. In the present work, the S- and L-lineages did not display a different feeding response (Figure 4.9), which shows that differences in growth could not be explained by changes in energy acquisition. Then, it is possible that fish from the selected lines are allocating the acquired energy in different ways, with the L-lineage allocating more energy for growth. The hypothesis that gene expression of genes from the IGF pathway is differentially regulated between the two selected lines in response to a growth stimulus was then tested.

In a previous work, the transcriptional response of the IGF pathway in skeletal muscle of the zebrafish after seven days of fasting with a single-meal as the growth stimulus has been characterized (Amaral and Johnston, 2011). Here a slight modification of the previous experiment, with *ad libitum* feeding after seven days of fasting to observe the recovery response after fasting was used. The results of

transcriptional regulation in response to fasting obtained here are very similar to those described in the previous work (Amaral and Johnston, 2011) and 23 genes showed no difference in level or pattern expression between the S- and L-lineages. In addition to the transcripts studied in the previous work, the transcriptional response of the MRFs to fasting and refeeding was investigated, with the expression of three MRFs not being affected by experimental selection. *Myf5*, a member of the MRF family involved in muscle differentiation and proliferation (Chen and Tsai, 2008), showed a clear response to fasting-refeeding with downregulation during fasting and gradual upregulation with feeding (Figure 4.10). This pattern of *myf5* expression was independent of the zebrafish lineage and has been previously described in Atlantic salmon (Bower and Johnston, 2010a). Expression of two other MRFs, *myogenin* and *myf6*, was not affect by the experimental selection with no discernible pattern in response to fasting-refeeding (Figure 4.10). Expression of *myoD* had a clear response to fasting and refeeding, with a peak of expression at 1h after fish were re-fed and expression returned to basal levels from 3h after refeeding (Figure 4.12C). MyoD was the only MRF whose expression was affected by selection. Peak expression of myoD in response to refeeding was considerably higher in fish from the S-lineage (Figure 4.12C). The pattern described here is similar to the *MyoD1b* paralogue in Atlantic salmon (Bower and Johnston, 2010a).

Only 9 genes showed different levels of expression between the S- and L-lineages, with very similar patterns of expression in response to the fasting-refeeding in the two lineages. Genes with differential expression between the two lineages included two ligands (*igf1a* and *igf2a*), the three receptors (*igf1ar*, *igf1br* and *igf2r*), two binding proteins of the IGF-axis (*igfbp1a* and *igfbp1b*), one MRF (*myoD*) and one nutritionally-responsive gene (*klf11b*).

In the zebrafish, *igf1a* is downregulated during fasting with a peak of expression in response to a single-meal, while its receptors (*igf1ar* and *igf1br*) show an opposite pattern of expression with upregulation during fasting with subsequent downregulation during refeeding (Amaral and Johnston, 2011). The selection regime affected the level of expression of these three transcripts, with the L-lineage having a higher basal expression of *igf1a* across the fasting-refeeding experiment and higher expression of the IGF receptors during the prolonged fasting period only (Figure 4.11A,C,D). IGF promotes cell growth after binding to its respective receptors, activating the

AKT/PI3K/mTOR pathway (Laplante and Sabatini, 2009). The present work shows that the L-lineage might be more responsive to the same level of energy due to a higher expression of *igf1a* and more sensitive to the ligand during fasting due to a higher availability of the respective receptors.

The present approach allowed for a better observation of the transcriptional response of *igf2r* and *igf2a* to refeeding which was not observed in the previous work due to differences in experimental conditions (Figure 4.11B,E). Transcripts of *igf2r* and *igf2a* were upregulated with prolonged fasting and a downregulation was observed during refeeding, with the *igf2r* transcripts showing a very gradual change in transcript level in relation to *igf2a* (Figure 4.11B,E). This pattern of expression and correlation between *igf2r* and *igf2* were as observed previously in Atlantic salmon (Bower et al., 2008; Bower and Johnston, 2010a). The results show that the basal expression of *igf2r* was affected by the selection experiment, while only a transient change during fasting was observed for *igf2a*. Absence of a functional allelic copy of the maternal *igf2r* leads to perinatal overgrowth and lethality, with elevated levels of *igf2* in mice embryos due to the absence of the degrading *igf2* function of the *igf2r* (Lau et al., 1994; Wang et al., 1994). In the zebrafish two copies of the *igf2* gene exist, with distinct transcriptional regulation during embryonic and adult phases (Zou et al., 2009; Nelson and Van Der Kraak, 2010) with differential regulation in response a single-meal (Amaral and Johnston, 2011) and fasting-refeeding (present work).

It is known that overexpression of *igfbp1a/b* in zebrafish embryos under normoxia causes growth and developmental retardations (Kajimura et al., 2005; Kamei et al., 2008). Igfbp1 causes its growth inhibiting action by rendering igf1 less available to tissues. This negative regulation of growth by *igfbp1* genes might explain the downregulation of these genes during the growth stimuli of satiation (Amaral and Johnston, 2011) and hints at a putative role of igfbp1 in the differential response to growth stimuli in zebrafish lineages selected for divergent body size at age (Figure 4.12A,B).

Klf11b was also found to have different levels of expression between the S- and L-lineages. *Klf11b* is a zebrafish paralogue of the KLF family of transcription factors which has members involved in many biological processes including differentiation, proliferation and apoptosis (McConnell and Yang, 2010). In mice *klf11* functions in growth inhibition (Fernandez-Zapico et al., 2003) while in fish its functions are not

known. There is evidence that KLF is not strictly necessary for normal development and growth in knockout mice, probably due to overlap in function of the different members of the KLF family (Song et al., 2005). A strong upregulation of *klf11b* with prolonged fasting in zebrafish skeletal muscle has been previously reported (Amaral and Johnston, 2011). In the present work a strong effect of selection on the transcriptional regulation of this gene was observed, with fish from the L-lineage having twice as many transcripts during prolonged fasting (Figure 4.12D).

The artificial selection experiment reported in this chapter successfully produced three lineages of zebrafish with divergent body size. Selection for larger body size had positive effects on offspring during embryonic and adult stage in terms of growth (during both phases) and absolute number of fish per spawning, with no clear trade-off for the increased body size at adult stage. A change in expression of a limited number of genes from the IGF pathway was demonstrated in the present work, which points to a better growth opportunity for fish from the L-lineage in response to a growth stimulus (higher basal expression of *igf1a,* higher transient expression of *igf1* receptors and lower transient expression of *igfbp1* genes in response to fasting-refeeding). However, the L-lineage also had higher expression of the *klf11b*, which has negative effects on growth in other organisms. Directional changes in transcript levels as a result of selective breeding are based on the maintenance of alleles and loci that are beneficial to the affected trait. Small changes in the regulatory sequence of genes and single nucleotide polymorphisms in the coding sequence (SNPs) are two important variations within an allele that could contribute to phenotypical differences within families. The current work provides a good starting point for future research on the regulatory sequence and SNPs of candidate genes that were changed after experimental selection.

5. General Discussion

The overall objective of this thesis was to characterize the transcriptional change in response to nutrition, photoperiod and selective breeding in the zebrafish, with special attention to the IGF system. These three factors were chosen for their importance for growth physiology of fish, with the intention of understanding in more detail the molecular mechanisms of regulation. Transcription of DNA into mRNA is a fundamental process for the production of protein, and recent findings point to a good correlation between mRNA and protein levels in a teleost (Rees et al., 2011). However, care must be exercised when extrapolating the results of transcript levels to biological outputs due to the complex regulatory mechanisms that exist within the cells (e.g., mRNA stability and degradation, translation control). In this section the main findings made during this study and their impact on the literature will be discussed, together with ideas for future experiments.

5.1. IGF signalling in zebrafish skeletal muscle

In chapters 2 and 4 the transcriptional response to nutrition was investigated in skeletal muscle of zebrafish. In both experiments the concurrent expression of the 16 known zebrafish genes of the IGF signaling was investigated. In zebrafish, the transcription of the ligands *igf1a, igf2a and igf2b,* the receptors *igf1ar, igf1br* and *igf2r*, and the binding proteins *igfbp1a* and *igfbp1b* changed in response to nutritional status. Some of the duplicated genes showed a marked difference in expression. For example, *igf1a* was detected in skeletal muscle but *igf1b* was not. The patterns of transcription for *igf1a, igf1ar* and *igf1br* described here for the zebrafish are similar to other fish species (Chauvigne et al., 2003; Bower et al., 2008). However, the timing of changes in transcription were dramatically faster in this small tropical species. For example, previous research has demonstrated a marked increase in *igf1* transcripts within days in skeletal muscle of fasted rainbow trout and Atlantic salmon following refeeding (Chauvigne et al., 2003; Bower et al., 2008). It is important to notice that those studies investigated the transcriptional response during recovery for a period of days, and that fast (<2d) transcriptional responses were not investigated. Thus the present work provides a detailed description of the fast transcriptional response of IGF components during the post-prandial period.

The transcription of IGF binding proteins was another noteworthy difference between zebrafish and Atlantic salmon. Only the paralogues *igfbp1a* and *igfbp1b* showed a clear response to feeding, with upregulation during fasting in skeletal muscle of zebrafish. In Atlantic salmon, *igfbp2.1* was upregulated during maintenance feeding with a gradual downregulation with refeeding whereas *igfbp4* showed the opposite pattern to *igfbp2.1* (Bower et al., 2008). It is possible that the differences in IGF binding protein regulation found between zebrafish and salmonids derived from the massive genome rearrangements after WGD events, with retained gene paralogues sharing the molecular functions of genes that were lost over evolutionary time. For example, *igfbp4* was apparently lost in the zebrafish genome, whereas it is conserved in the salmonid lineage functioning in the transcriptional response to nutritional status.

Igf2r is known to have a fundamental function in development and embryonic growth in mice (Lau et al., 1994; Wang et al., 1994). The function of this receptor has not been investigated in fish. In chapter 4 a clear upregulation with fasting with a very gradual downregulation with feeding was observed for this receptor. This finding, together with previous report in Atlantic salmon, point to a function of the *igf2r* in the nutritional response in fish (Bower et al., 2008). Transient loss-of-function using antisense morpholino in zebrafish embryos could shed light on this matter and would be an important model to study the signaling downstream of the igf2r (to confirm that the ligands are targeted for lysosomal degradation, for example).

In addition to the expression of the genes of the IGF signaling, the microarray analysis revealed approximately 147 genes differentially regulated in skeletal muscle in response to nutritional status (chapter 2). For example, ornithine decarboxylase 1 (ODC1) was strongly upregulated with feeding. This enzyme catalyses the rate limiting step of polyamine biosynthesis pathway by converting ornithine to putrescine (Figure 5.1). Polyamines interact with a number of macromolecules within the cell, including the DNA and can cause changes in transcriptional regulation. They have been implicated in various biological processes and are known to play an important role in control of cell cycle (Nasizadeh et al., 2005; Larqué et al., 2007; Alm and Oredsson, 2009). Previous research has demonstrated the changes in activity of hepatic ODC in mice and fish in response to the nutritional status (Moore and Swendseid, 1983; Benfey, 1992). For example, hepatic ODC activity decreased exponentially during fasting and was elevated 4h after refeeding in brook trout (*Salvelinus fontinalis*) (Benfey, 1992). Furthermore,

ODC mRNA and activity levels in muscle of Atlantic salmon and brook trout were strongly positively correlated with growth rate (Arndt et al., 1994; Benfey et al., 1994). The description of ODC in this study as a nutritionally-responsive gene is an example of the importance of a gene discovery approach, revealing the importance of other genes than the candidate ones. Future investigation on the transcriptional changes triggered by polyamines in cell culture could shed light on the molecular mechanisms controlling cell cycle control in fish muscle.

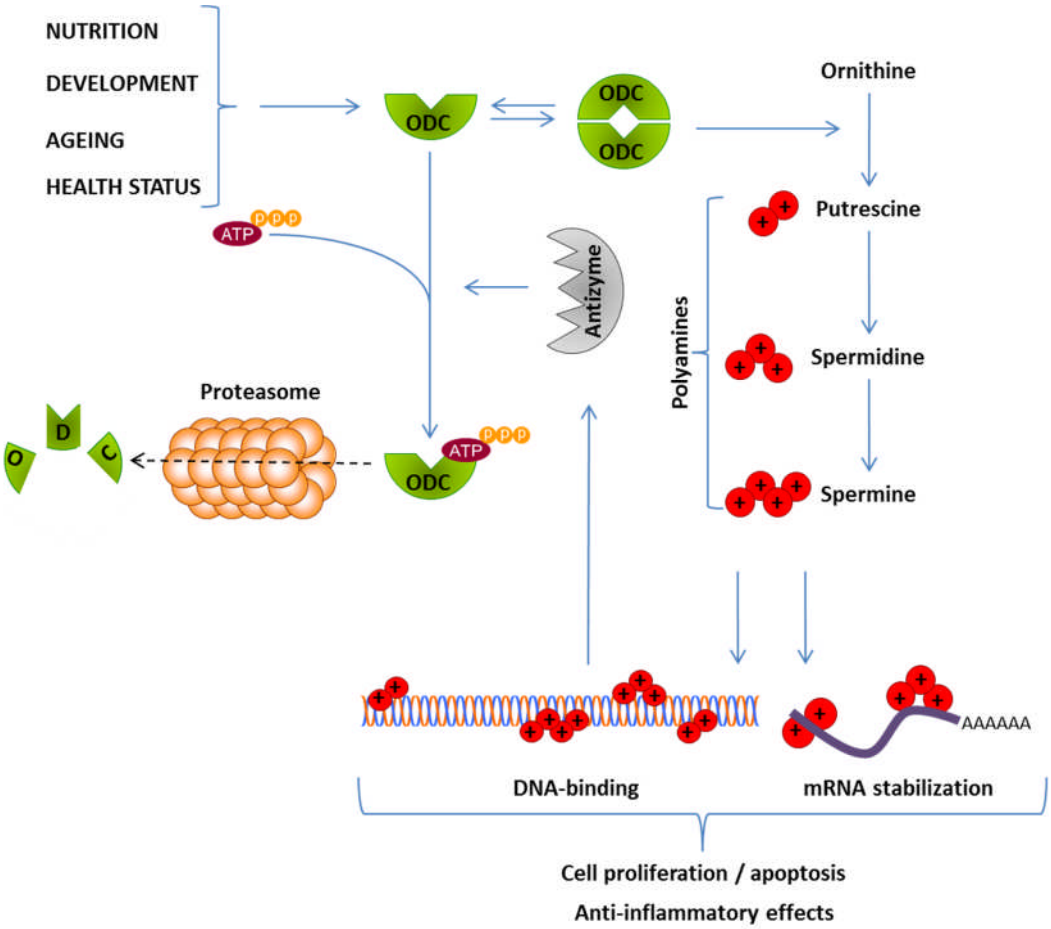

Figure 5.1 – Role of ornithine decarboxylase (ODC) in the biosynthesis of polyamines (putrescine, spermidine and spermine). ODC has high turnover rates due to fast degradation by the proteasome. In contrast to other proteins, ODC is targeted to proteasome degradation by conjugation to ATP by antizyme, whose expression is positively correlated with polyamine levels. The biological functions of polyamines are many, and are thought to be based on their poly-cationic nature by binding and stabilizing DNA and mRNA molecules, for example. This diagram was modified from (Pegg, 2006; Larqué et al., 2007).

The expression of different nutritionally-responsive IGF muscle genes was also differentially expressed in two lineages of zebrafish divergently selected for body size at age (chapter 4). The changes in transcription could not be linked to differences in feed intake, since fish from both lineages showed similar relative gut food content. It is possible that experimental selection resulted in fish with different feeding conversion, affecting the metabolism rather than the appetite control. In line with this hypothesis, fish from the L-lineage had a transcriptional profile compatible with a higher anabolic state (higher constitutive levels of *igf1a* that became more pronounced during feeding and higher levels of *igf1* receptor during satiation feeding). Furthermore, fish from the L-lineage had lower levels of *igfbp1a/1b* during feeding, pointing to a higher availability of *igf1a*. The promoter region of these genes are interesting candidates for investigating variations in *cis*-regulatory sequences responsible for the modifications observed in size in the zebrafish lineages. Another possibility that was not explored in the present study is that there could exist small variations in the coding sequence of genes, and that experimental selection is purifying favourable alleles in a certain direction. Occurrence of single nucleotide polymorphisms (SNPs) in many species is one example of well documented sequence variation, with correlations with changes of phenotype. For example, SNPs have been used in breeding programs to improve qualities of trait in the production of meat from cattle (Goddard et al., 2010). A web data-base is available for SNPs markers in cattle, allowing a quick glance at annotation and gene ontology of affected genes (Wang et al., 2011). It is possible that experimental selection and domestication in fish cause a directional shift in frequency of alleles bearing SNPs related to growth and fillet quality traits. Next generation sequencing of genomic DNA and RNAseq techniques could prove very useful in the investigation of differences in regulatory and coding sequence of selected fish, respectively. The availability of a well annotated genome sequence would certainly be a great advantage in analysing the results of such a large-scale experiment.

Adult fish from the L-lineage were ~12% larger and ~41% heavier than fish from the S-lineage after three rounds of experimental selection for body size at age. Although these results are significant, it is important to notice that around 45-75% of fish were selected from each generation to produce offspring for the following generation. These percentages were chosen to keep a minimum number of fish per population in order to avoid an extensive loss of genetic variation. If the circumstances

allowed, it would have been better to have more fish per replicate line allowing for an increase in the selective pressure, which could result in even more clear-cut effects. In addition, genetic material from the founding populations and the selected lineages could have been stored. By doing so it would have been possible to assert parentage, to calculate the heritability of the traits under investigation, and to analyse the extent of loss of genetic variation per generation, which are very important factors in selective breeding of captive fish.

Apart from the effects on body size and gene expression in skeletal muscle, experimental selection caused several changes on the early-life traits of zebrafish. The higher number of eggs produced per spawning is maybe the most significant difference for successful propagation of a fish lineage in a competitive environment. Five times more fish were produced by the L-lineage compared to the S-lineage. However, it remains to be established whether the experimental selection affected the timing of sexual maturation or the fertilization rate. To properly address this question, the number of eggs produced at age by single pairs of fish could have been calculated over a period from the juvenile to early adult stages. It is also possible that the selective breeding did not affect sexual maturation or fertilization rate and that the number of eggs produced is simply a result of the positive correlation between body size and egg production, as observed previously (Forbes et al., 2010).

Differential deposition of maternal transcripts was another important early-life trait change triggered by the experimental selection experiment. The functions of maternal transcripts are far from completely understood and more experiments to specifically investigate the importance of these maternally-deposited transcripts in fish eggs are necessary.

5.2. Molecular clock machinery in zebrafish skeletal muscle

Zebrafish have strong circadian locomotory, breeding and feeding rhythm (Blanco-Vives and Sanchez-Vazquez, 2009; del Pozo et al., 2011). The experiments in chapter 3 were first designed to provide evidence whether the changes in expression observed in genes of the IGF pathway and nutritionally-responsive genes were due to metabolic changes triggered by circadian food-anticipatory activities or to the nutrient levels. The experiments in that chapter were then expanded to characterize the circadian

expression of the core-clock machinery and putative clock-controlled genes in skeletal muscle, an underexplored field in fish biology.

The experiments in chapter 3 confirmed that the differences observed in the IGF muscle genes were due to nutritional status since no circadian pattern was found for *igf* ligands, *igf* receptors or *igfbp1a*/*b*. Furthermore, expression of *igfbp3* and *igfbp5b* followed a circadian pattern and were described as putative clock-controlled genes. The photoperiod experiment was also important in discovering genes that integrate metabolism with the molecular clock machinery. For example, two nutritionally-responsive genes (*nr1d1* and *hsf2*) were found to have a strong circadian pattern of expression, highlighting the importance of the comparison of the different experiments performed in this study.

Concurrent expression of 17 known circadian genes in skeletal muscle was investigated and differences in responsiveness were found between three gene paralogues. Expression of the main positive (*clock1a/b* and *bmal1a/b*) and negative oscillators (*cry1a*, *per1a*/*1b*, *per2*, and *per3*) in skeletal muscle followed a strong circadian pattern similar to those described in central pacemaker organs of the circadian mechanism (eye, brain and pineal gland) in zebrafish and Senegalese sole (*Solea senegalensis*) (Whitmore et al., 1998; Martín-Robles et al., 2011; Vatine et al., 2011). From the known circadian genes investigated, c*ry1b* was the only one with no strong circadian pattern. Thus, this gene might not participate in the pool of cryptochrome proteins that form heterodimers with period proteins in the cytoplasm to block dimerization of clock with bmal. The apparent synchronization of peripheral clock in skeletal muscle and central pacemaker organs remains to be established and has been a contentious subject in this field (Vatine et al., 2011; Weger et al., 2011).

To investigate the fundamentals of integration and synchronization of the peripheral organs to central pacemakers in adult fish the first step would be to disrupt the molecular clock in either tissue. Disruption of the molecular clock in the central pacemakers would have a systemic effect and would possibly make the interpretation of specific effects in peripheral tissues impossible. However, there are two advantages in this scenario: it would be possible (a) to assert the putative direct responsiveness of peripheral tissues to light and establish the hierarchy of the central pacemakers, and (b) to establish the importance of the central molecular clock for peripheral homeostasis. Disruption of the molecular clock in the peripheral tissue of interest would possibly

render the tissue irresponsive to the central pacemakers, allowing for direct observation of the importance of the clock mechanism in the peripheral tissue. This approach also has the advantage of investigating the effect of disruption of clock-controlled genes in tissue-specific manner. To achieve such objectives in adult tissues, a long-term change in the transcriptional machinery would be necessary which excludes the possibility of using anti-sense morpholinos. Loss-of-function of the main oscillators *clock* and *bmal* could theoretically be achieved by the RNA interference technique, affecting the positive arm of the clock pathway. However, there are difficulties in establishing RNA interference in zebrafish (Lawson and Wolfe, 2011). Maybe a more feasible way to disrupt the molecular clock would be to use gain-of-function experiments in which a constitutive expression of the clock and bmal dimerization inhibitors (cryptochrome and period proteins) would disrupt the control of the negative oscillators of the clock pathway.

References

Allendorf, F. W. (1979). Rapid loss of duplicate gene-expression by natural-selection. *Heredity* **43**, 247-258.

Alm, K. and Oredsson, S. (2009). Cells and polyamines do it cyclically. In *Essays in Biochemistry, Vol 46: The Polyamines: Small Molecules in the Omics Era*, vol. 46 (ed. H. Wallace), pp. 63-76. London: Portland Press Ltd.

Amali, A. A., Lin, C. J. F., Chen, Y. H., Wang, W. L., Gong, H. Y., Lee, C. Y., Ko, Y. L., Lu, J. K., Her, G. M., Chen, T. T. et al. (2004). Up-regulation of muscle-specific transcription factors during embryonic somitogenesis of zebrafish (Danio rerio) by knock-down of myostatin-1. *Developmental Dynamics* **229**, 847-856.

Amaral, I. P. G. and Johnston, I. A. (2011). Insulin-like growth factor (IGF) signalling and genome-wide transcriptional regulation in fast muscle of zebrafish following a single-satiating meal. *The Journal of Experimental Biology* **214**, 2125-2139.

Andrews, J. L., Zhang, X., McCarthy, J. J., McDearmon, E. L., Hornberger, T. A., Russell, B., Campbell, K. S., Arbogast, S., Reid, M. B., Walker, J. R. et al. (2010). CLOCK and BMAL1 regulate MyoD and are necessary for maintenance of skeletal muscle phenotype and function. *Proceedings of the National Academy of Sciences of the United States of America* **107**, 19090-19095.

Appelbaum, L., Vallone, D., Anzulovich, A., Ziv, L., Tom, M., Foulkes, N. S. and Gothilf, Y. (2006). Zebrafish arylalkylamine-N-acetyltransferase genes - targets for regulation of the circadian clock. *Journal of Molecular Endocrinology* **36**, 337-347.

Arndt, S. K. A., Benfey, T. J. and Cunjak, R. A. (1994). A comparison of RNA concentrations and ornithine decarboxylase activity in Atlantic salmon (Salmo-salar) muscle-tissue, with respect to specific growth-rates and diel variations. *Fish Physiology and Biochemistry* **13**, 463-471.

Banos, N., Planas, J. V., Gutierrez, J. and Navarro, I. (1999). Regulation of plasma insulin-like growth factor-I levels in brown trout (Salmo trutta). *Comparative Biochemistry and Physiology C-Toxicology & Pharmacology* **124**, 33-40.

Barnes, P. J. (1998). Anti-inflammatory actions of glucocorticoids: molecular mechanisms. *Clin. Sci.* **94**, 557-572.

Barresi, M. J. F., D'Angelo, J. A., Hernandez, L. P. and Devoto, S. H. (2001). Distinct mechanisms regulate slow-muscle development. *Current Biology* **11**, 1432-1438.

Barrett, P., Conway, S. and Morgan, P. J. (2003). Digging deep - structure-function relationships in the melatonin receptor family. *J. Pineal Res.* **35**, 221-230.

Benfey, T. J. (1992). Hepatic ornithine decarboxylase activity during short-term starvation and refeeding in brook trout, Salvelinus-fontinalis. *Aquaculture* **102**, 105-113.

Benfey, T. J., Saunders, R. L., Knox, D. E. and Harmon, P. R. (1994). Muscle ornithine decarboxylase activity as an indication of recent growth in pre-smolt Atlantic salmon, Salmo-salar. *Aquaculture* **121**, 125-135.

Benjamini, Y. and Hochberg, Y. (1995). Controlling the false discovery rate - a practical and powerful approach to multiple testing. *Journal of the Royal Statistical Society Series B-Methodological* **57**, 289-300.

Bernier, N. J. (2006). The corticotropin-releasing factor system as a mediator of the appetite-suppressing effects of stress in fish. *General and Comparative Endocrinology* **146**, 45-55.

Besseau, L., Benyassi, A., Moller, M., Coon, S. L., Weller, J. L., Boeuf, G., Klein, D. C. and Falcon, J. (2006). Melatonin pathway: breaking the 'high-at-night' rule in trout retina. *Experimental Eye Research* **82**, 620-627.

Björnsson, B. T., Hemre, G. I., Bjornevik, M. and Hansen, T. (2000). Photoperiod regulation of plasma growth hormone levels during induced smoltification of underyearling Atlantic salmon. *General and Comparative Endocrinology* **119**, 17-25.

Björnsson, B. T., Johansson, V., Benedet, S., Einarsdottir, I. E., Hildahl, J., Agustsson, T. and Jonsson, E. (2002). Growth hormone endocrinology of salmonids: regulatory mechanisms and mode of action. *Fish Physiology and Biochemistry* **27**, 227-242.

Blanco-Vives, B. and Sanchez-Vazquez, F. J. (2009). Synchronisation to light and feeding time of circadian rhythms of spawning and locomotor activity in zebrafish. *Physiology & Behavior* **98**, 268-275.

Boujard, T. and Leatherland, J. F. (1992). Circadian pattern of hepatosomatic index, liver-glycogen and lipid-content, plasma nonesterified fatty-acid, glucose, T3, T4, growth-hormone and cortisol concentrations in Oncorhynchus-mykiss held under different photoperiod regimes and fed using demand-feeders. *Fish Physiology and Biochemistry* **10**, 111-122.

Bower, N. I. and Johnston, I. A. (2010a). Discovery and characterization of nutritionally regulated genes associated with muscle growth in Atlantic salmon. *Physiol. Genomics* **42A**, 114-130.

Bower, N. I. and Johnston, I. A. (2010b). Transcriptional Regulation of the IGF Signaling Pathway by Amino Acids and Insulin-Like Growth Factors during Myogenesis in Atlantic Salmon. *PLoS One* **5**.

Bower, N. I., Taylor, R. G. and Johnston, I. A. (2009). Phasing of muscle gene expression with fasting-induced recovery growth in Atlantic salmon. *Frontiers in Zoology* **6**.

Bower, N. I., Li, X. J., Taylor, R. and Johnston, I. A. (2008). Switching to fast growth: the insulin-like growth factor (IGF) system in skeletal muscle of Atlantic salmon. *Journal of Experimental Biology* **211**, 3859-3870.

Braun, T., Rudnicki, M. A., Arnold, H. H. and Jaenisch, R. (1992). Targeted inactivation of the muscle regulatory gene myf-5 results in abnormal rib development and perinatal death. *Cell* **71**, 369-382.

Bunger, L. and Hill, W. G. (1999). Role of growth hormone in the genetic change of mice divergently selected for body weight and fatness. *Genetical Research* **74**, 351-360.

Bustin, S. A., Benes, V., Garson, J. A., Hellemans, J., Huggett, J., Kubista, M., Mueller, R., Nolan, T., Pfaffl, M. W., Shipley, G. L. et al. (2009). The MIQE Guidelines: Minimum Information for Publication of Quantitative Real-Time PCR Experiments. *Clinical Chemistry* **55**, 611-622.

Cahill, G. M. (2002). Clock mechanisms in zebrafish. *Cell and Tissue Research* **309**, 27-34.

Capecchi, M. R. (2005). Gene targeting in mice: functional analysis of the mammalian genome for the twenty-first century. *Nature Reviews Genetics* **6**, 507-512.

Carr, J. A. and Patino, R. (2011). The hypothalamus-pituitary-thyroid axis in teleosts and amphibians: Endocrine disruption and its consequences to natural populations. *General and Comparative Endocrinology* **170**, 299-312.

CarterSu, C., Schwartz, J. and Smit, L. S. (1996). Molecular mechanism of growth hormone action. *Annual Review of Physiology* **58**, 187-207.

Castro, R., Zou, J., Secombes, C. J. and Martin, S. A. M. (2011). Cortisol modulates the induction of inflammatory gene expression in a rainbow trout macrophage cell line. *Fish Shellfish Immunol.* **30**, 215-223.

Celeghin, A., Benato, F., Pikulkaew, S., Rabbane, M. G., Colombo, L. and Dalla Valle, L. (2011). The knockdown of the maternal estrogen receptor 2a (esr2a) mRNA affects embryo transcript contents and larval development in zebrafish. *General and Comparative Endocrinology* **172**, 120-129.

Cermakian, N., Whitmore, D., Foulkes, N. S. and Sassone-Corsi, P. (2000). Asynchronous oscillations of two zebrafish CLOCK partners reveal differential clock control and function. *Proceedings of the National Academy of Sciences of the United States of America* **97**, 4339-4344.

Chauvigne, F., Gabillard, J. C., Weil, C. and Rescan, P. Y. (2003). Effect of refeeding on IGFI, IGFII, IGF receptors, FGF2, FGF6, and myostatin mRNA expression in rainbow trout myotomal muscle. *General and Comparative Endocrinology* **132**, 209-215.

Chen, J. Y., Chen, J. C., Huang, W. T., Liu, C. W., Hui, C. F., Chen, T. T. and Wu, J. L. (2004). Molecular cloning and tissue-specific, developmental-stage-specific, and hormonal regulation of IGFBP3 gene in zebrafish. *Marine Biotechnology* **6**, 1-7.

Chen, Y. H. and Tsai, H. J. (2008). Myogenic regulatory factors Myf5 and Mrf4 of fish: current status and perspective. *Journal of Fish Biology* **73**, 1872-1890.

Chiba, S., Arnott, S. A. and Conover, D. O. (2007). Coevolution of foraging behavior with intrinsic growth rate: risk-taking in naturally and artificially selected growth genotypes of Menidia menidia. *Oecologia* **154**, 237-246.

Chizinski, C. J., Sharma, B., Pope, K. L. and Patino, R. (2008). A bioenergetic model for zebrafish Danio rerio (Hamilton). *Journal of Fish Biology* **73**, 35-43.

Chong, S. W., Korzh, V. and Jiang, Y. J. (2009). Myogenesis and molecules- insights from zebrafish Danio rerio. *Journal of Fish Biology* **74**, 1693-1755.

Chu, M. X., Jia, L. H., Zhang, Y. J., Jin, M., Chen, H. Q., Fang, L., Di, R., Cao, G. L., Feng, T., Tang, Q. Q. et al. (2011). Polymorphisms of coding region of BMPR-IB gene and their relationship with litter size in sheep. *Molecular Biology Reports* **38**, 4071-4076.

Clark, T. D., Brandt, W. T., Nogueira, J., Rodriguez, L. E., Price, M., Farwell, C. J. and Block, B. A. (2010). Postprandial metabolism of Pacific bluefin tuna (Thunnus orientalis). *Journal of Experimental Biology* **213**, 2379-2385.

Costas, B., Aragão, C., Ruiz-Jarabo, I., Vargas-Chacoff, L., Arjona, F., Dinis, M., Mancera, J. and Conceição, L. (2010). Feed deprivation in Senegalese sole (<i>Solea senegalensis</i> Kaup, 1858) juveniles: effects on blood plasma metabolites and free amino acid levels. *Fish Physiology and Biochemistry*, 1-10.

Craig, R. W. and Padrón, R. (2004). Molecular structure of the sarcomere. In: Engel AC, Franzini-Armstrong C, editors. *Myology. 3. New York: McGraw-Hill;*, pp 129-144.

Crumbley, C. and Burris, T. P. (2011). Direct regulation of CLOCK expression by REV-ERB. *PLoS One* **6**, e17290.

Dai, W., Kamei, H., Zhao, Y., Ding, J., Du, Z. and Duan, C. M. (2010). Duplicated zebrafish insulin-like growth factor binding protein-5 genes with split functional domains: evidence for evolutionarily conserved IGF binding, nuclear localization, and transactivation activity. *Faseb Journal* **24**, 2020-2029.

Davie, A., Minghetti, M. and Migaud, H. (2009). Seasonal Variations in Clock-Gene Expression in Atlantic Salmon (Salmo salar). *Chronobiology International* **26**, 379-395.

Davis, K. B. and Peterson, B. C. (2006). The effect of temperature, stress, and cortisol on plasma IGF-I and IGFBPs in sunshine bass. *General and Comparative Endocrinology* **149**, 219-225.

del Pozo, A., Sanchez-Ferez, J. A. and Sanchez-Vazquez, F. J. (2011). Circadian Rhythms of Self-feeding and Locomotor Activity in Zebrafish (Danio Rerio). *Chronobiology International* **28**, 39-47.

Delvecchio, C., Tiefenbach, J. and Krause, H. M. (2011). The Zebrafish: A Powerful Platform for In Vivo, HTS Drug Discovery. *Assay Drug Dev. Technol.* **9**, 354-361.

Desterro, J. M. P., Rodriguez, M. S. and Hay, R. T. (1998). SUMO-1 modification of I kappa B alpha inhibits NF-kappa B activation. *Molecular Cell* **2**, 233-239.

Devlin, R. H., Yesaki, T. Y., Donaldson, E. M., Du, S. J. and Hew, C. L. (1995). Production of germline transgenic Pacific salmonids with dramatically increased growth-performance. *Canadian Journal of Fisheries and Aquatic Sciences* **52**, 1376-1384.

Devlin, R. H., Sakhrani, D., Tymchuk, W. E., Rise, M. L. and Goh, B. (2009). Domestication and growth hormone transgenesis cause similar changes in gene expression in coho salmon (Oncorhynchus kisutch). *Proceedings of the National Academy of Sciences of the United States of America* **106**, 3047-3052.

Devoto, S. H., Melancon, E., Eisen, J. S. and Westerfield, M. (1996). Identification of separate slow and fast muscle precursor cells in vivo, prior to somite formation. *Development* **122**, 3371-3380.

Dibner, C., Schibler, U. and Albrecht, U. (2010). The Mammalian Circadian Timing System: Organization and Coordination of Central and Peripheral Clocks. *Annual Review of Physiology* **72**, 517-549.

Dosch, R., Wagner, D. S., Mintzer, K. A., Runke, G., Wiemelt, A. P. and Mullins, M. C. (2004). Maternal Control of Vertebrate Development before the Midblastula Transition: Mutants from the Zebrafish I. *Developmental Cell* **6**, 771-780.

Duan, C. M., Ren, H. X. and Gao, S. (2010). Insulin-like growth factors (IGFs), IGF receptors, and IGF-binding proteins: Roles in skeletal muscle growth and differentiation. *General and Comparative Endocrinology* **167**, 344-351.

Duez, H. and Staels, B. (2008). The nuclear receptors Rev-erbs and RORs integrate circadian rhythms and metabolism. *Diabetes Vasc. Dis. Res.* **5**, 82-88.

Eames, S. C., Philipson, L. H., Prince, V. E. and Kinkel, M. D. (2010). Blood Sugar Measurement in Zebrafish Reveals Dynamics of Glucose Homeostasis. *Zebrafish* **7**, 205-213.

Eaton, R. C. and Farley, R. D. (1974). Growth and reduction of depensation of zebrafish, Brachydanio-rerio, reared in laboratory. *Copeia*, 204-209.

Eliason, E. J., Djordjevic, B., Trattner, S., Pickova, J., Karlsson, A., Farrell, A. P. and Kiessling, A. K. (2010). The effect of hepatic passage on postprandial plasma lipid profile of rainbow trout (Oncorhynchus mykiss) after a single meal. *Aquac. Nutr.* **16**, 536-543.

Emery, P. and Reppert, S. M. (2004). A Rhythmic Ror. *Neuron* **43**, 443-446.

Engert, J. C., Berglund, E. B. and Rosenthal, N. (1996). Proliferation precedes differentiation in IGF-I-stimulated myogenesis. *Journal of Cell Biology* **135**, 431-440.

Etard, C., Roostalu, U. and Strahle, U. (2008). Shuttling of the chaperones Unc45b and Hsp90a between the A band and the Z line of the myofibril. *Journal of Cell Biology* **180**, 1163-1175.

Falcon, J. (1999). Cellular circadian clocks in the pineal. *Progress in Neurobiology* **58**, 121-162.

Falcon, J., Besseau, L., Sauzet, S. and Boeuf, G. (2007). Melatonin effects on the hypothalamo-pituitary axis in fish. *Trends in Endocrinology and Metabolism* **18**, 81-88.

Falcon, J., Besseau, L., Magnanou, E., Herrero, M. J., Nagai, M. and Boeuf, G. (2011). Melatonin, the time keeper: biosynthesis and effects in fish. *Cybium* **35**, 3-18.

Falcon, J., Besseau, L., Fazzari, D., Attia, J., Gaildrat, P., Beauchaud, M. and Boeuf, G. (2003). Melatonin modulates secretion of growth hormone and prolactin by trout pituitary glands and cells in culture. *Endocrinology* **144**, 4648-4658.

Farchi-Pisanty, O., Sternberg, H. and Moav, B. (1997). Transcriptional regulation of fish growth hormone gene. *Fish Physiology and Biochemistry* **17**, 237-246.

Feng, D., Liu, T., Sun, Z., Bugge, A., Mullican, S. E., Alenghat, T., Liu, X. S. and Lazar, M. A. (2011). A Circadian Rhythm Orchestrated by Histone Deacetylase 3 Controls Hepatic Lipid Metabolism. *Science* **331**, 1315-1319.

Fernandes, J. M. O., MacKenzie, M. G., Wright, P. A., Steele, S. L., Suzuki, Y., Kinghorn, J. R. and Johnston, I. A. (2006). Myogenin in model pufferfish species: Comparative genomic analysis and thermal plasticity of expression during early development. *Comparative Biochemistry and Physiology D-Genomics & Proteomics* **1**, 35-45.

Fernandez-Zapico, M. E., Mladek, A., Ellenrieder, V., Folch-Puy, E., Miller, L. and Urrutia, R. (2003). An mSin3A interaction domain links the transcriptional activity of KLF11 with its role in growth regulation. *EMBO J* **22**, 4748-4758.

Figueiredo, M. D., Lanes, C. F. C., Almeida, D. V. and Marins, L. F. (2007). Improving the production of transgenic fish germlines: In vivo evaluation of mosaicism in zebrafish (Danio rerio) using a green fluorescent protein (GFP) and growth hormone cDNA transgene co-injection strategy. *Genet. Mol. Biol.* **30**, 31-36.

Finn, P. F. and Dice, J. F. (2006). Proteolytic and lipolytic responses to starvation. *Nutrition* **22**, 830-844.

Firth, S. M. and Baxter, R. C. (2002). Cellular actions of the insulin-like growth factor binding proteins. *Endocr. Rev.* **23**, 824-854.

Flores, M. V., Hall, C., Jury, A., Crosier, K. and Crosier, P. (2007). The zebrafish retinoid-related orphan receptor (ror) gene family. *Gene Expression Patterns* **7**, 535-543.

Forbes, E. L., Preston, C. D. and Lokman, P. M. (2010). Zebrafish (Danio rerio) and the egg size versus egg number trade off: effects of ration size on fecundity are not mediated by orthologues of the Fec gene. *Reprod. Fertil. Dev.* **22**, 1015-1021.

Force, A., Lynch, M., Pickett, F. B., Amores, A., Yan, Y. L. and Postlethwait, J. (1999). Preservation of duplicate genes by complementary, degenerative mutations. *Genetics* **151**, 1531-1545.

Fuentes, E. N., Björnsson, B. T., Valdés, J. A., Einarsdottir, I. E., Lorca, B., Alvarez, M. and Molina, A. (2011). IGF-I/PI3K/Akt and IGF-I/MAPK/ERK pathways in vivo in skeletal muscle are regulated by nutrition and contribute to somatic growth in the fine flounder. *American Journal of Physiology - Regulatory, Integrative and Comparative Physiology* **300**, R1532-R1542.

Gabillard, J. C., Kamangar, B. B. and Montserrat, N. (2006). Coordinated regulation of the GH/IGF system genes during refeeding in rainbow trout (Oncorhynchus mykiss). *Journal of Endocrinology* **191**, 15-24.

Gabillard, J. C., Weil, C., Rescan, P. Y., Navarro, I., Gutierrez, J. and Le Bail, P. Y. (2003). Effects of environmental temperature on IGF1, IGF2, and IGF type I receptor expression in rainbow trout (Oncorhynchus mykiss). *General and Comparative Endocrinology* **133**, 233-242.

Gabillard, J. C., Weil, C., Rescan, P. Y., Navarro, I., Gutierrez, J. and Le Bail, P. Y. (2005). Does the GH/IGF system mediate the effect of water temperature on fish growth? A review. *Cybium* **29**, 107-117.

Geiss-Friedlander, R. and Melchior, F. (2007). Concepts in sumoylation: a decade on. *Nat Rev Mol Cell Biol* **8**, 947-956.

Girard, I., Rezende, E. L. and Garland, T. (2007). Leptin levels and body composition of mice selectively bred for high voluntary locomotor activity. *Physiol. Biochem. Zool.* **80**, 568-579.

Glass, D. J. (2003). Signalling pathways that mediate skeletal muscle hypertrophy and atrophy. *Nature Cell Biology* **5**, 87-90.

Glass, D. J. (2005). Skeletal muscle hypertrophy and atrophy signaling pathways. *International Journal of Biochemistry & Cell Biology* **37**, 1974-1984.

Goddard, M. E., Hayes, B. J. and Meuwissen, T. H. E. (2010). Genomic selection in livestock populations. *Genet. Res.* **92**, 413-421.

Gottlieb, P. D., Pierce, S. A., Sims, R. J., Yamagishi, H., Weihe, E. K., Harriss, J. V., Maika, S. D., Kuziel, W. A., King, H. L., Olson, E. N. et al. (2002). Bop encodes a muscle-restricted protein containing MYND and SET domains and is essential for cardiac differentiation and morphogenesis. *Nature Genetics* **31**, 25-32.

Guillaumond, F., Dardente, H., Giguere, V. and Cermakian, N. (2005). Differential control of Bmal1 circadian transcription by REV-ERB and ROR nuclear receptors. *J. Biol. Rhythms* **20**, 391-403.

Hall, T. E. and Johnston, I. A. (2003). Temperature and developmental plasticity during embryogenesis in the Atlantic cod Gadus morhua L. *Marine Biology* **142**, 833-840.

Hammond, C. L., Hinits, Y., Osborn, D. P. S., Minchin, J. E. N., Tettamanti, G. and Hughes, S. M. (2007). Signals and myogenic regulatory factors restrict pax3 and pax7 expression to dermomyotome-like tissue in zebrafish. *Dev. Biol.* **302**, 504-521.

Hardeland, R. (2009). Melatonin: Signaling mechanisms of a pleiotropic agent. *Biofactors* **35**, 183-192.

Hastings, M., O'Neill, J. S. and Maywood, E. S. (2007). Circadian clocks: regulators of endocrine and metabolic rhythms. *Journal of Endocrinology* **195**, 187-198.

Hasty, P., Bradley, A., Morris, J. H., Edmondson, D. G., Venuti, J. M., Olson, E. N. and Klein, W. H. (1993). Muscle deficiency and neonatal death in mice with a targeted mutation in the myogenin gene. *Nature* **364**, 501-506.

Hatori, M., Hirota, T., Iitsuka, M., Kurabayashi, N., Haraguchi, S., Kokame, K., Sato, R., Nakai, A., Miyata, T., Tsutsui, K. et al. (2011). Light-dependent and circadian clock-regulated activation of sterol regulatory element-binding protein, X-box-binding protein 1, and heat shock factor pathways. *Proceedings of the National Academy of Sciences* **108**, 4864-4869.

Hay, R. T. (2005). SUMO: A History of Modification. *Molecular Cell* **18**, 1-12.

Herrington, J., Smit, L. S., Schwartz, J. and Carter-Su, C. (2000). The role of STAT proteins in growth hormone signaling. *Oncogene* **19**, 2585-2597.

Hinits, Y. and Hughes, S. M. (2007). Mef2s are required for thick filament formation in nascent muscle fibres. *Development* **134**, 2511-2519.

Hinits, Y., Osborn, D. P. S. and Hughes, S. M. (2009). Differential requirements for myogenic regulatory factors distinguish medial and lateral somitic, cranial and fin muscle fibre populations. *Development* **136**, 403-414.

Hinits, Y., Osborn, D. P. S., Carvajal, J. J., Rigby, P. W. J. and Hughes, S. M. (2007). Mrf4 (myf6) is dynamically expressed in differentiated zebrafish skeletal muscle. *Gene Expression Patterns* **7**, 738-745.

Hirayama, J., Cho, S. and Sassone-Corsi, P. (2007). Circadian control by the reduction/oxidation pathway: Catalase represses light-dependent clock gene expression in the zebrafish. *Proceedings of the National Academy of Sciences* **104**, 15747-15752.

Hirayama, J., Miyamura, N., Uchida, Y., Asaoka, Y., Honda, R., Sawanobori, K., Todo, T., Yamamoto, T., Sassone-Corsi, P. and Nishina, H. (2009). Common light signaling pathways controlling DNA repair and circadian clock entrainment in zebrafish. *Cell Cycle* **8**, 2794-2801.

Hollway, G. E., Bryson-Richardson, R. J., Berger, S., Cole, N. J., Hall, T. E. and Currie, P. D. (2007). Whole-somite rotation generates muscle progenitor cell compartments in the developing zebrafish embryo. *Developmental Cell* **12**, 207-219.

Hunter, C. P., Shen-Orr, S. S. and Pilpel, Y. (2010). Composition and regulation of maternal and zygotic transcriptomes reflects species-specific reproductive mode. *Genome Biology* **11**.

Hurd, M. W., Debruyne, J., Straume, M. and Cahill, G. M. (1998). Circadian rhythms of locomotor activity in zebrafish. *Physiology & Behavior* **65**, 465-472.

Huxley, H. and Hanson, J. (1954). Changes in the cross-striations of muscle during contraction and stretch and their structural interpretation. *Nature* **173**, 973-976.

Jaillon, O., Aury, J. M., Brunet, F., Petit, J. L., Stange-Thomann, N., Mauceli, E., Bouneau, L., Fischer, C., Ozouf-Costaz, C., Bernot, A. et al. (2004). Genome duplication in the teleost fish Tetraodon nigroviridis reveals the early vertebrate proto-karyotype. *Nature* **431**, 946-957.

Jardine, D. and Litvak, M. K. (2003). Direct yolk sac volume manipulation of zebrafish embryos and the relationship between offspring size and yolk sac volume. *Journal of Fish Biology* **63**, 388-397.

Jenkins, N. L., McColl, G. and Lithgow, G. J. (2004). Fitness cost of extended lifespan in Caenorhabditis elegans. *Proc. R. Soc. Lond. Ser. B-Biol. Sci.* **271**, 2523-2526.

John, T. (1992). Understanding the functions of titin and nebulin. *Febs Letters* **307**, 44-48.

Johnston, I. A. (1980). Specialization of fish muscle. In *Goldspink, D. F.*, pp. P123-148.

Johnston, I. A. (1982). Capillarization, oxygen diffusion distances and mitochondrial content of carp muscles following acclimation to summer and winter temperatures. *Cell and Tissue Research* **222**, 325-337.

Johnston, I. A. (2006). Environment and plasticity of myogenesis in teleost fish. *Journal of Experimental Biology* **209**, 2249-2264.

Johnston, I. A. and Goldspink, G. (1973). Some effects of prolonged starvation on metabolism of red and white myotomal muscles of plaice pleuronectes-platessa. *Marine Biology* **19**, 348-353.

Johnston, I. A., Davison, W. and Goldspink, G. (1977). ENERGY-METABOLISM OF CARP SWIMMING MUSCLES. *Journal of Comparative Physiology* **114**, 203-216.

Johnston, I. A., Temple, G. K. and Vieira, V. L. A. (2001). Impact of temperature on the growth and differentiation of muscle in herring larvae: BIOS Scientific Publishers Ltd., 9 Newtec Place, Magdalen Road, Oxford, OX4 1RE, UK; Society for Experimental Biology, Burlington House, Piccadilly, London, W1V OlQ, UK.

Johnston, I. A., Bower, N. I. and Macqueen, D. J. (2011). Growth and the regulation of myotomal muscle mass in teleost fish. *The Journal of Experimental Biology* **214**, 1617-1628.

Johnston, I. A., Manthri, S., Smart, A., Campbell, P., Nickell, D. and Alderson, R. (2003). Plasticity of muscle fibre number in seawater stages of Atlantic salmon in response to photoperiod manipulation. *Journal of Experimental Biology* **206**, 3425-3435.

Johnston, I. A., Lee, H. T., Macqueen, D. J., Paranthaman, K., Kawashima, C., Anwar, A., Kinghorn, J. R. and Dalmay, T. (2009). Embryonic temperature affects muscle fibre recruitment in adult zebrafish: genome-wide changes in gene and microRNA

expression associated with the transition from hyperplastic to hypertrophic growth phenotypes. *Journal of Experimental Biology* **212**, 1781-1793.

Kajimura, S., Aida, K. and Duan, C. (2005). Insulin-like growth factor-binding protein-1 (IGFBP-1) mediates hypoxia-induced embryonic growth and developmental retardation. *Proceedings of the National Academy of Sciences of the United States of America* **102**, 1240-1245.

Kamei, H., Lu, L., Jiao, S., Li, Y., Gyrup, C., Laursen, L. S., Oxvig, C., Zhou, J. F. and Duan, C. M. (2008). Duplication and Diversification of the Hypoxia-Inducible IGFBP-1 Gene in Zebrafish. *PLoS One* **3**.

Kapitonov, V. V. and Jurka, J. (2004). Harbinger transposons and an ancient HARBI1 gene derived from a transposase. *DNA and Cell Biology* **23**, 311-324.

Kassar-Duchossoy, L., Gayraud-Morel, B., Gomes, D., Rocancourt, D., Buckingham, M., Shinin, V. and Tajbakhsh, S. (2004). Mrf4 determines skeletal muscle identity in Myf5:Myod double-mutant mice. *Nature* **431**, 466-471.

Kawauchi, H. and Sower, S. A. (2006). The dawn and evolution of hormones in the adenohypophysis. *General and Comparative Endocrinology* **148**, 3-14.

Kimmel, C. B., Warga, R. M. and Schilling, T. F. (1990). Origin and organization of the zebrafish fate map. *Development* **108**, 581-594.

Kimmel, C. B., Ballard, W. W., Kimmel, S. R., Ullmann, B. and Schilling, T. F. (1995). Stages of embryonic-development of the zebrafish. *Developmental Dynamics* **203**, 253-310.

Kitano, J., Lema, S. C., Luckenbach, J. A., Mori, S., Kawagishi, Y., Kusakabe, M., Swanson, P. and Peichel, C. L. (2010). Adaptive Divergence in the Thyroid Hormone Signaling Pathway in the Stickleback Radiation. *Current Biology* **20**, 2124-2130.

Kobayashi, Y., Ishikawa, T., Hirayama, J., Daiyasu, H., Kanai, S., Toh, H., Fukuda, I., Tsujimura, T., Terada, N., Kamei, Y. et al. (2000). Molecular analysis of zebrafish photolyase/cryptochrome family: two types of cryptochromes present in zebrafish. *Genes to Cells* **5**, 725-738.

Koenig, B. B., Cook, J. S., Wolsing, D. H., Ting, J., Tiesman, J. P., Correa, P. E., Olson, C. A., Pecquet, A. L., Ventura, F. S., Grant, R. A. et al. (1994). Characterization and cloning of a receptor for bmp-2 and bmp-4 from NIH 3T3 cells. *Mol. Cell. Biol.* **14**, 5961-5974.

Labeur, M. and Holsboer, F. (2010). Molecular mechanisms of glucocorticoid receptor signaling. *Med.-Buenos Aires* **70**, 457-462.

Lahiri, K., Vallone, D., Gondi, S. B., Santoriello, C., Dickmeis, T. and Foulkes, N. S. (2005). Temperature regulates transcription in the zebrafish circadian clock. *Plos Biology* **3**, 2005-2016.

Lankford, T. E., Billerbeck, J. M. and Conover, D. O. (2001). Evolution of intrinsic growth and energy acquisition rates. II. Trade-offs with vulnerability to predation in Menidia menidia. *Evolution* **55**, 1873-1881.

Laplante, M. and Sabatini, D. M. (2009). mTOR signaling at a glance. *J Cell Sci* **122**, 3589-3594.

Larqué, E., Sabater-Molina, M. and Zamora, S. (2007). Biological significance of dietary polyamines. *Nutrition* **23**, 87-95.

Larsen, P. F., Nielsen, E. E., Williams, T. D., Hemmer-Hansen, J., Chipman, J. K., Kruhoffer, M., Gronkjaer, P., George, S. G., Dyrskjot, L. and Loeschcke, V. (2007). Adaptive differences in gene expression in European flounder (Platichthys flesus). *Molecular Ecology* **16**, 4674-4683.

Lau, M. M. H., Stewart, C. E. H., Liu, Z. Y., Bhatt, H., Rotwein, P. and Stewart, C. L. (1994). Loss of the imprinted igf2/cation-independent mannose 6-phosphate receptor results in fetal overgrowth and perinatal lethality. *Genes Dev.* **8**, 2953-2963.

Lawson, N. D. and Wolfe, S. A. (2011). Forward and Reverse Genetic Approaches for the Analysis of Vertebrate Development in the Zebrafish. *Developmental Cell* **21**, 48-64.

Lee, C. Y., Hu, S. Y., Gong, H. Y., Chen, M. H. C., Lu, J. K. and Wu, J. L. (2009). Suppression of myostatin with vector-based RNA interference causes a double-muscle effect in transgenic zebrafish. *Biochemical and Biophysical Research Communications* **387**, 766-771.

Lee, S. J. (2004). Regulation of muscle mass by myostatin. *Annu. Rev. Cell Dev. Biol.* **20**, 61-86.

Li, X., Nie, F., Yin, Z. and He, J. Y. (2011). Enhanced hyperplasia in muscles of transgenic zebrafish expressing Follistatin1. *Sci. China-Life Sci.* **54**, 159-165.

Li, Y., Xiang, J. H. and Duan, C. M. (2005). Insulin-like growth factor-binding protein-3 plays an important role in regulating pharyngeal skeleton and inner ear formation and differentiation. *Journal of Biological Chemistry* **280**, 3613-3620.

Lieschke, G. J. and Currie, P. D. (2007). Animal models of human disease: zebrafish swim into view. *Nature Reviews Genetics* **8**, 353-367.

Liu, L. and Ge, W. (2007). Growth differentiation factor 9 and its spatiotemporal expression and regulation in the zebrafish ovary. *Biol. Reprod.* **76**, 294-302.

Lubzens, E., Young, G., Bobe, J. and Cerdà, J. (2010). Oogenesis in teleosts: How fish eggs are formed. *General and Comparative Endocrinology* **165**, 367-389.

Luther, P. K., Munro, P. M. G. and Squire, J. M. (1995). Muscle ultrastructure in the teleost fish. *Micron* **26**, 431-459.

MacKenzie, D. S., VanPutte, C. M. and Leiner, K. A. (1998). Nutrient regulation of endocrine function in fish. *Aquaculture* **161**, 3-25.

Macqueen, D. J. and Johnston, I. A. (2008a). Evolution of follistatin in teleosts revealed through phylogenetic, genomic and expression analyses. *Development Genes and Evolution* **218**, 1-14.

Macqueen, D. J. and Johnston, I. A. (2008b). An update on MyoD evolution in teleosts and a proposed consensus nomenclature to accommodate the tetraploidization of different vertebrate genomes. *PLoS One* **3**.

Macqueen, D. J., KristjÁNsson, B. K., Paxton, C. G. M., Vieira, V. L. A. and Johnston, I. A. (2011). The parallel evolution of dwarfism in Arctic charr is accompanied by adaptive divergence in mTOR-pathway gene expression. *Molecular Ecology* **20**, 3167-3184.

Macqueen, D. J., Robb, D. H. F., Olsen, T., Melstveit, L., Paxton, C. G. M. and Johnston, I. A. (2008). Temperature until the 'eyed stage' of embryogenesis programmes the growth trajectory and muscle phenotype of adult Atlantic salmon. *Biology Letters* **4**, 294-298.

Mambrini, M., Labbe, L., Randriamanantsoa, F. and Boujard, T. (2006). Response of growth-selected brown trout (Salmo trutta) to challenging feeding conditions. *Aquaculture* **252**, 429-440.

Martín-Robles, Á. J., Isorna, E., Whitmore, D., Muñoz-Cueto, J. A. and Pendón, C. (2011). The clock gene Period3 in the nocturnal flatfish Solea senegalensis: Molecular cloning, tissue expression and daily rhythms in central areas. *Comparative Biochemistry and Physiology - Part A: Molecular & Integrative Physiology* **159**, 7-15.

Martin, A. M., Elliott, J. A., Duffy, P., Blake, C. M., Ben Attia, S., Katz, L. M., Browne, J. A., Gath, V., McGivney, B. A., Hill, E. W. et al. (2010). Circadian regulation of locomotor activity and skeletal muscle gene expression in the horse. *Journal of Applied Physiology* **109**, 1328-1336.

Mathavan, S., Lee, S. G. P., Mak, A., Miller, L. D., Murthy, K. R. K., Govindarajan, K. R., Tong, Y., Wu, Y. L., Lam, S. H., Yang, H. et al. (2005). Transcriptome analysis of zebrafish embryogenesis using microarrays. *Plos Genetics* **1**, 260-276.

Maures, T., Chan, S. J., Xu, B., Sun, H., Ding, J. and Duan, C. M. (2002). Structural, biochemical, and expression analysis of two distinct insulin-like growth factor I receptors and their ligands in zebrafish. *Endocrinology* **143**, 1858-1871.

Maures, T. J. and Duan, C. M. (2002). Structure, developmental expression, and physiological regulation of zebrafish IGF binding protein-1. *Endocrinology* **143**, 2722-2731.

Mazurais, D., Brierley, I., Anglade, I., Drew, J., Randall, C., Bromage, N., Michel, D., Kah, O. and Williams, L. M. (1999). Central melatonin receptors in the rainbow trout: Comparative distribution of ligand binding and gene expression. *Journal of Comparative Neurology* **409**, 313-324.

McCarthy, J. J., Andrews, J. L., McDearmon, E. L., Campbell, K. S., Barber, B. K., Miller, B. H., Walker, J. R., Hogenesch, J. B., Takahashi, J. S. and Esser, K. A. (2007). Identification of the circadian transcriptome in adult mouse skeletal muscle. *Physiological Genomics* **31**, 86-95.

McConnell, B. B. and Yang, V. W. (2010). Mammalian Krüppel-Like Factors in Health and Diseases. *Physiol. Rev.* **90**, 1337-1381.

McCormick, S. D. (2001). Endocrine control of osmoregulation in teleost fish. *American Zoologist* **41**, 781-794.

McElhinny, A. S., Kazmierski, S. T., Labeit, S. and Gregorio, C. C. (2003). Nebulin: The Nebulous, Multifunctional Giant of Striated Muscle. *Trends in Cardiovascular Medicine* **13**, 195-201.

Medeiros, E. F., Phelps, M. P., Fuentes, F. D. and Bradley, T. M. (2009). Overexpression of follistatin in trout stimulates increased muscling. *American Journal of Physiology-Regulatory Integrative and Comparative Physiology* **297**, R235-R242.

Menke, A. L., Spitsbergen, J. M., Wolterbeek, A. P. M. and Woutersen, R. A. (2011). Normal Anatomy and Histology of the Adult Zebrafish. *Toxicol. Pathol.* **39**, 759-775.

Miller, B. H., McDearmon, E. L., Panda, S., Hayes, K. R., Zhang, J., Andrews, J. L., Antoch, M. P., Walker, J. R., Esser, K. A., Hogenesch, J. B. et al. (2007). Circadian and CLOCK-controlled regulation of the mouse transcriptome and cell proliferation. *Proceedings of the National Academy of Sciences* **104**, 3342-3347.

Miller, N. and Gerlai, R. (2007). Quantification of shoaling behaviour in zebrafish (Danio rerio). *Behavioural Brain Research* **184**, 157-166.

Moeller, L. C., Cao, X., Dumitrescu, A. M., Seo, H. and Refetoff, S. (2006). Thyroid hormone mediated changes in gene expression can be initiated by cytosolic action of the thyroid hormone receptor beta through the phosphatidylinositol 3-kinase pathway. *Nuclear receptor signaling* **4**, e020.

Mommsen, T. P. and Moon, T. W. (2001). 8. Hormonal regulation of muscle growth. In *Fish Physiology*, vol. Volume 18 (ed. J. Ian), pp. 251-308: Academic Press.

Moore, P. and Swendseid, M. E. (1983). Dietary-regulation of the activities of ornithine decarboxylase and s-adenosylmethionine decarboxylase in rats. *Journal of Nutrition* **113**, 1927-1935.

Nabeshima, Y., Hanaoka, K., Hayasaka, M., Esumi, E., Li, S. W. and Nonaka, I. (1993). Myogenin gene disruption results in perinatal lethality because of severe muscle defect. *Nature* **364**, 532-535.

Nasevicius, A. and Ekker, S. C. (2000). Effective targeted gene 'knockdown' in zebrafish. *Nature Genetics* **26**, 216-220.

Nasizadeh, S., Myhre, L., Thiman, L., Alm, K., Oredsson, S. and Persson, L. (2005). Importance of polyamines in cell cycle kinetics as studied in a transgenic system. *Experimental Cell Research* **308**, 254-264.

Neely, K. G., Myers, J. M., Hard, J. J. and Shearer, K. D. (2008). Comparison of growth, feed intake, and nutrient efficiency in a selected strain of coho salmon (Oncorhynchus kisutch) and its source stock. *Aquaculture* **283**, 134-140.

Nei, M. (2007). The new mutation theory of phenotypic evolution. *Proceedings of the National Academy of Sciences of the United States of America* **104**, 12235-12242.

Nelson, S. N. and Van Der Kraak, G. (2010). Characterization and regulation of the insulin-like growth factor (IGF) system in the zebrafish (Danio rerio) ovary. *General and Comparative Endocrinology* **168**, 111-120.

Nicieza, A. G. and Metcalfe, N. B. (1997). Growth compensation in juvenile Atlantic salmon: Responses to depressed temperature and food availability. *Ecology* **78**, 2385-2400.

Nordgarden, U., Fjelldal, P. G., Hansen, T., Björnsson, B. T. and Wargelius, A. (2006). Growth hormone and insulin-like growth factor-I act together and independently when regulating growth in vertebral and muscle tissue of atlantic salmon postsmolts. *General and Comparative Endocrinology* **149**, 253-260.

Ogawa, H., Ishiguro, K.-i., Gaubatz, S., Livingston, D. M. and Nakatani, Y. (2002). A Complex with Chromatin Modifiers That Occupies E2F- and Myc-Responsive Genes in G0 Cells. *Science* **296**, 1132-1136.

Okada, T., Yoshida, H., Akazawa, R., Negishi, M. and Mori, K. (2002). Distinct roles of activating transcription factor 6 (ATF6) and double-stranded RNA-activated protein kinase-like endoplasmic reticulum kinase (PERK) in transcription during the mammalian unfolded protein response. *Biochemical Journal* **366**, 585-594.

Pando, M. P., Pinchak, A. B., Cermakian, N. and Sassone-Corsi, P. (2001). A cell-based system that recapitulates the dynamic light-dependent regulation of the vertebrate clock. *Proceedings of the National Academy of Sciences* **98**, 10178-10183.

Pegg, A. E. (2006). Regulation of ornithine decarboxylase. *Journal of Biological Chemistry* **281**, 14529-14532.

Pelegri, F. (2003). Maternal factors in zebrafish development. *Developmental Dynamics* **228**, 535-554.

Peng, C., Clelland, E. and Tan, Q. (2009). Potential role of bone morphogenetic protein-15 in zebrafish follicle development and oocyte maturation. *Comparative Biochemistry and Physiology - Part A: Molecular & Integrative Physiology* **153**, 83-87.

Penton, A., Chen, Y. J., Staehlinghampton, K., Wrana, J. L., Attisano, L., Szidonya, J., Cassill, J. A., Massague, J. and Hoffmann, F. M. (1994). Identification of 2 bone morphogenetic protein type-i receptors in drosophila and evidence that BRK25D is a decapentaplegic receptor. *Cell* **78**, 239-250.

Perez-Sanchez, J., Calduch-Giner, J. A., Mingarro, M., de Celis, S. V. R., Gomez-Requeni, P., Saera-Vila, A., Astola, A. and Valdivia, M. M. (2002). Overview of fish growth hormone family. New insights in genomic organization and heterogeneity of growth hormone receptors. *Fish Physiology and Biochemistry* **27**, 243-258.

Peschel, N. and Helfrich-Forster, C. (2011). Setting the clock - by nature: Circadian rhythm in the fruitfly Drosophila melanogaster. *Febs Letters* **585**, 1435-1442.

Peterson, B. C., Small, B. C., Waldbieser, G. C. and Bosworth, B. G. (2008). Endocrine responses of fast- and slow-growing families of channel catfish. *North American Journal of Aquaculture* **70**, 240-250.

Plaut, I. and Gordon, M. S. (1994). Swimming metabolism of wild-type and cloned zebrafish Brachydanio-rerio. *Journal of Experimental Biology* **194**, 209-223.

Plautz, J. D., Kaneko, M., Hall, J. C. and Kay, S. A. (1997). Independent photoreceptive circadian clocks throughout Drosophila. *Science* **278**, 1632-1635.

Power, D. M., Llewellyn, L., Faustino, M., Nowell, M. A., Björnsson, B. T., Einarsdottir, I. E., Canario, A. V. M. and Sweeney, G. E. (2001). Thyroid hormones in growth and development of fish. *Comparative Biochemistry and Physiology C-Toxicology & Pharmacology* **130**, 447-459.

Powers, D. A. and Schulte, P. M. (1998). Evolutionary adaptations of gene structure and expression in natural populations in relation to a changing environment: A multidisciplinary approach to address the million-year saga of a small fish. *Journal of Experimental Zoology* **282**, 71-94.

Rees, B. B., Andacht, T., Skripnikova, E. and Crawford, D. L. (2011). Population Proteomics: Quantitative Variation Within and Among Populations in Cardiac Protein Expression. *Molecular Biology and Evolution* **28**, 1271-1279.

Ren, H. X., Accili, D. and Duan, C. M. (2010). Hypoxia converts the myogenic action of insulin-like growth factors into mitogenic action by differentially regulating multiple signaling pathways. *Proceedings of the National Academy of Sciences of the United States of America* **107**, 5857-5862.

Rescan, P. Y., Montfort, J., Ralliere, C., Le Cam, A., Esquerre, D. and Hugot, K. (2007). Dynamic gene expression in fish muscle during recovery growth induced by a fasting-refeeding schedule. *Bmc Genomics* **8**.

Ripperger, J. A., Jud, C. and Albrecht, U. (2011). The daily rhythm of mice. *Febs Letters* **585**, 1384-1392.

Robison, B. D. and Rowland, W. (2005). A potential model system for studying the genetics of domestication: behavioral variation among wild and domesticated strains of zebra danio (Danio rerio). *Canadian Journal of Fisheries and Aquatic Sciences* **62**, 2046-2054.

Rome, L. C., Loughna, P. T. and Goldspink, G. (1984). Muscle-fiber activity in carp as a function of swimming speed and muscle temperature. *Am. J. Physiol.* **247**, R272-R279.

Rommel, C., Bodine, S. C., Clarke, B. A., Rossman, R., Nunez, L., Stitt, T. N., Yancopoulos, G. D. and Glass, D. J. (2001). Mediation of IGF-1-induced skeletal myotube hypertrophy by PI(3)K/Akt/mTOR and PI(3)K/Akt/GSK3 pathways. *Nature Cell Biology* **3**, 1009-1013.

Rosa, C. E. d., Kuradomi, R. Y., Almeida, D. V., Lannes, C. F. C., Figueiredo, M. d. A., Dytz, A. G., Fonseca, D. B. and Marins, L. F. (2010). GH overexpression modifies muscle expression of anti-oxidant enzymes and increases spinal curvature of old zebrafish. *Experimental Gerontology* **45**, 449-456.

Rowlerson, A. and Veggetti, A. (2001). 5. Cellular mechanisms of post-embryonic muscle growth in aquaculture species. In *Fish Physiology*, vol. Volume 18 (ed. J. Ian), pp. 103-140: Academic Press.

Rudnicki, M. A., Braun, T., Hinuma, S. and Jaenisch, R. (1992). Inactivation of myod in mice leads to up-regulation of the myogenic HLH gene myf-5 and results in apparently normal muscle development. *Cell* **71**, 383-390.

Rudnicki, M. A., Schnegelsberg, P. N. J., Stead, R. H., Braun, T., Arnold, H. H. and Jaenisch, R. (1993). Myod or myf-5 is required for the formation of skeletal-muscle. *Cell* **75**, 1351-1359.

Ruijter, J. M., Ramakers, C., Hoogaars, W. M. H., Karlen, Y., Bakker, O., van den Hoff, M. J. B. and Moorman, A. F. M. (2009). Amplification efficiency: linking baseline and bias in the analysis of quantitative PCR data. *Nucleic Acids Res.* **37**.

Ruzzante, D. E. and Doyle, R. W. (1991). Rapid behavioral-changes in medaka (Oryzias-latipes) caused by selection for competitive and noncompetitive growth. *Evolution* **45**, 1936-1946.

Saele, O., Solbakken, J. S., Watanabe, K., Hamre, K. and Pittman, K. (2003). The effect of diet on ossification and eye migration in Atlantic halibut larvae (Hippoglossus hippoglossus L.). *Aquaculture* **220**, 683-696.

Sakamoto, T. and McCormick, S. D. (2006). Prolactin and growth hormone in fish osmoregulation. *General and Comparative Endocrinology* **147**, 24-30.

Salem, M., Silverstein, J., Iii, C. E. R. and Yao, J. (2007). Effect of starvation on global gene expression and proteolysis in rainbow trout (Oncorhynchus mykiss). *Bmc Genomics* **8**.

Salem, M., Nath, J., Rexroad, C. E., Killefer, J. and Yao, J. (2005). Identification and molecular characterization of the rainbow trout calpains (Capn1 and Capn2): their expression in muscle wasting during starvation. *Comparative Biochemistry and Physiology B-Biochemistry & Molecular Biology* **140**, 63-71.

Sanchez, J. A. and Sanchez-Vazquez, F. J. (2009). Feeding Entrainment of Daily Rhythms of Locomotor Activity and Clock Gene Expression in Zebrafish Brain. *Chronobiology International* **26**, 1120-1135.

Sanchez, J. A., Lopez-Olmeda, J. F., Blanco-Vives, B. and Sanchez-Vazquez, F. J. (2009). Effects of feeding schedule on locomotor activity rhythms and stress response in sea bream. *Physiology & Behavior* **98**, 125-129.

Sarup, P., Sorensen, P. and Loeschcke, V. (2011). Flies selected for longevity retain a young gene expression profile. *Age* **33**, 69-80.

Schlueter, P. J., Peng, G., Westerfield, M. and Duan, C. (2007). Insulin-like growth factor signaling regulates zebrafish embryonic growth and development by promoting cell survival and cell cycle progression. *Cell Death and Differentiation* **14**, 1095-1105.

Schlueter, P. J., Royer, T., Farah, M. H., Laser, B., Chan, S. J., Steiner, D. F. and Duan, C. M. (2006). Gene duplication and functional divergence of the zebrafish insulin-like growth factor 1 receptors. *Faseb Journal* **20**, 1230-+.

Schoneveld, O., Gaemers, I. C. and Lamers, W. H. (2004). Mechanisms of glucocorticoid signalling. *Biochim. Biophys. Acta-Gene Struct. Expression* **1680**, 114-128.

Schulte, P. M. (2001). Environmental adaptations as windows on molecular evolution. *Comparative Biochemistry and Physiology B-Biochemistry & Molecular Biology* **128**, 597-611.

Segal, J. A., Schulte, P. M., Powers, D. A. and Crawford, D. L. (1996). Descriptive and functional characterization of variation in the Fundulus heteroclitus Ldh-B proximal promoter. *Journal of Experimental Zoology* **275**, 355-364.

Seiliez, I., Gabillard, J. C., Skiba-Cassy, S., Garcia-Serrana, D., Gutierrez, J., Kaushik, S., Panserat, S. and Tesseraud, S. (2008). An in vivo and in vitro assessment of TOR signaling cascade in rainbow trout (Oncorhynchus mykiss). *American Journal of Physiology-Regulatory Integrative and Comparative Physiology* **295**, R329-R335.

Shimizu, M., Cooper, K. A., Dickhoff, W. W. and Beckman, B. R. (2009). Postprandial changes in plasma growth hormone, insulin, insulin-like growth factor (IGF)-I, and

IGF-binding proteins in coho salmon fasted for varying periods. *American Journal of Physiology-Regulatory Integrative and Comparative Physiology* **297**, R352-R361.

Siccardi, A. J., Garris, H. W., Jones, W. T., Moseley, D. B., D'Abramo, L. R. and Watts, S. A. (2009). Growth and Survival of Zebrafish (Danio rerio) Fed Different Commercial and Laboratory Diets. *Zebrafish* **6**, 275-280.

Sidi, S., Goutel, C., Peyrieras, N. and Rosa, F. M. (2003). Maternal induction of ventral fate by zebrafish radar. *Proceedings of the National Academy of Sciences of the United States of America* **100**, 3315-3320.

Silverstein, J. T. (2002). Using genetic variation to understand control of feed intake in fish. *Fish Physiology and Biochemistry* **27**, 173-178.

Song, C. Z., Gavriilidis, G., Asano, H. and Stamatoyannopoulos, G. (2005). Functional study of transcription factor KLF11 by targeted gene inactivation. *Blood Cells Mol. Dis.* **34**, 53-59.

Stefansson, S. O., Nilsen, T. O., Ebbesson, L. O. E., Wargelius, A., Madsen, S. S., Björnsson, B. T. and McCormick, S. D. (2007). Molecular mechanisms of continuous light inhibition of Atlantic salmon parr-smolt transformation. *Aquaculture* **273**, 235-245.

Stellabotte, F. and Devoto, S. H. (2007). The teleost dermomyotome. *Developmental Dynamics* **236**, 2432-2443.

Stricker, D. (2008). BrightStat.com: Free statistics online. *Computer Methods and Programs in Biomedicine* **92**, 135-143.

Sumariwalla, V. M. and Klein, W. H. (2001). Similar myogenic functions for myogenin and MRF4 but not MyoD in differentiated murine embryonic stem cells. *Genesis* **30**, 239-249.

Summerton, J. and Weller, D. (1997). Morpholino antisense oligomers: Design, preparation, and properties. *Antisense Nucleic Acid Drug Dev.* **7**, 187-195.

Tadros, W. and Lipshitz, H. D. (2009). The maternal-to-zygotic transition: a play in two acts. *Development* **136**, 3033-3042.

Takahashi, J. S., Hong, H. K., Ko, C. H. and McDearmon, E. L. (2008). The genetics of mammalian circadian order and disorder: implications for physiology and disease. *Nature Reviews Genetics* **9**, 764-775.

Tamai, T. K., Young, L. C. and Whitmore, D. (2007). Light signaling to the zebrafish circadian clock by Cryptochrome 1a. *Proceedings of the National Academy of Sciences of the United States of America* **104**, 14712-14717.

Tan, X. G., Rotllant, J., Li, H. Q., DeDeyne, P. and Du, S. J. (2006). SmyD1, a histone methyltransferase, is required for myofibril organization and muscle contraction in zebrafish embryos (vol 103, pg 2713, 2006). *Proceedings of the National Academy of Sciences of the United States of America* **103**, 7935-7935.

Taylor, J. F., Migaud, H., Porter, M. J. R. and Bromage, N. R. (2005). Photoperiod influences growth rate and plasma insulin-like growth factor-I levels in juvenile rainbow trout, Oncorhynchus mykiss. *General and Comparative Endocrinology* **142**, 169-185.

Thisse, C., Thisse, B., Schilling, T. F. and Postlethwait, J. H. (1993). tructure of the zebrafish snail1 gene and its expression in wild-type, spadetail and no tail mutant embryos. *Development* **119**, 1203-1215.

Tintignac, L. A., Lagirand, J., Batonnet, S., Sirri, V., Leibovitch, M. P. and Leibovitch, S. A. (2005). Degradation of MyoD mediated by the SCF (MAFbx) ubiquitin ligase. *J Biol Chem* **280**, 2847-2856.

Tyler, C. R. and Sumpter, J. P. (1996). Oocyte growth and development in teleosts. *Reviews in Fish Biology and Fisheries* **6**, 287-318.

Ullmann, J. F. P., Cowin, G., Kurniawan, N. D. and Collin, S. P. (2010). A three-dimensional digital atlas of the zebrafish brain. *Neuroimage* **51**, 76-82.

Van Leeuwen, J. L. (1999). A mechanical analysis of myomere shape in fish. *Journal of Experimental Biology* **202**, 3405-3414.

Vandesompele, J., De Preter, K., Pattyn, F., Poppe, B., Van Roy, N., De Paepe, A. and Speleman, F. (2002). Accurate normalization of real-time quantitative RT-PCR data by geometric averaging of multiple internal control genes. *Genome Biol* **3**, RESEARCH0034.

Vanella, F. A., Boy, C. C., Lattuca, M. E. and Calvo, J. (2010). Temperature influence on post-prandial metabolic rate of sub-Antarctic teleost fish. *Comparative Biochemistry and Physiology a-Molecular & Integrative Physiology* **156**, 247-254.

Vatine, G., Vallone, D., Gothilf, Y. and Foulkes, N. S. (2011). It's time to swim! Zebrafish and the circadian clock. *Febs Letters* **585**, 1485-1494.

Vatine, G., Vallone, D., Appelbaum, L., Mracek, P., Ben-Moshe, Z., Lahiri, K., Gothilf, Y. and Foulkes, N. S. (2009). Light Directs Zebrafish period2 Expression via Conserved D and E Boxes. *Plos Biology* **7**.

Velleman, S. G. (1999). The role of the extracellular matrix in skeletal muscle development. *Poult. Sci.* **78**, 778-784.

Vesterlund, L., Jiao, H., Unneberg, P., Hovatta, O. and Kere, J. (2011). The zebrafish transcriptome during early development. *BMC Developmental Biology* **11**, 30.

Vieira, V. L. A. and Johnston, I. A. (1992). Influence of temperature on muscle-fiber development in larvae of the herring Clupea-harengus. *Marine Biology* **112**, 333-341.

Volff, J. N. (2005). Genome evolution and biodiversity in teleost fish. *Heredity* **94**, 280-294.

Wang, H. (2008a). Comparative Analysis of Period Genes in Teleost Fish Genomes. *Journal of Molecular Evolution* **67**, 29-40.

Wang, H. (2008b). Comparative analysis of teleost fish genomes reveals preservation of different ancient clock duplicates in different fishes. *Marine Genomics* **1**, 69-78.

Wang, H. (2009). Comparative genomic analysis of teleost fish bmal genes. *Genetica* **136**, 149-161.

Wang, Q. S., Zhao, H. B. and Pan, Y. C. (2011). SNPknow: a web server for functional annotation of cattle SNP markers. *Can. J. Anim. Sci.* **91**, 247-253.

Wang, X. L., Lu, L., Li, Y., Li, M. Y., Chen, C., Feng, Q., Zhang, C. Y. and Duan, C. M. (2009). Molecular and functional characterization of two distinct IGF binding protein-6 genes in zebrafish. *American Journal of Physiology-Regulatory Integrative and Comparative Physiology* **296**, R1348-R1357.

Wang, Y. H., Li, C. K., Lee, G. H., Tsay, H. J., Tsai, H. J. and Chen, Y. H. (2008). Inactivation of zebrafish mrf4 leads to myofibril misalignment and motor axon growth disorganization. *Developmental Dynamics* **237**, 1043-1050.

Wang, Y. X., Qian, L. X., Dong, Y. X., Jiang, Q., Gui, Y. H., Zhong, T. P. and Song, H. Y. (2006). Myocyte-specific enhancer factor 2A is essential for zebrafish posterior somite development. *Mechanisms of Development* **123**, 783-791.

Wang, Y. X., Qian, L. X., Yu, Z., Jiang, Q., Dong, Y. X., Liu, X. F., Yang, X. Y., Zhong, T. P. and Song, H. Y. (2005). Requirements of myocyte-specific enhancer factor 2A in zebrafish cardiac contractility. *Febs Letters* **579**, 4843-4850.

Wang, Z. Q., Fung, M. R., Barlow, D. P. and Wagner, E. F. (1994). Regulation of embryonic growth and lysosomal targeting by the imprinted igf2/mpr gene. *Nature* **372**, 464-467.

Weger, B. D., Sahinbas, M., Otto, G. W., Mracek, P., Armant, O., Dolle, D., Lahiri, K., Vallone, D., Ettwiller, L., Geisler, R. et al. (2011). The Light Responsive Transcriptome of the Zebrafish: Function and Regulation. *PLoS One* **6**, e17080.

Wheatcroft, S. B. and Kearney, M. T. (2009). IGF-dependent and IGF-independent actions of IGF-binding protein-1 and-2: implications for metabolic homeostasis. *Trends in Endocrinology and Metabolism* **20**, 153-162.

White, Y. A. R., Kyle, J. T. and Wood, A. W. (2009). Targeted Gene Knockdown in Zebrafish Reveals Distinct Intraembryonic Functions for Insulin-Like Growth Factor II Signaling. *Endocrinology* **150**, 4366-4375.

Whitehead, A. and Crawford, D. L. (2006). Neutral and adaptive variation in gene expression. *Proceedings of the National Academy of Sciences of the United States of America* **103**, 5425-5430.

Whitmore, D., Foulkes, N. S., Strahle, U. and Sassone-Corsi, P. (1998). Zebrafish Clock rhythmic expression reveals independent peripheral circadian oscillators. *Nat Neurosci* **1**, 701-707.

Winkler, G. S. (2010). The Mammalian Anti-Proliferative BTG/Tob Protein Family. *J. Cell. Physiol.* **222**, 66-72.

Witt, S. H., Granzier, H., Witt, C. C. and Labeit, S. (2005). MURF-1 and MURF-2 Target a Specific Subset of Myofibrillar Proteins Redundantly: Towards Understanding MURF-dependent Muscle Ubiquitination. *Journal of Molecular Biology* **350**, 713-722.

Wood, A. W., Duan, C. M. and Bern, H. A. (2005a). Insulin-like growth factor signaling in fish. *International Review of Cytology - a Survey of Cell Biology, Vol 243* **243**, 215-285.

Wood, A. W., Schlueter, P. J. and Duan, C. (2005b). Targeted knockdown of insulin-like growth factor binding protein-2 disrupts cardiovascular development in zebrafish embryos. *Mol. Endocrinol.* **19**, 1024-1034.

Wood, C. M., Walsh, P. J., Kajimura, M., McClelland, G. B. and Chew, S. F. (2010). The influence of feeding and fasting on plasma metabolites in the dogfish shark (Squalus acanthias). *Comparative Biochemistry and Physiology Part A Molecular & Integrative Physiology* **155**, 435-444.

Woods, I. G., Kelly, P. D., Chu, F., Ngo-Hazelett, P., Yan, Y. L., Huang, H., Postlethwait, J. H. and Talbot, W. S. (2000). A comparative map of the zebrafish genome. *Genome Res.* **10**, 1903-1914.

Xie, S. Q., Mason, P. S., Wilkes, D., Goldspink, G., Fauconneau, B. and Stickland, N. C. (2001). Lower environmental temperature delays and prolongs myogenic regulatory factor expression and muscle differentiation in rainbow trout (Onchrhynchus mykiss) embryos. *Differentiation* **68**, 106-114.

Yamada, P. M. and Lee, K. W. (2009). Perspectives in mammalian IGFBP-3 biology: local vs. systemic action. *Am. J. Physiol.-Cell Physiol.* **296**, C954-C976.

Yamaguchi, M., Hirai, Y., Takehana, K., Oba, T., Yamamoto, S., Muguruma, M., Masty, J. and Yamano, S. (1990). Dense bands and polarity of thin filament at myotendinous junction in guppy muscle. *Protoplasma* **158**, 121-129.

Yang, R. and Su, Z. (2010). Analyzing circadian expression data by harmonic regression based on autoregressive spectral estimation. *Bioinformatics* **26**, i168-i174.

Yang, X. J., Xie, J. J., Wu, T. X., Yue, G. H., Chen, J. and Zhao, R. Q. (2007). Hepatic and muscle expression of thyroid hormone receptors in association with body and muscle growth in large yellow croaker, Pseudosciaena crocea (Richardson). *General and Comparative Endocrinology* **151**, 163-171.

Yen, P. M. (2001). Physiological and molecular basis of thyroid hormone action. *Physiol. Rev.* **81**, 1097-1142.

Zhao, R. M. and Houry, W. A. (2007). Molecular interaction network of the Hsp90 chaperone system. In *Molecular Aspects of the Stress Response: Chaperones, Membranes and Networks*, vol. 594 eds. P. Csermely and L. Vígh), pp. 27-36. Berlin: Springer-Verlag Berlin.

Zhou, J. F., Li, W. H., Kamei, H. and Duan, C. M. (2008). Duplication of the IGFBP-2 Gene in Teleost Fish: Protein Structure and Functionality Conservation and Gene Expression Divergence. *PLoS One* **3**.

Zou, S., Kamei, H., Modi, Z. and Duan, C. (2009). Zebrafish IGF genes: gene duplication, conservation and divergence, and novel roles in midline and notochord development. *PLoS One* **4**, e7026.